DISSERTATION FOR DOCTORAL (PHD) DEGREE

University of Sopron (Soproni Egyetem)

Faculty of Wood Engineering and Creative Industry,

József Cziráki Doctoral School of Wood Sciences and Technologies

Creep and fatigue analysis of furniture joints

in

Material Science and Technology

PhD Program: Wood Sciences and Technologies

Author: Seda Baş

Research Supervisors: Dr. habil. Csiha Csilla

Dr. habil. Dénes Levente

University of Sopron

Faculty of Wood Engineering and Creative Industries

Sopron, 2024

CREEP AND FATIGUE ANALYSIS OF FURNITURE JOINTS

Dissertation for doctoral (PhD) degree

University of Sopron József Cziráki Doctoral School

of Wood Sciences and Technologies

Wood Sciences and Technologies programme

Written by:

Seda Baş

Made in the framework of

…..... programme

of the József Cziráki Doctoral School, University of Sopron

Supervisors: Dr. habil. Csiha Csilla and Dr. habil. Dénes Levente

I recommend for acceptance (yes / no)

(signature)

The candidate reached …..... % at the complex exam,

Sopron, 2024 .....

Chairman of the Examination Board

As assessor I recommend the dissertation for acceptance (yes/no)

First assessor: Prof. Dr. Bejó László yes/no

(signature)

Second assessor: Prof. Dr. Kovács Zsolt yes/no

(signature)

(Possible third assessor (Dr. .....) yes/no

(signature)

The candidate reached .....% in the public debate of the dissertation

Sopron, 2024

.....

Chairman of the Assessor Committee

Qualification of the doctoral (PhD) degree ….....

.....

Chairman of the University Doctoral
and Habilitation Council (UDHC)

DECLARATION

I, the undersigned **Seda Baş** by signing this declaration declare that my PhD thesis entitled "**Creep and fatigue analysis of furniture joints"** was my own work; during the dissertation I complied with the regulations of Act LXXVI of 1999 on Copyright and the rules of the doctoral dissertation prescribed by the Cziráki József Doctoral School, especially regarding references and citations.[1]

Furthermore, I declare that during the preparation of the dissertation I did not mislead my supervisor(s) or the programme leader with regard to the independent research work.

By signing this declaration, I acknowledge that if it can be proved that the dissertation is not self-made or the author of a copyright infringement is related to the dissertation, the University of Sopron is entitled to refuse the acceptance of the dissertation.

Refusing to accept a dissertation does not affect any other legal (civil law, misdemeanour law, criminal law) consequences of copyright infringement.

Sopron, ... 2024

……..

Seda Baş

[1] **Act LXXVI of 1999** Article 34 (1) Anyone is entitled to quote details of the work, to the extent justified by the nature and purpose of the recipient work, by designating the source and the author specified therein.

Article 36 (1) Details of publicly lectures and other similar works, as well as political speeches, may be freely used for the purpose of information to the extent justified by the purpose. For such use, the source, along with the name of the author, shall be indicated, unless this is impossible.

Acknowledgements

The thesis is an important result and realization of life. Without the continuous support, help and cooperation of my supervisors, Dr. Csilla Csiha and Dr. Levente Dénes, the research work presented in the dissertation would probably not have been possible. I have received enormous support from both of them through the sharing of technological knowledge, material procurement, guidance and advice.

Furthermore, the results presented here would not have been achieved without the administrative support received from Vera Tolvaj, the coordinator of the József Cziráki Doctoral School, the cordial cooperation of the teachers and administrators and the workers of the various laboratories of the University of Sopron. I would like to thank Gábor Kun, István Schantl, Gábor Buranics and Antal Labozár for their continuous help and support. Furthermore, appreciation and special thanks go to the administrative bodies of the University of Sopron for their kind support during the various official arrangements during my PhD studies. Moreover, I would like to express my sincere gratitude to the "Tempus Public Foundation" for providing me financial assistance through awarding "Stipendium Hungaricum Scholarship" in 2019.

Once and for all, I would like to express my sincere thanks to my family and my dear fiance for providing great support, enthusiasm, and motivation during my difficult situations, which was a huge support during my PhD studies.

Finally, I am also grateful to the almighty creators of the Universe for providing me with a beautiful life with the right powers, abilities, and knowledge.

Table of Contents

DECLARATION I
Acknowledgements II
Table of Contents III
List of Figures VI
List of Tables IX
List of Abbreviations VIII
Abstract 1
1. INTRODUCTION AND LITERATURE REVIEW 2
1.1. Furniture 2
1.1.1. Square-Ended Butt Joint 5
1.1.2. Mitred Butt Joint 5
1.1.3. Dowel Joint 5
1.1.4. Lap Joint 6
1.1.5. Splined Mitre Joint 6
1.1.6. Corner Bridle Joint 7
1.1.7. Stopped Mortise&Tennon 7
1.1.8. Through Mortise&Tennon 8
1.1.9. Butt T-Joint 8
1.1.10. T-Halving Joint 9
1.1.11. Cross Halving Joint 9
1.1.12. Pinned Mortise&Tennon 10
1.1.13. Groove and Tenon Joints 10
1.1.14. Biscuit Joint 10
1.1.15. Edge-to-Edge Butt Joint 11
1.1.16. Tongue&Groove Joint 11
1.1.17. Splined Edge-to-Edge Joint 12
1.2. Domino wood dowels 13
1.3. Domino metallic connectors 14
1.4. Static and Dynamic Strength of Joints 17
1.4.1. Static Strength 17
1.4.2. Dynamic strength 18
1.5. Creep Behaviour of Furniture Joints 20
2. MATERIALS AND METHOD 30
2.1. Material 30

2.2. Method....33
2.2.1. Static Tensile (withdrawal) Test....33
2.2.2. Static bending tests by diagonal compression and tension....34
2.2.3. Creep Test....35
2.2.4. Cyclic Test....38
2.2.5. Statistical analysis....38
2.2.6. Other calculations....39
3. RESULTS AND DISCUSSIONS....39
3.1. Static bending tests by diagonal compression and tension and T-joint withdrawal tests....40
3.1.1. Compression and tension test results of joints fastened with Domino wood dowel..40
3.1.1.1. Compression test results of the joints of code LBWD....40
3.1.1.2. Compression test results of the joints of code TBWD.....44
3.1.1.3. Compression test results of the joints of code LSWD....45
3.1.1.4. Compression test results of joints of code TSWD....46
3.1.2.5. Tension test results of the joints of code LBWD.....46
3.1.1.6. Tension test results of the joints of code TBWD.....47
3.1.1.7. Tension test results of the joints of code LSWD....48
3.1.1.8. Tension test results of the joints of code TSWD....48
3.1.2.1. Compression test results the joints of code LBC....49
3.1.2.2. Compression test results of the joints of code TBC....49
3.1.2.3. Compression test results of the joints of code LSC....50
3.1.2.4. Compression test results of the joints of code TSC....51
3.1.2.5. Tension test results of the joints of code LBC....51
3.1.2.6. Tension test results for the of the joints of code TBC....52
3.1.2.7. Tension test results of the joints of code LSC....53
3.1.2.8. Tension test results of the joints of code TSC....53
3.1.3 Observations on the behaviour of test pieces in the course of tests....54
3.1.4 Comparison and statistical analysis of static tests data obtained for the different joint types....56
3.2. Cyclic test results....64
3.2.1. Cyclic test results of Domino wood dowel fastened joints....64
3.2.1.1. Cyclic test results of the joints coded LBWD:....64
3.2.1.2. Cyclic test results for the TBWD-type joints....65
3.2.1.3. Cyclic test results for the LSWD-type joints....66
3.2.1.4. Cyclic test results for the TSWD-type joints....67
3.2.2. Cyclic test results of metallic Domino connector fastened joints:....68
3.2.2.1. Cyclic test results for the LBC-type joints:....68

3.2.2.2. Cyclic test results for the TBC fastened joints.....69
3.2.2.3. Cyclic test results for the LSC-type joints.....70
3.2.2.4. Cyclic test results for the TSC-type joints.....71
3.3. Creep Test Results.....72
3.3.1 Creep factor curves.....72
3.3.5. Comparison and statistical analysis of the change of rotation/moment ratio as a measure of creep.....89
3.3.6. Comparison of the loss of rigidity of the different joint types in the course of sustained loading 91
4. CONCLUSIONS.....93
THESES.....97
APPENDIX.....100
5. REFERENCES.....141

List of Figures

Figure 1.1 Square-Ended Butt Joint (drawing by S.Baş).....5
Figure 1.2 Mitred Butt Joint (drawing by S.Baş).....5
Figure 1.3 Dowel Joint (drawing by S.Baş).....5
Figure 1.4 Corner Halving Joint (drawing by S.Baş).....6
Figure 1.5 Splined Mitre Joint (drawing by S.Bas).....6
Figure 1.6 Corner Bridle Joint (drawing by S.Baş).....7
Figure 1.7 Stopped Mortise& Tennon Joint (drawing by S.Baş).....7
Figure 1.8 Through Mortise& Tennon Joint (drawing by S.Baş).....8
Figure 1.9 Butt Joint (drawing by S.Baş).....8
Figure 1.10 T-Halving Joint (drawing by S.Baş).....9
Figure 1.11. Cross Halving Joint (drawing by S.Baş).....9
Figure 1.12. Pinned Mortise& Tennon Joint (drawing by S.Baş).....10
Figure 1.13 Groove and Tenon Joint (drawing by S.Baş).....10
Figure 1.14 Biscuit Joint (drawing by S.Baş).....10
Figure 1.15 Edge-to-Edge Butt Joint (drawing by S.Baş).....11
Figure 1.16 Tongue&Groove Joint (drawing by S.Baş).....11
Figure 1.17 Splined Edge-to-Edge Joint12 (drawing by S.Baş).....12
Figure 1.18 Different domino wood dowel sizes (S. Baş).....14
Figure 1.19 Different domino metallic connectors (S. Baş).....15
Figure 1.20 Domino system.....16
Figure 1.21 The two types of Domino elements in the same joint.....17
Figure 1.22 Stress-strain curve of an elastic-plastic material (Yiğiter, H., 2006).....18
Figure 1.23 Deformation graph resulting from the creep test [65].....21
Figure 1.24 Strain-time graph (Costa and Barros, 2015).....26
Figure 2.1 Corner joint and T-joint specimens - Type 1 (big size) (drawing: S.Baş).....30
Figure 2.2 Corner joint and T-joint specimens - Type 2 (small size) (drawing: S.Baş).....31
Figure **2.3** Domino wood dowel (a) (source: Festool) metallic Domino connector (b) (source: Festool) and the anchoring effect of the metallic Domino connector (c) (source: beavertools.com) for small-size test-pieces.....32
Figure 2.4 Static bending test arrangement for T- and L-joints in compression (a, b) as well as in tension (c, d) (drawing: S.Baş).....33
Figure 2.5 Domino joint elements, static tensile test of big L joint (a), withdrawal test of T joint (b). (Photo: S. Baş).....34
Figure 2.6 Bending test by diagonal loading: compressive load application (Photo: S. Baş).35
Figure 2.7 Digital gauge (Photo: S. Baş).....36
Figure 2.8 Creep test setup for the big samples (Photo: S. Baş).....37
Figure 2.9 Weights used in the creep test fort the big test pieces.....37
Figure 2.10 Creep test setup for the small test pieces (Photo:S.Baş)..... 37

List of Tables

Table 1.1 Different sizes of wood dowels and metallic connectors 15
Table 2.1 Specimen codes and names.....31
Table 2.2. Properties of the PVAc adhesive.....32
Table 3.1 Tests performed and number of samples used.....39
Table 3.2 Compression test results of the joints of code LBWD 43
Table 3.3 Compression test results of the joints of code TBWD. 44
Table 3.4 Compression test results of the joints of code LSWD.....45
Table 3.5 Compression test results of joints of code TSWD 46
Table 3.6 Tension test results of the joints of code LBWD 46
Table 3.7 Tension test results of the joints of code TBWD 47
Table 3.8 Tension test results of the joints of code LSWD. 48
Table 3.9 Tension test results of the joints of code TSWD. 48
Table 3.10 Compression test results of the joints of code LBC 49
Table 3.11 Compression test results of the joints of code TBC 50
Table 3.12 Compression test results of the joints of code LSC 50
Table 3.13 Compression test results of the joints of code TSC 51
Table 3.14 Tension test results of the joints of code LBC 51
Table 3.15 Tension test results of the joints of code TBC 52
Table 3.16 Tension test results of the joints of code LSC 53
Table 3.17 Tension test results of the joints of code TSC 53
Table 3.18 Displacement amplitudes applied in the course of the cyclic loading test 64
Table 3.19 Displacement amplitudes applied in the course of the cyclic loading test 65
Table 3.20 Displacement amplitudes applied in the course of the cyclic loading test 66
Table 3.21 Displacement amplitudes applied in the course of the cyclic loading test 67
Table 3.22 Displacement amplitudes applied in the course of the cyclic loading test 68
Table 3.23 Displacement amplitudes applied in the course of the cyclic loading test 69
Table 3.24 Displacement amplitudes applied in the course of the cyclic loading test 70
Table 3.25 Displacement amplitudes applied in the course of the cyclic loading test 71
Table 3.26 Logarithmic equations fitted on creep factor data for the individual test pieces in 78
each group, with the respective coefficient of determination; yi is the time-dependent creep.78
factor value of the i^{th} specimen in a group.....78
Table 3.27 Creep factor data of test pieces by joint types after the first 24 hours. X - tests....79
pieces omitted from the analysis. 79
Table 3.28 Creep factor data of test pieces by joint types after seven days loading; 186 test .81
piece omitted from the analysis.....81
Table 3.29 Z-coefficient increment data of test pieces by joint types. X - test pieces omitted from the analysis; corner joints 1^{st} day (a), corner joints 7 days (b); T- joints 1^{st} day (a), T-joints 7 days (b). 90

List of Abbreviations

ANOVA Analysis of Variance

ASTM American Society for Testing and Materials

EN European Standard

LBC **L** join, **B**ig size, with **C**onnector

LBWD **L** join, **B**ig size, with **W**ood **D**owel

LSC **L** join, **S**mall size, with **C**onnector

LSWD **L** join, **S**mall size, with **W**ood **D**owel

MOE Modulus of elasticity

MOR Modulus of rupture

PBAT Poly butylene adipate-terephthalate

PLA Polylactic acid

PVAc Polyvinyl acetate

TBC **T** join, **B**ig size, with **C**onnector

TBWD **T** join, **B**ig size, with **W**ood **D**owel

TSC **T** join, **S**mall size, with **C**onnector

TSWD **T** join, **S**mall size, with **W**ood **D**owel

Abstract

Selection of joint type and its characteristics is one of the most important decisions in furniture design. In this study, the behaviour of Domino-type furniture joints under sustained as well as cyclic loading was investigated. Corner-joints and T-joints were prepared for loading in bending. Joints with two types of connectors, Domino wood dowel and dismountable Domino metallic connector were tested, both with two different sizes: 8x22x40 mm and 14x28x75 mm. Specimens were made of European beech wood and for glued samples a D3 grade PVAc adhesive was used. For a proper planning of the sustained and the cyclic loading, it was necessary to obtain information on the performance of the individual joint types in static loading. Because of the static bending tests, ranking of the joint types with respect to load carrying capacity and deformation was possible. The flexibility coefficient (rotation/moment ratio) of the studied joints were also determined taking into account their nonlinear behaviour. Cyclic loading tests were conducted on the principles of the standard EN 12512:200. The joints started to lose their original strength during the repetitions of the 75% amplitude level. At the end of the fatigue tests, it was possible to pull out the Domino wood dowels from the mortise, whilst this was not the case with the metallic Domino connectors. The load levels to be applied in sustained loading were determined not to exceed 50% of the maximum load obtained from the static load tests. The creep results were evaluated in terms of creep factor and the increase in joint flexibility. Considering creep factor the wood dowel fastened small size corner joints (LSWD) as well as T-joints (TSWD) performed best, while the big size T-joint with wood dowel (TBWD) proved to be the worst; the differences are quite important between the two ends of the rank (0.56 vs. 2.23). With the exception of T-joints with metallic connector, small-size samples performed 1.4 to 3.2 times better than their big-size counterparts did. Logarithmic functions were fitted on the creep factor data with high value of the coefficient of determination. The coefficient *a* in the equation as a measure of the initial creep rate is 1.4 to 2.8 times higher in the case of big-size specimens, as reflected in the creep curves; T-joints with metallic connector did not follow this trend. Increase of joint flexibility or loss of joint rigidity is 1.1 to 11.7 times higher in the case of big-size joint types. The increase of the rotation/moment ratio of joints with wood dowel is 1.5 to 2.8 times higher than that of similar joints with metal connector. The two main finding of the research were the superiority of small-size joints with respect to sustained loading attributable to the more advantageous positioning of the connecting elements, as well as the better performance of the dismountable joints both in sustained and cyclic loading.

1. INTRODUCTION AND LITERATURE REVIEW

1.1. Furniture

Furniture is a product that combines art and technique, which affects the usefulness of the place with its functional value, makes the place look beautiful or ugly with its aesthetic value, makes the places we live or work in a warm and colourful environment [1].

Human life passes in various places. These spaces should be suitable for the purpose of construction and provide the necessary comfort level to the user. Physical factors such as heat, light, sound, colour, odour, and equipment in the place should be installed in a balanced way according to the needs and living habits of the person. In addition to structural elements such as walls, floorings, columns, doors, windows, spatial elements such as furniture and accessories play a very effective role in creating space. The choice of the colour and texture of the furniture, their densities and the arrangement in the space can affect the liveability of that space in a positive or negative way [2].

Furniture and building elements are structures formed by combining more than one element in a construction with various shapes and methods, while gaining some features and functions. In this direction, when listing the factors that determine the quality or performance of a furniture or building element, it is necessary to count the quality of the material used in its construction, as well as its design in accordance with the purpose of use and various features and functions that it gains during the design and construction [3].

When it comes to furniture, the first thing that comes to mind is wooden furniture. Wooden materials are mostly used in housing equipment such as desks, cabinets, bedsteads, nightstands, bookshelves, various office equipment, school desks and desks. Today, although other materials such as steel, aluminium, glass, and plastic have been used in furniture making, wood still maintains its popularity in this regard.

Features such as being easily processed, easily combined with each other, having high resistance, being easily changed when old and being painted are the main reasons why wood is more preferred in furniture making [4].

Various wood species and wood-based materials are used in the furniture industry including the solid wood, veneers, plywood, particleboards, fibreboards and other wood composites. In recent years, problems have started to be seen in international trade due to the shortage of raw materials, and there have been changes over time due to reasons such as changing fashion conditions in the use of wood material in production and the availability of the preferred wood material in the market or the difficulties in obtaining it. So much so that

Elm (Ulmus spp), which was abundant in the past, was used in furniture production, and later on due to insufficient supply, Eastern Beech (Fagus orientalis), Scots Pine (Pinus sylvestris), Alder (Alnus spp), Walnut (Juglans nigra), Oak (Tree species such as Quercus spp), Ash (Fraxinus spp), Chestnut (Castanea spp), Maple (Acer spp), Linden (Tilia spp), Spruce and Yew have been used. Among the broad-leaved tree species mentioned above, beech and white oaks and coniferous tree species like spruce and pine are widely used for furniture manufacturing. Since other tree species are difficult to obtain, they are mostly preferred for special orders and coatings [5]. Meeting the personal wishes and needs of people, the decrease in natural materials as a result of the forced use of wood materials by some sectoral areas has caused some negativities and deficiencies. In today's furniture industry, limited resources and unlimited human needs have forced manufacturers to produce different alternatives. Wood species such as Elm, Walnut, Oak, which were frequently preferred in furniture production in the past, are now available in small quantities in the market. Due to this situation beech started to be more frequently requested and used by furniture manufacturers than before. Therefore, in this study, furniture joints made from **beech wood** have been studied, because it is easily available and has been frequently used in furniture production. Beech (Fagus sylvatica) is one of the most common wood species in Central and Western Europe, although it can be found as shrub or tree between the 40th and 60th degrees of latitude. Beech wood is widely used, especially in the production of chairs, armchairs, office furniture, school furniture, where resistance to load and deformations is required [6]. At the same time, it can be finished very well and the texture of expensive and rare precious woods on the market can be imitated on the beech surface with varnish and paint. Likewise, this tree species takes its place as a preferred species in the market due to its resistance, hardness and suitability of bending properties [7].Beech can be found in mixed forests as well as in homogenous beech forests particularly in lowlands but also in low mountainous regions. The European beech (Fagus sylvatica) is the most useful of beech timbers and is therefore known simply as beech. The prefix red is sometimes used to describe the light red colouring of the wood. The copper beech with brown or red leaves is a special variety and has no commercial relevance. The white beech or hornbeam (Carpinus betulus L.) which is an accompanying species of beech belongs to another botanical family and has quite different properties. Beech trees can grow to 300 years or more, although trees of between 100 and 140 years old are typically felled. They can reach a height of 30 to 35 metres. Beech belongs to the heartwood trees. Sap and heartwood have an even pale yellow to reddish-white colouring, red-brown when steam-treated. The wood has an even fine-pored structure without noticeable markings. Older trees (over 80 years old) can develop a reddish core of irregular colour intensity

and shape. Furniture connections are an important element to consider when manufacturing or assembling furniture. A piece of furniture is mounted together by **joints**, which are a variety of hardware and techniques used to join and secure furniture pieces together [8]. These connections increase the durability of the furniture and ensure its longevity. They are also important from an aesthetic point of view, because the smooth and solid joints of the furniture are important for both appearance and use.

Reasons for using furniture mounts may be:

- Durability: furniture connections extend the life of furniture by connecting furniture parts strongly and durably.
- Safety: solid connections ensure that the furniture does not pose any danger during use.
- Aesthetics: well-made connections provide the furniture with a more professional and aesthetic appearance.
- Convenience: proper connection methods make furniture easier to assemble, resulting in a better experience for users.
- Repairs and Replacements: proper connections make it easy to repair or replace furniture parts when necessary.

Choosing the right fastening methods can increase the lifespan and durability of the furniture. Structural joints are extremely important during furniture design. Structural rigidity and strength is known as a critical part of the design [9]. Wood fasteners are used to join individual pieces in a perfectly and functionally satisfactory piece such as a furniture component, furniture or overall structure [10]. In joint elements, internal forces are mostly distributed between compressive contact and an element due to external stress [9, 11]. The areas where the elements are in contact with each other must be carefully bonded so that internal forces can be transmitted evenly across the surface [12]. Positioning of the joints is often known as a limiting factor in the design process [13-15]. There is a difference between glued (permanent) and non-glued (temporary and dismountable) joints. Connection and mounting means should be selected according to the connection type. Glued joints reduce vibration in the material compared to other joints and positively affect the strength of the structure [16]. Various fasteners and connection techniques are used for joining furniture constructions. The traditional ones are manufactured from wood and the strength of the connection is offered by the conveniently big surface area of the connected elements. Some of the most relevant **traditional furniture joint types** are represented below:

1.1.1. Square-Ended Butt Joint

A square-ended butt joint is a basic woodworking joint where two pieces of wood are joined together by placing their square ends against each other. This joint is simple to create and is often used when the appearance of the joint is not critical, or when additional strength or reinforcement is provided through other means [17].

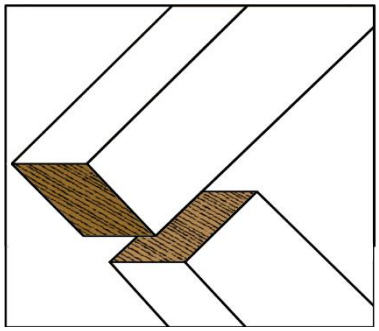

Figure 1.1 Square-Ended Butt Joint (drawing by S.Baş)

It is important to note that while a square-ended butt joint is easy to create, it may not be the strongest joint on its own, especially for heavy loads or structural applications. Consider using additional reinforcement or exploring other types of joints, such as mortise and tenon or dovetail joints, for projects that require greater strength and stability[18].

1.1.2. Mitred Butt Joint

A mitred butt joint is a woodworking joint where two pieces of wood are cut at an angle and joined together to form a 90-degree corner. This type of joint is commonly used in carpentry and woodworking for constructing frames, boxes, and other projects where a clean and seamless corner is desired. The angle at which the two pieces are cut is typically 45 degrees for a standard 90-degree corner [19].

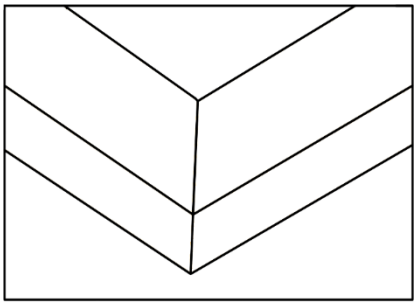

Figure 1.2 Mitred Butt Joint (drawing by S.Baş)

The success of the joint depends on the accuracy of the angle cuts and the quality of the glue bond, so attention to detail is crucial for a strong and aesthetically pleasing mitred butt joint [20].

1.1.3. Dowel Joint

A dowel joint is a type of woodworking joint that involves joining two pieces of wood by inserting dowels (cylindrical rods) into corresponding holes in each piece. The dowels serve as simple, effective, and durable connectors, providing both alignment and strength to the joint. Dowel joints are commonly used in furniture making, cabinet construction, and other woodworking projects[21].

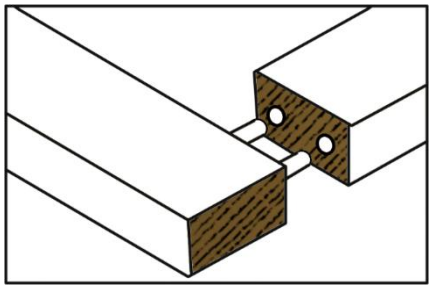

Figure 1.3 Dowel Joint (drawing by S.Baş)

Dowel joints offer several advantages, such as simplicity, strength, and ease of construction. They are particularly useful in applications where a clean appearance is desired, as the dowels are often hidden within the joint. However, dowel joints may not be suitable for extremely heavy loads or high-stress applications, where more complex joinery methods such as mortise and tenon joints or dovetails might be preferred [22].

1.1.4. Lap Joint

A corner halving joint, also known as a lap joint or halving joint, is a woodworking joint where two pieces of wood are notched at their ends and then fit together to form a right angle. The joint involves removing half the thickness of each piece of wood at the point where they intersect. This creates a flush and strong connection between the two pieces.

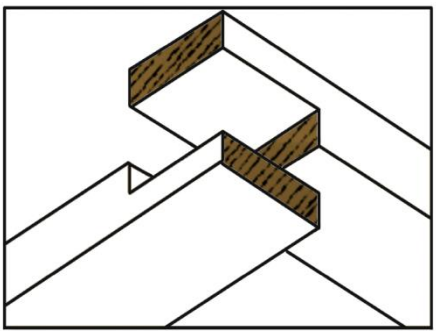

Figure 1.4 Corner Halving Joint
(drawing by S.Baş)

The corner-halving joint is commonly used in woodworking for various projects, such as constructing frames, boxes, or other structures where a strong corner connection is required. It's a relatively simple joint to create and provides good stability when done correctly [23].

1.1.5. Splined Mitre Joint

A splined mitre joint is a woodworking joint that combines the elements of a mitre joint and a spline joint. A mitre joint involves joining two pieces of wood at an angle, typically 45 degrees, to create a corner. While mitre joints can provide a clean look, they may lack strength and stability over time [19].

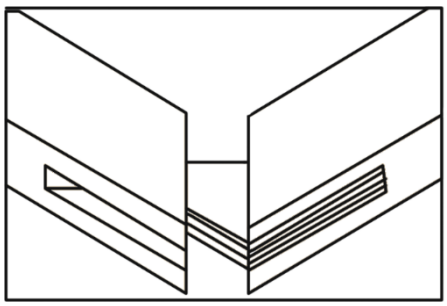

Figure 1.5 Splined Mitre Joint
(drawing by S.Bas)

To enhance the strength of a mitre joint, a spline can be added. A spline is a thin strip of wood or another material that is inserted into matching slots or grooves cut into the mating surfaces of the joined pieces[24]. In the case of a splined mitre joint, a groove or slot is cut into both mitred surfaces, and a spline is inserted to reinforce and stabilize the joint.

The addition of splines reinforces the mitre joint, preventing separation and adding durability. This type of joint is commonly used in projects where both strength and aesthetics are important, such as in picture frames or decorative corners of furniture [25].

1.1.6. Corner Bridle Joint

A corner bridle joint, also known simply as a bridle joint, is a woodworking joint that connects two pieces of wood at a right angle. This joint is commonly used in carpentry and joinery for constructing frames, boxes, and other wooden structures. The joint gets its name from the fact that one piece of wood forms a "bridle" that fits into a notch or recess cut into the other piece.

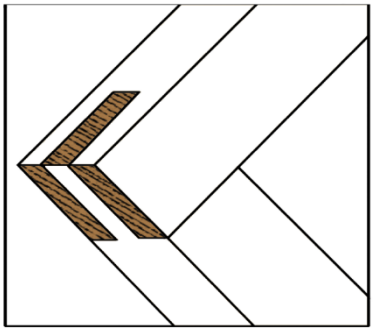

Figure 1.6 Corner Bridle Joint
(drawing by S.Baş)

Corner bridle joints are valued for their strength and simplicity. They provide a good amount of surface area for gluing, making them sturdy. However, it is important to note that the joint is visible, so it might not be suitable for projects where a seamless appearance is desired. Additionally, it requires precise cutting for a proper fit, and careful attention must be paid to the alignment of the joint during assembly [26].

1.1.7. Stopped Mortise&Tennon

A "stopped" mortise and tenon joint refers to a specific type of woodworking joint where either the mortise or the tenon (or both) do not extend all the way through the work piece. Instead, it stops before reaching the edge, creating a joint that is not visible from the outside.

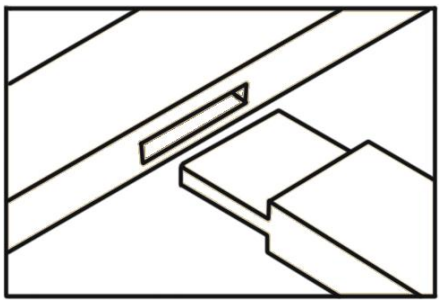

Figure 1.7 Stopped Mortise& Tennon Joint
(drawing by S.Baş)

This technique is often used for aesthetic reasons, providing a cleaner and more refined look to the finished woodworking project. It can be particularly useful in situations where you want to hide the joint for design purposes or where a through-tenon might not be appropriate.

Creating a stopped mortise and tenon joint requires careful planning and precision during the cutting and fitting process. Woodworkers use various tools such as chisels, saws, and other cutting tools to create these joints [27].

1.1.8. Through Mortise&Tennon

The mortise and tenon joint is a traditional woodworking joint that is widely used in carpentry and furniture making. It is known for its strength, durability, and ability to provide a tight connection between two pieces of wood. The joint consists of two parts: the mortise, which is a cavity or hole, and the tenon, which is a projection or tab.

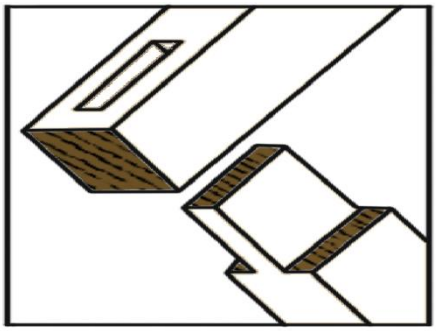

Figure 1.8 Through Mortise& Tennon Joint (drawing by S.Baş)

The mortise and tenon joint comes in different forms, including through mortise and tenon (where the tenon passes completely through the thickness of the mortised piece) and blind mortise and tenon (where the tenon does not extend completely through the mortised piece) [28].

This joint is valued for its simplicity, strength, and resistance to being pulled apart. It is commonly used in woodworking to join structural elements like table and chair legs, frame construction, and other applications where a strong, durable connection is essential [29].

1.1.9. Butt T-Joint

A butt joint is a basic woodworking and metalworking joint where two pieces of material are joined by aligning their ends and securing them together. The joint is formed by placing the squared or cut end of one pieces of material against the side of the other. This type of joint is commonly used in various applications, including woodworking, welding, and metal fabrication [19].

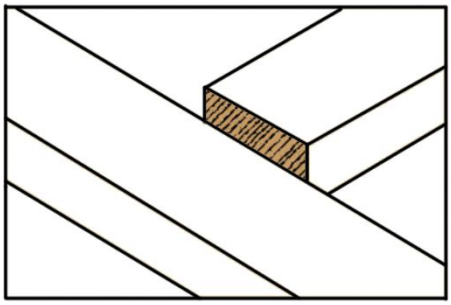

Figure 1.9 Butt Joint (drawing by S.Baş)

In woodworking, butt joints are often reinforced with additional fasteners or adhesives to enhance their strength. Common methods of reinforcing butt joints in woodworking include using screws, nails, dowels, or biscuits. These reinforcements help prevent the joint from separating over time and increase its overall stability [30].

While butt joints are simple to create, they may not be as strong as other types of joints, such as mortise and tenon or dovetail joints in woodworking. The strength of a butt joint depends on the materials used, the quality of the joint preparation, and any additional reinforcement applied [31].

Overall, butt joints are versatile and widely used, but the choice of joint depends on the specific application, the materials involved, and the desired strength and appearance of the final product.

1.1.10. T-Halving Joint

Creating a T-halving joint involves cutting a slot (or groove) into one piece of wood and then fitting another piece into that slot to form a T-shape.

T-halving joint is commonly used in carpentry and woodworking, providing a strong and flush connection between two pieces of wood [32].

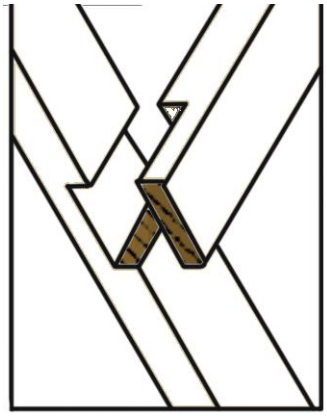

Figure 1.10 T-Halving Joint
(drawing by S.Baş)

1.1.11. Cross Halving Joint

A cross halving joint is a woodworking joint where two pieces of wood intersect each other at right angles, and each piece has a notch or slot cut into it to allow for a snug fit. This joint is often used in carpentry and joinery to create a strong and stable connection between two pieces of wood, particularly when building frames or other structures.

The joint is called "cross halving" because the material is halved in both directions, forming a cross when the two pieces come together. Each piece has a slot or groove cut into it, and when the two pieces are assembled, the slots interlock, creating a sturdy connection [33].

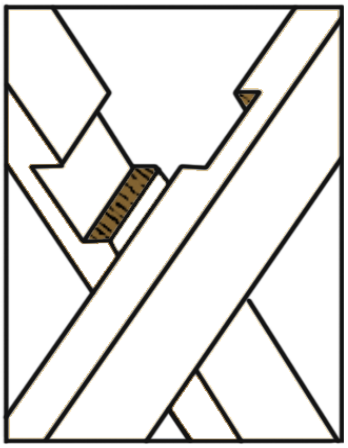

Figure 1.11. Cross Halving Joint
(drawing by S.Baş)

Creating a cross halving joint typically involves careful measuring, marking, and cutting to ensure a precise fit. This joint is commonly used in various woodworking projects, such as constructing frames for doors, windows, or cabinets. It provides good strength and stability when properly executed, making it a reliable choice for certain applications in woodworking [8].

1.1.12. Pinned Mortise&Tennon

A pinned mortise and tenon joint is a traditional woodworking joint that involves connecting two pieces of wood by fitting a projecting tenon on one piece into a corresponding hole or mortise on the other. The joint is secured with a pin or dowel, adding strength and stability to the connection. This type of joint is commonly used in furniture making, carpentry, and timber framing [34].

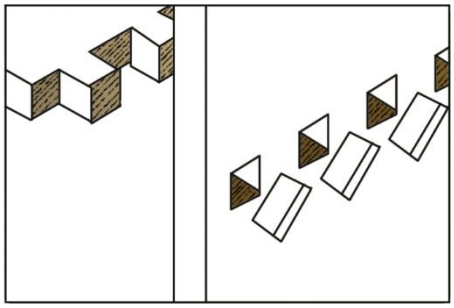

Figure 1.12. Pinned Mortise& Tennon Joint
(drawing by S.Baş)

1.1.13. Groove and Tenon Joints

The groove and tenon joint is a type of woodworking joint where a groove is cut into one piece of wood, and a tenon is formed on the end of another piece. The tenon is then inserted into the groove, creating a strong and secure connection. The joint is often secured with glue or other fasteners, such as dowels or screws, to enhance its strength. Overall, the groove and tenon joint is a versatile and strong method of joining wood, providing both functional and aesthetic benefits in woodworking projects [35].

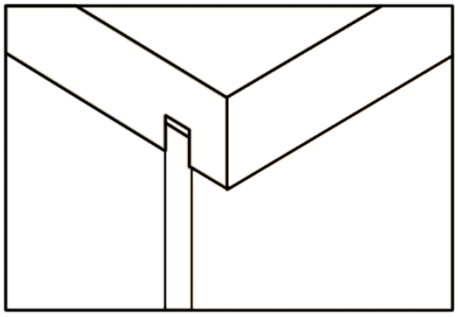

Figure 1.13 Groove and Tenon Joint
(drawing by S.Baş)

1.1.14. Biscuit Joint

A biscuit joint refers to a woodworking technique that involves using wooden biscuits to join two pieces of wood together. The term "biscuit" in this context does not refer to the baked goods but rather to small, flat, oval-shaped pieces of compressed wood, usually made from beech. These biscuits are inserted into corresponding slots or mortises in the pieces of wood being joined [36].

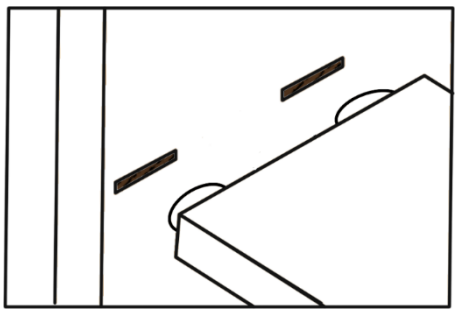

Figure 1.14 Biscuit Joint
(drawing by S.Baş)

Biscuit joints are commonly used in woodworking to join boards edge-to-edge (for panel glue-ups), end-to-end, or at mitred corners. The biscuits provide additional surface area for glue, making the joint stronger. The technique is particularly

useful in cabinetry, furniture making, and other woodworking projects where a strong and inconspicuous joint is desired [37].

1.1.15. Edge-to-Edge Butt Joint

An "edge-to-edge butt joint" is a type of woodworking joint where two pieces of material are joined together by aligning their edges. In this joint, the edges of the two pieces meet squarely without any overlapping or notching. The term "butt" in this context refers to the squared or beveled ends of the materials coming together.

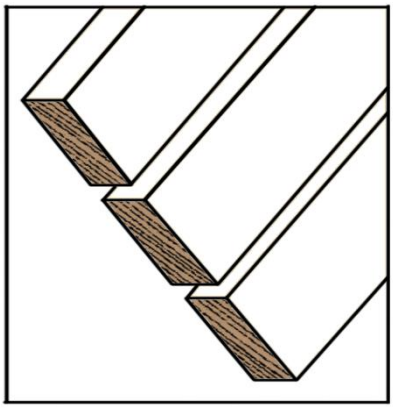

Figure 1.15 Edge-to-Edge Butt Joint
(drawing by S.Baş)

This type of joint is commonly used in various woodworking and metalworking projects, providing a simple and clean appearance when properly executed. However, it's worth noting that an edge-to-edge butt joint may not be as strong as some other types of joints, such as a dovetail joint or a mortise and tenon joint, which provide more mechanical interlocking [38] .

To enhance the strength of an edge-to-edge butt joint, additional methods can be employed, such as using glue, screws, dowels, or other reinforcing elements. Reinforcing the joint helps to create a more stable and durable connection between the two pieces of material [39].

In woodworking, edge-to-edge butt joints are often used in applications where the joint will not be highly stressed, and where a clean, seamless appearance is desired, such as in the construction of tabletops, panels, or other flat surfaces. Proper preparation of the mating edges and the use of appropriate adhesives or fasteners are crucial for achieving a reliable edge-to-edge butt joint [19].

1.1.16. Tongue&Groove Joint

A tongue and groove joint is a type of woodworking joint that is commonly used to join two pieces of wood edge-to-edge. This joint creates a strong and seamless connection between the two pieces. It is often employed in flooring, panelling, and other applications where a tight, flush fit is desired [40].

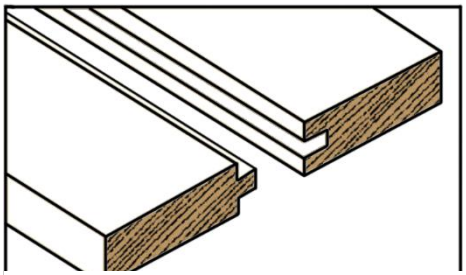

Figure 1.16 Tongue&Groove Joint
(drawing by S.Baş)

Tongue and groove joints are versatile and widely used, providing a reliable method for joining wood pieces seamlessly. The precise fit of the tongue into the groove helps create a visually appealing and durable connection [41].

1.1.17. Splined Edge-to-Edge Joint

A splined edge-to-edge joint in woodworking involves joining two pieces of wood together with a spline—a thin strip of wood that is inserted into matching grooves on the edges of the two boards. This joint is often used to add strength, alignment, and decorative elements to the connection between two boards [19].

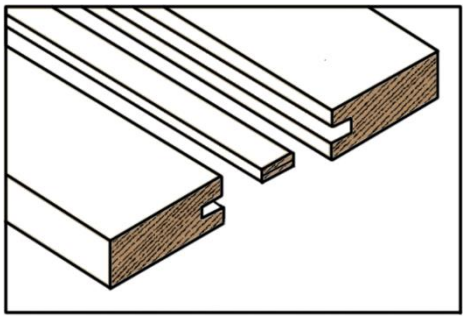

Figure 1.17 Splined Edge-to-Edge Joint (drawing by S.Baş)

This method creates a strong and visually appealing joint. The spline adds strength to the joint, and the contrasting colours of the wood can enhance the overall aesthetic of the project.

The advantages of the above traditional wood joints are that they are manufactured from wood, which is usually available in the woodworking workshop, and can be manufactured independently, even in a small microenterprise. They are manufactured in well-established process relaying on long-time experience. In the same a disadvantage can be, that in most cases their manufacturing needs ~~or~~ detailed preliminary process planning (in case of machine production) or many workhours (in case of hand making).

For example, a mortise and tenon joint is manufactured in the following steps:

1. Marking and Measuring:
    - Determine where the joint will be located on each piece of wood.
    - Mark the location of the mortise and tenon on each piece, ensuring that they align properly when assembled.
2. Creating the Mortise:
    - The mortise is typically cut into the thicker piece of wood. It is a rectangular or square hole.
    - Various tools can be used to cut the mortise, including chisels, drill press, or dedicated mortising machines.
    - The mortise should be accurately sized to match the tenon for a snug fit.
3. Crafting the Tenon:
    - The tenon is created on the end of the thinner piece of wood. A protruding tab fits into the mortise.

- The tenon can be formed using saws, chisels, or specialized tenoning jigs on machines.
- The tenon should be precisely shaped to fit snugly into the mortise.

4. Assembly:
    - Once the mortise and tenon are cut and fitted, the joint is ready for assembly.
    - Apply glue to the surfaces of the mortise and tenon to enhance the bond.
    - Insert the tenon into the mortise, ensuring a tight fit.
    - Clamp the pieces together until the glue dries.
5. Optional Additions:
    - Some variations of the joint include additional features such as wedges or pegs to add extra strength and stability.

However, the biggest disadvantage of the traditional joints is that they are NOT dismountable joints, whilst in many cases this is considered an advantage of the furniture both by the customer (due to a mobile lifestyle of people) and the producer and retail seller (requesting flat mounted furniture during storing). Based on the need of dismountable jointing, mechanical fasteners are also used to provide furniture piece connections. As metal fasteners, trapezoidal fasteners, minifix fasteners, corner fasteners, raffix and pipe fasteners to moon fasteners are the fasteners frequently used in furniture constructions during assembly.

Round dowels are some of the most important fasteners used in furniture assembly. Dowel is known as one of the preferred connecting elements for frames and shelves. However, because round dowels do not allow misalignment, exact positioning is often required on benchtop or semi-stationary machines. Biscuit dowels are usually placed on the writing line using hand-held machines. Since the biscuit dowels are shorter than the guided grooves, a slight protrusion is not a problem since the joint can be moved while the dowel is inserted. However, this requires additional alignment when gluing. The lately developed **Domino joint** system is a mixture of both. It is an important component in wood joining.

1.2. Domino wood dowels

The Domino is a loose mortise and tenon joining tool manufactured by the German company Festool. In 2006, the company Festool introduced a reliable domino joiner system that creates strong hidden joints. This is a special type of joint using a loose tenon, or Domino pin, and mortises into which the Domino pin is inserted and glued [42]. This is a joining element with rounded edges, oval cross sections, and grooved surfaces. It is supplied in 14 different sizes.

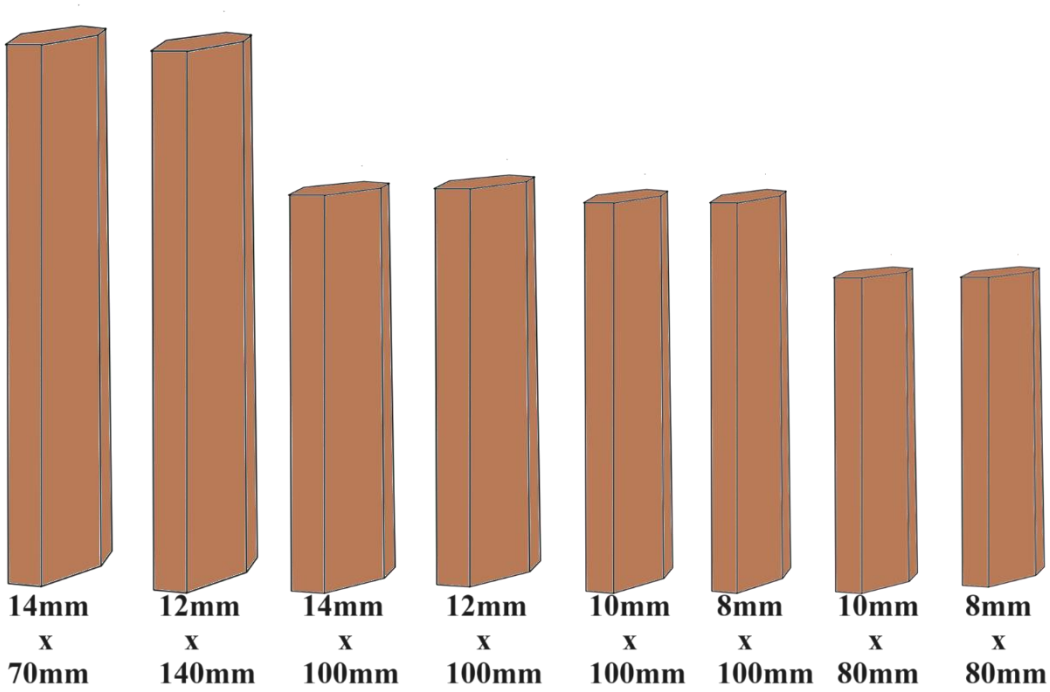

Figure 1.18 Different domino wood dowel sizes (S. Baş)

1.3. Domino metallic connectors

As a detachable interlocutor of the fixed wood Domino tenons, the so-called Domino metallic “connectors” were also developed. The domino wood dowels can be glued to the wood material by means of adhesives [42]. The metallic fasteners make flat or corner joints in wood components, providing simple, quick, and dismountable joints. The same tool is used to form the mortises in both mating work pieces, then depending on the joint type, a custom drilling template fits into the mortise to drill a hole that accepts the mating component of the connector. The metallic Domino connector joints are suitable to connect frames, panels, tops, sides, and other large joints, assure a robust connection strength and provide a rapid building, moving and reassembling of furniture components. The simple placement of the Domino tenons and connectors allow for the economical production of individual parts and small batches, for chairs, tables, beds, cabinets, and shelves[43].

Figure 1.19 Different domino metallic connectors (S. Baş)

Table 1.1 Different sizes of wood dowels and metallic connectors

Joint Sizes	Joint Type	
	Domino wood dowel	Domino metallic connector
4x20mm	+	+
5x30mm	+	+
6x40mm	+	+
8x36mm	+	+
8x40mm	+	+
8x50mm	+	+
8x80mm	+	+
8x100mm	+	+
8x750mm	+	+
10x50mm	+	+
10x80mm	+	+
10x100mm	+	+
10x750mm	+	+
12x100mm	+	+
12x140mm	+	+
12x750mm	+	+
14x70mm	+	+
14x100mm	+	+
14x140mm	+	+
14x750mm	+	+

In this study, **Domino wood dowel and metallic Domino connectors** were evaluated. It was aimed to prove that the Domino wood dowel and metallic Domino connector are suitable to make them the most widely used joining methods in the manufacture of upholstered furniture. Figure A is an example showing that the rail of a seat frame is connected with a Domino wood

dowel and a metallic Domino connector applied at a 90-degree angle to the seat post; it is known that this joint is subject to lateral loads during sitting.

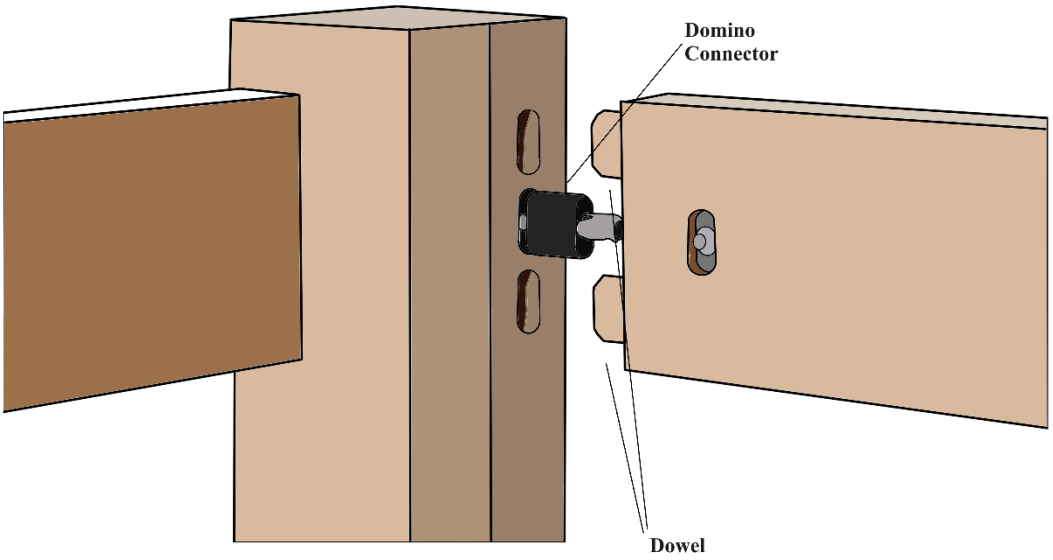

Figure 1.20 Domino system

After the adhesive is applied, the Domino wood dowel adheres to the sides of the hole more tightly because of the swelling properties of wood, which makes the glued joint even stronger. The grooves on the Domino pin facilitate even glue distribution [14, 44].

Another method of joining is using metallic Domino connectors. The reason for using a connector is to get a more robust joint. Thus, it can be assumed that the joints are more powerful. The Domino joints are suitable for both panel joints and frame and rack joints. The simple placement of the Domino wood dowel allows for the economical production of individual parts and small batches, for chairs, tables, and shelving.

It is an advantage of the Domino system, that the Domino wood dowel can be used in combination with the metallic Domino connector (Fig. 1.21).

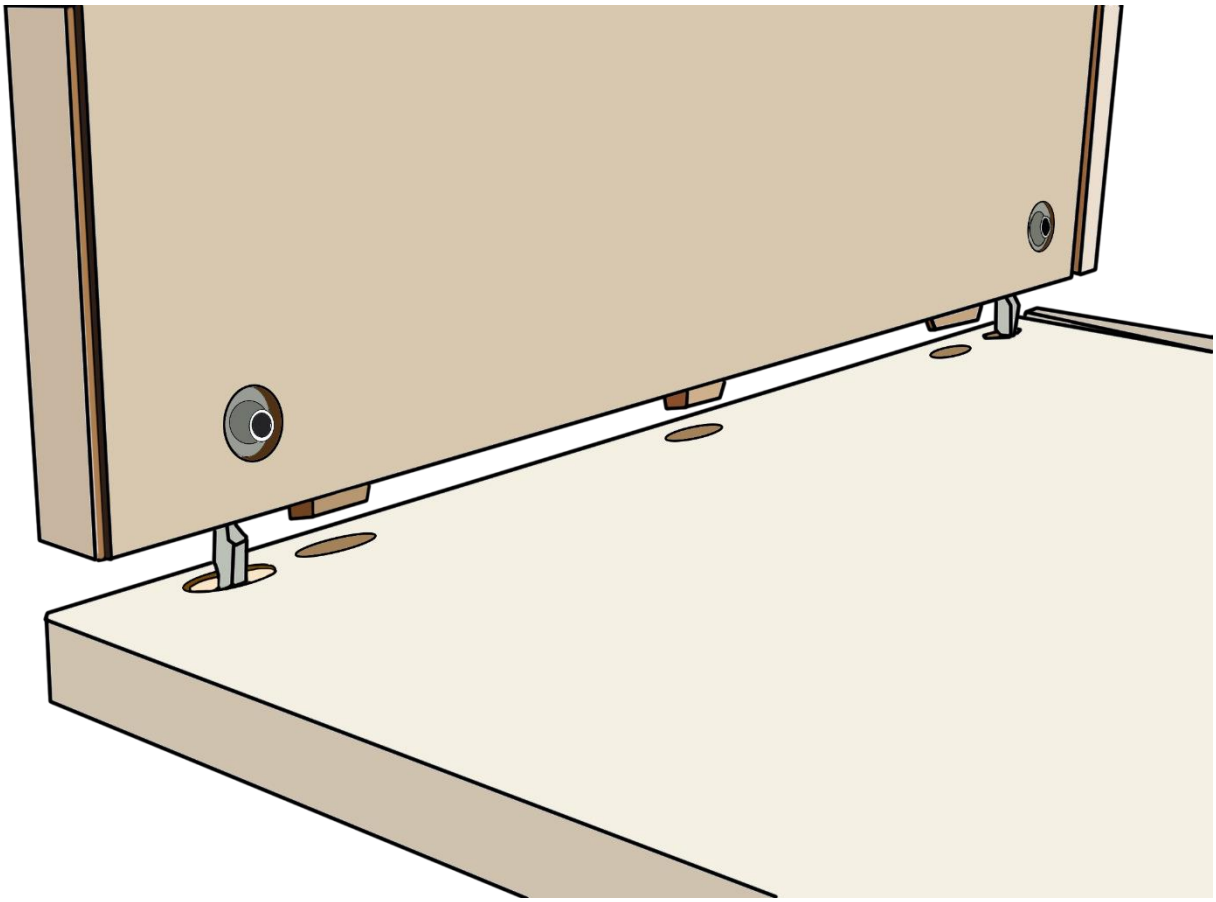

Figure 1.21 The two types of Domino elements in the same joint

1.4. Static and Dynamic Strength of Joints

Although a properly glued joint is stronger than wood fibre itself, bond alone is seldom able to withstand the forces exerted on tables, chairs, cabinets, and doors during normal use.
Most of all joints provide mechanical strength to the jointed elements and contribute to the beauty of the products sometimes [8].
The joint types used in furniture production vary according to the furniture production system. Joints are points of low resistance in furniture, and their strength affects the entire furniture structure. In this context, the joints must be designed to be robust enough to carry the loads that they may be exposed to during use [45].

1.4.1. Static Strength

Static tests are performed to measure the short-term resistance of test pieces made of solid wood or wood-based materials, such as moment resistance, axial strength (in tension and compression), hardness, and in-plane and lateral shear strength. A load is applied to the test sample until destruction occurs in the materials. In static tests, the load is applied to the test

piece gradually, reaches its maximum value; in the course of loading the test piece undergo deformation[45].

Elasticity means that the deformations produced by the low stress can be fully recovered after the loads are removed. Plastic deformation or failure occurs when the joint is loaded to higher stress levels and the shape cannot fully recover after the load is eliminated. Elastic constants of wood vary between species, and within a species with moisture content and specific gravity [46]. The direct proportionality between stress and deformation is valid up to a certain point. The point where this stage is reached is called the elasticity limit of the material. If the material continues to be under load after this point, cracks or breaks may occur in the material. At this point, the material becomes unable to maintain its current volume and shape. In other words, elastic deformation turns into plastic deformation [47]. In plastic deformation, permanent shape changes occur in the material. Materials usually undergo elastic deformation and then plastic deformation under loading.

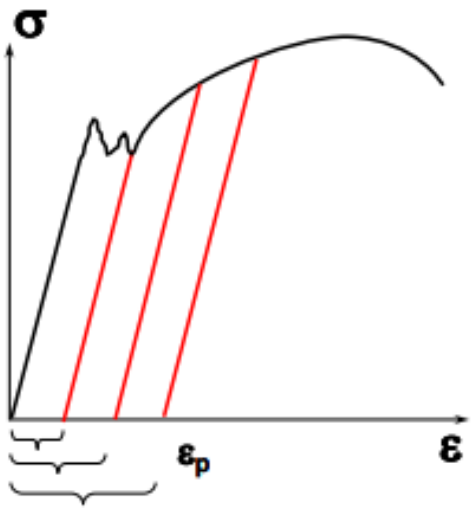

Figure 1.22 Stress-strain curve of an elastic-plastic material (Yiğiter, H., 2006)

If the force is removed in the plastic deformation region, the deformation will be recovered parallel to the elastic line from the point where the force was released, see Figure 1.22. The lines of unloading shown in red mark the amount of plastic deformation ε_p on the horizontal axis. [48].

1.4.2. Dynamic strength

Building materials such as bridges, buildings and houses are exposed to cyclic loads during service. The study of cyclical behaviour is very important for a joint. Wood and wood

composites are major building materials and therefore fatigue and cyclic behaviour are of great importance in the design of safer wooden structures. Cyclic loading, fatigue, environmental and loading conditions in wood and wood composites have been studied in previous years. The effects of loading conditions such as wave loading, and frequency loading have been reported in various studies. Marsoem et al. [49] studied the tensile fatigue of solid wood in triangular and square waveforms and found that the square form was most damaged. A similar result was obtained in compression fatigue of solid wood. Gong and Smith [50] proposed a fatigue life criterion independent of fluctuating loading on fatigue life at tensile strength, based on the strain energy loss behaviour of solid wood material. Frequency of loading also affects the fatigue life of wood and wood composites (EN 12512:2006).

In recent years, there has been some success with traditional timber frames and mortise and tenon connections [14]. Related test results showed significant nonlinearity and inelasticity in load-displacement curves and moment-rotation relationships under both static and cyclic lateral load [10, 15, 44]. Many studies have been done on the stiffness properties of furniture joints [46]. For example, Pan et al.[47] and Xie et al. [51] discussed the ~~mechanical~~ mechanism of straight tenon connections and dovetail joints, respectively. The gap in ~~the tenon~~ mortice and tenon joints caused by wood shrinkage or loading history has been investigated by Chang et al. [52-54] and Ogawa et al.[55] to explore the effect of such insufficient contact on the mechanical performance of joints.

Cyclic tests are very important in terms of predicting the lifetime of furniture. According to EN 12512:2001, a cyclic test consists of four phases [56]. These are 1^{st} cycle, 2^{nd} cycle, 3^{rd}-4^{th}-5^{th} cycles (set of three cycles) and 6^{th}-7^{th}-8^{th} cycles (set of three cycles).

First cycle:

1. Apply the load in compression, until a slip of 25% of the estimated yield slip $V_{y,est}$ is reached. Yield slip is the joint slip (elongation or angle change) corresponding to the yield load, which is the load at the entry into the plastic range. The value of $V_{y,est}$ may be evaluated by calculation, by experience or by previous monotonic tests according to EN 26891;
2. Unload the specimen and reload it in tension to zero-slip;
3. Continue to load in tension up to a slip of 25% of $V_{y,est}$ on the tension side;
4. Unload the specimen and reload it in compression to zero-slip.

Second cycle:

1. Continue to load in compression, up to a slip of 50% of $V_{y,est}$;
2. Unload the specimen and reload in tension to zero-slip;

3. Continue to load in tension, up to a slip of 50% of $V_{y,est}$;
4. Unload the specimen and reload it in compression to zero-slip.

3^{rd}-4^{th}-5^{th} cycles (set of three cycles):

Repeat 2nd cycle three times but up to a slip corresponding to 75% of $V_{y,est}$.

6^{th}-7^{th}-8^{th} cycles (set of three cycles):

Repeat 2nd cycle three times but up to a slip of $V_{y,est}$

1.5. Creep Behaviour of Furniture Joints

Wood material can be considered as a product today; it is used to achieve many purposes at functional, environmental and aesthetic levels. Most wood-based products are exposed to long lasting loads. This situation causes a continued mechanical deformation in the wood called '**creep**' [51-54]. The main factors affecting the creep behaviour of wood material~~;~~ **:** material itself (species of wood, growing characteristics etc.), time, temperature, load level and humidity [57, 58]. Wood is classified as a viscoelastic material that will exhibit creep under prolonged loading [59].

Creep deformation plays a significant role in the design of many products. Even when the Modulus of Elasticity (MOE) is within an acceptable range, customers tend to find creep deformation more concerning. Hence, addressing creep deformation is a matter that requires attention [60].

The power law characterises creep behaviour, where the moisture content (MC) is generally assumed constant. However, the MC of wood structures is constantly changing in service conditions; it follows the relative humidity of the air in the environment due to the hygroscopic nature of wood [57]. Creep of wood under humidity conditions varying between dry and wet is much greater than at constant MC. In other words, creep of wood can be accelerated by MC changes, defined as the mechano-absorbent effect (MSE) resulting from interactions between stress and MC changes [61]. As Armstrong first described the phenomenon of mechano-absorbent (MS) creep, the initial deformation nearly doubled at a rapid rate during the first adsorption phase, while the loaded wooden beam showed partial recovery and then increased deflection occurred during the next adsorption phase. This unique property of wood has attracted a lot of attention to give physical interpretations. Some interpretations, such as the breaking and recombination of hydrogen bonds [62, 63] and deformation kinetics, were based on the molecular level.

In creep tests, the test specimen is subjected to a constant load at a point - the midpoint generally - and the deflection of that point is registered over a certain period. The typical deformation graph for wood and wood-based materials under creep load is shown in Figure 1.23 [64].

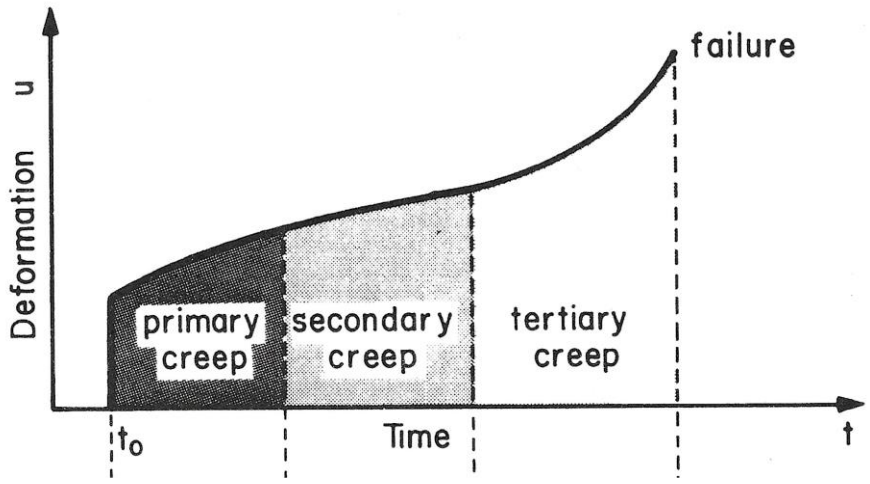

Figure 1.23 Deformation graph resulting from the creep test [65].

Literature studies have determined a three-stage deformation for wood materials subjected to creep load; each stage is characterised by the rate of deformation. In the initial stage, a continuing increase of deformation was observed with decreasing deformation rate. In the second stage, a nearly constant deformation rate was observed lasting for a period of time depending on the applied load level. In the third and final stage, a creep flow with increasing rate was detected, finally-resulting in rupture.

$$H = \frac{d_t - d_0}{d_0} \quad (1)$$

Here, H = Relative creep, d_t = deflection at time *t* (mm), d_0 = instantaneous (elastic) deflection (mm)

A material having both viscous and elastic properties is termed viscoelastic. Wood material can therefore be defined as a viscoelastic material [66]. When wood material undergoes a creep deformation and afterwards the load is removed, the instantaneous (elastic) part of the deformation vanishes; the rest of deformation (viscous part) ceases only after some time.

Humidity increases the creep deformation in wood up to the fibre saturation point (FSP). The strength (MOR) of a material is a very important factor especially in developing the product and enhancing its durability. In the design of most products made of the same material, MOR is not of great concern, but creep deformation is. Even if the MOR is satisfactory, customers perceive creep deformation as a disturbing effect. Customer satisfaction is considered as a very

important element in the design of furniture products [67]. Therefore, creep deformation is an issue to be considered.

Thanks to the modern wood-processing industry, various wood-based materials are available to manufacture furniture frames or panel assemblies using various joint types [36]. It can be a problem to predict the creep behaviour of such constructions. Creep deformation is influenced both by the dimension of the joined materials and by the dimensions of the joint. Time-dependent motion of wood material is being widely observed and investigated in experimental studies including time-dependent creep variation under constant load, relaxation, stress loss at constant deformation; change in hardness during dynamic analysis [68] and the effect of loading rate [69]. These main research techniques can be generalized to restore the material to its original state when the load is removed [70].

The mentioned tests can mostly be associated with the change of the load, which appears in the load-displacement graph of the material, within linear limits. When measuring the behaviour of materials under load for extended periods of time, transitive tests (static tests) are normally preferred to establish a reasonable load ratio. For relatively hard materials, the creep test is normally the preferred test for measuring the post-relaxation of the material. The creep test also has the character to better analyse a structure exposed to dead and live loads [69].

Wood is a material that interacts with its environment and is affected by these changes with its structure. Creep properties of wood are more sensitive to temperature, humidity and physical aging then its elastic properties are.[52].

The performance of a wooden structure is closely related to the behaviour of the joints between its individual members. Analytical models predicting the behaviour of joints are very complex due to the large number of influencing variables such as fastener properties, joint geometry, and material variation. Also, due to the large number of special fasteners on the market, no unified design method has been developed for the joints, even for short-term loading. Consequently, due to the complexity of the situation, several models have been developed to predict the long-term performance of wood joints. Most creep models associated with joints are based on studies of lateral shear stiffness. For example, the reduction of lateral shear stiffness of dowel-nail and nut-screw joints over time has been investigated and models have been developed [71-77].

In the most comprehensive study to date, Whale [78] developed six models based on heritable integrals to predict lateral displacements at dowel joints subjected to varying load histories. Whale [36] noted that the creep in the metal connector is almost negligible at operating load levels and most of the joint creep is due to bearing slip of the wood in the

immediate vicinity of the joint. This suggests that models based on polymer theories have the potential to predict creep at junctions. However, due to the complex mechanisms of charge transfer, such models can be difficult to develop.

Various studies have been carried out on the creep properties of wood as a material. However, practical applications and necessary rules have not yet been developed to examine the effects on the service life of wood material. While there are many creep studies on wooden structures and wood materials used for construction purposes [52], creep studies on the joints that make up furniture constructions such as armchairs in the furniture industry are very scares. The aim of this study is to examine the creep and fatigue strength of beech and oak wood samples furniture joints made with Domino fasteners. In this sense, it is aimed to add a new one to the limited number of studies in the literature and to expand the research range on this subject.

1.6 Various types of creep

"Creep" can refer to various concepts in different contexts. A few different types of "creep" with their respective meanings are listed as follows:

-Nabarro–Herring Creep:

is a mode of deformation of fine-grained crystalline materials (and amorphous materials) that occurs at low stresses at elevated temperatures. In Nabarro–Herring creep (NH creep), atoms diffuse through the crystals, and the creep rate varies inversely with the square of the grain size so fine-grained materials creep faster than coarser-grained ones.[79].

-Cople Creep:

is a form of diffusion creep, is a mechanism for deformation of crystalline solids. Coble creep is a deformation mechanism characterized by the diffusion of atoms along the grain boundaries of a material. It is one of several types of "creep," or time-dependent permanent deformation, caused by constantly applied loads at elevated temperatures. Contrasted with other diffusional creep mechanisms, Coble creep is similar to Nabarro–Herring creep in that it is dominant at lower stress levels and higher temperatures than creep mechanisms utilizing dislocation glide [80].

-Solute drag creep

Solute drag creep is one of the mechanisms for power-law creep (PLC), involving both dislocation and diffusional flow. Solute drag creep is observed in certain metallic alloys [81].

The above-mntioned types of creeps are material specific. In case of wood joints, the most relevant one is the dislocation creep.

Dislocation creep

In crystalline materials at high stresses (relative to the shear modulus), creep is controlled by the movement of dislocations. Dislocation creep has a strong dependence on the applied stress and the intrinsic activation energy (Q) and a weaker dependence on grain size. As grain size gets smaller, grain boundary area gets larger, so dislocation motion is impeded [82] . The degree of stress-dependence is described by the stress-exponent □ of the power law equation. Diffusional creep exhibits an □ of 1 to 2, climb-controlled creep an □ of 3 to 5, and glide-controlled dislocation creep an □ of 5 to 7.

Some alloys exhibit a very large stress exponent (m>10), and this has typically been explained by introducing a "threshold stress," σ_{th}, below which creep cannot be measured. The modified power law equation describing creep rate then becomes:

$$\frac{d\varepsilon}{dt} = A(\sigma - \sigma\text{th})^m e\frac{-Q}{RT} \quad (2)$$

where R is the ideal gas constant, T is the temperature and A is a constant depending on the creep mechanism. The creep increases with increasing applied stress, since the applied stress tends to drive the dislocation past the barrier, and make the dislocation get into a lower energy state after bypassing the obstacle, which means that the dislocation is inclined to pass the obstacle. In other words, part of the work required to overcome the energy barrier of passing an obstacle is provided by the applied stress and the remainder by thermal energy [83].

A **constant load creep** test is performed by applying a fixed load to a specimen and measuring the change in length or strain over time. The load is usually applied by a lever arm or a dead weight, and an extensometer or a dial gauge records the strain. The advantage of this method is that it is simple and easy to set up and operate. The disadvantage is that the stress on the specimen varies with the change in cross-sectional area of some materials (mostly metals) due to creep deformation [84]. This means that the test results may not reflect the true creep behaviour of the material under constant stress conditions in case of all materilas.

A **constant stress creep** test is performed by applying a fixed stress to a specimen and measuring the change in length or strain over time. The stress is usually applied by a hydraulic or pneumatic system that adjusts the load to maintain a constant force per unit area on the specimen. An extensometer or a dial gauge records the strain. The advantage of this method is that it mimics the actual service conditions of the material under constant stress. The

disadvantage is that it requires a more complex and sophisticated equipment and control system, and it may be affected by factors such as temperature fluctuations, friction, and leakage [85]. According to Yuxiang Huang [78], load and MC changes are essential conditions for studying mechano-absorbent (MS) creep of wood. To understand mechano-absorbent creep from our point of view, an experiment was conducted on poplar. Three sets of well-matched samples were loaded in third point bending process under different humidity cycles, to restore the authenticity of the MS creep behaviour especially in the initial dampening stage. The applied load for each set varied between 15% and 35% of the short-term breaking load. It was found that the wood samples showed partial recovery during the entire adsorption phase and increased deflection during the entire desorption phase when low load level was applied. This phenomenon was very different from a notable creep event at the initial adsorption observed by large bodies.

Researchers distinguish false creep attributable to the difference in wood's normal longitudinal swelling and shrinkage. The results also showed that there was an enhanced load effect in the creep under cyclical moisture changes, which usually resulted in the shroud pseudo-recovery with rapidly increasing viscoelastic creep in the initial dampening step.

Costa and Barros [86] presented a study to experimentally characterize the tensile creep behaviour of an epoxy-based adhesive used with polymer-reinforced carbon fibre (CFRP) systems currently used in the reinforcement of concrete structures. During the study, creep tests were carried out in a climatic chamber programmed to maintain a constant temperature of 20°C and 60% relative humidity. During the creep test, 3 different load levels, 20%, 40% and 60% were determined and applied. The modified Burger model for the observation of the stress creep behaviour was fitted to the experimental creep curves and the results revealed that the used model could predict with very good accuracy the tensile strength and long-term behaviour up to a sustained stress level of 60%. The strain-time graph obtained by Costa and Barros in their creep study conducted on epoxy adhesive protective materials is shown in Figure 1.24.

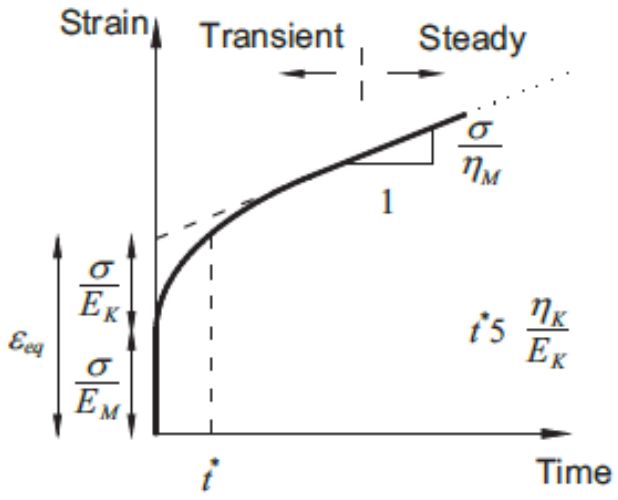

Figure 1.24 Strain-time graph (Costa and Barros, 2015).

Jerzy Smardzewski, Robert Klos and Beata Fabisiak [87] present research results on the effect of creep on changes in stiffness of selected joints used in upholstered furniture making, expressed as the modulus of substitution of elasticity Ez. In the study, ~~it~~ this modulus was calculated analytically using the Maxwell-Mohr constitutive equation for this purpose, and a theoretical model that gave the best results was selected for the results. At the same time, a detailed statistical analysis was carried out. As a result of the study, it was determined that the creep behaviour caused a significant effect on the mechanical quality of the investigated joints by reducing the modulus of elasticity by 11-16%. It has been estimated that this module can be used in numerical calculations using the finite element method.

Wei Xu et al.[88], investigated the effects of the pressure load size of the seat cushions commonly used in upholstered furniture and the force-deformation-time behaviour of the material used in the cushion covers. The results showed that the Burger and Kelvin models can be used to describe the creep and rebound behaviour of furniture seat cushions composed of foam, spring and cover materials. Statistical analyses of the experimental data in this study showed that the magnitude of the loads in examining the creep behaviour had significant effects on the viscoelastic constants in the mathematical expressions derived from the Burger Model to describe the force-deformation-time behaviour of the evaluated mattresses. It has been observed that foam mattresses with spiral springs have greater viscoelastic constants than they do. Changing the cushion cover material from leather to fabric did not have a significant effect on the elastic constant of the cushion materials tested but increased the viscous constant and delayed elastic deformation.

In their study, Johansson and Nilsson [66] aimed to observe the creep behaviour of a wood-based lightweight sandwich panel and to see if this type of panel has a creep characteristic similar to that of solid wood. Beech veneer was used for the surface part of the panels, and layers of pine wood battens glued crosswise to each other formed the core. Twenty-seven samples were used, with solid beech panel as reference material. The study consisted of two stages, the bending test and the creep test. The bending test was performed to determine the maximum load to failure for the panel; 30% of the crushing load was used for the creep test. The best panel was the one with the lowest density, the highest value for bending load, and the smallest creep deformation. The results from the bending tests ranked in terms of load capacity with respect to density ranged from 9.0 to 18.0 m4/s2 for the light panels, compared to the reference panel's value of 27.3 m4/s2. This ratio measured how effective the panel was in withstanding bending tests, depending on its density. When creep deformation was related to density, the light panel results rangeđ from 10.4 to 33.7 kg/m compared to the reference panel's value of 45.5 kg/m. As in the bending test, these values show how effective the panel is in resisting creep deformation depending on the density. The results of the tests show that it is possible for this type of panel to influence physical properties such E-modulus, bending strength and resistance to creep deformation through varying density.

Takahisa Nakai et al. [89], investigated the temporal changes in creep and stress-relaxation behaviour in both microscopic crystalline cellulose and macroscopic stretching of wood samples using Japanese cypress to understand the viscoelastic properties of wood cell walls. In this study, 600-micron thick samples were observed by X-ray diffraction and subjected to tensile load. The crystal cross-stress and the macroscopic stretch of the sample were continuously controlled during the creep and stress-relaxation tests, and differences between the macroscopic and microscopic levels were observed. The microfibril angle (MFA) of the wood cell wall involved in the study influences mechanical behaviour at the microscopic level; the crystal cross stresses are less than those ođ occurring with increasing MFA in both creep and stress-relaxation processes. At the macroscopic level, creep decreased, and the stress relaxation modulus increased with increasing MFA. Results on viscoelastic behaviour at the microscopic level demonstrated its dependence on MFA.

Güntekin, E.[90], investigated the factors affecting the creep behaviour of wood and wood-based composites. He mentioned that creep is an important property in constructions in general; materials such as metals and ceramics exhibit creep when exposed to high temperatures, but temperature is not a necessary factor in polymer materials such as wood and wood-based composites, thus creep can be experienced under normal conditions under long-

term loading. As a result of the study, it was determined that ~~the~~ creep will cause image distortion or breakage in wood and wood-based composites. As a solution, it was stated that care should be taken to prioritize the creep values of wood and its composites, especially during the design phase.

P. Navi, V. Pittet, CJG Plummer [91] in their study "Transient moisture effects on wood creep", used creep/recovery and relaxation/drying tests in a controlled humidity environment to gain insight into the physical nature of the link between mechanical stress and moisture changes. The behaviour of thin wood strips was investigated using a specially developed apparatus. The loading time and viscoelastic creep rate were found to have little effect on mechano-absorbent creep. In addition, the creep trajectory curves for samples with continuous and discontinuous moisture cycles showed deviation from simple creep limit behavior. The effect of transient moisture was also numerically modelled at the molecular level using an idealized cellulose-based composite. Preliminary results show: (i) during free contraction, cellulose chains in elementary fibrils can bend perpendicular to the planes of hydrogen bonded layers forming a crystal lattice; (ii) temporary hydrogen bonding due to the addition or removal of water between the crystalline cellulose and the amorphous polymer can accelerate the shear shift between the two phases in the presence of an external charge.

Fahimeh Hoseinzadeh, Seyed Majid Zabihzadeh, Foroogh Dastoorian [92] evaluated the creep behaviour of wood heat treated at 160, 175 and 190°C and that of modified wood at various moisture contents. Fourier transform infrared spectroscopy (FTIR) was conducted to find a relationship between creep behaviour and structural changes, aiming to improve its applications for construction purposes. The FTIR results showed major structural changes: removal of extractants, hemicelluloses and amorphous portions of cellulose, and partial degradation of lignin. Creep results showed that, in contrast to the elastic short-term modulus, the creep modulus decreases at operating temperatures above 160°C. Samples treated at 160°C were observed to have improved creep behaviour in humid conditions, which can be attributed to lower degradation of cell wall components and lower hygroscopicity.

Panayiotis Georgiopoulos, Evagelia Kontou, Aggelos Christopoulos [93]~~,~~ extensively studied the short-term creep behaviour in tension and single cantilever deformation mode for a range of biodegradable composites. The composites contained a biodegradable polymer matrix formed as a mixture of poly butylene adipate-terephthalate (PBAT) copolyester and Polylactic acid (PLA) produced by non-renewable resources. The matrix was reinforced with three different wood fibre types at 20% and 30% proportion by weight. Experimental data were analysed in terms of Findley's and Burger's viscoelastic models. The effects of stress,

temperature, and wood fibre type on the material's creep response were analysed analytically, while Burger's model parameters were related to the composite morphology. In all cases, wood fibres were observed to improve the creep resistance of the composites.

1.7 Research aims

This study aimed to enhance the understanding of the behaviour of wood joints under static load, dynamic load and long-term load using different size Domino wood dowels and metallic Domino connectors. Special focus is on creep deformation. One of the main points in ~~a~~ design process for furniture production is to reduce the weight while keeping the strength of the wood parts at a sufficient level. Using different wood materials in furniture production can have technical, aesthetic, and economic advantages.

The main purpose of this study was to investigate the load bearing capacity of the corner and T-joints made of beech species and assembled using with Domino wood dowels and metallic Domino connectors. The research focused specifically on the following aspects:

- Determining the static, in-plane bending load bearing capacity of the Domino wood dowel and metallic Domino connector fastened corner and T-joints, by applying both compression and tension loading in the case of corner joints.
- Determining the dynamic, in-plane load bearing capacity of the Domino wood dowel and metallic Domino connector fastened corner and T-joints, by applying both compression and tension loading.
- Testing the pulling (withdrawal) resistance of T- joints connectors and the bending moment capacity of corner joints in the case of tension and pressure made with glued Domino dowels and removable Domino connecting elements.
- Studying and comparing the creep behavior of the Domino wood dowel and metallic Domino connector fastened corner and T-joints under sustained static load.

2. MATERIALS AND METHOD

2.1. Material

For the test samples preparation European beech wood (*Fagus sylvatica L.*) was used with a mean density of 705 kg/m^3 and 43 kg/m^3 standard deviation. Beech wood species was selected due to its wide range of application in the European furniture industry. A part of the wood material contained red heartwood. From the conditioned boards slats and bars were prepared with uniform width and thickness and in various lengths. From the slats and bars, corner joints (L-joints) for bending tests and T-joints for bending and withdrawal tests were prepared with the geometry shown in Figures 2.1 to 2.6.

Joints of two different configurations were prepared. In the case of big-size specimens the 41.5 mm by 65 mm members were joined with their wider face perpendicular to the plane of frame, while the small-size were prepared of 22 mm by 40 mm members with their wider face in the plane of the frame. The orientation of the member cross-section defined the orientation of the connecting elements (Domino wood dowel and Domino metallic connector) as well with respect to the plane of the frame.

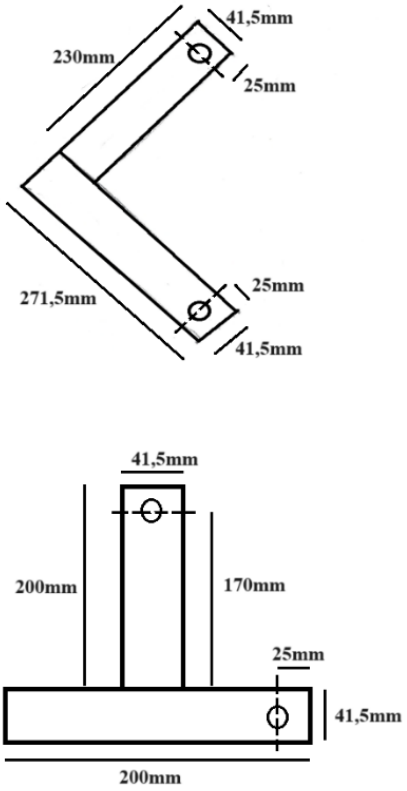

Figure 2.1 Corner joint and T-joint specimens - Type 1 (big size) (drawing: S.Baş)

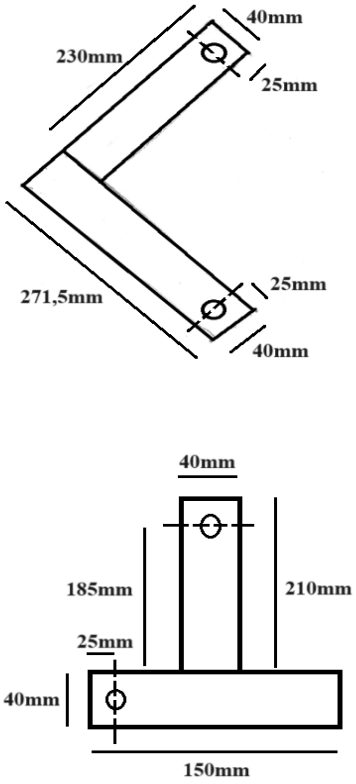

Figure 2.2 Corner joint and T-joint specimens - Type 2 (small size) (drawing: S.Baş)

Eight different types of joints were produced and tested. The codes and names used for the identification of the specimens are summarized in Table 2.1.:

Table 2.1 Specimen codes and names

Code	**Joint type**
LBC	**L** joint, **B**ig size, with **C**onnector
LBWD	**L** joint, **B**ig size, with **W**ood **D**owel
LSC	**L** joint, **S**mall size, with **C**onnector
LSWD	**L** joint, **S**mall size, with **W**ood **D**owel
TBC	**T** joint, **B**ig size, with **C**onnector
TBWD	**T** joint, **B**ig size, with **W**ood **D**owel
TSC	**T** joint, **S**mall size, with **C**onnector
TSWD	**T** joint, **S**mall size, with **W**ood **D**owel

A total of 186 samples were prepared. The average moisture content of the samples was 10.8 %.

For **small size** Domino wood dowels, the sizes of the fasteners were 40mm×22mm×8mm; the metallic Domino connectors were of size 42mm×22mm×8mm.

For **big size** Domino wood dowels, the sizes of the fasteners were 75mm×28mm×14mm; the metallic Domino connectors were of size 82mm×29mm×14mm with an additional 15 mm drill hole placed on the side to house the anchor nut. The fixing of the joint is made possible by a split anchor with threaded sides and a wedge inserted into one of the pieces and an anchor nut secured with a plastic tray in the other piece. The tight connection is achieved by turning the threaded shaft of the bolt, which stretches the anchor with the help of the wedge, and the wedge-grooved shaft of the bolt enables the stretching of the clamping screw. For the joint's preparations, the Festool's Domino Joiner DF 500 Q-Plus machine was used.

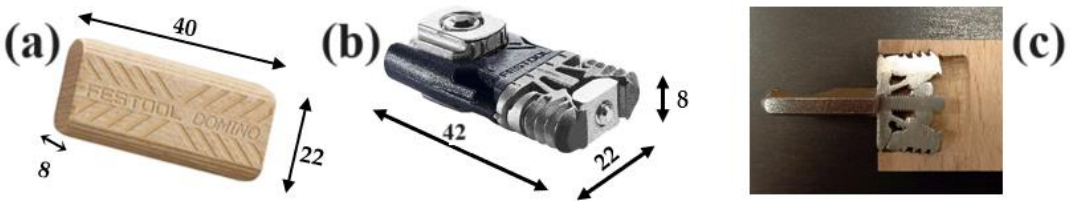

Figure **2.3** Domino wood dowel (a) (source: Festool) metallic Domino connector (b) (source: Festool) and the anchoring effect of the metallic Domino connector (c) (source: beavertools.com) for small-size test-pieces

The joints using Domino wood dowels were glued with a polyvinyl acetate (PVAc) type adhesive, specifically Ponal Super 3 from Henkel Ltd., with a solid content of 50+/-2% and D3 class of water resistance. The main properties of the D3 type adhesive used to glue the wood dowels are shown in Table 2.2. The glue was applied with a small brush on both sides of the drill hole and on the Domino wood dowel at a spread rate of 160-180 g/m^2. To separate the extra bonding strength provided by the glued joint shoulders, a set of joints were prepared without adhesive on shoulders, by using a masking tape to cover the shoulder area. In this way, we could compare more accurately the joint strength of the Domino wood dowel and metallic Domino connector joints. The connectors were installed based on Festool's instructions. Holes the same as for the dowels were prepared. Extra drill holes of 15 mm diameter were prepared on the sides of the shorter pieces. The cross anchors with threaded pin were positioned and fixed with the plastic trays, the split anchors were inserted in the mortises made in the longer pieces, the threaded bolts were tightened to expand the anchor sides laterally, the other side of bolts were fit into the cross anchors and stiffened with the pins.

Table 2.2. Properties of the PVAc adhesive

Water resistance class	D3

Spread rate	120/180 g/m^2
Storage temperature	Over 5°C
Recommended bonding temperature	20°C
Pressure	2-6 kp/cm^2

2.2. Method

Static in-plane bending tests and T-joint withdrawal tests were conducted in order to calibrate the load levels to be applied in the creep tests and cyclic test of the joints. The bending tests were performed by diagonally loading the test pieces with compressive as well as tensile load in the case of L-joints; T-joints were tested for bending with diagonal compressive load only.

2.2.1. Static Tensile (withdrawal) Test

40 test pieces each prepared from beech wood using Domino wood dowel and metallic Domino connectors were subjected to static tensile test in Instron Model 5566 Universal testing machine and static tensile values of the joints were obtained. This test was conducted based on the ASTM D 1761 standard. Founded in 1898, ASTM (American Society for Testing and Materials). Organizations operating in many industries refer to ASTM publications in their production. That is why we use ASTM standards. Figure 2.4 shows the static bending test arrangement for T and L-joints.

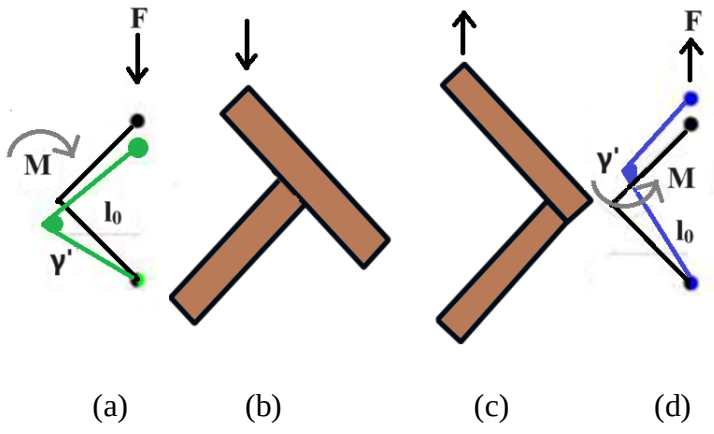

Figure 2.4 Static bending test arrangement for T- and L-joints in compression (a, b) as well as in tension (c, d) (drawing: S.Baş)

Figure 2.9 shows big-size specimens set up for bending in tension and withdrawal test respectively.

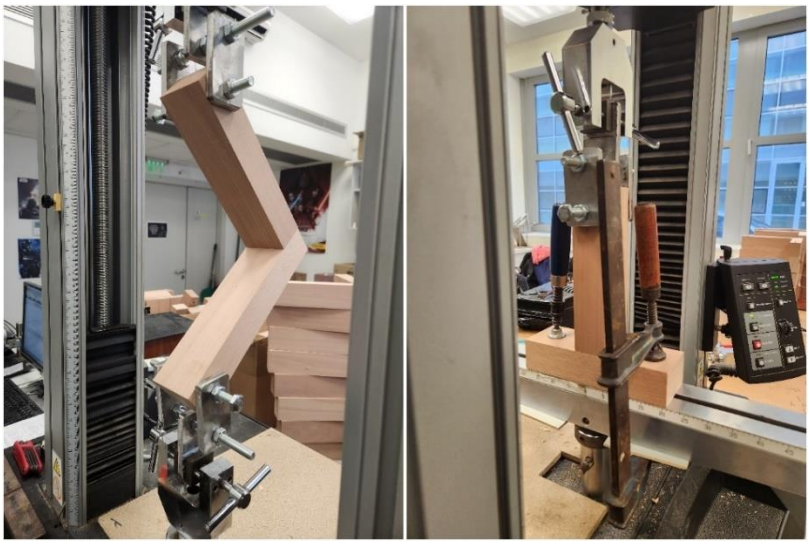

(a) (b)

Figure 2.5 Domino joint elements, static tensile test of big L joint (a), withdrawal test of T joint (b). (Photo: S. Baş)

2.2.2. Static bending tests by diagonal compression and tension

To determine their strength performance 30 L-joints and 16 T-joints of beech wood, each prepared using Domino wood dowels and metallic Domino connectors, were subjected to static diagonal compression test, as well as 40 L-joints for diagonal tension test on Instron Model 5566 Universal testing machine. This test was conducted based on the ASTM D 1761 standard. Figure 2.10 shows the bending by diagonal load test of an L-joint for both tension and compression.

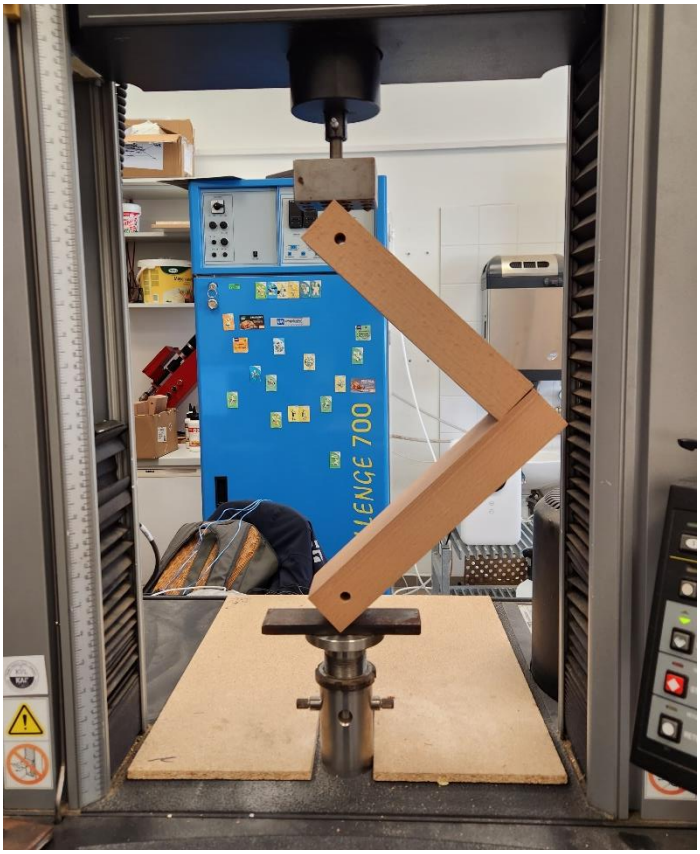

Figure 2.6 Bending test by diagonal loading: compressive load application (Photo: S. Baş)

The load levels measured at compression were good indicators for fatigue testing.

2.2.3. Creep Test

For the creep measurement process, deflection gauges (comparators), some of them with digital display were used. Constant follow-up of the deflection of test specimens was performed during a period of 1 to 7 days, depending on the behaviour of the test sample under load. The specimen's deflection due to creep deformation occurring at the joints was recorded as a function of time. Figure 2.11 shows the digital indicators from which the creep movements were read.

Figure 2.7 Digital gauge (Photo: S. Baş)

In order to determine the load levels suitable for the creep test, first of all, the results of static tensile and compression strengths were analysed. The load rate was checked to not to be too close with the weights used for creep test, to the load of deterioration (braking).

Based on preliminary experimentation, the load level of 50% based on the static test results seemed to be a limit. It would not risk the braking of the joints but may result measurable creep within the planned loading period of one week. Because of these considerations, the use of weights of 25 kg in case of big samples, and 10 kg in case of the small samples was decided, that accounted for the change in moment arm length too. The reason of testing with the same weigth was that this method enables a clear comparability of the results, because basically the general question was the performance of different joint types under the same load.

The **big samples** were tested with the setup as shown in Figure 2.12.

Figure 2.12 shows a representative test setup prepared for the creep test. In our study, we determined a procedure comprising several work steps. Costa and Barros (2015) presents a study aimed at experimentally characterizing the elastic behaviour of an epoxy-based adhesive used with polymer-reinforced carbon fibre (CFRP) systems currently used to strengthen concrete structures. This study was carried out in a climate programmed to ensure a constant temperature of 20°C and 60% relative humidity. Three different load levels were determined and applied, such as 20%, 40% and 60%. The modified Burger's model was used to describe the visco-elastic behavior. The experimentally adjusted elastic curves were used, and the obtained results revealed that the elastic bonding strength between this material and the adhesive can be predicted with a very good accuracy, along with the long-term behavior up to a constant stress level.

Figure 2.8 Creep test setup for the big samples (Photo: S. Baş)

Weights of 25 kg were used for each test sample when performing the creep test. These weights are shown in figure 8.

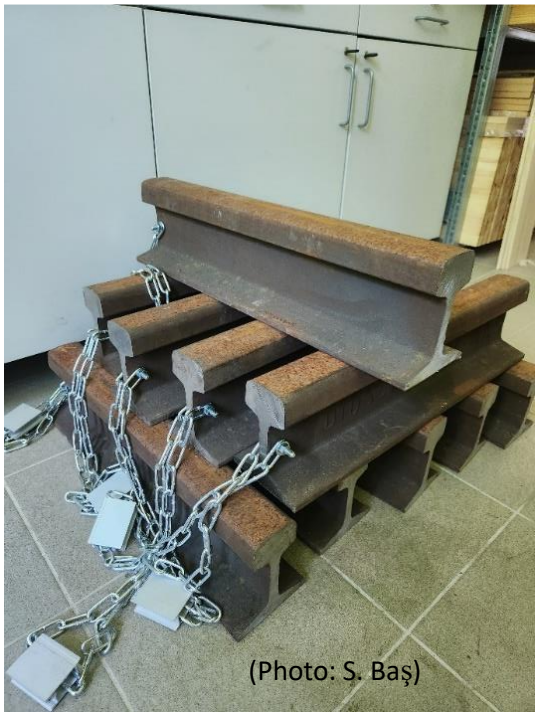

Figure 2.9 Weights used in the creep test fort the big test pieces

Figure 2.10 Creep test setup for the small test pieces (Photo: S. Baş)

The **small samples** were tested with a setup as shown in Figure 2.10.

Figure 2.10 shows a representative test setup prepared for the creep test. Here, a load of 10 kg was suspended over small-sized samples subjected to the creep test.

2.2.4. Cyclic Test

Cyclic loading tests help to determine the fatigue life of a product during use. In this study, the cyclic loading was applied to each specimen setting up a test programme based on EN 12512:2001 in the Instron machine as shown in Figure 2.11.

2.2.5. Statistical analysis

STATISTICA statistical program package was used in the analysis of the data. In order to determine the effects of different parameters, such as specimen size and connector type, on the bending strength and stiffness values of the joints, a test of variance was conducted at the 5% significance level.

Figure 2.11 Cyclic pressure test setup (Photo: S. Baş)

2.2.6. Other calculations

During this study, the static resistance values obtained in N on the Instron universal testing machine were converted to kg-force in N and the following relation was used for this conversion: 9.81 N corresponds to 1 kg. (3)

In addition, the final creep values of the tested joints were expressed as the percentage of the deflection in the static bending test by compression using the equation below:

$$Y = (dt / SM) * 100 \quad (4)$$

Here, Y = percent creep, dt = final creep deflection (mm), SM = deflection due to static bending test by compression (mm)

3. RESULTS AND DISCUSSIONS

Table 3.1 Tests performed and number of samples used

	14 mm thick (Bıg) Samples			
	L-Domino Wood Dowel	L- Metallic Domino Connector	T-Domino Wood Dowel	T-Metallic Domino Connector
Compression test	10	10	3	3
Tension Test	10	10	10	3
Cyclic Test	4	5	4	4
Creep Test	5	6	3	3
	8 mm thick (Small) Samples			
Compression test	5	5	5	5
Tension Test	10	10	10	3
Cyclic Test	5	5	5	5
Creep Test	5	5	5	5

3.1. Static bending tests by diagonal compression and tension and T-joint withdrawal tests

In the next tables we give the ultimate load results and in the case of bending by diagonal compression, the deformation of the joint at ultimate load. Load-displacement curves for the individual test pieces are shown in APPENDIX A. The ultimate load values are converted into bending moment, so they can be used for comparison in the case of different moment arm lengths, such as in creep tests. Part of the displacement values measured is due to the elastic deflection of the joined members which was calculated and subtracted from the measured displacement in order to get displacement values clearly due to the joint's internal deformation (slip) under the applied moment. In the case of T-joints the members' own deflection was shown negligible. We then converted the part of displacement caused by slip into angular value (angle change, or angle of rotation of the member end adjacent to the joint). This is a joint characteristic independent of the moment arm used in loading. As another joint characteristic, the rotation to moment ratio was calculated. From the load-deflection curves, it was clear that this ratio is decreasing with increase of load; the joints behave in a non-linear manner. Therefore, this ratio was calculated from the steepest slope of the load-deflection curves (Z1 (rad/Nm)) as well as from the ultimate load and corresponding deflection as a secant modulus of joint flexibility (Z (rad/Nm)) that may be termed apparent flexibility coefficient. In the tables that follow both values are listed multiplied by a factor of 104 for convenience. The reciprocal value of the Z coefficient is a measure of joint rigidity, hence the larger the Z value the less rigid the joint is.

3.1.1. Compression and tension test results of joints fastened with Domino wood dowel

3.1.1.1. Compression test results of the joints of code LBWD

In the next tables we give the ultimate load results and in the case of bending by diagonal compression, the deformation of the joint at ultimate load. Load-displacement curves for the individual test pieces are shown in APPENDIX A. In the tables, the ultimate load values are converted into bending moment, so they can be used for comparison in the case of different moment arm lengths, such as in creep tests. The elastic deflection of the joined members ~~which~~ was calculated and subtracted from the measured displacement in order to get displacement values clearly due to the joint's internal deformation (slip) under the applied moment. In the case of T-joints the members' own deflection was shown negligible. We converted the part of displacement caused by slip into angular value (angle change, or angle of rotation of the member end adjacent to the joint). This is a joint characteristic independent of the moment arm

used in loading. As another joint characteristic, the rotation to moment ratio was calculated. From the load-deflection curves, it was clear that this ratio is decreasing with increase of load; the joints behave in a non-linear manner. Therefore, this ratio was calculated from the steepest slope of the load-deflection curves (Z1 (rad/Nm)) as well as from the ultimate load and corresponding deflection as a secant modulus of joint flexibility (Z (rad/Nm)) that may be termed apparent flexibility coefficient. In the tables that follow both values are listed multiplied by a factor of $\mathbf{10^4}$ for convenience. The reciprocal value of the Z coefficient is a measure of joint rigidity, hence the larger the Z value the less rigid the joint is.

When calculating the angle change of the joints the assumptions as follow were applied.

The displacement measured is the sum of that due to the deformation of the members and the rotation of the members as rigid bodies around the centre of the deformable joint. The member deformation is the deflection of a cantilever beam fixed rigidly to the joint. The final deformation is independent on the sequence of the two partial deformations, so we consider the rigid body rotation to happen first, through which the points of load application come closer to each other.

When the member deflection is superimposed, the distance of the points of load application further reduces. The lengthwise elongation of the members is negligible according to the beam theory of small deflections. It follows that the length of the line connecting the centre of the joint with the centre of member end does not change in the bent member. The same holds for the line connecting the joint's centre with the point of load application.

The change of the originally right angle between the axes of the two members is the same as the angle change between the lines connecting the point of load application and centre of joint in both members. This is taken use of in the case of compressive load when no point on the member axes will move along the line of displacement measurement. For the calculation of the angle change, we draw a triangle with sides connecting the joint centre and points of load application on both members. The angle between the two sides starting from the joint centre is calculated by trigonometric functions using member dimensions. After loading, the vertical side of the triangle will shorten with the amount of the measured (then corrected) displacement and the angle between the two other sides of unchanged length diminishes, see Figure 3.1 A horizontal line that divides the triangle into two right-angle triangles allows calculating the new angle.

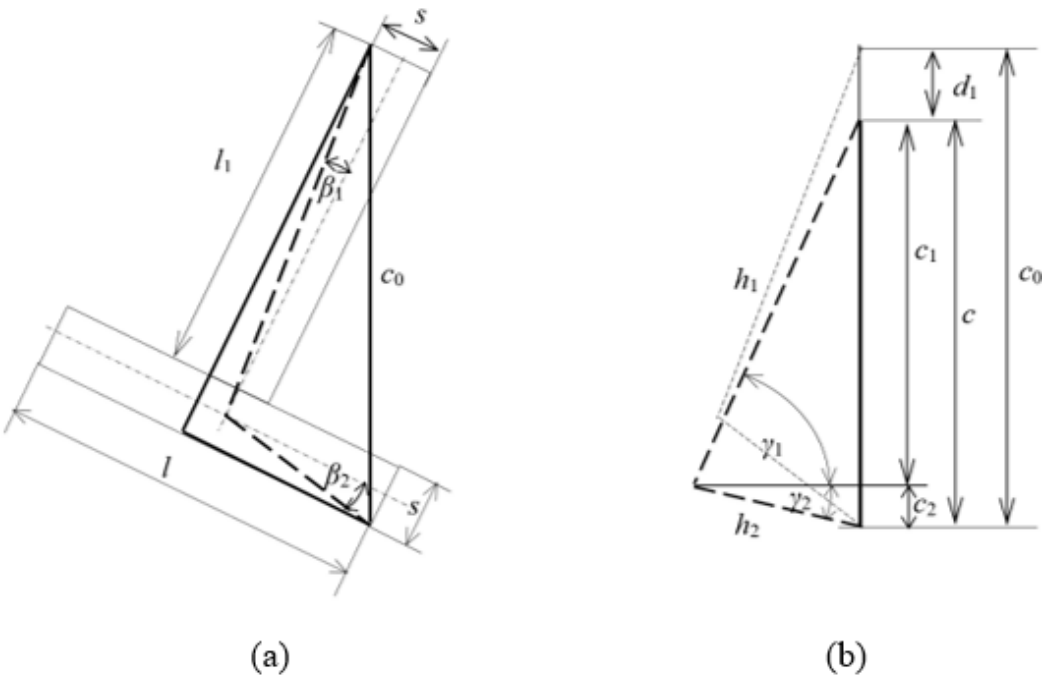

Figure 3.1 Graphical representation of calculating angel change; test piece and lines of reference in unloaded condition (a); lines of reference under load (b).

The calculation of the angle change in the case of a T-joint is as follows. The distance of the points of load application (lower supported corner and upper loaded corner):

$$c_0 = \left((l_1 + s)^2 + \left(\frac{l+s}{2}\right)^2\right)^{\frac{1}{2}}$$

The line connecting the joint's centre with the point of upper load application:

$$h_1 = \left(\left(\frac{s}{2}\right)^2 + \left(l_1 + \frac{s}{2}\right)^2\right)^{\frac{1}{2}}$$

The line connecting the joint's centre with the point of lower load application:

$$h_2 = \left(\left(\frac{s}{2}\right)^2 + \left(\frac{l}{2}\right)^2\right)^{\frac{1}{2}}$$

The angle between the above lines (shown bold dashed lines in the figure) before load application:

$$\alpha_1 = \frac{\pi}{2} + \beta_1 + \beta_2 = \frac{\pi}{2} + arctan\left(\frac{s/2}{l_1 + s/2}\right) + arctan\left(\frac{s/2}{l/2}\right)$$

The angle between the bold dashed lines and the horizontal line:

$$\gamma_1 = arcsin\left(\frac{c_1}{h_1}\right) \qquad \gamma_2 = arcsin\left(\frac{c_2}{h_2}\right)$$

d_1 = measured displacement (crosshead movement) corrected with the members' own deformation (no correction is needed in the case of T-joints).

The angle change is

$$\alpha = \alpha_1 - (\gamma_1 + \gamma_2)$$

In the case of L-joints the calculation simplifies: $c_1 = c_2 = c/2$, furthermore $\beta_1 = \beta_2$ and $\gamma_1 = \gamma_2$.

The members' own deformation:

$$y_1 = \frac{\left(\sin(\frac{\pi}{8})\right)\cdot F\cdot {k_1}^3}{3\cdot E\cdot I} \quad \text{and} \quad y_2 = \frac{\left(\sin(\frac{\pi}{8})\right)\cdot F\cdot {k_2}^3}{3\cdot E\cdot I}$$

where k_1 and $k_2$are the deflected member lengths (for the butt member the whole length, for the other member from the joint centre to the end); F is the ultimate load, E is the Modulus of elasticity of the wood used, I is the moment of inertia of the member's cross section. The corrected displacement is obtained by subtracting the projection of the members' deflection onto the direction of crosshead movement:

$$d_1 = d - \left(\sin\left(\frac{\pi}{8}\right)\right)\cdot(y_1 + y_2)$$

The load-deflection curves of the LBWD-type specimens demonstrate linear or close to linear behaviour up to a first peak followed by an abrupt drop then slow, non-linear increase of load; the ultimate load mostly exceed the first peak. Such nature of the curves clearly indicates high initial rigidity of joints until slipping of the wood dowel comes about. With wood dowel tightened in its new position, the joint is capable of supporting increased load until the final failure, with deteriorated rigidity. Data in Table 3.2 demonstrate this behaviour of the joints.

Table 3.2 Compression test results of the joints of code LBWD

Sample No	First peak displ. (mm)	Final displ. (mm)	d1 I (mm)	d1 II (mm)	Z1 10^{-4} rad/Nm	α degree I
1	1.2	13.45	0.79	12.75	0.593	0.28
2	2.38	4.41	1.66	3.68	0.712	0.58
3	2.24	7.43	1.41	6.59	0.525	0.49
4	1.24	12.52	0.65	11.93	0.348	0.23
5	1.91	5.68	1.16	4.87	0.481	0.41
6	1.69	8.33	1.14	7.66	0.638	0.40

7	1.91	10.9	1.14	10.12	0.458	0.40
8	1.92	10.65	1.09	10.03	0.405	0.38
9	2.43	2.43	1.31	1.31	0.366	0.46
10	1.89	9.73	1.10	9.09	0.430	0.39
Average	1.88	8.55	1.14	7.80	0.50	0.40
Max	2.43	13.45	1.66	12.75	0.71	0.58
Min	1.20	2.43	0.65	1.31	0.35	0.23
SD	0.42	3.58	0.29	3.69	0.12	0.10
COV	0.22	0.42	0.25	0.47	0.24	0.25

Sample No	Z 10^{-4} rad/Nm	α degree II	First peak Load (N)	First peak moment (Nm)	Ultimate Load (N)	Ultimate moment (Nm)
1	5.58	4.39	500.8	81.4	844.7	137.35
2	1.56	1.29	877	142.6	884.3	143.79
3	2.43	2.30	1010.1	164.2	1014.7	164.99
4	6.14	4.12	709.6	115.4	719	116.91
5	1.86	1.70	909.39	147.9	980.8	159.48
6	3.54	2.66	672.1	109.3	808.0	131.38
7	3.98	3.50	937.4	152.4	944.5	153.58
8	4.92	3.47	1010.9	164.4	757.0	123.09
9	0.37	0.46	1353.9	220.1	1353.9	220.14
10	4.38	3.15	961.6	156.4	773.1	125.71
Average	3.48	2.70	894.28	145.41	908.00	147.64
Max	6.14	4.39	1353.90	220.14	1353.90	220.14
Min	0.37	0.46	500.80	81.43	719.00	116.91
SD	1.88	1.27	231.78	37.69	185.03	30.09
COV	0.54	0.47	0.26	0.26	0.20	0.20

3.1.1.2. Compression test results of the joints of code TBWD.

The load-deflection curves of the TBWD-type specimens do not imply any discontinuity in the deterioration of the joints; no mark of sudden slipping of the wood dowel can be detected. However, linearity is maintained over an important part of the curves from the early stage of ramp loading. Data in Table 3.3 demonstrate this behaviour of the joints.

Table 3.3 Compression test results of the joints of code TBWD.

Sample No	Displacement (mm)	slope N/mm	Z1 10^{-4} rad/Nm	Z 10-4 rad/Nm	α degree	Ultimate Load (N)	Ultimate moment (Nm)
1	9.33	831.00	1.71	4.28	6.46	3346.1	263.0

2	8.14	830.40	1.87	4.02	5.65	3119.5	245.19
3	13.69	499.33	3.16	7.93	9.34	2617.7	205.75
Average	10.39	720.24	2.25	5.41	7.15	3027.77	237.98
Max	13.69	831.00	3.16	7.93	9.34	3346.10	263.00
Min	8.14	499.33	1.71	4.02	5.65	2617.70	205.75
SD	2.79	168.85	0.73	1.98	1.86	365.16	28.70
COV	0.27	0.23	0.33	0.37	0.26	0.12	0.12

3.1.1.3. Compression test results of the joints of code LSWD

Just as in the case of LBWD-type specimens, the load-deflection curves of the LSWD-type specimens indicate slipping of the wood dowel after a first peak until which linear behaviour prevails. The non-linear increase of load that follows the intermediate drop leads to an ultimate load mostly exceed the first peak. Such nature of the curves clearly indicate high initial rigidity of joints until slipping of the wood dowel comes about. With wood dowel tightened in its new position, the joint is capable of supporting increased load until the final failure, with deteriorated rigidity. Data in Table 3.4 demonstrate this behaviour of the joints.

Table 3.4 Compression test results of the joints of code LSWD

Sample No	Displacement (mm)	Slope N/mm	d1 (mm)	Z1 10^{-4} rad/Nm	Z 10-4 rad/Nm	α degree	Ultimate Load (N)	Ultimate moment (Nm)
1	8.80	158.60	6.59	2.38	6.59	2.29	648.4	105.4
2	9.59	165.20	6.72	2.28	6.72	2.34	840.4	136.6
3	11.20	173.00	8.74	2.18	8.74	3.03	719.9	117.1
4	8.29	169.20	5.47	2.23	5.47	1.91	824.8	134.1
5	16.87	126.40	14.49	2.99	14.49	4.98	696	113.2
Average	10.95	158.48	8.40	2.41	8.40	2.91	745.90	121.28
Max	16.87	173.00	14.49	2.99	14.49	4.98	840.40	136.65
Min	8.29	126.4	5.47	2.18	5.47	1.91	648.40	105.43
SD	3.49	18.71	3.60	0.33	3.60	1.23	83.41	13.56
COV	0.32	0.12	0.43	0.14	0.43	0.42	0.11	0.11

3.1.1.4. Compression test results of joints of code TSWD

Similarly, to the behaviour of the LSWD-type specimens, the load-deflection curves of the TSWD-type specimens indicate slipping of the wood dowel, roughly at the half of the ultimate load. The second part of the curves follows the slope of the initial part then starts then decreases moderately until the ultimate load. It follows that the secant modulus of joint flexibility is with one exception less than double of the initial one, as witnessed by the data in Table 3.5.

Table 3.5 Compression test results of joints of code TSWD

Sample No	Displacement (mm)	slope N/mm	Z1 10^{-4} rad/Nm	Z 10-4 rad/Nm	α degree	Ultimate Load (N)	Ultimate moment (Nm)
1	5.41	230.7	3.33	5.59	4.80	2478.8	149.9
2	7.74	789.0	3.39	6.59	6.81	2980.4	180.3142
3	6.94	640.7	3.15	7.46	6.12	2368.4	143.2882
4	6.78	689.7	3.74	6.72	5.99	2568.1	155.37005
5	7.29	569.6	4.38	6.38	6.42	2905.2	175.7646
Average	6.83	583.9	3.60	6.55	6.03	2660.2	160.9
Max	7.74	789.0	4.38	7.46	6.81	2980.4	180.3
Min	5.41	230.7	3.15	5.59	4.80	2368.4	143.3
SD	0.88	213.0	0.49	0.67	0.75	268.8	16.3
COV	0.13	0.36	0.14	0.10	0.13	0.10	0.10

3.1.2.5. Tension test results of the joints of code LBWD.

Contrary to what was experienced with the LBWD-type test pieces when bending by compressive force, load-deflection curves of bending by tension have not revealed any abrupt change due to an incidental slipping of the dowel during ramp loading up to ultimate load. The secant coefficient of joint flexibility is roughly the double of the initial one as can be seen in Table 3.6.

Table 3.6 Tension test results of the joints of code LBWD

Sample No.	Displacement (mm)	slope N/mm	Z1 10^{-4} rad/Nm	Z 10^{-4} rad/Nm	α degree	Ultimate Load (N)	Ultimate moment (Nm)
1	2.55	671.4	0.75	1.46	1.01	763.7	121.0
2	3.29	355.0	1.42	2.46	1.27	571.0	90.4
3	4.79	358.8	1.41	2.44	1.81	814.9	129.1
4	7.46	323.5	1.56	4.32	2.74	699.9	110.9

5	5.25	423.1	1.19	2.35	1.97	924.0	146.4
6	4.70	382.8	1.32	1.75	1.77	1114.9	176.6
7	4.50	422.3	1.20	2.43	1.70	772.2	122.3
8	4.71	416.7	1.21	2.92	1.78	671.3	106.3
9	6.38	408.8	1.23	3.05	2.37	854.3	135.3
10	5.37	321.2	1.57	3.30	2.01	671.1	106.3
Average	4.90	408.34	1.29	2.65	1.84	785.7	124.5
Max	7.46	671.36	1.57	4.32	2.74	1114.9	176.6
Min	2.55	321.16	0.75	1.46	1.01	571.0	90.4
SD	1.39	100.23	0.24	0.81	0.49	154.0	24.4
COV	0.28	0.25	0.18	0.31	0.27	0.20	0.20

3.1.1.6. Tension test results of the joints of code TBWD.

The withdrawal test done on T-joints confirm the supposition that joint distortion due to shear and axial force is negligible. While axial and shear elongation of a joint is of the order of tenth of a millimetre per 1 kN of load as witnessed by the data in Table 3.7, angle change of the same type of joints may attain 3.5 to 6.8 degrees at loads of 150 Nm typically acting in service conditions of furniture.

Table 3.7 Tension test results of the joints of code TBWD

Sample No.	Ultimate Load (N)	Max. Slope N/mm
1	5163.5	4758.7
2	8548.1	4756.3
3	5322.4	6053.1
4	4315.6	4677.3
5	4752.1	3382.2
6	5237.6	5036.1
7	5252.6	5767.5
8	5319.6	5381.3
9	4040.7	4928.1
10	4832.9	5135.5
Average	5278.5	4987.6
Max	8548.1	6053.1
Min	4040.7	3382.2
SD	1231.3	723.1
COV	0.23	0.14

3.1.1.7. Tension test results of the joints of code LSWD.

Bending load capacity by using tensile force, shown in Table 3.8 was determined for the joints of type LSWD for comparing the same with the results obtained by compressive force. Comparison comes in Section 3.1.3.

Table 3.8 Tension test results of the joints of code LSWD.

Sample No	Ultimate Load (N)	Ultimate moment (Nm)
1	639.6	100.8
2	502.4	79.2
3	611.4	96.4
4	452.6	71.3
5	600.2	94.6
6	626.2	98.7
7	647.1	102.0
8	664.6	104.7
9	551.4	86.9
10	570.6	89.9
Average	586.61	92.45
Max	664.58	104.74
Min	452.63	71.34
SD	67.86	10.69
COV	0.12	0.12

3.1.1.8. Tension test results of the joints of code TSWD

Withdrawal load capacity of the joints of type TSWD shown in Table 3.9 was determined for comparing the same with the results obtained for the other T-joint types tested. Comparison comes in Section 3.1.3.

Table 3.9 Tension test results of the joints of code TSWD.

Sample No	Ultimate Load (N)
1	3587.5
2	3499.8
3	3597.4
4	2180.5
5	2769.0
6	3327.0
7	3253.5
8	2690.0
9	3622.0

10	3697.8
Average	3222.5
Max	3697.8
Min	2180.5
SD	508.05
COV	0.16

3.1.2 Compression and tension test results of joints fastened with **metallic Domino connector**

3.1.2.1. Compression test results the joints of code LBC

When bending LBC-type specimens by compressive force, load-deflection curves obtained show continuous decrease of their initial slope. The secant coefficient of joint flexibility as related to the initial one therefore grows at a rate varying from test piece to test piece, as shown in Table 3.10.

Table 3.10 Compression test results of the joints of code LBC

Sample No	Displacement (mm)	Slope N/mm	d1 (mm)	Z1 10^{-4} rad/Nm	Z 10^{-4} rad/Nm	α degree	Ultimate Load (N)	Ultimate moment (Nm)
1	6.84	210.9	6.29	1.79	3.54	2.19	664.90	108.11
2	6.36	235.2	5.80	1.60	3.21	2.02	676.10	109.93
3	4.64	279.7	4.17	1.35	2.78	1.46	563.70	91.66
4	3.16	276.3	2.73	1.37	1.98	0.96	518.40	84.29
5	3.99	279.2	3.61	1.35	2.92	1.26	464.60	75.54
6	7.4	306.0	6.82	1.24	3.64	2.37	700.60	113.92
7	5.43	322.7	4.95	1.17	3.22	1.73	576.00	93.66
8	4.75	329.3	4.36	1.15	3.47	1.52	471.50	76.67
9	6.26	356.5	5.68	1.06	3.03	1.98	702.40	114.21
10	7.42	404.4	6.96	0.93	4.61	2.42	563.30	91.59
Average	5.63	300.01	5.14	1.30	3.24	1.79	590.15	95.96
Max	7.42	404.35	6.96	1.79	4.61	2.42	702.40	114.21
Min	3.16	210.90	2.73	0.93	1.98	0.96	464.60	75.54
SD	1.46	56.80	1.41	0.25	0.68	0.49	90.91	14.78
COV	0.26	0.19	0.27	0.19	0.21	0.27	0.15	0.15

3.1.2.2. Compression test results of the joints of code TBC

The general shape of the load-deflection curves obtained for TBC-type specimens is similar to that of LBC-type specimens, leading to identical finding concerning the ratio of secant to initial coefficient of joint flexibility, see the data in Table 3.11.

Table 3.11 Compression test results of the joints of code TBC

Sample No	Displacement (mm)	slope N/mm	Z1 10^{-4} rad/Nm	Z 10^{-4} rad/Nm	α degree	Ultimate Load (N)	Ultimate moment (Nm)
1	10.04	373.1	4.24	8.06	6.93	1910.5	150.1653
2	9	696.6	2.06	5.65	6.23	2449	192.4914
3	7.73	629.7	2.51	4.55	5.38	2623.8	206.23068
Average	8.92	566.47	2.94	6.09	6.18	2327.77	182.96
Max	10.04	696.60	4.24	8.06	6.93	2623.80	206.23
Min	7.73	373.10	2.06	4.55	5.38	1910.50	150.17
SD	1.16	162.78	1.10	1.76	0.78	358.36	28.17
COV	0.13	0.29	0.37	0.29	0.13	0.15	0.15

3.1.2.3. Compression test results of the joints of code LSC

Load-deflection curves obtained for the LSC-type specimens in bending by compression show a continuous decrease of the initial slope; ultimate load is reached with the curves still ascendant. The ratio of secant to initial flexibility coefficients of Table 3.12 varies between 2.0 and 4.0.

Table 3.12 Compression test results of the joints of code LSC

Sample No	Displacement (mm)	slope N/mm	d1 (mm)	Z1 10^{-4} rad/Nm	Z 10^{-4} rad/Nm	α degree
1	18.16	35.84	17.10	10.50	20.19	5.85
2	20.01	48.99	18.87	7.70	20.78	6.44
3	33.9	52.85	32.52	7.14	28.80	10.87
4	25.15	37.58	23.95	10.02	24.77	8.11
5	12.33	47.46	11.41	7.95	15.64	3.94
Average	21.91	44.54	20.77	8.66	22.04	7.04
Max	33.90	52.85	32.52	10.50	28.80	10.87
Min	12.33	35.84	11.41	7.14	15.64	3.94
SD	8.12	7.44	7.95	1.50	4.98	2.61
COV	0.37	0.17	0.38	0.17	0.23	0.37

Sample No	d1	Ultimate Load (N)	Ultimate moment (Nm)
1	17.99	311.00	50.57
2	19.83	332.70	54.10
3	33.68	405.00	65.85
4	24.95	351.40	57.14
5	12.18	270.40	43.97
Average	21.72	334.10	54.32

Max	33.68	405.00	65.85
Min	12.18	270.4	43.97
SD	8.09	49.80	8.10
COV	0.37	0.15	0.15

3.1.2.4. Compression test results of the joints of code TSC

Load-deflection curves obtained for the TSC-type specimens in bending by compression show a continuous, slow decrease of the initially moderate slope; ultimate load is reached with the curves culminating then declining. The ratio of secant to initial flexibility coefficients in Table 3.13 varies between 1.4 and 3.3.

Table 3.13 Compression test results of the joints of code TSC

Sample No	Displacement (mm)	slope N/mm	Z1 10^{-4} rad/Nm	Z 10^{-4} rad/Nm	α degree	Ultimate Load (N)	Ultimate moment (Nm)
1	11.92	268.30	9.73	17.87	10.32	1665.7	100.8
2	14.74	163.67	15.92	22.67	12.63	1608.1	97.3
3	14.42	317.50	8.22	18.05	12.37	1977.6	119.6
4	12.98	524.60	4.99	16.57	11.19	1949	117.9
5	14.08	403.00	6.48	17.38	12.10	2007.8	121.5
Average	13.63	335.41	9.07	18.51	11.72	1841.6	111.4
Max	14.74	524.60	15.92	22.67	12.63	2007.8	121.5
Min	11.92	163.67	4.99	16.57	10.32	1608.1	97.3
SD	1.16	136.64	4.23	2.39	0.95	189.2	11.4
COV	0.09	0.41	0.47	0.13	0.08	0.10	0.10

3.1.2.5. Tension test results of the joints of code LBC

Load-deflection curves of bending by tension of the LBC-type specimens show continuously decreasing initial slope with no or very short linear response at the beginning of ramp loading. The secant coefficient of joint flexibility is around the double of the initial one as show by the data in Table 3.14.

Table 3.14 Tension test results of the joints of code LBC

Sample No	Displacement (mm)	slope N/mm	Z1 10^{-4} rad/Nm	Z 10^{-4} rad/Nm	α degree	Ultimate Load (N)	Ultimate moment (Nm)
1	6.64	279.6	1.80	3.73	2.46	725.6	114.9
2	5.69	236.8	2.13	3.70	2.12	632.6	100.2
3	4.81	186.7	2.70	4.26	1.81	469.1	74.3
4	4.56	252.7	2.00	3.28	1.72	579.5	91.8
5	4.88	292.8	1.72	3.40	1.84	605.3	94.3
6	8.58	223.6	2.26	4.72	3.14	731.9	115.9
7	6.96	248.5	2.03	3.80	2.57	745.1	118.0
8	6.53	160.1	3.15	4.60	2.42	578.9	91.7
9	6.44	277.7	1.82	3.50	2.39	750.5	118.9
10	8.52	234.5	2.15	4.86	3.12	706.1	111.8
Average	6.36	239.3	2.18	3.99	2.36	652.5	103.2
Max	8.58	292.8	3.15	4.86	3.14	750.5	118.9
Min	4.56	160.1	1.72	3.28	1.72	469.1	74.3
SD	1.43	41.5	0.44	0.58	0.50	94.1	15.0
COV	0.22	0.17	0.20	0.15	0.21	0.14	0.15

3.1.2.6. Tension test results for the of the joints of code TBC

The withdrawal test done on T-joints with metallic connector confirm the supposition that joint distortion due to shear and axial force is negligible. While axial and shear elongation of a joint is of the order of tenth of a millimetre per 1 kN of load as can be deduced from the data in Table 3.15, angle change of the same type of joints may attain 3.9 to 6.9 degrees at loads of 150 Nm typically acting in service conditions of furniture.

Table 3.15 Tension test results of the joints of code TBC

Sample No	Ultimate Load (N)	Max. Slope N/mm
1	4875.2	3731.5
2	4659.6	3876.5
3	4345.8	2834.2
4	5164.9	3692.2
5	5455.0	2809.1
6	5058.8	3321.2
7	5303.4	3014.1
8	4979.3	2828.0
9	4971.4	3429.3
10	4818.0	3279.0
Average	4963.14	3281.51
Max	5455.05	3876.47

Min	4345.83	2809.11
SD	317.96	401.24
COV	0.06	0.12

3.1.2.7. Tension test results of the joints of code LSC

Bending load capacity by using tensile force, shown in Table 3.16 was determined for the joints of type LSC for comparing the same with the results obtained by compressive force. Comparison comes in Section 3.1.3.

Table 3.16 Tension test results of the joints of code LSC

Sample No	Ultimate Load (N)	Ultimate moment (Nm)
1	288.8	45.51
2	348.3	54.89
3	340.5	53.66
4	276.3	43.54
5	368.0	58.00
6	326.1	51.39
7	229.6	36.19
8	315.6	49.74
9	343.1	54.07
10	291.0	45.87
Average	312.72	49.29
Max	368.02	58.00
Min	229.61	36.19
SD	41.48	6.54
COV	0.13	0.13

3.1.2.8. Tension test results of the joints of code TSC

Withdrawal load capacity of the joints of type TSC shown in Table 3.17 was determined for comparing the same with the results obtained for the other T-joint types tested. Comparison comes in Section 3.1.3.

Table 3.17 Tension test results of the joints of code TSC

Sample No	Ultimate Load (N)
1	3135.448
2	3380.103
3	2362.086
4	3451.048

5	2671.698
6	3144.505
7	2041.053
8	2820.581
9	3618.77
10	3188.172
Average	2981.35
Max	3618.77
Min	2041.05
SD	502.05
COV	0.17

3.1.3 Observations on the behaviour of test pieces in the course of tests

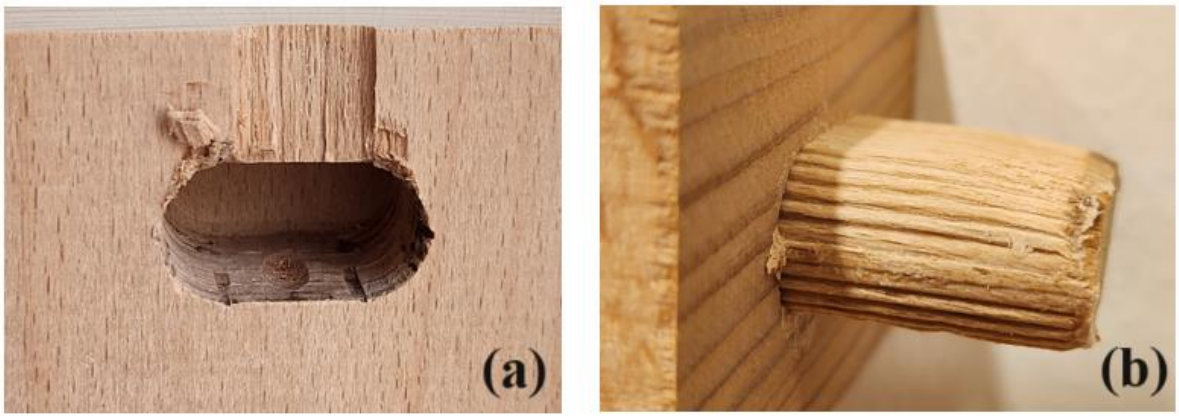

Figure 3.2 Deformation and damage caused by metallic Domino connector (a) and deformation of the wood dowel (b) (Photo: S. Baş)

In the first range of loading, the solid wood resist better to the pressure of the metal under a compressive force of 200 N, and in the second range, above a compressive force of 200 N, the metallic Domino connectors increase the deformation locally in the wood. Considering, that after the tests it was possible to pull out the wood dowel from the mortise, whilst this was not the case with ~~of~~ the metallic Domino connectors, the use of these latter can be considered more reliable as they maintain the integrity of the joint.

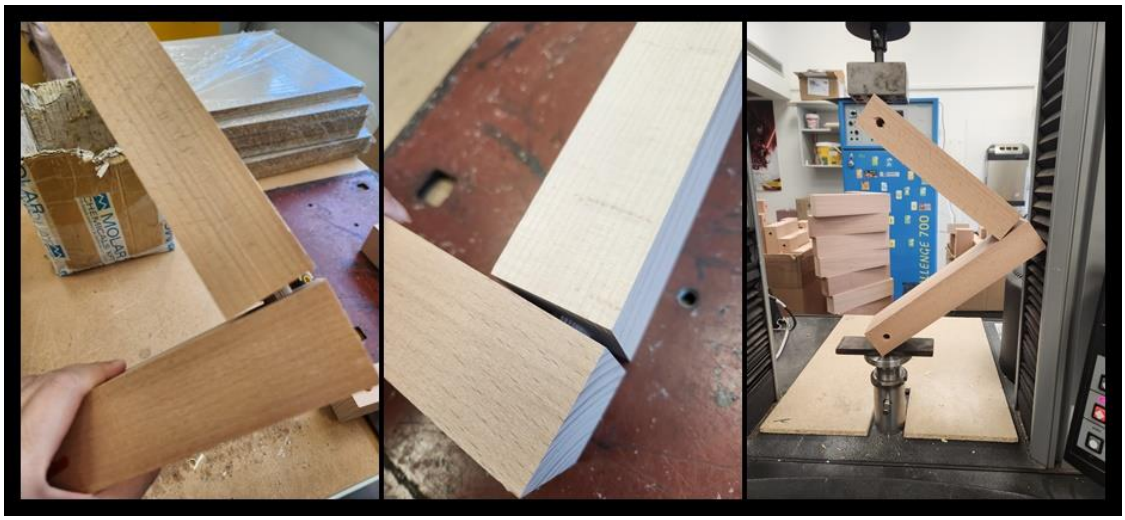

Figure 3.3 Typical deterioration of corner joints under compression: tightness of the fit was lost, the joints loosened. (Photo: S. Baş)

When evaluating the displacement, a characteristic difference between the T joints and L joints can be identified. Whilst T joints fastened with both Domino wood dowel and metallic Domino connector show similar behaviour during pullout, in the case of corner joints there is a difference between the joints fastened with Domino wood dowels and metallic Domino connectors. Metallic Domino connectors of corner joints under tension ~~showed~~ allowed a displacement proportional to the pulling force (with a slope of 45° of the force vs. displacement graph), indicating a continuous deformation. At the same time, the use of wood dowels results in importantly smaller displacement and steeper graphs, indicating a higher resistance to load. The distortion indicated by the graph of metallic Domino connectors is due to the fact, that the hard and strong metallic claws got pulled out by continuously, consistently deforming and scratching the wood (Fig. 3.3). The corner joints show similar trend of distortion for compression as well. However, deformations caused by the metallic parts appear, which do not occur during tension.

Figure 3.4 Typical deterioration of wood dowels during tension tests (Photo: S. Baş)

3.1.4 Comparison and statistical analysis of static tests data obtained for the different joint types

In Figures 3.4 to 3.11, we delineate the test results in the form of box whisker plot. Analysis of Variances, both One-way ANOVA and Factorial Anova were conducted to reveal significance of differences between the results of joint types (LBWD, LSWD, LBC, LSC, TBWD, TSWD, TBC, TSC) as well as joint features such as Big and Small, Wood connector and Metal connector.

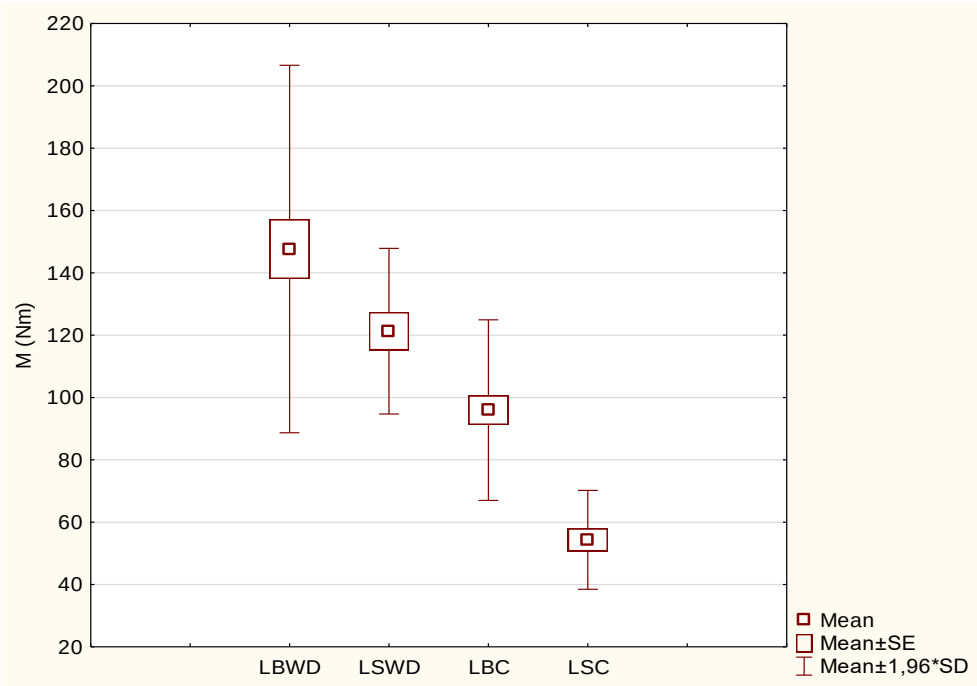

Figure 3.5 Ultimate moment diagram of bending by compressive force of corner joints made with dowels and metal connectors.

The differences between groups' means, small and big test specimens' and Wood and Metal connector results were found significant at the 5% level.

The compression test of the four types of corner joints indicated, that both the big and the small wood dowel fastened joint are stronger than the connector fastened joints.

The connector fastened big corner joints reached 65.0% of the strength of the wood dowel fastened big corner joints. The small metallic connector was far to reach even half of the strength of the small wood dowel fastened corner joints.

At the same time, the big metallic Domino connector fastened joints showed 81.1% of the strength of the small wood dowel fastened joints. Considering the individual samples test results, the strength of the big metallic Domino connector fastened corner joints exceeded in four cases the strength results of the small wood dowel fastened corner joints.

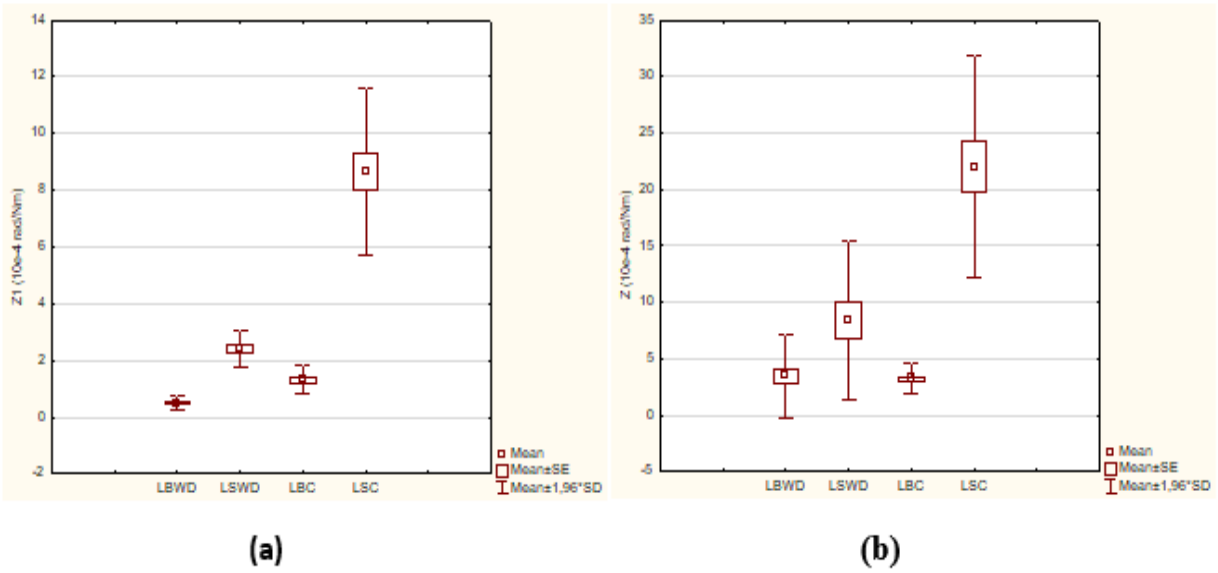

Figure 3.6. Joint flexibility diagrams of bending by compressive force of corner joints made with dowels and metal connectors; smallest flexibility (a), secant flexibility at ultimate load (b)

Factorial ANOVA showed that small and big test specimens' results were found significantly different, similarly Wood and Metal connectors performed at significantly different levels. Especially, the small test specimens with metallic connector proved to be very flexible. However, the test pieces with metallic connector exhibited only 2.5 times increase at ultimate load as opposed to the results of type LBWD (7 times) and LSWD (3.5 times). That is, joints with metallic connector proved to be more stable with respect to

deformation. The LBC-type specimens showed essentially the same level of secant flexibility coefficient than those of type LBWD.

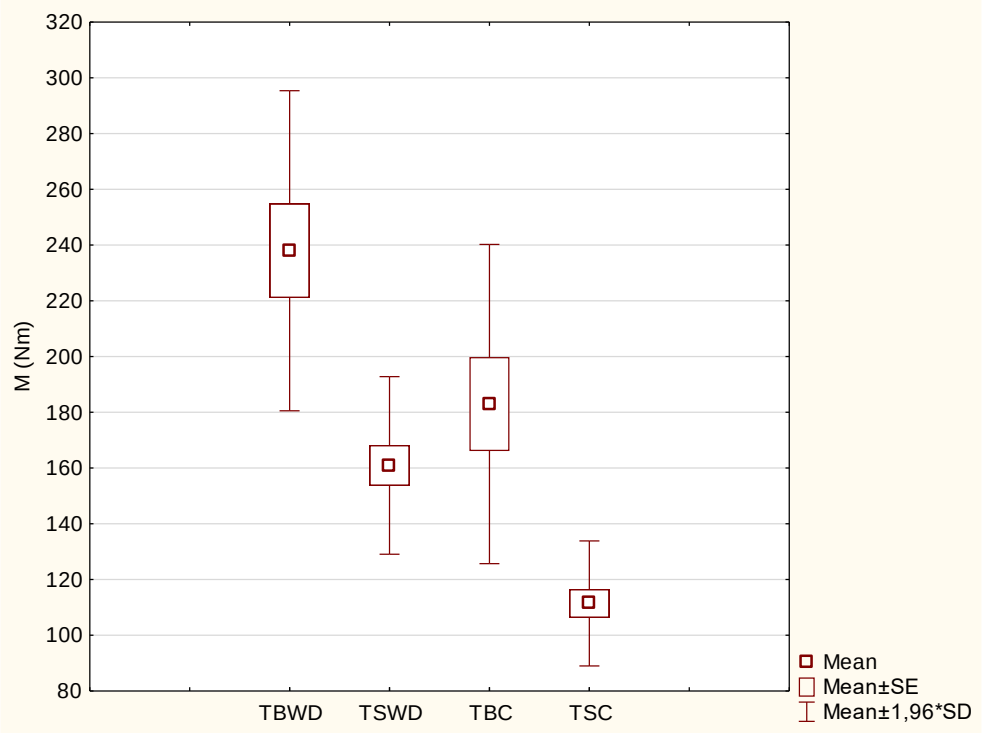

Figure 3.7. Ultimate moment diagram of bending by compressive force of T-joints made with dowels and metal connectors.

According to ANOVA conducted, the results obtained for the TSWD and TBC group were found not significantly different. By factorial ANOVA, significant differences could be detected between the results of Big and Small, as well as between Wood and Metal connector groups.

Both the big and the small wood dowel fastened joint are stronger than their metallic connector fastened pairs. At the same time, the big specimens performed around 1.5 better than the small ones. The strength of the groups TSWD and TBC did not prove significantly different.

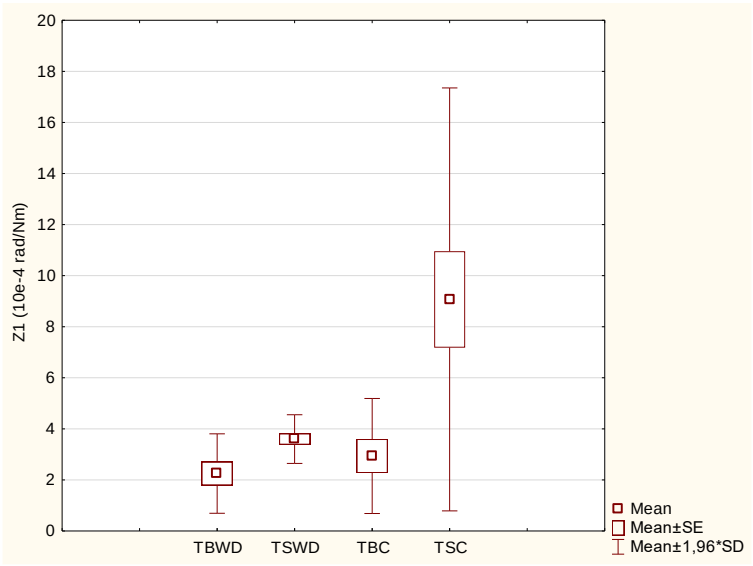

(a)

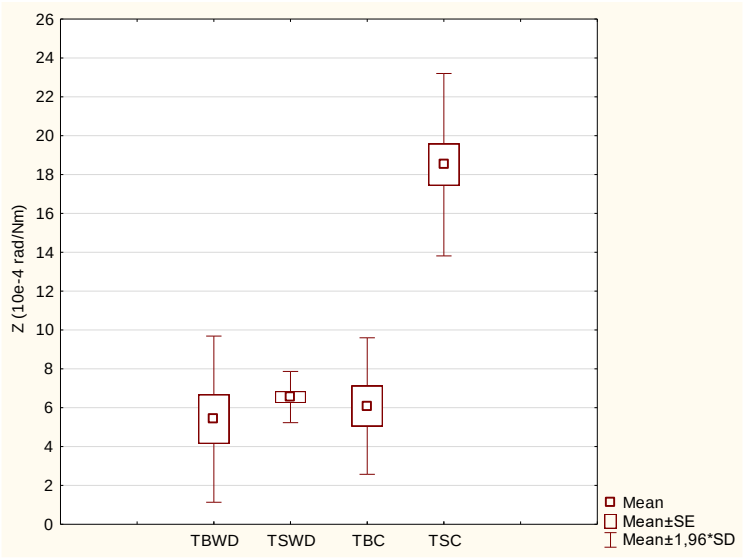

(b)

Figure 3.8 Joint flexibility diagrams of bending by compressive force of corner joints made with dowels and metal connectors; smallest flexibility (a), secant flexibility at ultimate load (b)

Factorial ANOVA showed significant difference between the results of Small and Big test specimens as well as between the results of specimens with Wood and Metal connectors. One-way ANOVA only showed the results of the group TSC to be significantly different from the other groups, both for Z1 and Z. As in the case of corner joints, the small test specimens with metallic connector proved to be outstandingly flexible. The flexibility coefficient increased quite uniformly at ultimate load with a factor of 1.8 to 2.4.

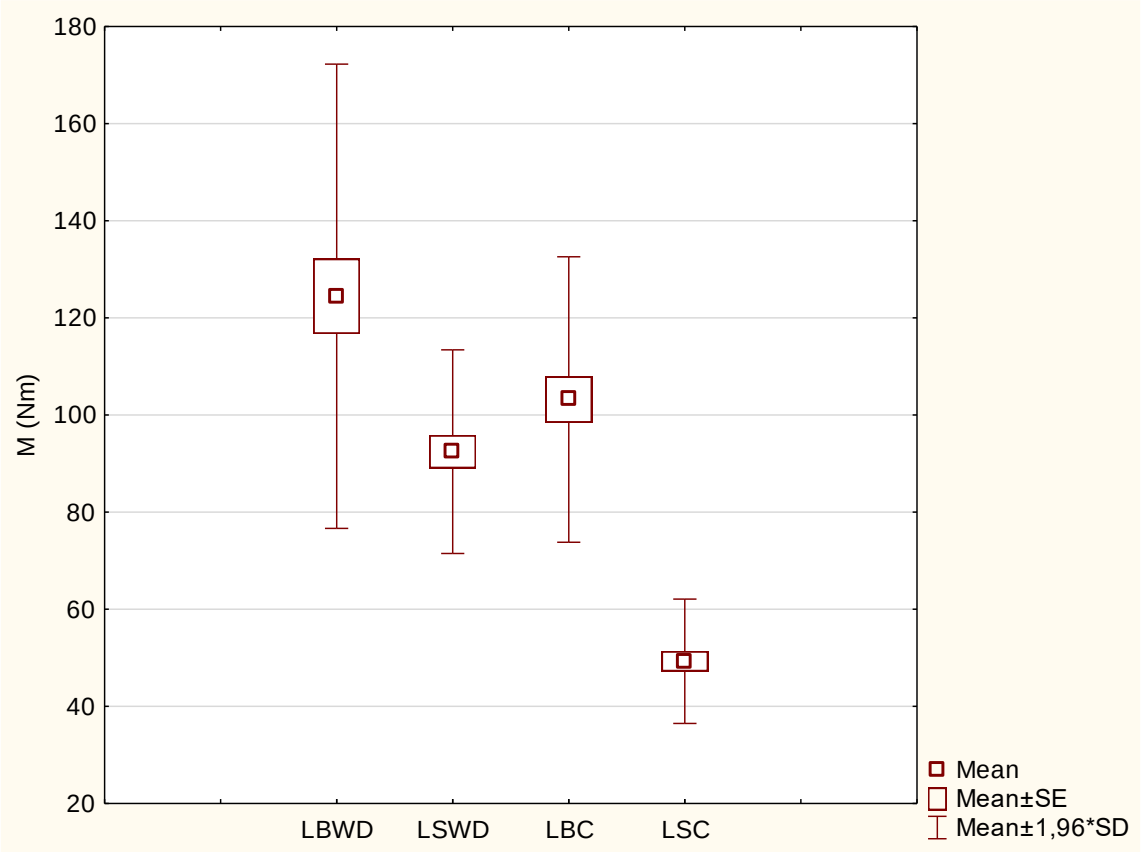

Figure 3.9 Ultimate moment diagram of bending by tensile force of L-joints made with dowels and metal connectors.

Factorial ANOVA showed significant difference between the results of small and big test specimens as well as between the results of specimens with Wood and Metal connectors. The strength of the groups LSWD and LBC did not prove to be significantly different.

In the case of both the metallic Domino connector and the wood dowel, the big size joint is stronger than the small ones. The metallic connector fastened big corner joint reached 83% of the strength of dowel fastened big corner joint. The small metallic Domino connector reached slightly more than half of strength of the small dowel fastened corner joints

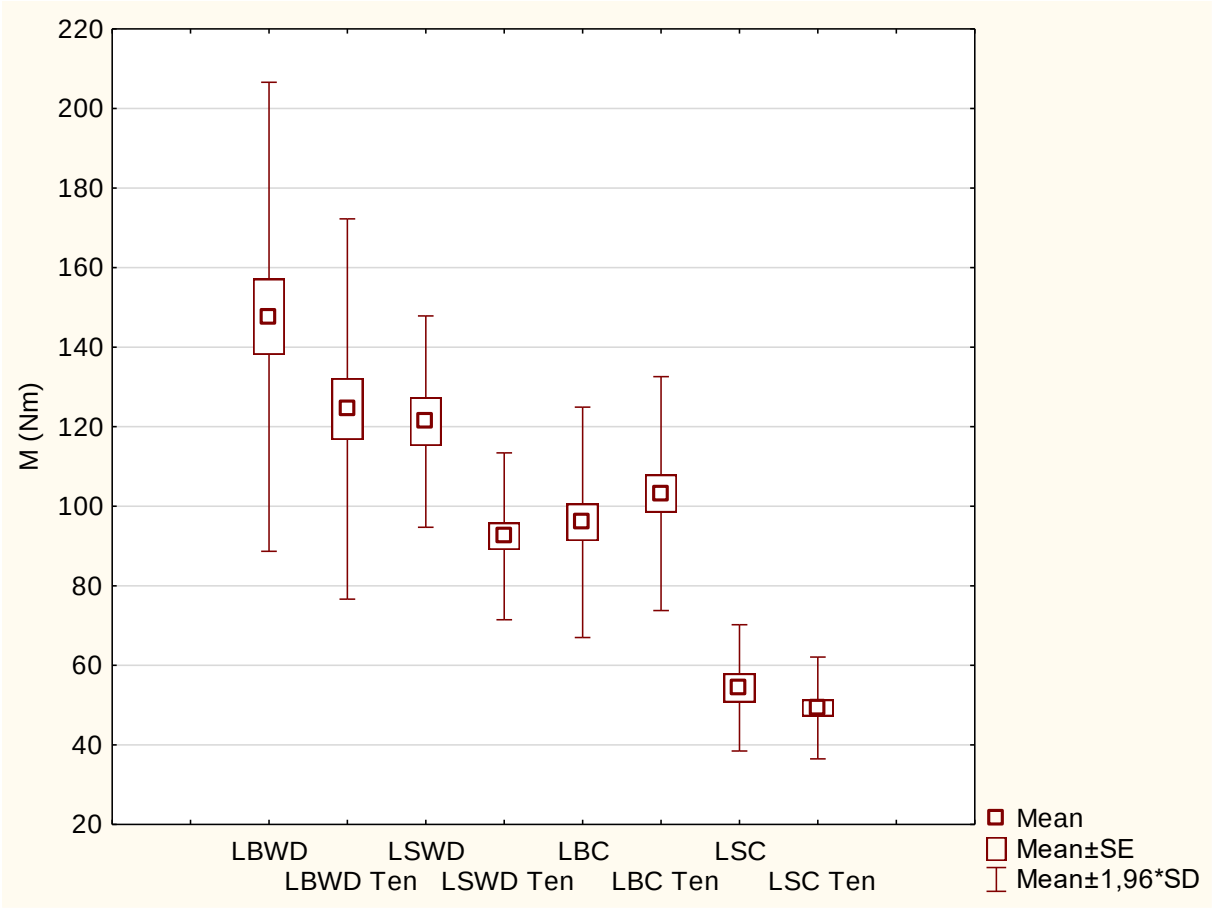

Figure 3.10 Comparison of ultimate bending moment of L-joints obtained by applying compressive and tensile force

The above figure suggests a similar trend in the alteration of bending resistance by joint types in the case of applying compressive and tensile force. Factorial ANOVA did not prove significant differences between the categories of compressive and tensile force.

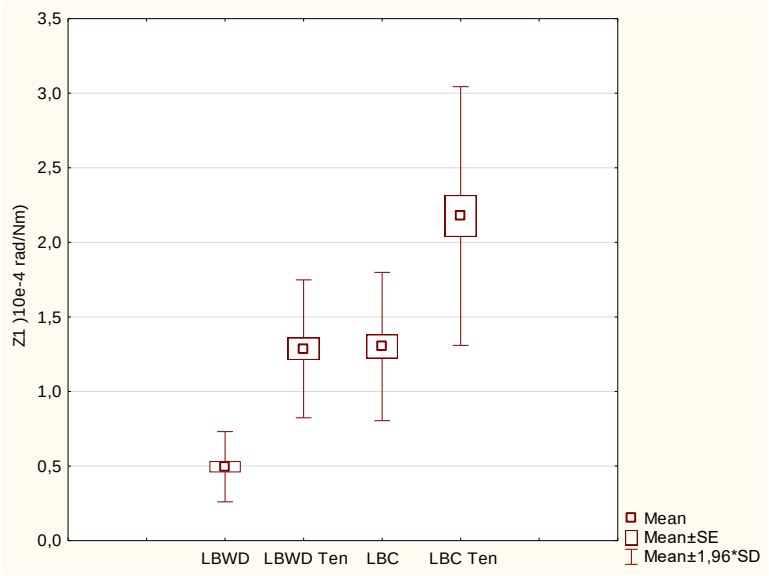

(a)

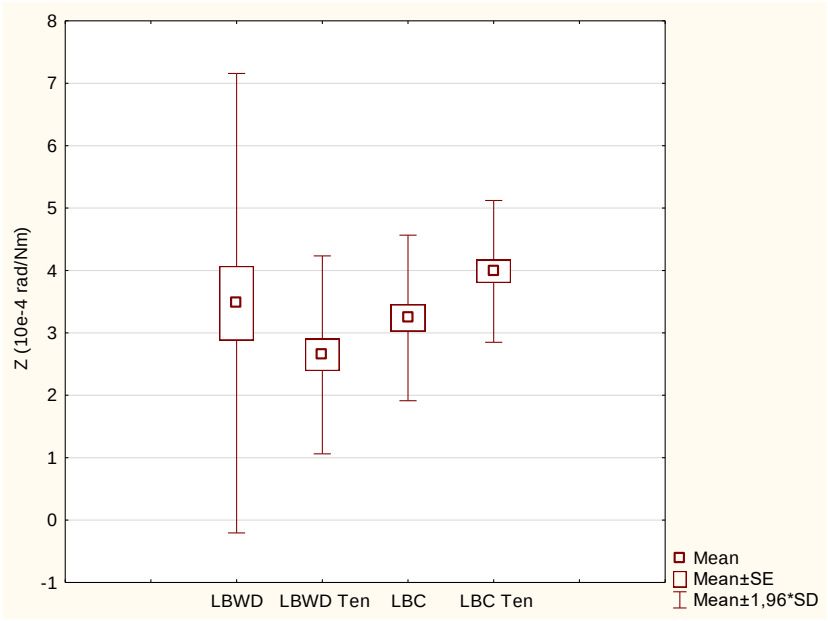

(b)

Figure 3.11 Comparison of flexibility coefficients of big size joints obtained by applying compressive and tensile force for bending; initial flexibility (a); secant flexibility (b)

Factorial ANOVA showed significant differences between the categories of compressive and tensile force in the case of the coefficient Z1. At ultimate load, this significant difference seemed to vanish. It is interesting that the ratio of Z to Z1 is quite low in the case of bending by tensile force (2.06 for LBWD and 1.83 for LBC).

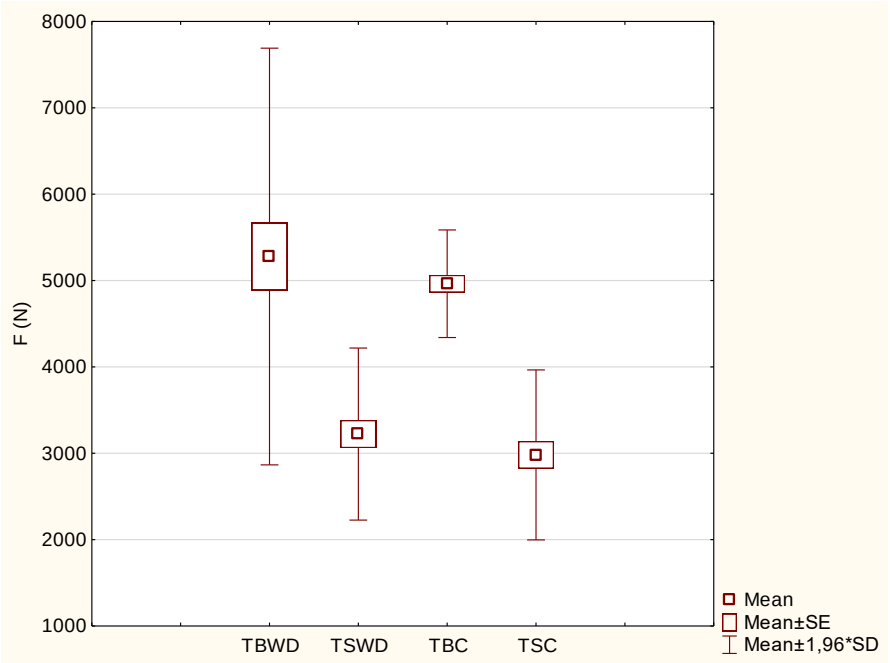

Figure 3.12 Ultimate load diagram of tension test of T-joints made with dowels and metal connectors.

One-way ANOVA showed that the results of the big samples were significantly higher than of the small samples while there was no significant difference between the TBWD and TBC as well as TSWD and TSC groups' results. Likewise, factorial ANOVA did not manifest the superiority of any of the connector types.

The metallic connector fastened big corner joints reached 94% of the strength of dowel fastened big corner joints. Small T wood dowel and small T metallic Domino connector fastened joints are almost at the same level. Differences between the performance of some of the groups are quite considerable. The big T dowel fastened joints show the highest resistance. The big metallic connector fastened joints exhibited 154% of the strength of the small wood dowel fastened joints. The big metallic connector fastened joints showed 166,4% of the strength of the small metallic connector fastened joints.

3.2. Cyclic test results

3.2.1. Cyclic test results of Domino wood dowel fastened joints

3.2.1.1. Cyclic test results of the joints coded LBWD:

Table 3.18 Displacement amplitudes applied in the course of the cyclic loading test

	1st cyclic		2nd scyclic		3rd;4rd;5th 6 cyclic						6th;7th;8th 6 cyclic					
Maximum deflection average																
	25%	25%	50%	50%	75%	75%	75%	75%	75%	75%	100%	100%	100%	100%	100%	100%
9,9	2,475	2,475	4,95	4,95	7,425	7,425	7,425	7,425	7,425	7,425	9,9	9,9	9,9	9,9	9,9	9,9

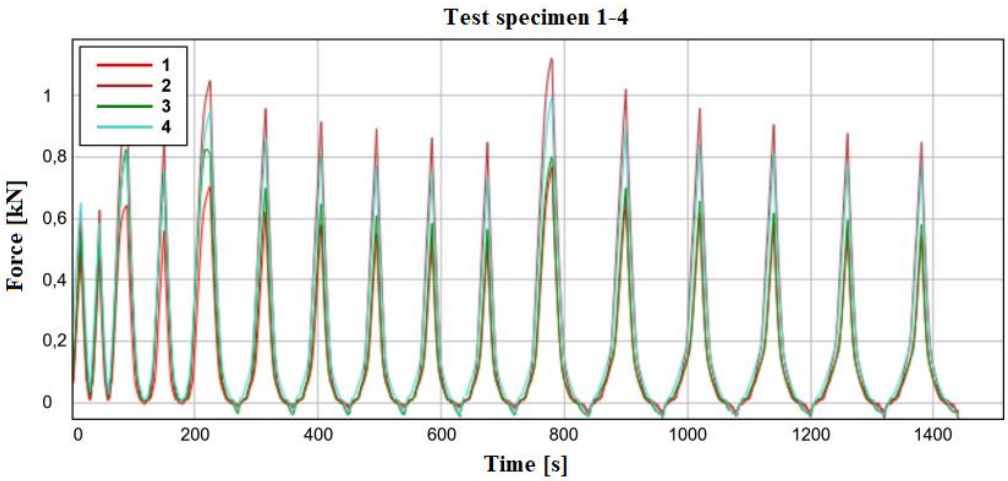

Figure 3.13 Force vs. load cycle diagram of the specimens tested

During cyclic tests, the big wood dowel fastened corner joints were subjected to 16 cycles of loading and unloading. During the first cycles performed under 25% of the deflection at ultimate load all the samples kept their strength associated with elastic behaviour and showed no loss of strength. During the next 2 cycles, performed under 50% of the deflection at ultimate load, the samples kept their strength and elastic load bearing capacity. The first test cycle performed under 75% of the deflection at ultimate load was reached by the joints in intact state, but at the end of the cycle, the joints started to weaken. The decreasing peaks refer to a gradual disintegration of the joints. It was an unexpected result, that when applying 100% of the load on the disintegrated sample, the joints continued to perform at the same level of strength as under the 75% of the deflection at ultimate load, without a total disintegration of the joints. The disintegration of the big wood dowel fastened corner joints started after the 5th cycle of dynamic testing.

3.2.1.2. Cyclic test results for the TBWD-type joints

Table 3.19 Displacement amplitudes applied in the course of the cyclic loading test

	1st cyclic		2nd cyclic		3rd;4rd;5th 6 cyclic						6th;7th;8th 6 cyclic					
Max. deflection average	25%	25%	50%	50%	75 %	75 %	75 %	75 %	75 %	75 %	100 %	100 %	100 %	100 %	100 %	100 %
51,1	12,7	12,7	25,5	25,5	38, 3	38, 3	38, 3	38, 3	38, 3	38, 3	51,1	51, 1	51, 1	51, 1	51, 1	51, 1

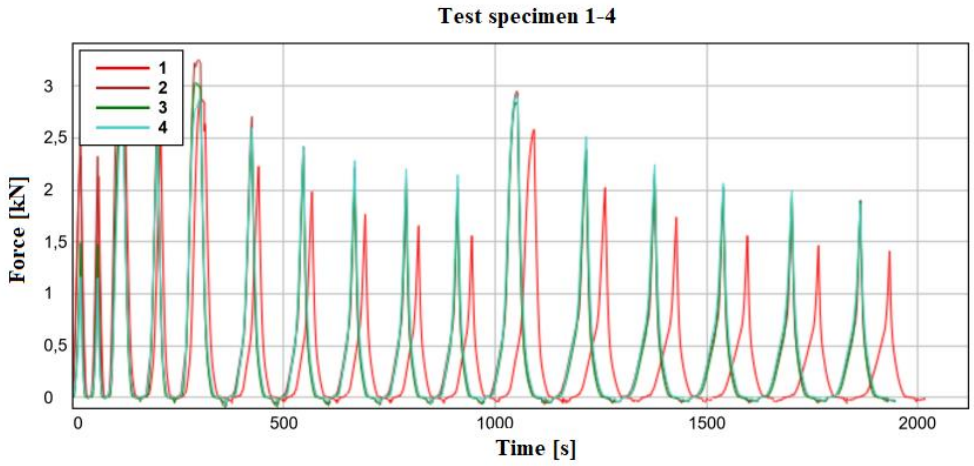

Figure. 3.14 Force vs. load cycle diagram of the specimens tested

During cyclic tests, the big wood dowel fastened T joints were subjected to 16 cycles of loading and unloading. During the first cycles performed under 25% of the deflection at ultimate load-all the samples kept their strength associated with ~~an~~ elastic behaviour and showed no loss of strength. During the next 2 cycles, performed under 50% of the deflection at ultimate load, the samples kept their strength and elastic load bearing capacity. The first test cycle performed under 75% of the deflection at ultimate load was reached by the joints in intact state, but the joints started to weaken. The decreasing peaks refer to a gradual disintegration of the joints. It was an unexpected result, that when applying 100% of the deflection at ultimate load on the disintegrated sample, the joints continued to perform at the same level of strength as under the 75% of the deflection at ultimate load, without a total disintegration of the joints. The disintegration of the big wood dowel fastened T joints started after the 3rd cycle of dynamic testing.

3.2.1.3. Cyclic test results for the LSWD-type joints

Table 3.20 Displacement amplitudes applied in the course of the cyclic loading test

	1st cyclic		2nd scyclic		3rd;4rd;5th 6 cyclic						6th;7th;8th 6 cyclic					
Maximum deflection average																
	25%	25%	50%	50%	75%	75%	75%	75%	75%	75%	100%	100%	100%	100%	100%	100%
13,74	3,43	3,43	6,87	6,87	10,3	10,3	10,3	10,3	10,3	10,3	13,75	13,75	13,75	13,75	13,75	13,75

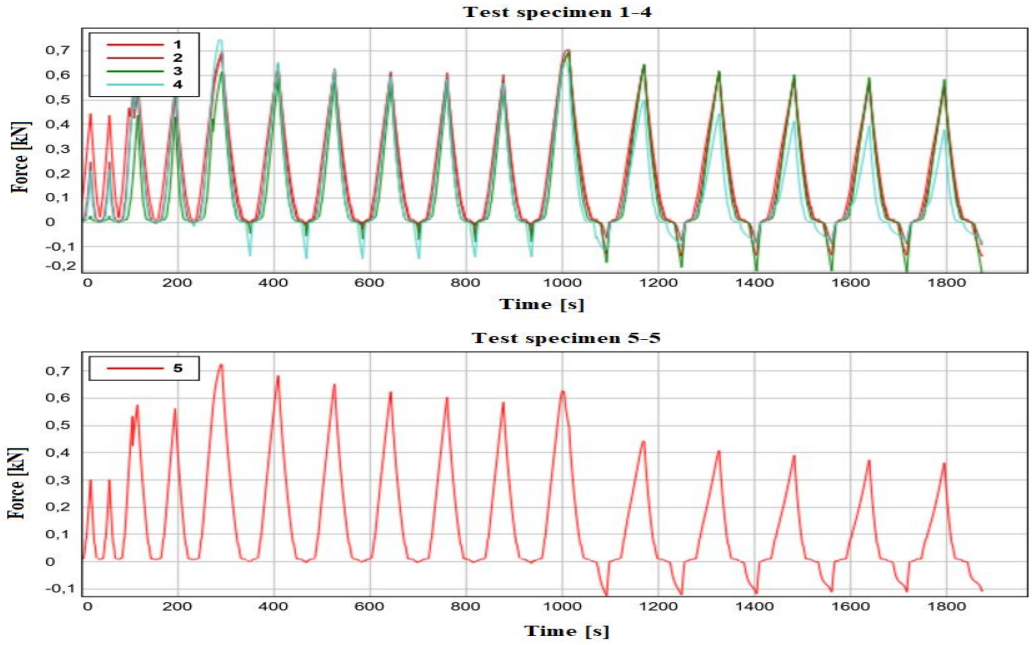

Figure 3.15 Force vs. load cycle diagram of the specimens tested

During cyclic tests, the small wood dowel fastened corner joints were subjected to 16 cycles of loading and unloading. During the first cycles performed under 25% of the ultimate load all the samples kept their strength associated with elastic behaviour and showed no loss of strength. During the next 2 cycles, performed under 50% of the deflection at ultimate load, the samples kept their strength and elastic load bearing capacity. The first test cycle performed under 75% of the deflection at ultimate load was reached by the joints in intact state; afterwards a gradual, but a moderate weakening of the joints could be observed. The decreasing peaks refer to a gradual disintegration of the joints. When applying 100% of the load on the disintegrated sample, at the beginning the joints continued to perform at the same level of strength as under the 75% load level, without a total disintegration. The disintegration of the small wood dowel fastened corner joints started after the 4th cycle of dynamic testing.

3.2.1.4. Cyclic test results for the TSWD-type joints

Table 3.21 Displacement amplitudes applied in the course of the cyclic loading test

	1st cyclic		2nd scyclic		3rd;4rd;5th 6 cyclic						6th;7th;8th 6 cyclic					
Maximum deflection average																
	25%	25%	50%	50%	75%	75%	75%	75%	75%	75%	100%	100%	100%	100%	100%	100%
9,84	2,46	2,46	4,92	4,92	7,38	7,38	7,38	7,38	7,38	7,38	9,84	9,84	9,84	9,84	9,84	9,84

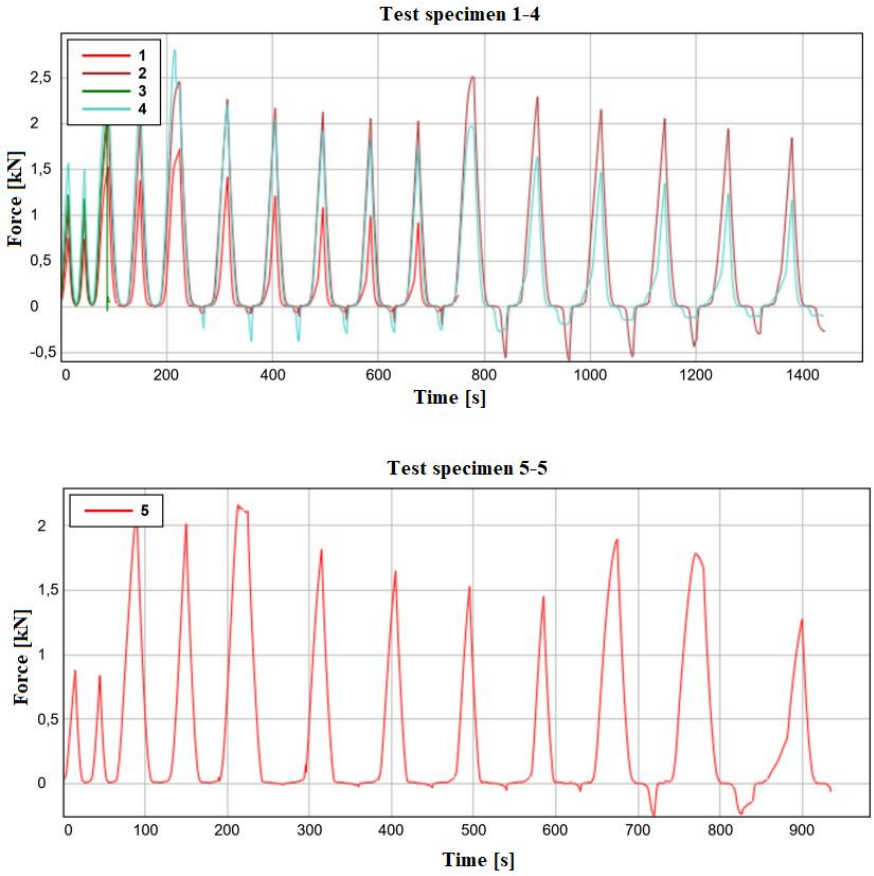

Figure 3.16 Force vs. load cycle diagram of the specimens tested

During cyclic tests, the small wood dowel fastened T joints were subjected to 16 cycles of loading and unloading. During the first cycles performed under 25% of the deflection at ultimate load all the samples kept their strength associated with elastic behaviour and showed no loss of strength. During the next 2 cycles, performed under 50% of the deflection at ultimate load, the samples still kept their strength and elastic load bearing capacity. The first test cycle performed under 75% of the deflection at ultimate load was reached by the joints in intact state, but at the end of the cycle, the joints started to weaken. The decreasing peaks refer to a gradual disintegration of the joints. When applying 100% of the load on the disintegrated sample, the joints continued to perform at the same level of strength as under the 75% of the deflection at

ultimate load, without a total disintegration of the joints. The disintegration of the small wood dowel fastened T joints started after the 5th cycle of dynamic testing.

3.2.2. Cyclic test results of metallic Domino connector fastened joints:

3.2.2.1. Cyclic test results for the LBC-type joints:

Table 3.22 Displacement amplitudes applied in the course of the cyclic loading test

	1st cyclic		2nd scyclic		3rd;4rd;5th 6 cyclic						6th;7th;8th 6 cyclic					
Maximum deflection average	25%	25%	50%	50%	75%	75%	75%	75%	75%	75%	100%	100%	100%	100%	100%	100%
7,01	1,7	1,7	3,5	3,5	5,25	5,25	5,25	5,25	5,25	5,25	7,01	7,01	7,01	7,01	7,01	7,01

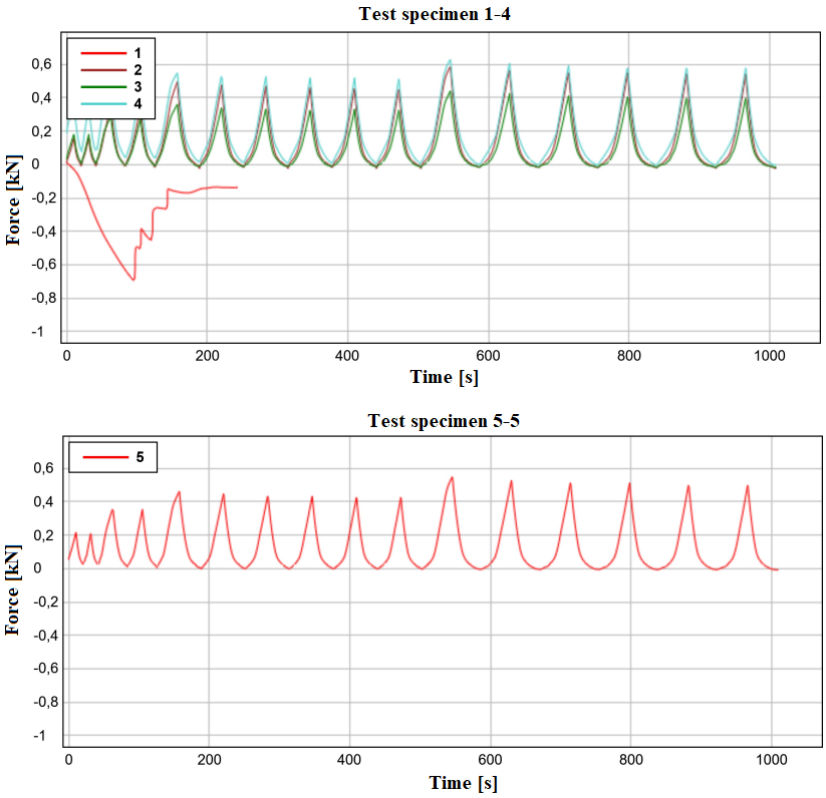

Figure 3.17 Force vs. load cycle diagram of the specimens tested

During cyclic tests, the big metallic Domino connector fastened corner joints were subjected to 16 cycles of loading and unloading. The first example showed a sudden break in the first cycle. During the first cycles performed under 25% of the deflection at ultimate load all the samples kept their strength associated with elastic behaviour and showed no loss of strength. During the next 2 cycles, performed under 50% of the deflection at ultimate load, the samples still kept their strength and elastic load bearing capacity. The first test cycle performed under 75% of the deflection at ultimate load was reached by the joints in intact state, but at the end of the cycle,

the joints started to weaken. There is no, or negligible decrease observed in peaks at a given load level. When applying 100% of the load on the disintegrated sample, the joints continued to perform at the same level of strength as under the 75% of the deflection at ultimate load, without a total disintegration of the joints. The disintegration of the big metallic Domino connector fastened corner joints started after the 5th cycle of dynamic testing.

3.2.2.2. Cyclic test results for the TBC fastened joints.

Table 3.23 Displacement amplitudes applied in the course of the cyclic loading test

	1st cyclic		2nd scyclic		3rd;4rd;5th 6 cyclic						6th;7th;8th 6 cyclic					
Maximum deflection average																
	25%	25%	50%	50%	75%	75%	75%	75%	75%	75%	100%	100%	100%	100%	100%	100%
9,44	2,36	2,36	4,72	4,72	7,08	7,08	7,08	7,08	7,08	7,08	9,44	9,44	9,44	9,44	9,44	9,44

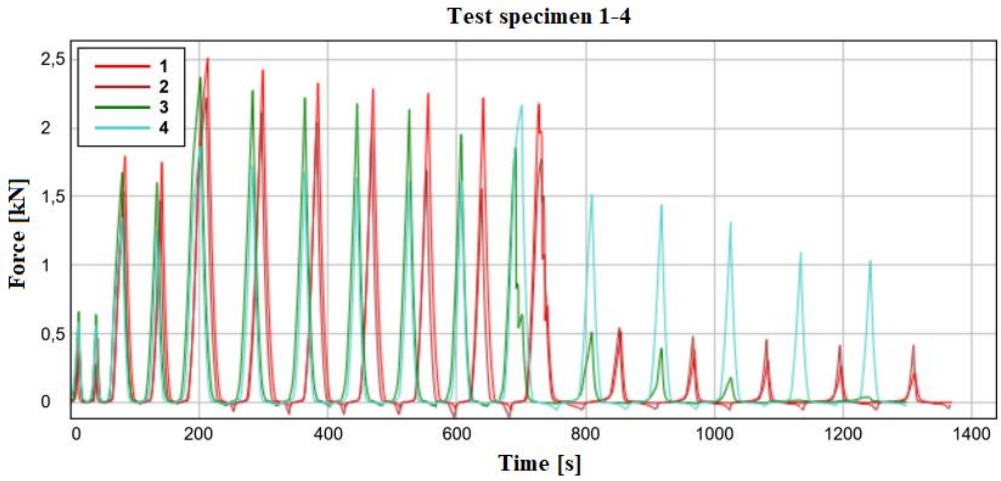

Figure 3.18 Force vs. load cycle diagram of the specimens tested

During cyclic tests, the big metallic Domino connector fastened T joints were subjected to 16 cycles of loading and unloading. During the first cycles performed under 25% of the deflection at ultimate load all the samples kept their strength associated with elastic behaviour and showed no loss of strength. During the next 2 cycles, performed under 50% of the deflection at ultimate load, the samples kept their strength and elastic load bearing capacity. The first test cycle performed under 75% of the deflection at ultimate load was reached by the joints in intact state, but at the end of the cycle, the joints started to weaken. The decreasing peaks refer to a gradual disintegration of the joints. It was an unexpected result, that when applying 100% of the load on the disintegrated sample, the joints continued to perform at the same level of strength as under the 75% of the deflection at ultimate load, without a total disintegration of the joints. The

disintegration of the big metallic Domino connector fastened T joints started after the 5th cycle of dynamic testing.

3.2.2.3. Cyclic test results for the LSC-type joints

Table 3.24 Displacement amplitudes applied in the course of the cyclic loading test

	1st cyclic		2nd scyclic		3rd;4rd;5th 6 cyclic						6th;7th;8th 6 cyclic					
Maximum deflection average																
	25%	25%	50%	50%	75%	75%	75%	75%	75%	75%	100%	100%	100%	100%	100%	100%
22,21	5,55	5,55	11,1	11,1	16,65	16,65	16,65	16,65	16,65	16,65	22,21	22,21	22,21	22,21	22,21	22,21

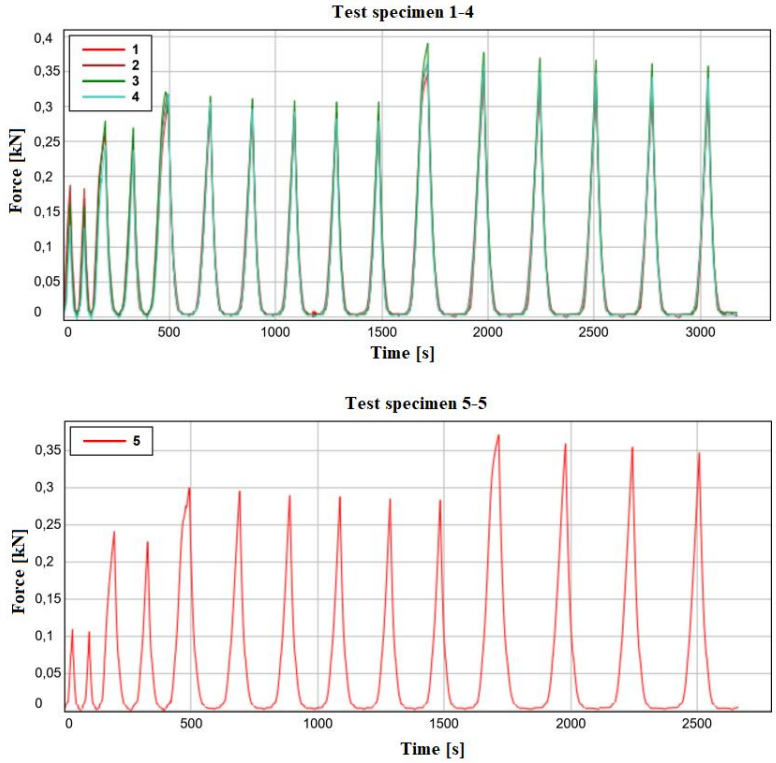

Figure 3.19 Force vs. load cycle diagram of the specimens tested

During cyclic tests, the small metallic Domino connector fastened corner joints were subjected to 16 cycles of loading and unloading. During the first cycles performed under 25% of the deflection at ultimate load all the samples kept their strength associated with elastic behaviour and showed no loss of strength. During the next 2 cycles, performed under 50% of the deflection at ultimate load, the samples kept their strength and elastic load bearing capacity. The first test cycle performed under 75% of the deflection at ultimate load was reached by the joints in intact state, but at the end of the cycle, the joints started to weaken. The decreasing peaks refer to a gradual disintegration of the joints. It was an unexpected result, that when applying 100% of the load on the disintegrated sample, the joints performed at proportionally higher level,

corresponding to their strength in static loading. This could be observed in spite of the fact that disintegration of the small metallic Domino connector fastened corner joints started already after the 1st cycle of dynamic testing. The test pieces did not totally disintegrate even at the end of the cyclic test.

3.2.2.4. Cyclic test results for the TSC-type joints

Table 3.25 Displacement amplitudes applied in the course of the cyclic loading test

	1st cyclic		2nd scyclic		3rd;4rd;5th 6 cyclic						6th;7th;8th 6 cyclic					
Maximum deflection average	25%	25%	50%	50%	75%	75%	75%	75%	75%	75%	100%	100%	100%	100%	100%	100%
17,8	4,4	4,4	8,9	8,9	13,3	13,3	13,3	13,3	13,3	13,3	17,8	17,8	17,8	17,8	17,8	17,8

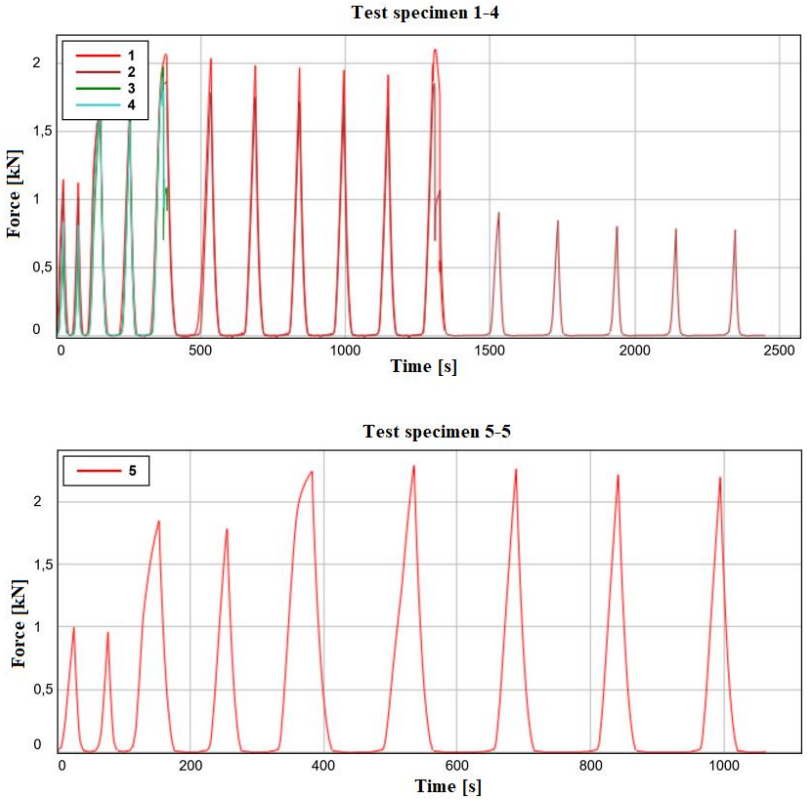

Figure 3.20 Force vs. load cycle diagram of the specimens tested

During cyclic tests, the small metallic Domino connector fastened T joints were subjected to 16 cycles of loading and unloading. During the first cycles performed under 25% of the deflection at ultimate load all the samples kept their strength associated with elastic behaviour and showed no loss of strength. During the next 2 cycles, performed under 50% of the deflection at ultimate load, the samples kept their strength and elastic load bearing capacity. The first test

cycle performed under 75% of the deflection at ultimate load was reached by the joints in intact state, but at the end of the cycle, the joints started to weaken. The decreasing peaks refer to a gradual disintegration of the joints. When applying 100% of the load on the disintegrated sample, the joints continued to perform at abruptly lower level of strength as under the 75% of the deflection at ultimate load, but without a total disintegration of the joints.

3.3. Creep Test Results

Creep results are presented in graphical form as creep curves. Two types of creep curves are used. The first type shows creep factor values defined by the formula

$$Creep\ factor = \frac{d_t - d_0}{d_0}$$

where:

- d_t is the measured deflection at time t and
- d_0 is the measured deflection after placing the dead load on the test piece.

When performing sustained loading tests, it seemed reasonable to wait for 10 to 20 minutes while the test piece settle down under the full load imposed on it. This practice was applied in researching into duration of load effect in timber joints [93].

Sections 3.3.1 to 3.3.3 demonstrate and analyse creep factor curves.

In the second type of creep curves, we plotted the increase in the members' relative rotation angle at unit bending moment versus time (Z). This kind of creep curves are demonstrated and analysed in Sections 3.3.4 to 3.3.6. The time-dependent deflection curves for all the test specimens subjected to sustained loading are shown in Appendix B. Two specimens failed shortly after the beginning of the test. In the case of a few others, there was either no increase of deflection with time or extremely high increase of the exceptionally small initial deflection, which do not show typical behaviour of the particular joint type. Measurement data for these specimens were omitted from further evaluation.

3.3.1 Creep factor curves

LBWD specimens

The curves of Figure 3.20 show that the LBWD-type test pieces reached the secondary creep

stage. Those with highest creep seem to attain zero creep rate within 3 days (1440 min) and somewhat more than 1 day (1440 min) respectively, while test piece No 4 demonstrated zero creep rate after the first 8 hours (480 min) of test

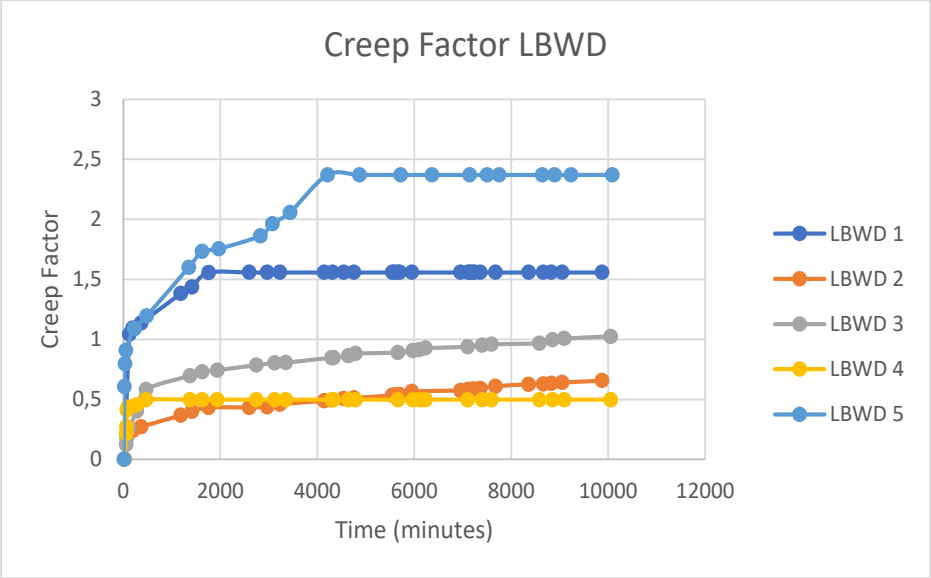

Figure 3.21 Creep curves of LBWD – type specimens

In the case of specimens, No 2 and 3, the creep continued to increase with constant, moderate rate at the end of the loading period. The individual specimens produced 61 to 100 per cent of the final creep after the first 24 hours (1440 min).

LSWD specimens

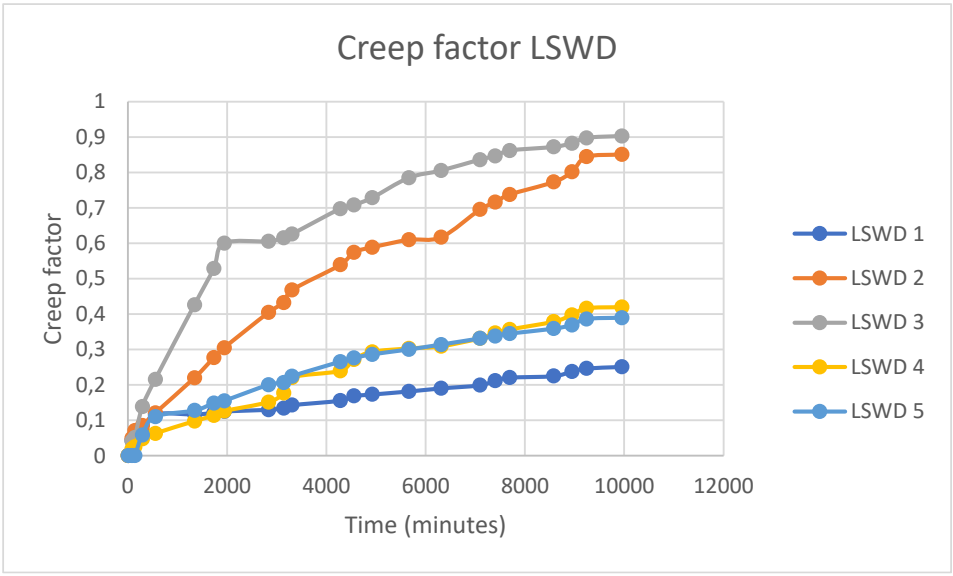

Figure 3.22 Creep curves of LSWD – type specimens

The curves of Figure 3.21 show that the LSWD-type test pieces did not reach the secondary creep stage: however, test pieces No. 1 and No 5 seem to have approached it. In all cases creep continued to increase with higher rate than in the case of the LBWD specimens at the end of the loading period. 24 to 50 per cent of the final creep was observed after the first 24 hours (1440 min)

TBWD specimens

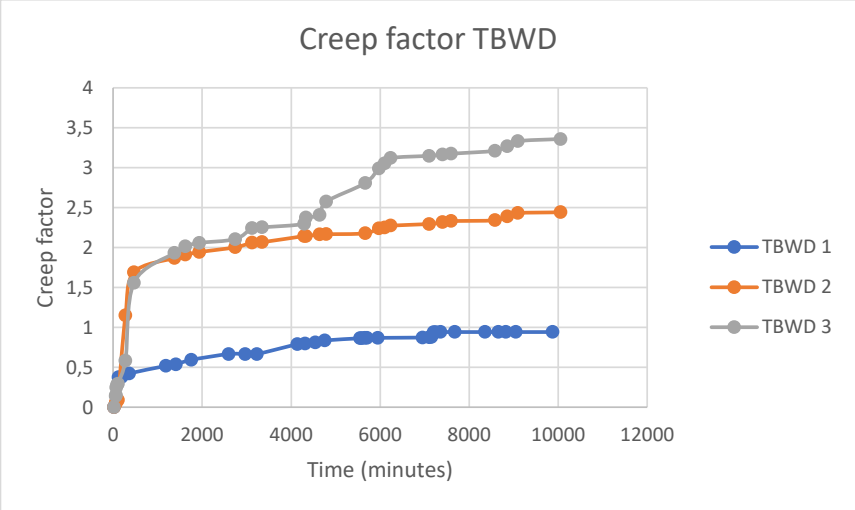

Figure 3.23 Creep curves of TBWD – type specimens

The creep curves of the TBWD-type test pieces demonstrate creep stages close to the secondary one; test piece No. 1 even seem to have attained it with zero creep rate. In the other two cases creep continued to increase with moderate rate at the end of the loading period. The individual specimens demonstrated that 57 to 77 per cent of the final creep occurred after the first 24 hours (1440 min).

TSWD specimens

The creep curves of the TSWD-type test pieces demonstrate that creep process attained or get close to the secondary stage. However, in the case of test piece No. 3 this statement is upported by only the last two deflection readings of slightly more than half a day (720 min) interval apart. In all cases creep rate decreased to zero at the end of the loading period. The individual specimens exhibited 13 to 42 per cent of the final creep after the first 24 hours (1440 min).

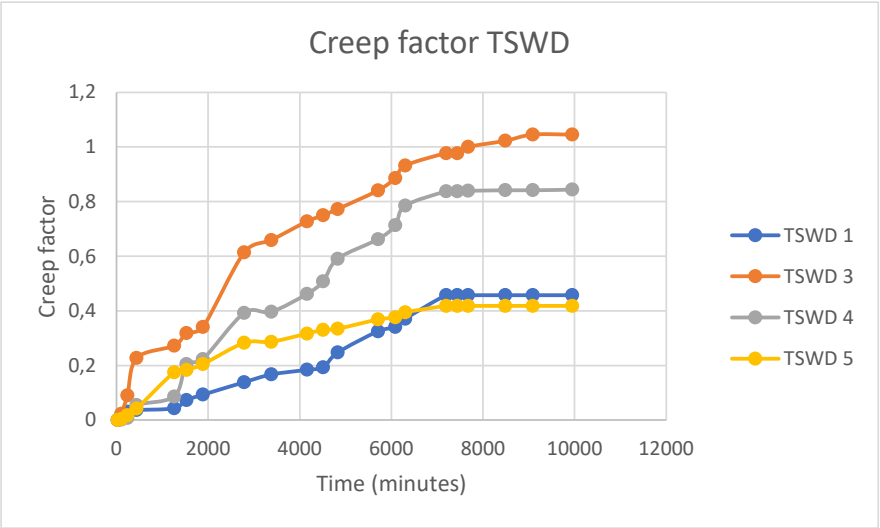

Figure 3.24 Creep curves of TSWD – type specimens

LBC specimens

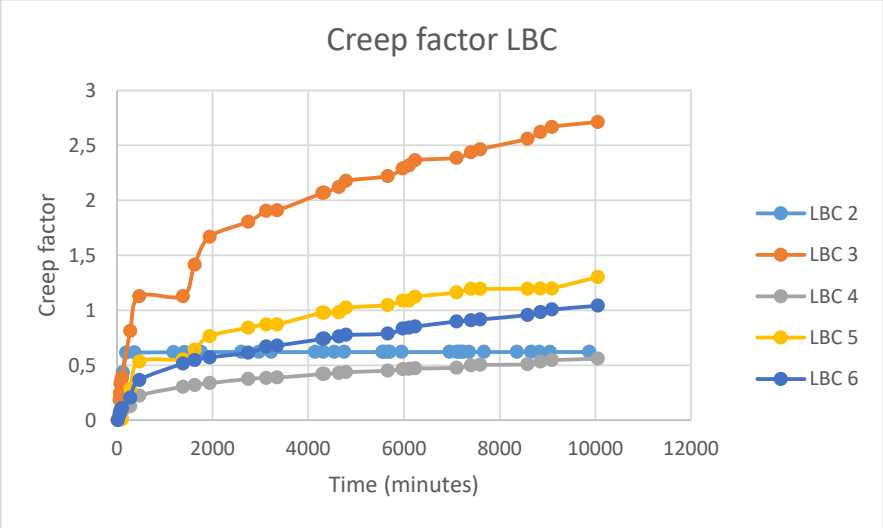

Figure 3.25 Creep curves of LBC – type specimens

The creep curves pertinent to the LBC - type test pieces show constant creep rate from the middle of the testing period with some modest fluctuations in the case of test piece No 3 and 5, having somewhat higher slope then the other three specimens. The curves of this group, except for that of LBC 2, let suppose the transition to tertiary creep stage over time, leading to failure. The individual specimens exhibited 50 to 100 per cent of the final creep after the first 24 hours (1440 min).

LSC specimens

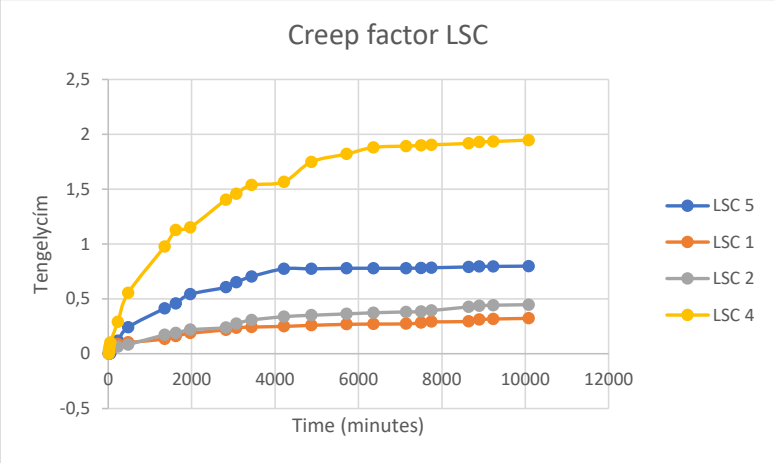

Figure 3.26 Creep curves of LSC – type specimens

The creep curves of the LSC-type test pieces demonstrate that creep process attained the secondary stage with low, in two cases zero creep rate. The individual specimens exhibited 39 to 52 per cent of the final creep after the first 24 hours (1440 min).

TBC specimens

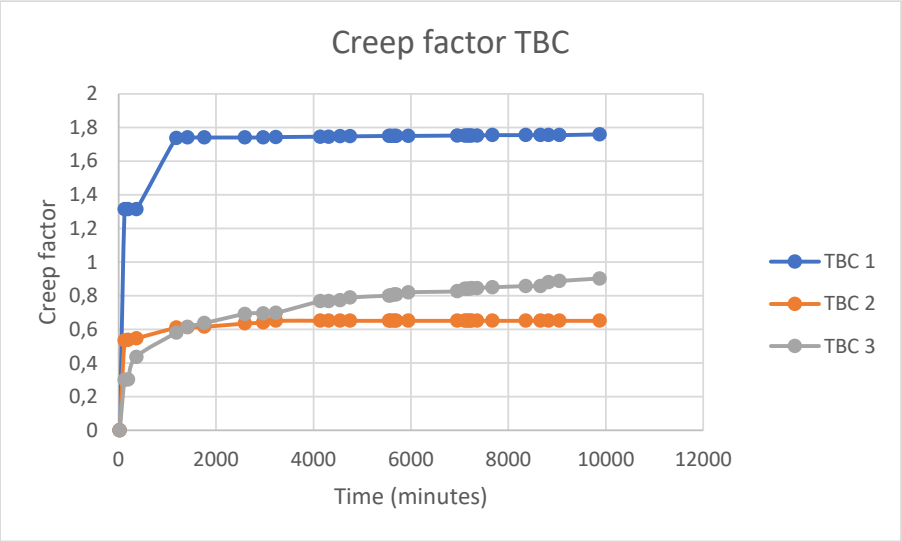

Figure 3.27 Creep curves of TBC – type specimens

The TBC - type test pieces have creep curves with initially very high but rapidly decreasing slope that becomes soon constant zero in the case of specimen No 1 and 2.
The individual specimens exhibited 68 to 100 per cent of the final creep after the first 24 hours (1440 min).

TSC specimens

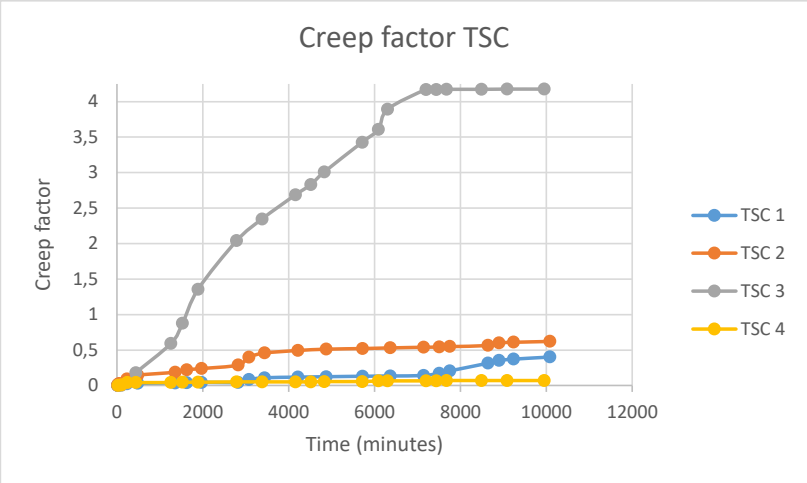

Figure 3.28 Creep curves of TSC – type specimens

The creep curves of to the TSC - type test pieces show different stages of creep process. Test specimens No 3 and No 4 seem to have attained the secondary stage towards the last days (cca. 8000 min) of the testing period with high creep but zero creep rate. The other two specimens still exhibit somewhat changing creep rate with low level of creep. The individual specimens exhibited only 9 to 30 per cent of the final creep after the first 24 hours (1440 min).

3.3.2 Analysis of the experimental creep data by curve fitting

Logarithmic curves have been fitted to the creep data of the individual test pieces. In most of the cases, the coefficient of determination R^2 was found quite high, over 0.8. The tables that follow demonstrate the equation of the curve and the coefficient of determination by type of joints for each test specimen. The fitted curves are shown in the diagrams of Appendix C.

LBWD		LSWD	
y1= 0.1894ln(t) - 0.0693	R^2 = 0.8145	y1= 0.0332ln(t) - 0.0997	R^2 = 0.853
y2= 0.0991ln(t) - 0.303	R^2 = 0.9647	y2 = 0.1297ln(t) - 0.5193	R^2 = 0.775
y3 = 0.1603ln(t) - 0.4768	R^2 = 0.9954	y3 = 0.1504ln(t) - 0.5508	R^2 = 0.885
y4= 0.0444ln(t) + 0.1264	R^2 = 0.5982	y4 = 0.0633ln(t) - 0.2604	R^2 = 0.734
y5= 0.3187ln(t) - 0.5188	R^2 = 0.9589	y5 = 0.0619ln(t) - 0.2454	R^2 = 0.820
LBC		LSC	
y2 = 0.0594ln(t) + 0.1168	R^2 = 0.562	y1 = 0.048ln(t) - 0.1521	R^2 = 0.945
y3 = 0.4503ln(t) - 1.6437	R^2 = 0.9718	y2 = 0.0664ln(t) - 0.2253	R^2 = 0.883
y4 = 0.0925ln(t) - 0.3395	R^2 = 0.9816	y4 = 0.3235ln(t) - 1.0967	R^2 = 0.942
y5 = 0.2336ln(t) - 0.9609	R^2 = 0.968	y5 = 0.1393ln(t) - 0.4804	R^2 = 0.943
y6 = 0.1717ln(t) - 0.6592	R^2 = 0.9664		
TBWD		TSWD	
y1 = 0.1524ln(t) - 0.4666	R^2 = 0.9507	y1 = 0.089ln(t) - 0.4525	R^2 = 0.672
y2 = 0.4521ln(t) - 1.6439	R^2 = 0.9563	y3 = 0.2073ln(t) - 0.9637	R^2 = 0.860
y3 = 0.5903ln(t) - 2.2854	R^2 = 0.9608	y4 = 0.1765ln(t) - 0.8866	R^2 = 0.769
		y5 = 0.0885ln(t) - 0.4091	R^2 = 0.907
TBC		TSC	
y1 = 0.1966ln(t) + 0.0697	R^2 = 0.7366	y1 = 0.0402ln(t) - 0.1677	R^2 = 0.488
y2 = 0.0678ln(t) + 0.07	R^2 = 0.685	y2 = 0.0958ln(t) - 0.3435	R^2 = 0.862
y3 = 0.1411ln(t) - 0.4129	R^2 = 0.9962	y3 = 0.8938ln(t) - 4.4591	R^2 = 0.799
		y5 = 0.0108ln(t) - 0.0323	R^2 = 0.906

Table 3.26 Logarithmic equations fitted on creep factor data for the individual test pieces in each group, with the respective coefficient of determination; yi is the time-dependent creep factor value of the i^{th} specimen in a group.

3.3.3 Comparison and statistical analysis of creep factor data

First day results

Test piece	TBWD 1 day	TSWD 1 day	TBC 1 day	TSC 1 day
1	0.54	0.06	1.74	0.04
2	1.87	X	0.61	0.2
3	1.93	0.3	0.62	0.75
4		0.15		X
5		0.18		0.05
AVERAGE	1.45	0.17	0.99	0.26
SD	0.79	0.10	0.65	0.33
CV	0.54	0.57		1.29

Test piece	LBWD 1 day	LSWD 1 day	LBC 1 day	LSC 1 day
1	1.44	0.12	X	0.14
2	0.4	0.29	0.62	0.18
3	0.7	0.45	1.13	X
4	0.5	0.1	0.3	1.03
5	1.6	0.13	0.55	0.42
6			0.52	
AVERAGE	0.93	0.22	0.62	0.44
SD	0.55	0.15	0.27	0.41
CV	0.60	0.69	0.44	0.93

Table 3.27 Creep factor data of test pieces by joint types after the first 24 hours. X - tests pieces omitted from the analysis.

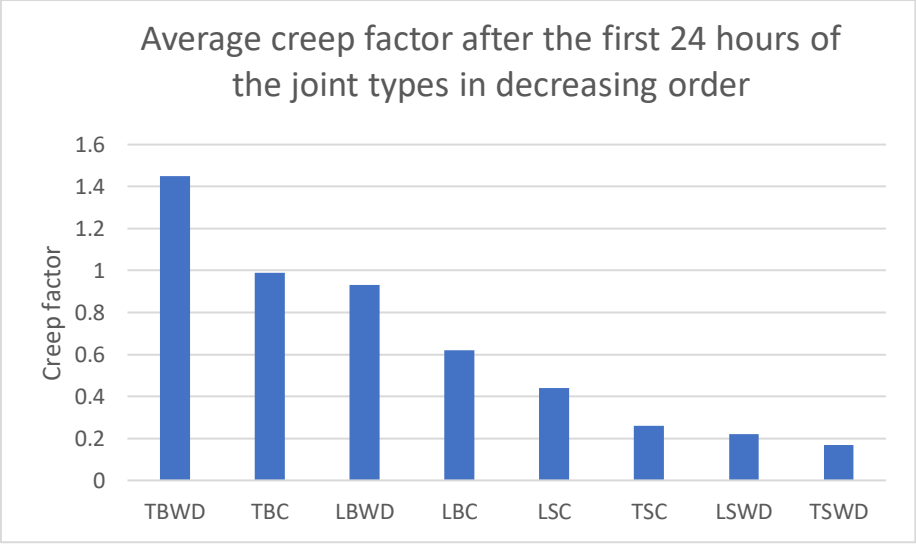

Figure 3.29 Average creep factor of the joint types after the first 24 hours

As Figure 3.28 suggests, big-size joint types attain higher creep factor than their small size counterparts within the first 24 hours. Big-size T-joints exhibit higher value than their corner joint mates do, while this is opposite in the case of small-size joints. Likewise, big-size joints with metallic connector perform better, while the opposite seems to be true for small-size samples.

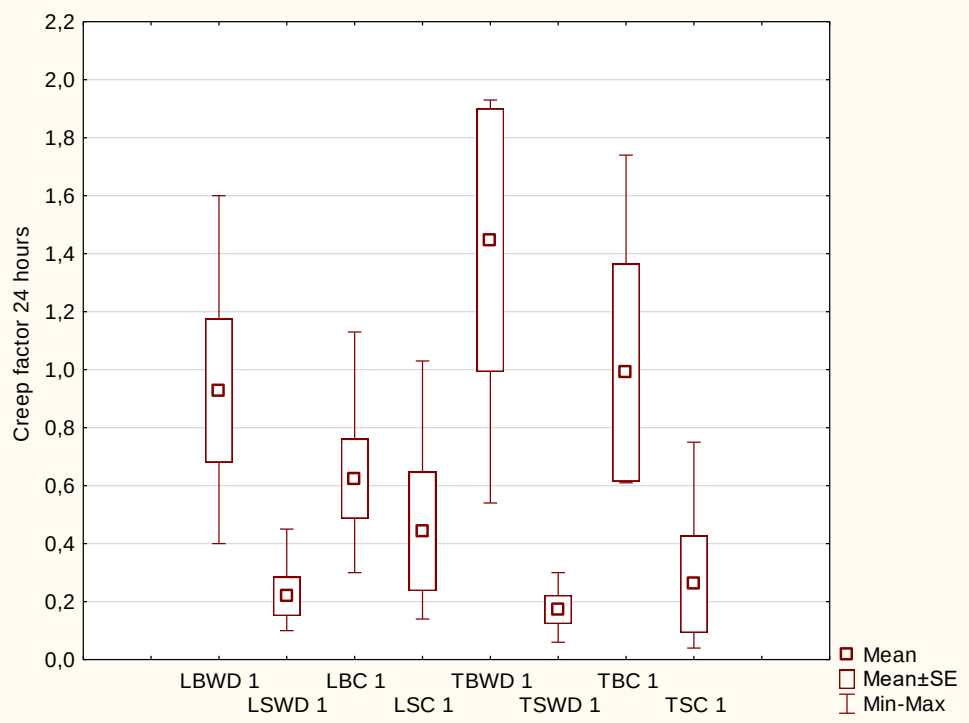

Figure 3.30 Box-Whiskers plot of the creep factor of the different joint types after 24 hours

Factorial ANOVA conducted on creep factor data proved significant difference between 24 hours creep results of big size, small-size test specimens as well as big wood dowel connected and small wood dowel connected samples, furthermore big wood dowel and small metal connector, as well as small wood dowel, and big metal connector fastened samples. One-way ANOVA pointed out significant differences at the 0.05 level of significance between groups as follows:

LBWD – LSWD; LBWD – TSWD; LSWD – LBC; LSWD – TBWD; LSWD – TBC; LBC – TSWD; TBWD – TSWD; TBWD – TSC; TBWD – LSC. those comparisons with bold were confirmed both by Scheffé- test and by Newman- Keuls test with respect to the high number of variables to be compared and the lack of fulfilling some the assumption of ANOVA.

7^{th} day results

Test piece No	LBWD 7 days	LSWD 7 days	LBC 7 days	LSC 7 days
1	1.56	0.25	X	0.32
2	0.66	0.85	0.62	0.45
3	1.02	0.9	2.71	X
4	0.5	0.42	0.56	1.95
5	2.37	0.39	1.3	0.8
6			1.04	
AVERAGE	1.22	0.56	1.25	0.88
SD	0.76	0.29	0.78	0.74
CV	0.62	0.52	0.63	0.84
Test piece No	TBWD 7 days	TSWD 7 days	TBC 7 days	TSC 7 days
1	0.9	0.46	1.76	0.4
2	2.44	X	0.65	0.62
3	3.36	1.05	0.9	4.18
4		0.84		X
5		0.42		0.08
AVERAGE	2.23	0.69	1.10	1.32
SD	1.24	0.30	0.58	1.92
CV	0.56	0.44	0.53	1.45

Table 3.28 Creep factor data of test pieces by joint types after seven days loading; 186 test piece omitted from the analysis

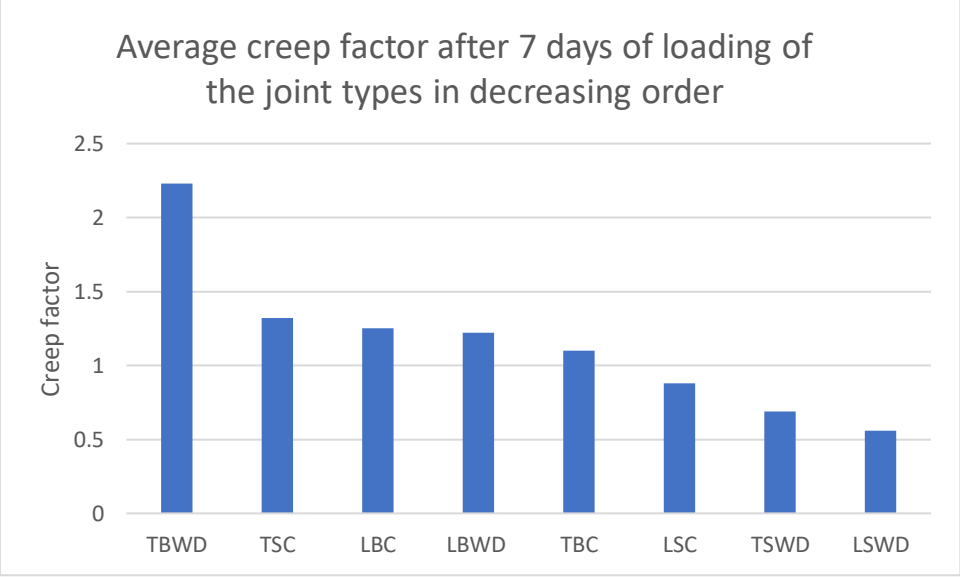

Figure 3.31 Average creep factor of the different joint types after 7 days

Figure 3.30 shows that big-size joint types attain higher creep factor than their small size counterparts with the exception of T-joints with metallic connector. No systematic difference can be traced with respect to connector type, L, or T joint configuration. As referenced before, the high scatter of the data in the TSC group may hide some effect of either the connector type or the T-joint configuration.

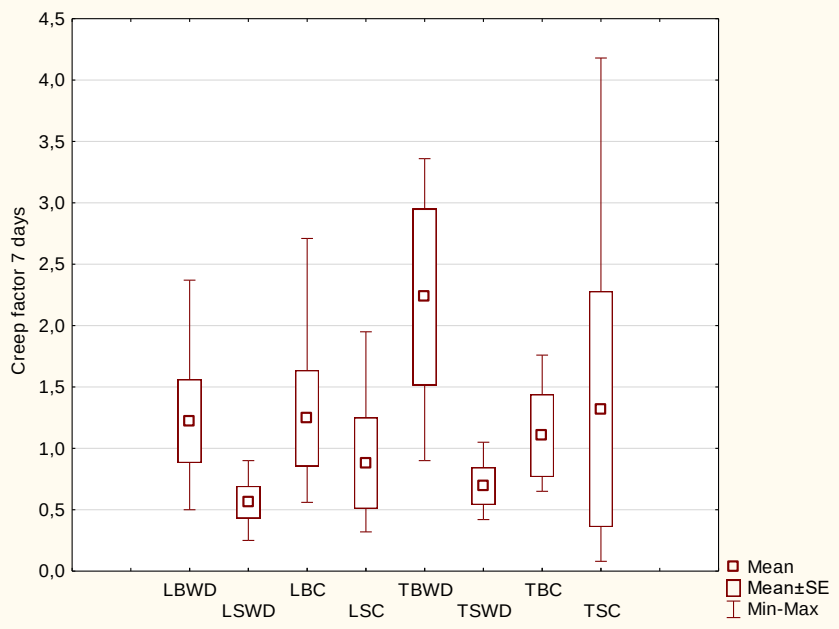

Figure 3.32 Box-Whisker's plot of the creep factor of the different joint types after 7 days

Factorial ANOVA conducted on creep factor data proved significant difference between 7 days creep results of big-size wood dowel and small-size wood dowel specimens only. One way ANOVA pointed out significant differences at the 0.05 level of significance between groups as follows: LSWD – TBWD; TBWD – TSWD.

Equations of logarithmic curve fitting

Figure 3.33 compares the average values of the coefficient of the logarithmic equation by joint type. The higher this coefficient the more rapid the increase of creep factor.

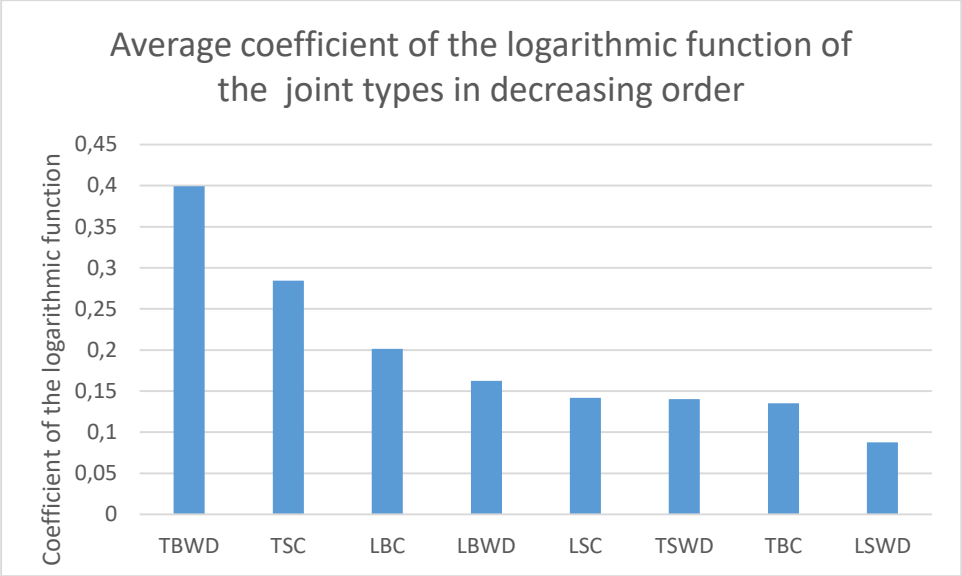

Figure 3.33 Comparison of the average values of the coefficient of logarithmic equation by joint type

It appears from Figure 3.32 that as a general trend creep is growing more rapidly in the case of big-size joint types. The value for the type TSC is an exception; however, the scatter of data in this group is exceptionally large making statistical inferences uncertain. T-joints have higher average coefficient than corner joints do in their cases. No systematic difference can be traced with respect to the kind of connector.

3.3.4 Evaluation of the change in joint flexibility

Just as in the case of static bending test, the deformation of the joints under sustained loading was evaluated in terms of angle change, i.e. rotation of the joint members with respect to each other as a function of loading time. The rotation caused by unit moment was calculated and plotted against time so that the responds of test specimens loaded by different bending moment could be compared. This value, as stated in connection with the static bending tests is a measure of joint flexibility Z, while its reciprocal value indicates joint rigidity. The figures that follow demonstrate the change of joint flexibility as a function of loading time by joint types for the individual test specimens. The values of the Z coefficients calculated represent the increments of the instantaneous flexibility coefficient in the course of the testing period, taking the first deflection reading as the starting point at which this increment is zero, just as how creep factor values were derived. It has to be noted, that the incremental Z-values

for an individual test specimen are proportional to the creep factor values. However, while the creep factor depends on the initial deflection, the incremental Z-value does not. Therefore, because of the differences in the initial deflection, the coefficient of proportionality varies from test piece to test piece within the same group. Nevertheless, the general shape of the two kinds of curves will be identical for individual specimens, thus these incremental Z-curves reflect the same creep stage as the creep curves do. However, the relative height of Z curves of the individual test pieces in a group will be different of that of the creep curves. On the other side, it also follows that these incremental Z-curves are not directly dependent on the load level, allowing the comparison between groups when the applied load level was not the same.

Big-size corner joints with Domino wood dowel

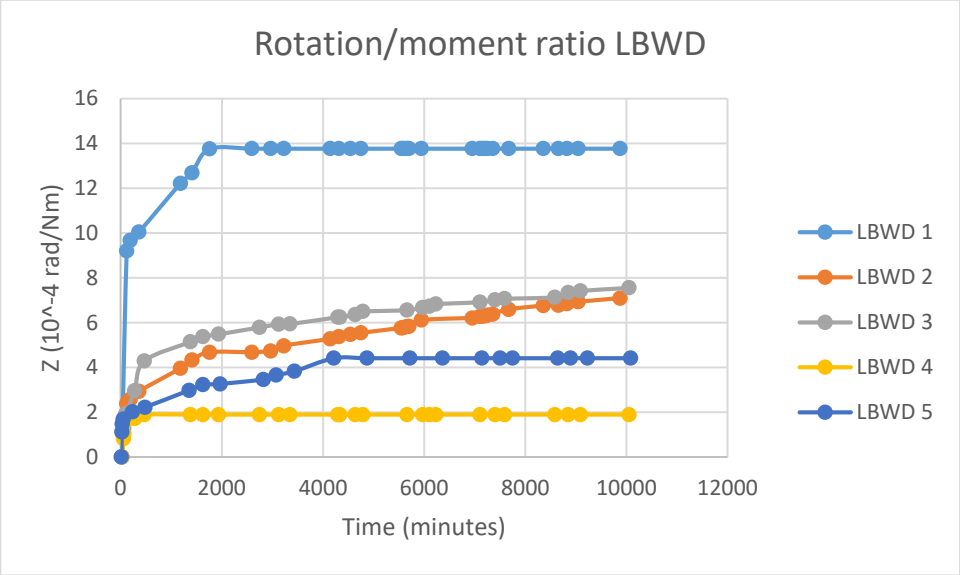

Figure 3.34 Rotation/moment ratio curves of the LBWD – type specimens

The average increase of the rotation/moment ratio by the end of the loading period of seven days was 6.94e-4 rad/Nm, which is close to 14 times the average Z – value of this type of joints in static loading in the steepest slope of load-deflection curve, which correspond to load levels up to about 60 per cent. If we take the secant coefficient at maximum load in static bending for basis of comparison, this increment in the flexibility coefficient is double as high, which means that is flexibility triples. This increment is approached, in some cases attained in the course of the first couple of days.

Small-size corner joints with Domino wood dowel

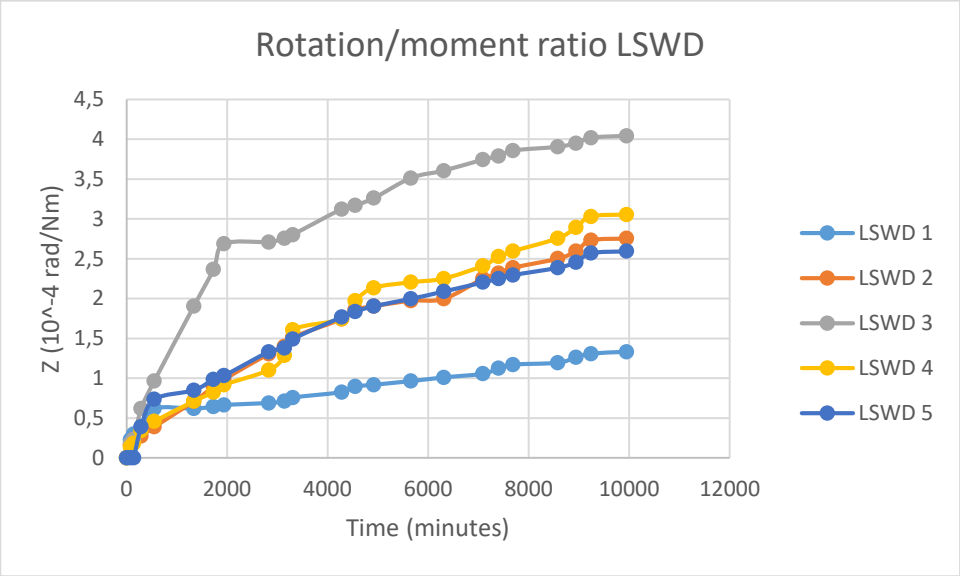

Figure 3.35 Rotation/moment ratio curves of the LSWD – type specimens

The average increase of the rotation/moment ratio by the end of the loading period of seven days was 2.75e-4 rad/Nm, which is just slightly higher than the average Z – value of this type of joints in static loading in the steepest slope of load-deflection curve, which correspond to load levels up to 50 to 60 per cent. If we take the secant coefficient at maximum load in static bending for basis of comparison, this increment in the flexibility coefficient is somewhat less As a rough comparison, we may say that flexibility of the LSWD-type joints doubles within a week of test period and will probably increase by continued loading, but with decreasing rate.

Big-size corner joints with metallic connector

The average increase of the rotation/moment ratio by the end of the loading period of seven days was 6.81e-4 rad/Nm, which is more than five times the average Z – value of this type of joints in static loading in the steepest slope of load-deflection curve, which correspond to load levels up to 30 to 35 per cent. If we take the secant coefficient at maximum load in static bending for basis of comparison, this increment in the flexibility coefficient is double as high. Further increase with continued loading can be expected.

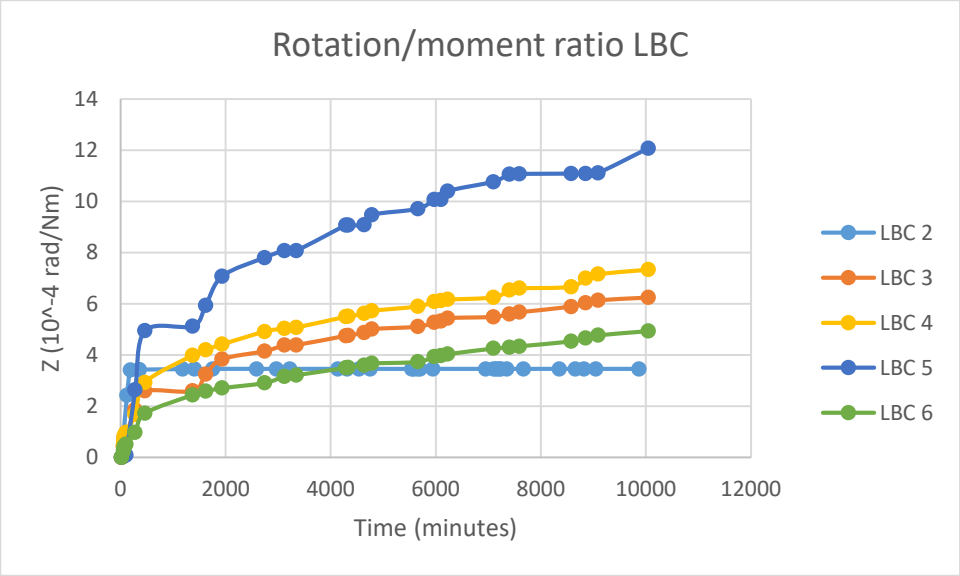

Figure 3.36 Rotation/moment ratio curves of the LBC – type specimens

Small-size corner joints with Domino metallic connector

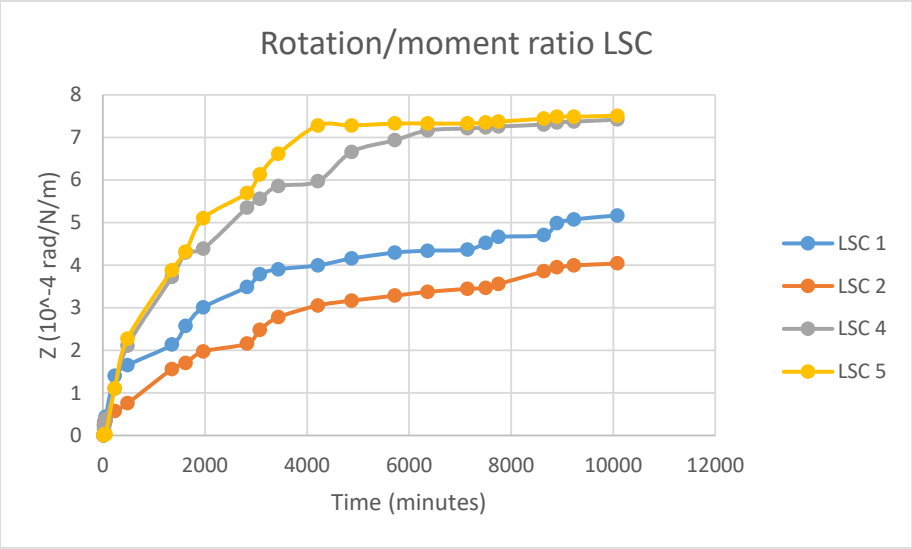

Figure 3.37 Rotation/moment ratio curves of the LSC – type specimens

The average increase of the rotation/moment ratio by the end of the loading period of seven days was 6.04e-4 rad/Nm, which is less than the average Z – value of 8.66e-4 rad/Nm of this type of joints in static loading in the steepest slope of load-deflection curve, corresponding to load levels up to 30 to 40 per cent. If we take the secant coefficient at maximum load in static bending for basis of comparison, this increment in the flexibility coefficient is just 27 per cent of the same. Further increase with continued loading can be foreseen except for the test specimen exhibiting the highest creep within the test period.

Big-size T-joints with Domino wood dowel

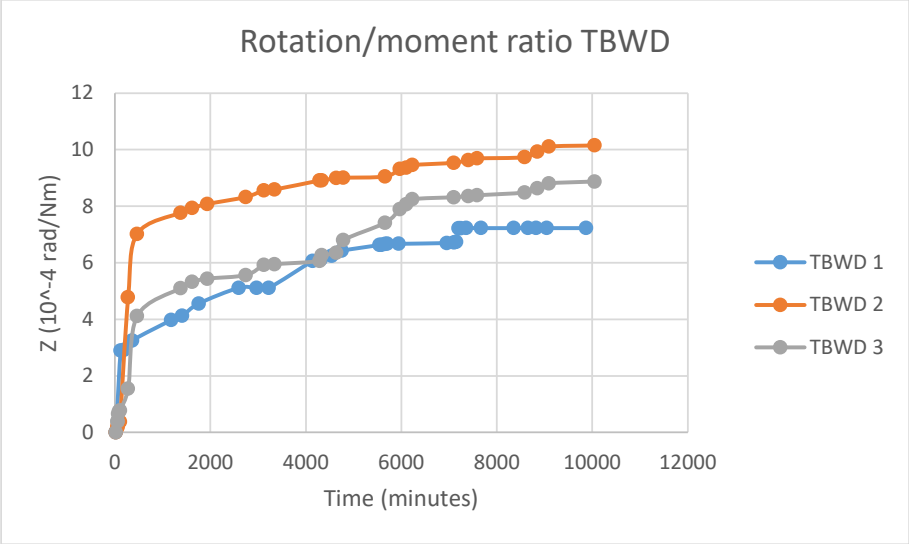

Figure 3.38 Rotation/moment ratio curves of the TBWD – type specimens

The average increase of the rotation/moment ratio by the end of the loading period of seven days was 8.75e-4 rad/Nm, which is almost four times the average Z – value of this type of joints in static loading in the steepest slope of load-deflection curve, corresponding to load levels up to 35 to 65 per cent. If we take the secant coefficient at maximum load in static bending for basis of comparison, this increment in the flexibility coefficient is 122 per cent per cent of the same. No further increase with continued loading can be foreseen.

Small-size T-joints with Domino wood dowel

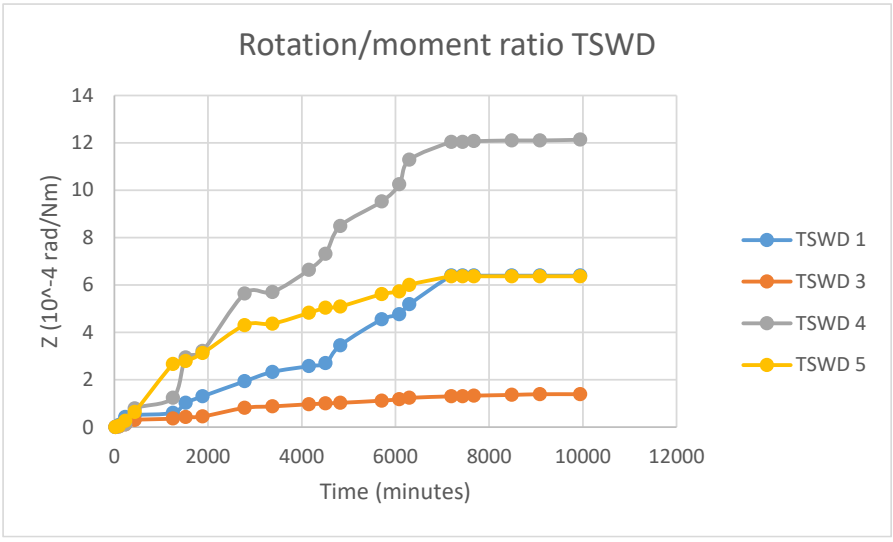

Figure 3.39 Rotation/moment ratio curves of the TSWD – type specimens

The average increase of the rotation/moment ratio by the end of the loading period of seven days was 6.57e-4 rad/Nm, which is 1.8 times the average Z – value of this type of joints in static loading in the steepest slope of load-deflection curve, corresponding to load levels up to 40 to 45 per cent. If we take the secant coefficient at maximum load in static bending for basis of comparison, this increment in the flexibility coefficient is essentially of the same magnitude. Further increase with continued loading cannot be expected. One may say that flexibility of the TSWD-type joints doubles within a week of test period and probably no further increase by continued loading will occur.

Big-size T-joints with Domino metallic connector

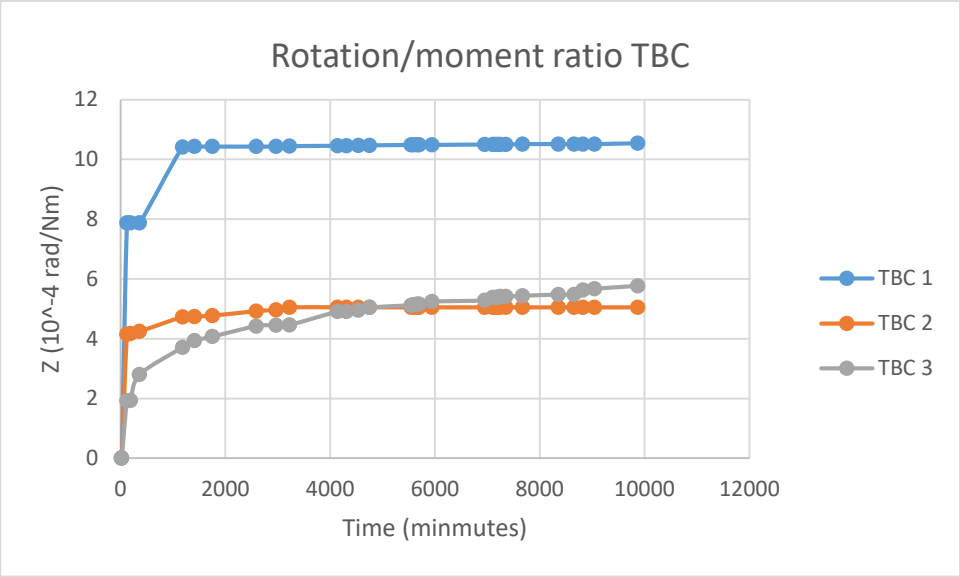

Figure 3.40 Rotation/moment ratio curves of the TBC – type specimens

The average increase of the rotation/moment ratio by the end of the loading period of seven days was 7.12e-4 rad/Nm, which is 2.4 times the average Z – value of this type of joints in static loading in the steepest slope of load-deflection curve, corresponding to load levels up to 40 to 45 per cent. If we take the secant coefficient at maximum load in static bending for basis of comparison, this increment in the flexibility coefficient is 1.2 times. Further increase with continued loading can be expected in one case of the three only.

Small-size T-joints with Domino metallic connector

The average increase of the rotation/moment ratio by the end of the loading period of seven

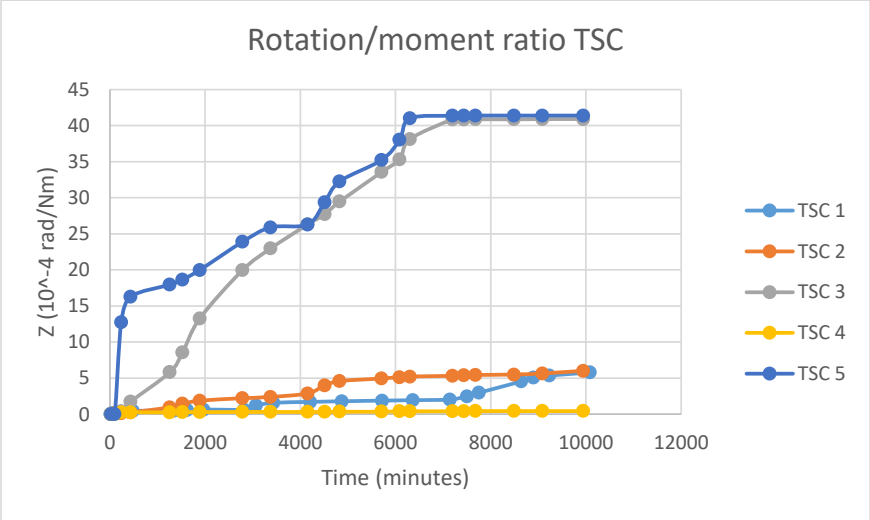

Figure 3.41 Rotation/moment ratio curves of the TSC – type specimens

days was 19.0e-4 rad/Nm, which is 2.2 times the average Z – value of this type of joints in static loading in the steepest slope of load-deflection curve, corresponding to load levels up to 25 to 35 per cent. If we take the secant coefficient at maximum load in static bending for basis of comparison, this coefficient is doubled. Further increase with continued loading can be foreseen in the case of test piece No 1. However, it has to be noted that creep results of the five test pieces in this group are so much scattered that any statistical inference can only considered with due discretion.

3.3.5 Comparison and statistical analysis of the change of rotation/moment ratio as a measure of creep

Increase of the initial Z coefficients of the joint types in the course of the creep test

The data in Table 3.29 were calculated, as outlined in Section 3.3.4, by subtracting the first deflection reading from every consecutive reading of time-dependent deflection values, and calculating first the corresponding angle changes. The angle changes divided by the bending moment acting on the test piece give the time-dependent increments of the Z-coefficient of the joint. The increment corresponding to the time of the first reading is hence zero, such as the creep belonging to the first reading is taken zero. The values in Table 3.29 are 104 times the actual values.

Test piece No	LBWD 1st day	LSWD 1st day	LBC 1st day	LSC 1st day
1	12.68	0.63	X	3.55
2	4.33	0.76	3.45	1.56
3	5.16	2.05	2.75	X
4	1.89	0.75	3.99	3.95
5	3.1	0.89	5.25	4.05
6			2.5	
AVERAGE	5.43	1.02	3.59	3.28
SD	4.24	0.59	0.98	1.17
CV	0.78	0.58	0.27	0.36

(a)

Test piece No	LBWD	LSWD	LBC	LSC
1	13.76	1.33	X	5.17
2	7.08	2.76	3.45	4.04
3	7.56	4.04	6.25	X
4	1.89	3.05	7.34	7.42
5	4.41	2.59	12.07	7.51
6			4.94	
AVERAGE	6.94	2.75	6.81	6.04
SD	4.44	0.97	2.93	1.71
CV	0.64	0.35	0.43	0.28

(b)

Test piece No	TBWD 1st day	TSWD 1st day	TBC 1st day	TSC 1st day
1	4.13	1.03	10.43	0.54
2	7.85	X	4.74	1.95
3	5.2	0.42	3.93	8.58
4		2.9		18.69
5		2.78		0.27
AVERAGE	5.73	1.78	6.37	2.84
SD	1.92	1.34	3.54	7.85
CV	0.33	0.75	0.56	2.77

(a)

Test piece No	TBWD	TSWD	TBC	TSC
1	7.23	6.4	10.54	5.79
2	10.15	X	5.05	6.22
3	8.87	1.39	5.77	40.9
4		12.13		41.4
5		6.37		0.45
AVERAGE	8.75	6.57	7.12	18.95
SD	1.46	4.81	2.98	20.39
CV	0.17	0.73	0.42	1.08

(b)

Table 3.29 Z-coefficient increment data of test pieces by joint types. X - test pieces omitted from the analysis; corner joints 1st day (a), corner joints 7 days (b); T- joints 1st day (a), T-joints 7 days (b).

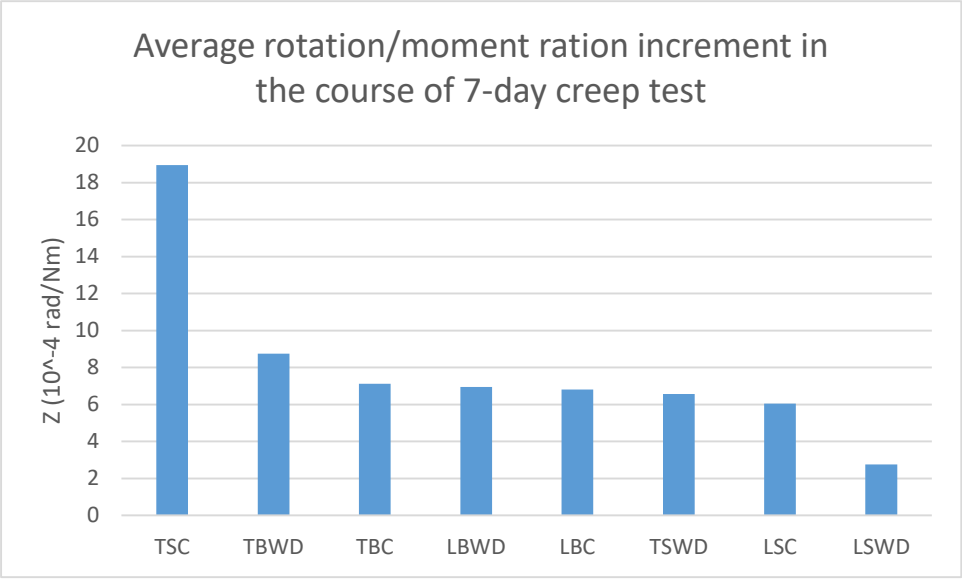

Figure 3.42 Comparison of the average rotation/ moment ratio increment by joint type

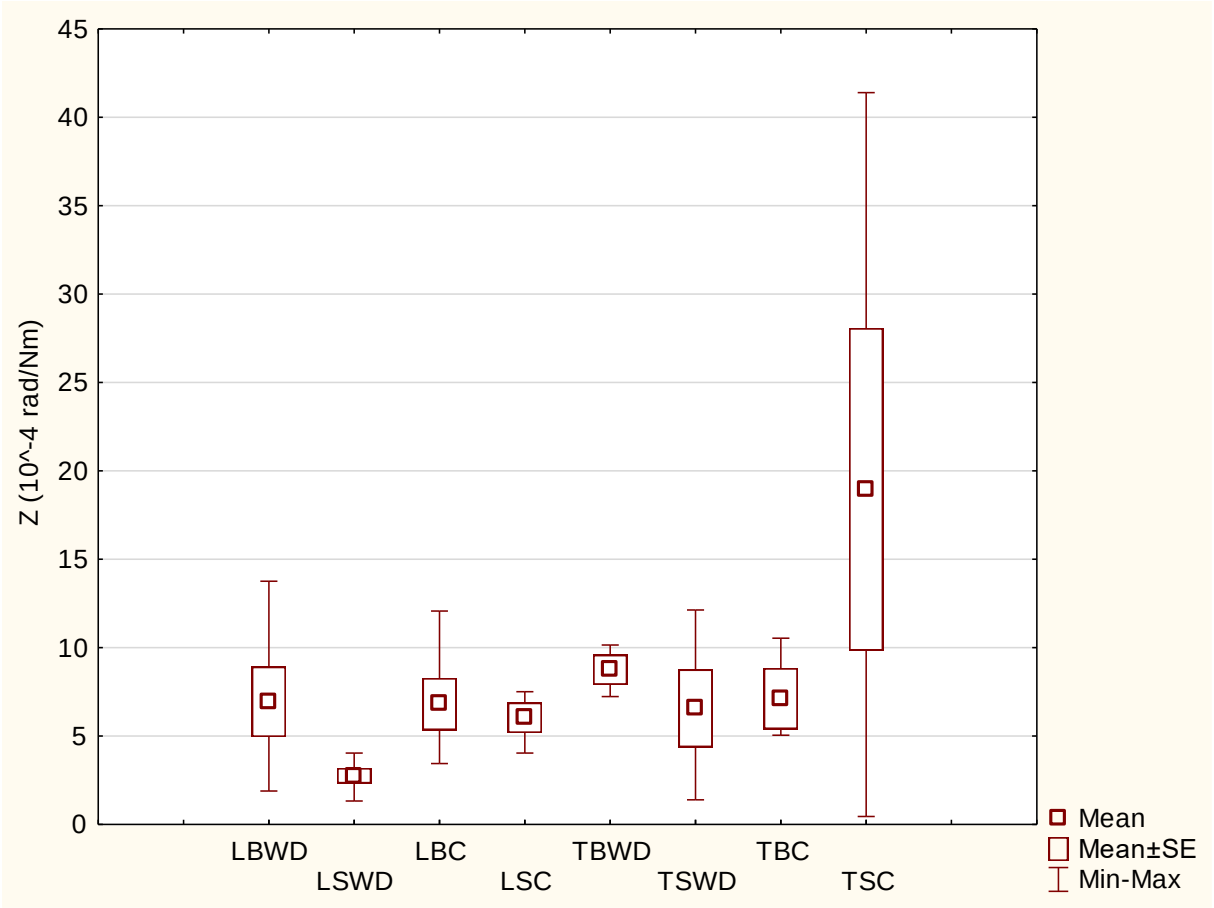

Figure 3.43 Box-plot of rotation/ moment ratio increment by joint type

Factorial ANOVA conducted on creep factor data proved significant difference between Z coefficient increment of small-size wood dowel and small-size metal connector specimens only. One-way ANOVA showed significant differences at the 0.05 level of significance between the results of TSC group and all other groups except for TBWD and TBC. These results should be considered with discretion because of the wide spread of data in the TSC group. However. *t*-test was found significant in the cases as follow: LSWD – LBC; LSWD – LSC; TBWD – LSWD; TBC – LSWD. i.e. the LSWD group's results are significantly different of the four above mentioned groups' results.

3.3.6 Comparison of the loss of rigidity of the different joint types in the course of sustained loading

Based on the load-deflection curves obtained in static bending test with compressive force. the load level applied in creep test fall within the range of highest rotational rigidity in the case of all joint types. Joint types with their respective loss of rigidity calculated as Z-value increment at the end of creep test over the initial Z-value in static bending are listed in Figure 3.43.

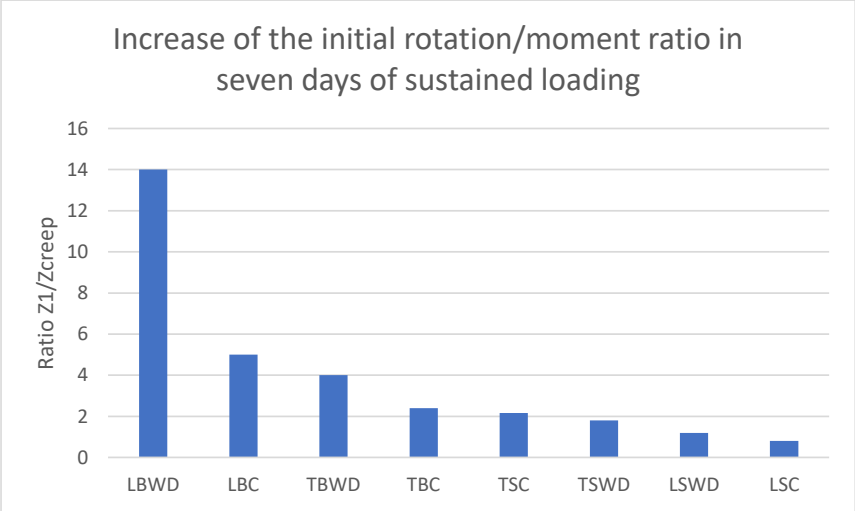

Figure 3.44 Loss of initial rigidity of the different joint types

According to Figure 3.43, the loss of rigidity in the course of sustained loading is higher in the case of big-size joint types. It can also be observed that the increase of the rotation/moment ratio of joints with wood dowel is higher than that of similar joints with metal connector. Furthermore, in the case of big-size samples corner joints seem to produce higher increase of the Z-value than T-joints do.

Probably the superiority of small-size joint types is due to the more favourable positioning of the connecting element in the wooden members with respect to the plane of bending. The loss of rigidity with respect to the secant rotation/moment ratio at ultimate load in static bending is shown in Figure 3.44.

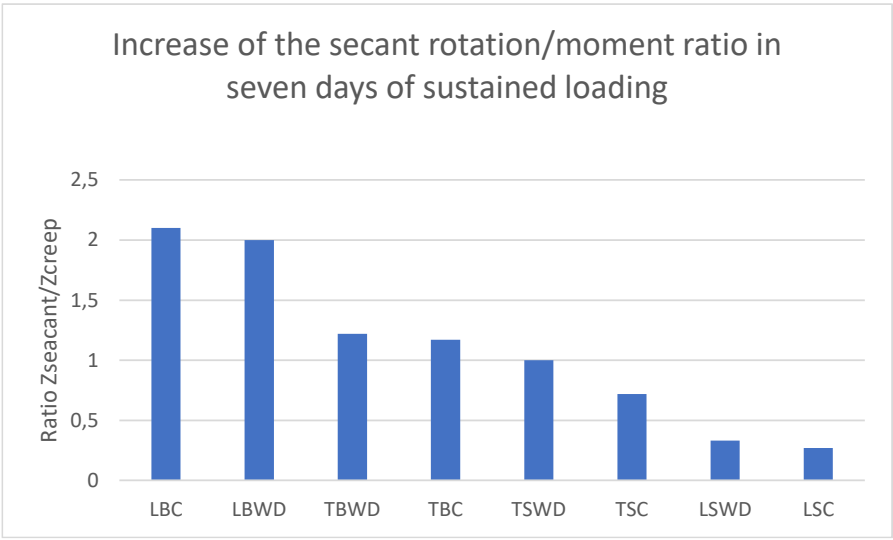

Figure 3.45 Loss of secant rigidity of the different joint types

The loss of rigidity as related to the secant value at ultimate load in static bending is higher at big-size specimens than small-size ones. In the case of big-size specimens, corner joints seem to produce higher increase of the Z-value than T-joints do. The contrary is evident with small-size specimens. The increase of the rotation/moment ratio of joints with wood dowel is higher than that of similar joints with metal connector in the case of small-size specimens as well as big-size T-joints. This is a further proof of superiority of joints with metal connectors in sustained loading.

In summary, we can state that the increase of the rotation/moment ratio of the tested Domino-type joints in the course of 7 days sustained loading may attain more than 10 times of the initial value. The increase of the secant ratio experienced at maximum load of static bending test does not exceed the double of this value.

4. CONCLUSIONS

This thesis work describes the completion of an experimental programme aiming to characterise the behaviour of Domino-type furniture joints under sustained as well as cyclic loading. Corner-joints and T-joints were prepared for loading in bending. Joints with two types of connectors. Domino wood dowel and dismountable Domino metallic connector were tested, both with two different sizes. For a proper planning of the sustained and the cyclic loading. it was necessary to obtain information on the performance of the individual joint types in static loading. Inplane bending using diagonal compressive as well as tensile force was applied to establish load-bearing capacity and deformation characteristics of the types of joints prepared for the study. As a result of the static bending tests, ranking of the joint types with respect to load carrying capacity and size of deformation was possible. Due to the differences in moment arm lengths and deflected member lengths used in static and duration of load tests for the different types of joints it seemed expedient to evaluate joint deformation in terms of angle change of the connected members per unit bending moment. From the load-deflection curves of the individual specimens, it was evident that the tested types of joints, as most of furniture joints fall into the category of semi-rigid or flexible joints. Angle change under unit bending moment is a usual measure of flexibility of these kinds of joints. As a spin-off of the research, work was the establishment of flexibility coefficients of the joint types under study. Based on the load-deflection curves the studied joints perform non-linear behaviour in terms of angle change; hence, their flexibility coefficient (rotation/moment ratio) is changing in the course of ramp

loading up to the ultimate load. In most of the cases, a linear or quasi-linear section occurs at lower load levels corresponding to the lowest flexibility (highest rigidity). Fortunately, loads in service conditions of furniture do not exceed this level. At ultimate load. a secant modulus of flexibility is revealing; the same was calculated for comparison.

As general trends in the responses to static bending loading, we found that big-size samples performed better than small size samples, corner-joints proved more resistant that T- joints, as well as joints with Domino wood dowel were superior to those with Domino metallic connector in terms of both load carrying capacity and deformation. The same applied to bending with compressive force and tensile force alike.

Cyclic loading tests conducted on the principles delineated in the standard EN 12512:2001 provided useful information on the fatigue properties of furniture joints tested. Generally, the joints started to lose their original strength during the repetition of the 75% amplitude level. At the end of the fatigue tests. It was possible to pull out the Domino wood dowels from the mortise, whilst this was not the case for the metallic Domino connectors. Therefore, the joints with metallic Domino connector can be considered more reliable, even if they deform more, but still maintain the integrity of the joint.

Creep behaviour of the joints was studied using dead loads for bending with load acting perpendicular to the deflecting member. The duration of creep tests was one week; two specimens suffered premature failure. Creep was evaluated by using two indices. One was creep factor, which is the ratio of time-dependent excess deflection divided by the initial elastic deflection. For the other index, we chose the option of using angle change of the joint per unit moment, as a measure of the change in joint flexibility in the course of creep test. This index calculated from the time-dependent deflection values is independent of the initial deflection. Besides, as mentioned above, it is independent of the moment arm and deflecting member length.

Both creep factor and the change of joint flexibility allowed ranking of the joint types with respect to their creep behaviour.

In terms of creep factor, the joint types LSWD and TSWD performed best, while the type TSWD proved to be the worst; the differences are quite important between the two ends of the rank (0.56 vs. 2.23). As a general trend, small-size samples performed better than their big-size

counterparts did. This finding is contrary to what we experienced in connection with the joints' behaviour in static bending. The possible reason for this may lie in the fact that big-size specimens are not only different with respect the member cross section and connector size. But in the positioning of the connecting element in the members as related to plane of the acting forces. Connectors in the big-size specimens are placed with their larger face perpendicular to the plane of bending moment, resulting this way smaller resistance that may not be counterbalanced by the larger sizes in the long term.

During the first day, the joints with metallic connector performed better than those with wood dowel did. However these differences vanished by the end of the 7-day test.

Logarithmic curves of the form

$$y = a \cdot \ln(t) + b$$

fitted to the creep factor data resulted generally high coefficient of determination. The coefficient a as a measure of initial creep rate turned out to be higher in the case of big-size specimens. This coefficient was also higher with T-joints in three of the four cases.

Considering the increase of rotation/moment ratios in the course of creep tests small-size joint types showed less increase than their big-size mates did, with the exception of the type TSC. It should be noted, that the TSC-type specimens exhibited exceptionally large scattering of this index, making their ranking uncertain.

Comparing the increase of flexibility coefficient to the initial value obtained in static bending for the same type of joints provided a more relevant kind if index for the change in joint rigidity in the course of sustained loading.

The loss of rigidity is higher in the case of big-size joint types. It can also be observed that the increase of the rotation/moment ratio of joints with wood dowel is higher than that of similar joints with metal connector. Furthermore. In the case of big-size samples corner joints seem to produce higher increase of the Z-value than T-joints do.

The superiority of small-size joint types can be attributed to the more favourable positioning of the connecting element in the wooden members with respect to the plane of bending.

When relating loss of rigidity to the secant modulus obtained in static bending, small-size specimens performed better than their big-size counterparts did. Furthermore, the increase of the rotation/moment ratio of joints with wood dowel is higher than that of similar joints with

metal connector I again with the exception of the type TSC. This is a further proof of superiority of joints with metal connectors in sustained loading.

In summary, we can state that the increase of the rotation/moment ratio of the tested Domino-type joints in the course of 7 days sustained loading may attain more than 10 times of the initial value. The increase of the secant ratio experienced at maximum load of static bending test does not exceed the double of this value. The positioning of the connecting elements with their wider face parallel with the plane of bending is beneficial from the point of stability of deformation in sustained loading. Furthermore, joints with Domino metallic connectors, while inferior in static loading regarding both load carrying capacity and the size of deformation, exhibit themselves less vulnerably by sustained loading.

THESES

1. Load carrying capacity of furniture joints made by using Domino wood dowels and Domino metallic connectors in static bending is governed by the size of connectors and member cross sections. Regardless of the position of their wider face when using the same wood species for the joint members. The ratio of small size specimens' load bearing capacity to that of big size ones is 57 to 82 per cent in case of the tested joint types.
2. T-joints have higher resistance in static bending than corner joints do. Their load carrying capacity is more than double of that of corner joints in the case of metallic connector; the ratio is 1.22 for small size and 1.61 for big size joints with wood dowel connector.
3. Deformation under unit moment of dismountable joints prepared with Domino metallic connector does not differ from that of their mates with wood dowel connector in the case of big size joints. In the case of small size joints, those with metallic connector are significantly more flexible.
4. Rotation/moment coefficients expressed in $10^{\wedge -4}$ rad /Nm indicating joint flexibility of semi-rigid joints in static bending were established for the types of joints under investigation. Both "working" values. i.e. measure of flexibility exhibited under service load (Z1) and final secant values based on deflection under ultimate load (Z) were established as below:

Joint type	Z1 (10^{-4} rad/Nm)	Z ($10^{\wedge -4}$ rad/Nm)
LBWD	0.51	3.4
LSWD	2.4	8.4
LBC	1.3	3.2
LSC	8.7	22
TBWD	2.2	5.4
TSWD	3.6	6.6
TBC	2.9	6.1
TSC	8.7	19

In summary "working" joint flexibility coefficients spread over the order of magnitude of $10^{\wedge -4}$ rad/Nm in case of joints using Domino connectors for joining beach wood members 40.0

to 41.5 mm wide in the plane of bending. Around double of this value can be accounted for as the secant flexibility coefficient at ultimate load.

5. Cyclic bending tests prove that joints of all tested types preserve their original strength after the completion of loading at 25% and 50% load level, and the first cycle of 75% load level based on deflection at ultimate load in static bending. The start of disintegration of the joining members can be accounted in the course of repeated cycles at 75% load level. Further load cycles lead to separation of the joining members in the case of joints with Domino wood dowel. In contrast, dismountable joints do not let the members separate after the test, allowing further functioning. This proves the superiority of dismountable Domino-type joints in dynamic loading.
6. Big size joints under sustained loading exhibit significantly higher creep than their small-size counterparts, despite the fact that big-size joints are stronger than small size ones. At the end of the seven days loading period, no systematic difference can be traced with respect to connector type. L. or T joint configuration. Average creep factors after the first 24 hours range between 0.17 and 1.25 while at the end of the sustained loading test between 0.56 and 2.23.
7. Logarithmic functions of the form

   $$y = a \cdot \ln(t) + b$$

   can be fitted on the creep factor data with high value of the coefficient of determination. The coefficient a in the equation as a measure of the initial creep rate is higher in the case of big-size specimens. This is reflected in the creep curves. The coefficient is also higher with T-joints with the exception of the TSC joint group of exceptionally high scattering of creep data.

8. Creep test results expressed as the increase of the joint's flexibility (Z rad/Nm) do not depend on the initial deflection of test pieces. These increments related to the initial "working" value of joint flexibility as well as to the secant flexibility of the same type are indicators of the joints' creep behavior. The ratios of increment to initial value are higher in the case of big-size joint types. In the case of big-size samples, corner joints produce higher increase of the Z-value than T-joints do. The increase of the Z-value of joints with wood dowel is higher than that of similar joints with metal connectors.

This is a further proof of the superiority of joints with metal connectors in sustained loading.

These statements are confirmed when the Z-value increments due to creep are related to the secant valuesobserbved at ultimate load in static bending.

9. In summary, we can state that the increase of the rotation/moment ratio of the tested Domino-type joints in the course of 7 days sustained loading may attain more than 10 times of the initial value. The increase of the secant ratio experienced at maximum load of static bending test may grow to the double of this value.

The superiority of small-size joint types to big size ones in sustained loading is due to the more favourable positioning of the connecting element in the wooden members with respect to the plane of bending that overmounts the effect of larger size of connector and member cross section.

APPENDIX

A - Load–displacement curves of static tests

1. Bending by compressive force

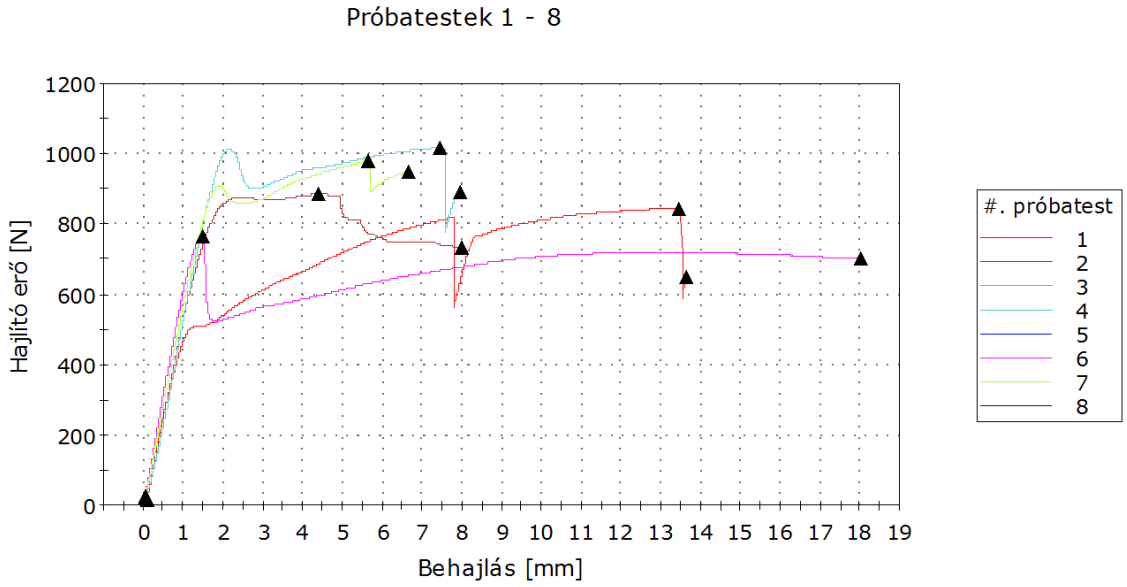

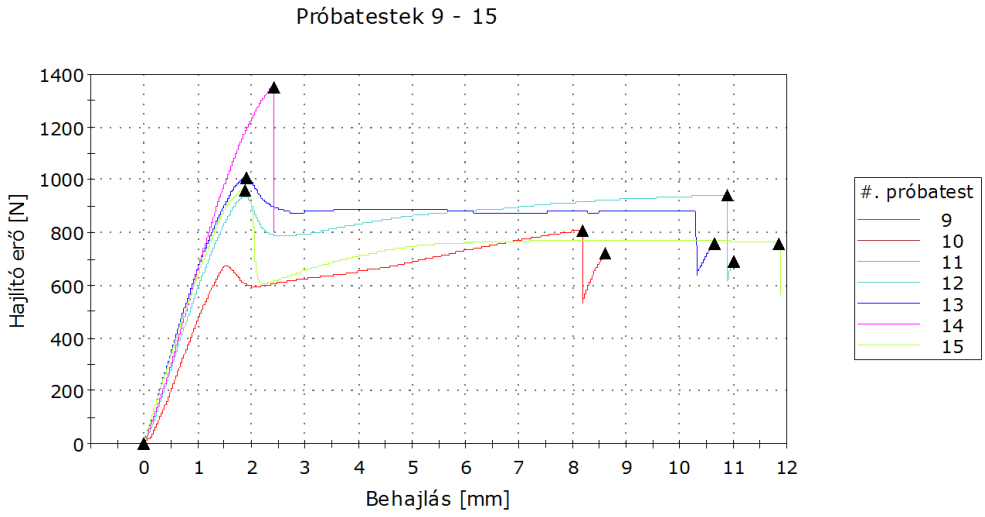

Figures A-1 Load-displacement curves. LBWD-type specimens, bending by compressive force

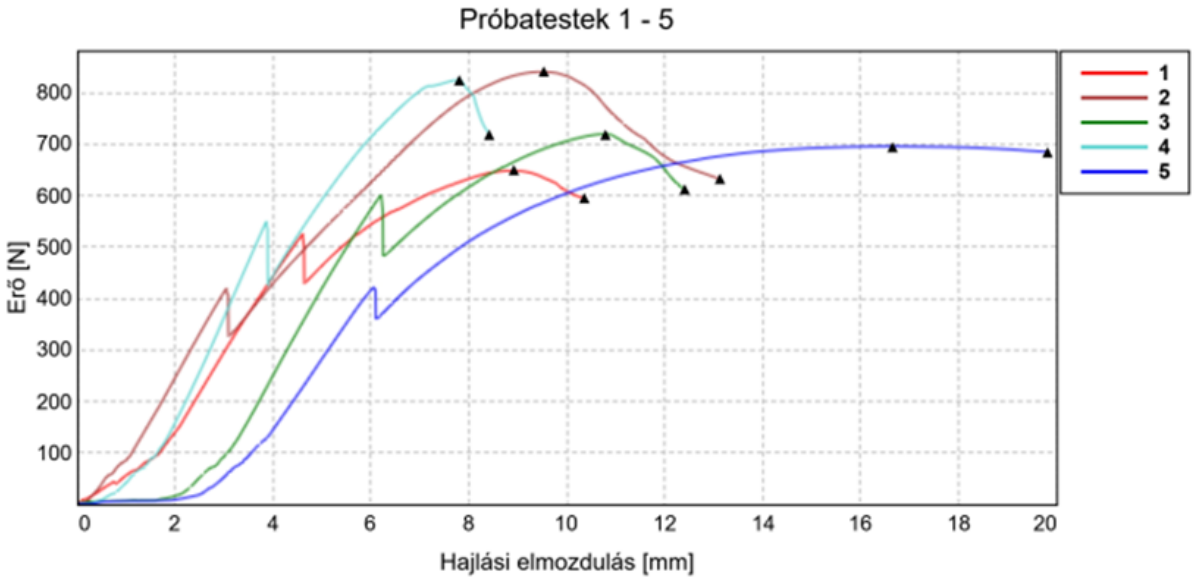

Figure A-2 Load-displacement curves. LSWD-type specimens, bending by compressive force

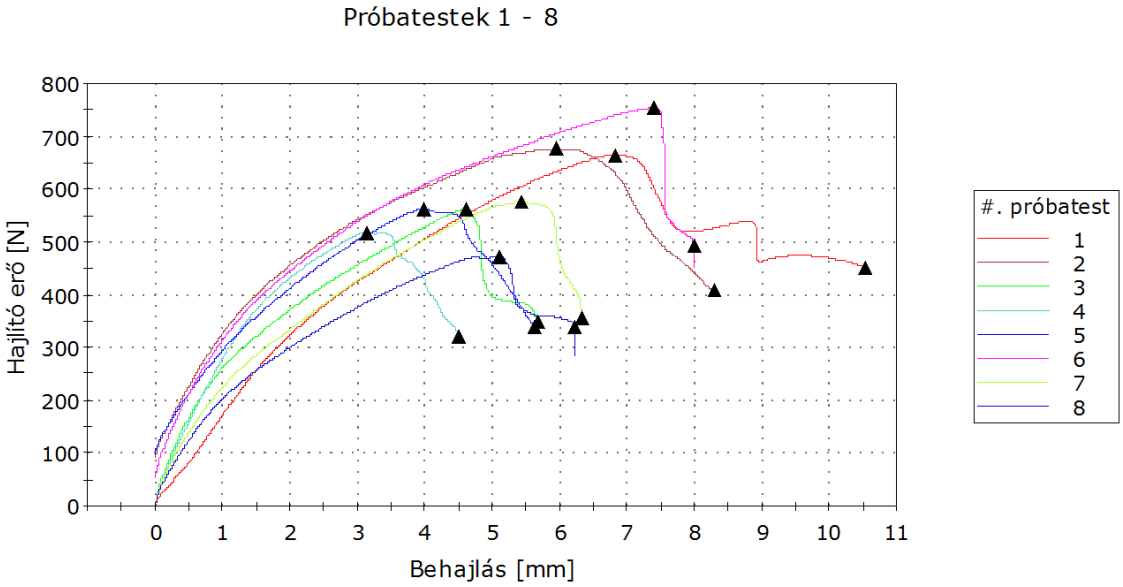

Figure A-3 Load-displacement curves. LBC-type specimens, bending by compressive force

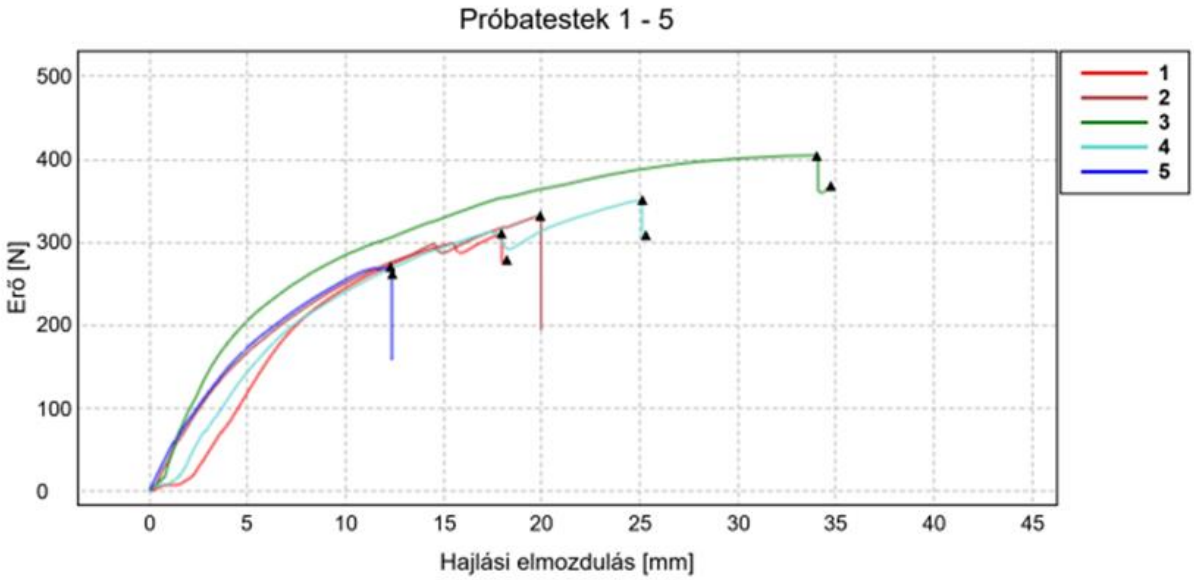

Figure A-4 Load-displacement curves. LSC-type specimens, bending by compressive force

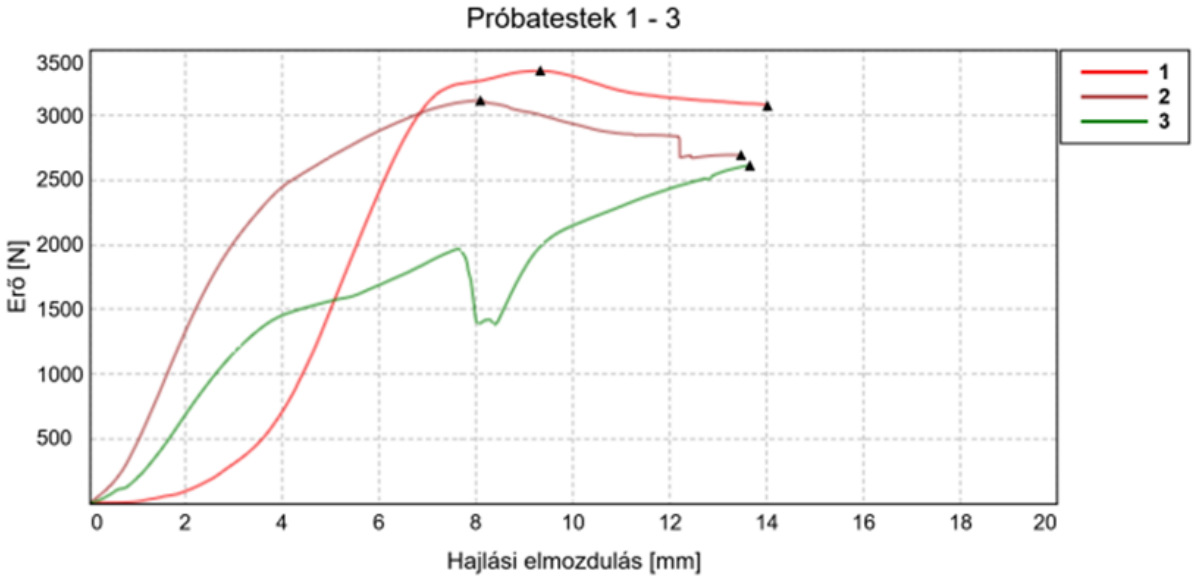

Figure A-5 Load-displacement curves. TBWD-type specimens, bending by compressive force

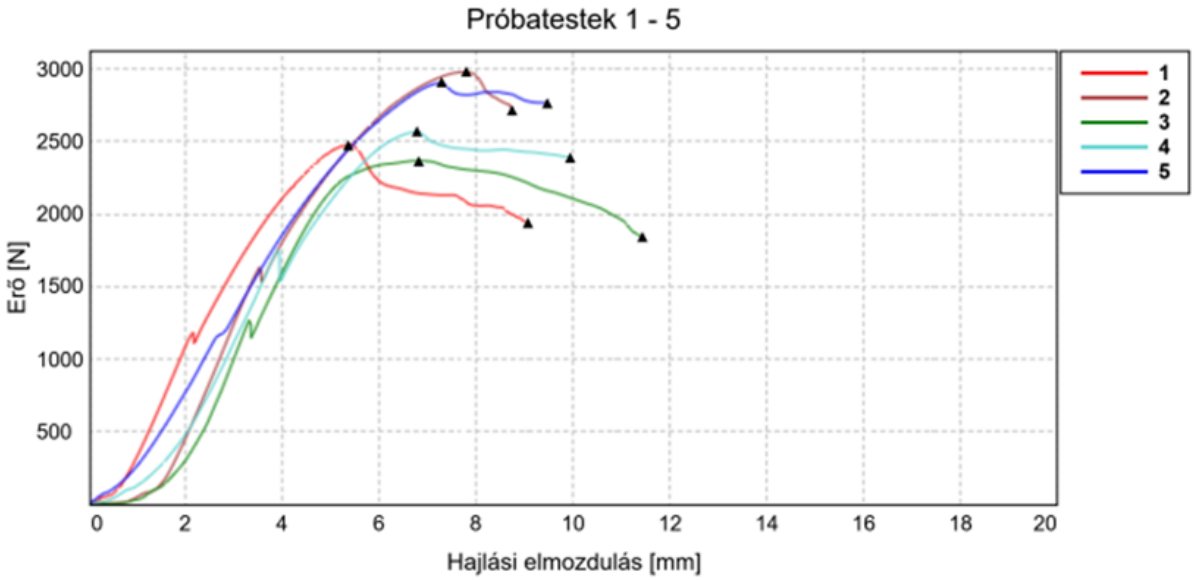

Figure A-6 Load-displacement curves. TSWD-type specimens, bending by compressive force

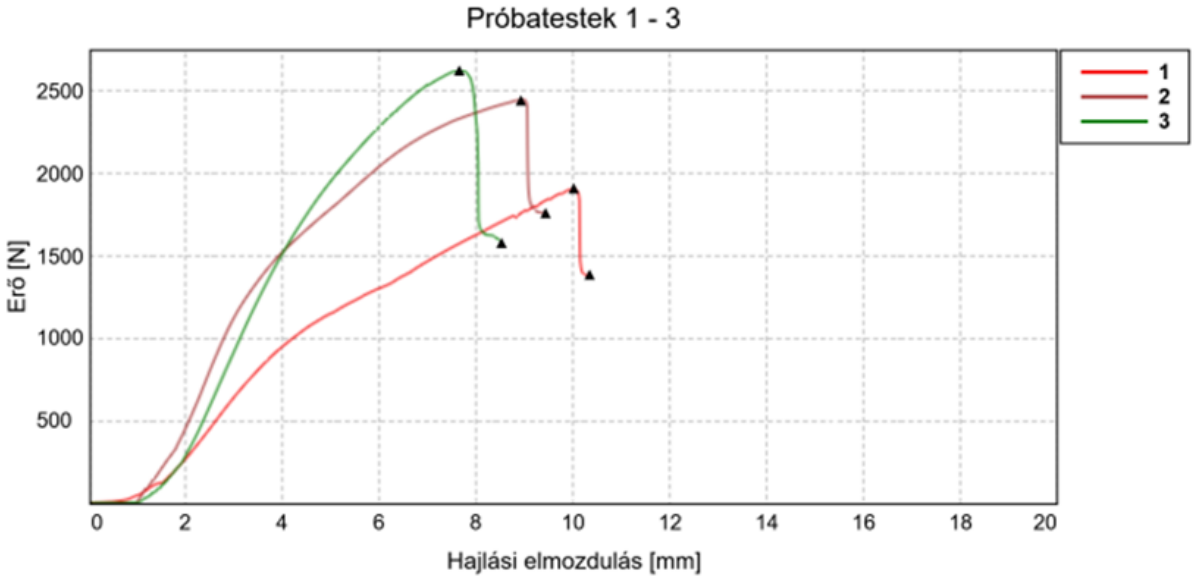

Figure A-7 Load-displacement curves. TBC-type specimens, bending by compressive force

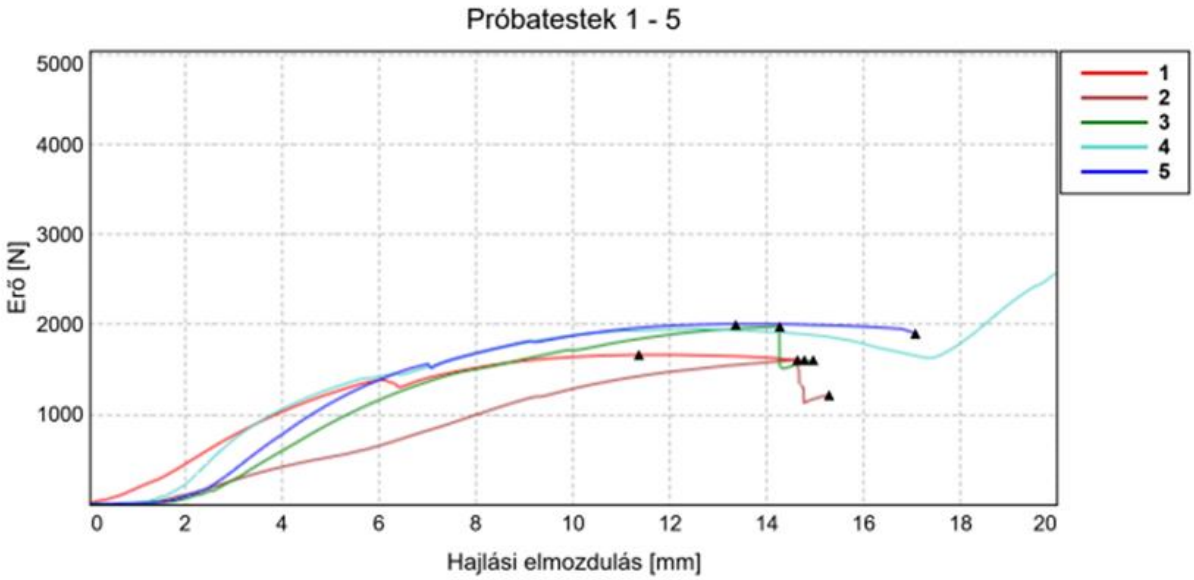

Figure A-8 Load-displacement curves. TSC-type specimens, bending by compressive force

2. Bending by tensile force

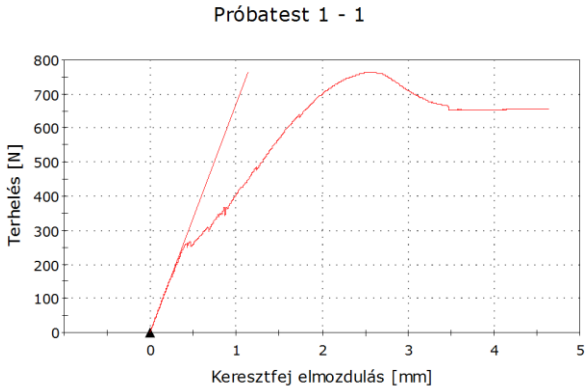

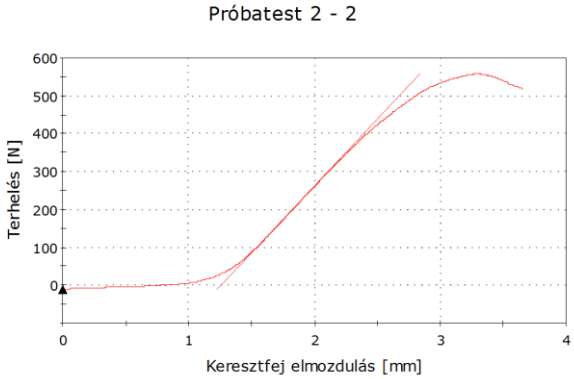

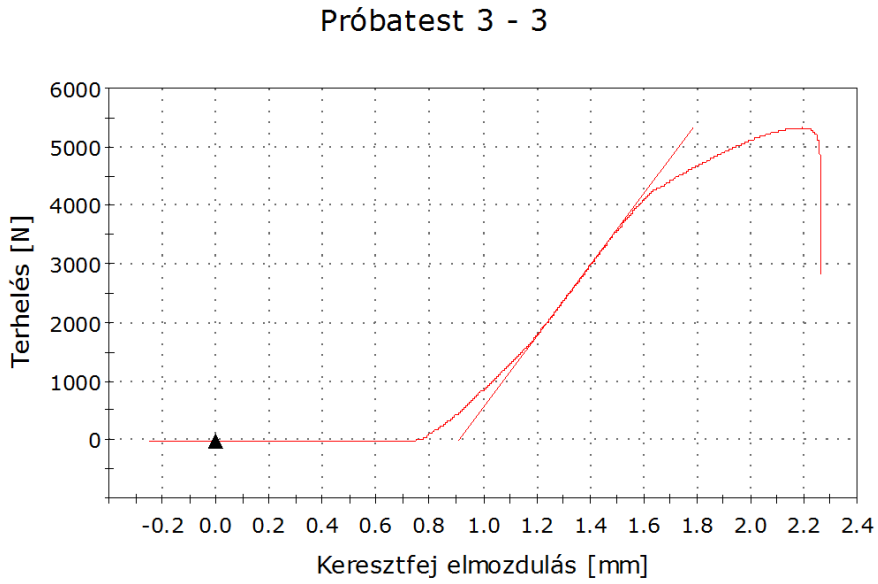

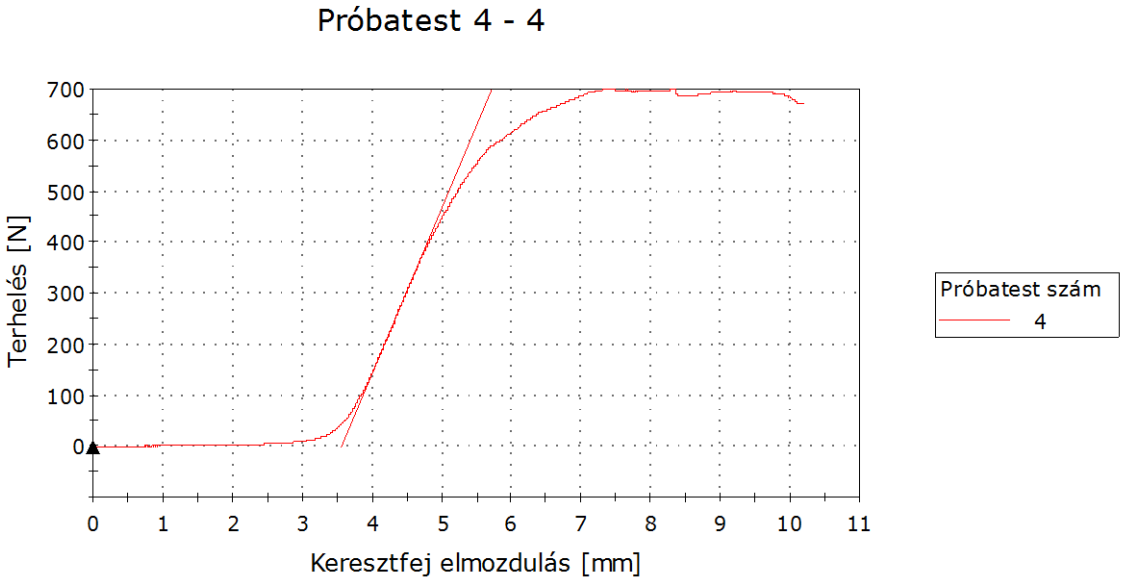
Próbatest 4 - 4
Terhelés [N]
700
600
500
400
300
200
100
0
0 1 2 3 4 5 6 7 8 9 10 11
Keresztfej elmozdulás [mm]
Próbatest szám
4

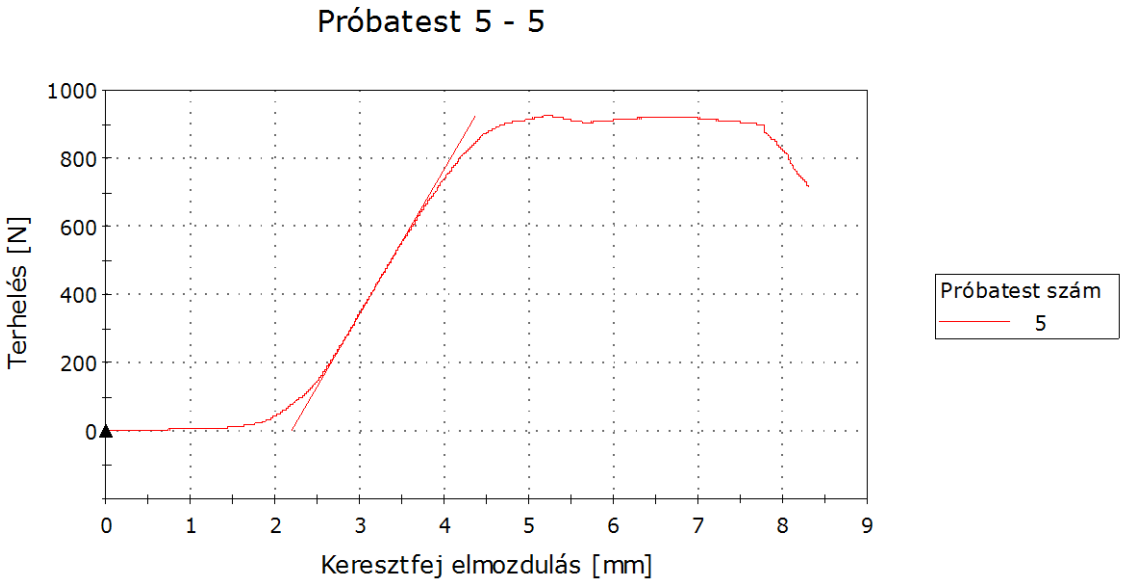
Próbatest 5 - 5
Terhelés [N]
1000
800
600
400
200
0
0 1 2 3 4 5 6 7 8 9
Keresztfej elmozdulás [mm]
Próbatest szám
5

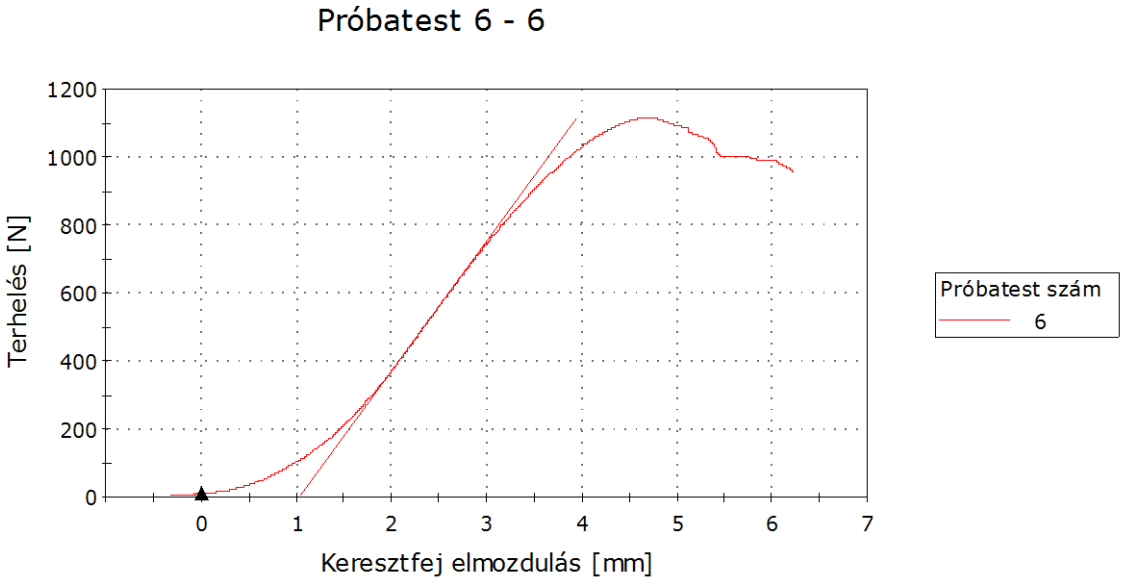
Próbatest 6 - 6
Terhelés [N]
1200
1000
800
600
400
200
0
0
1
2
3
4
5
6
7
Keresztfej elmozdulás [mm]
Próbatest szám
6

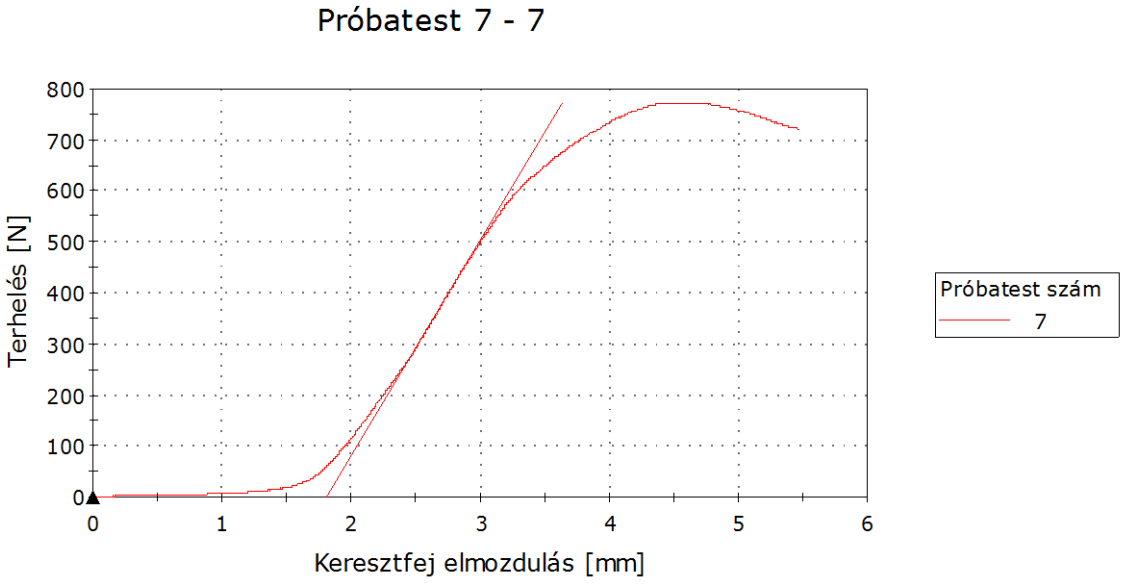
Próbatest 7 - 7
Terhelés [N]
800
700
600
500
400
300
200
100
0
0
1
2
3
4
5
6
Keresztfej elmozdulás [mm]
Próbatest szám
7

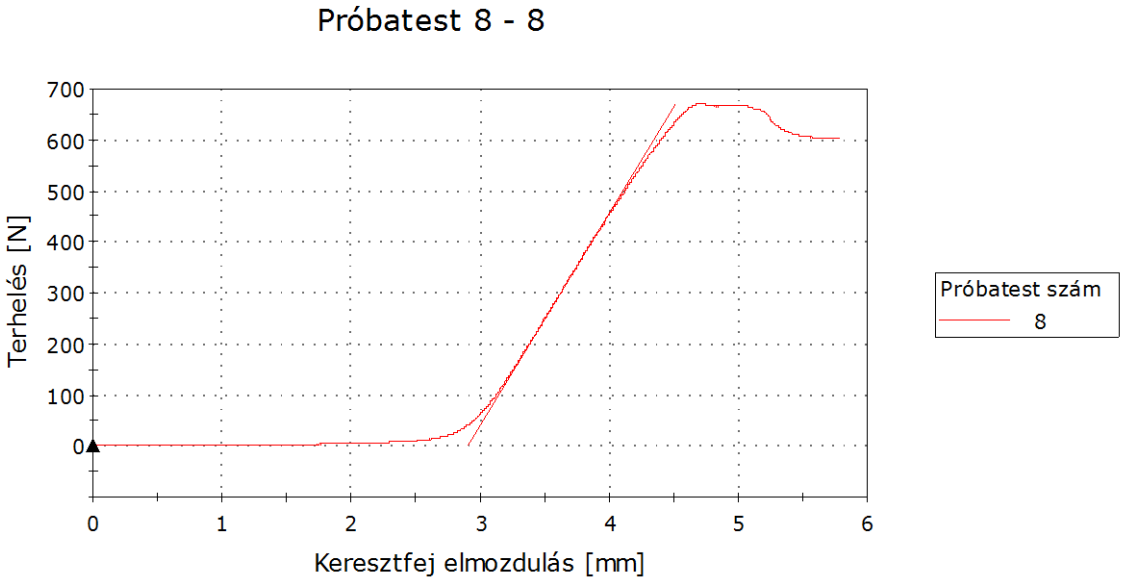
Próbatest 8 - 8
Terhelés [N]
700
600
500
400
300
200
100
0
0
1
2
3
4
5
6
Keresztfej elmozdulás [mm]
Próbatest szám
8

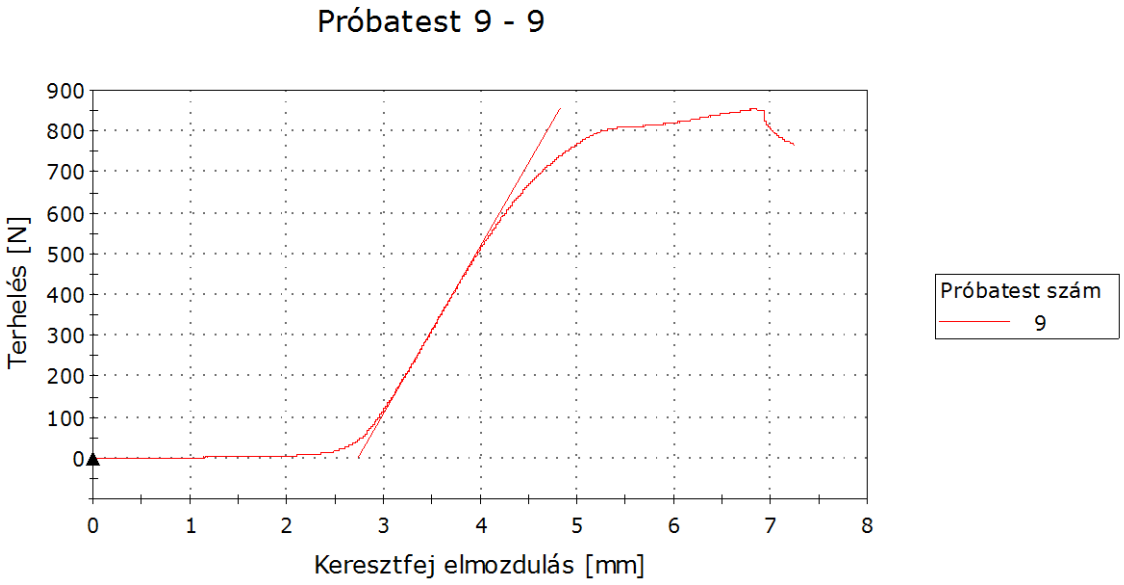
Próbatest 9 - 9
Terhelés [N]
900
800
700
600
500
400
300
200
100
0
0
1
2
3
4
5
6
7
8
Keresztfej elmozdulás [mm]
Próbatest szám
9

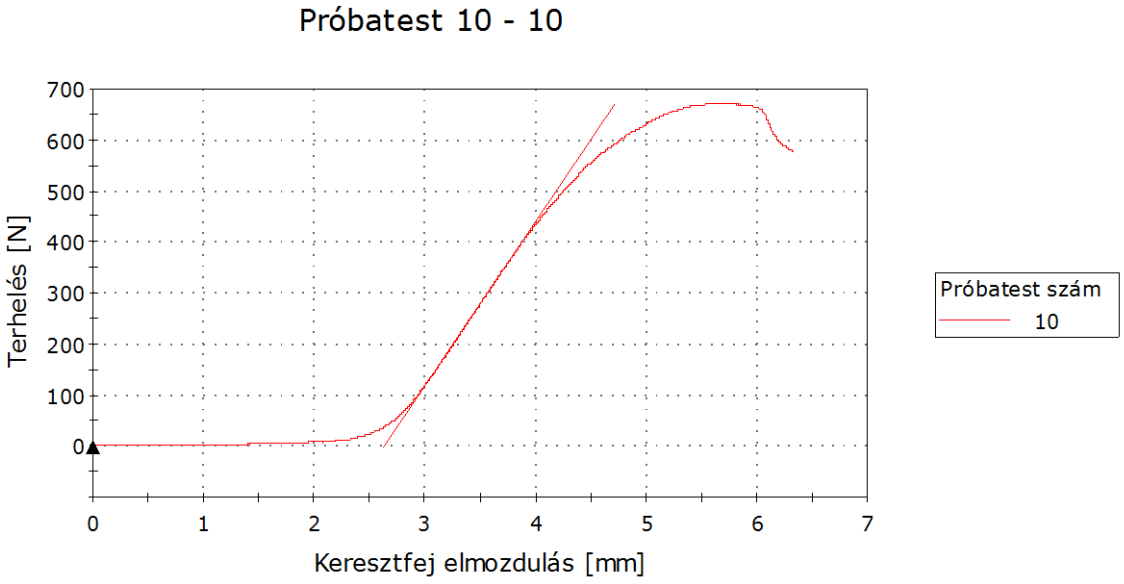

Figures A-9 to -18 Load-displacement curves. LBWD-type specimens, bending by tensile force

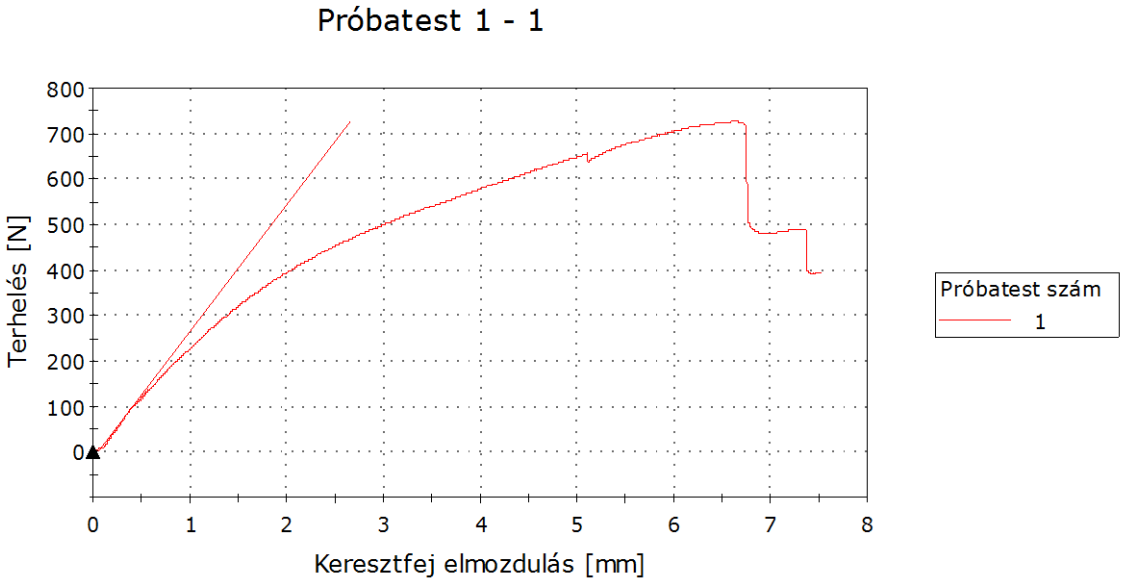

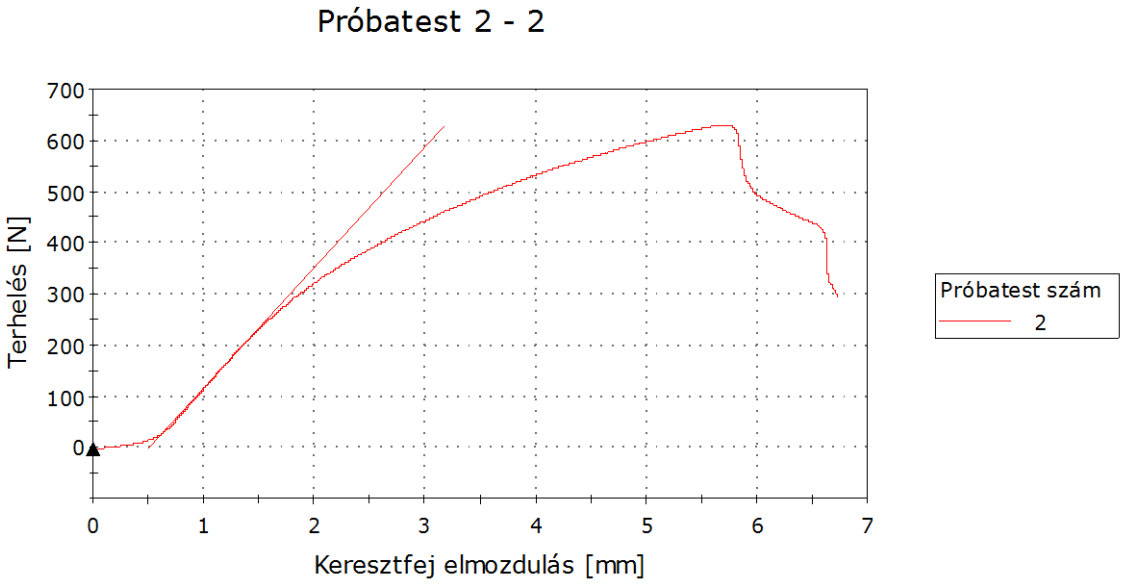
Próbatest 2 - 2
Terhelés [N]
700
600
500
400
300
200
100
0
0
1
2
3
4
5
6
7
Keresztfej elmozdulás [mm]
Próbatest szám
2

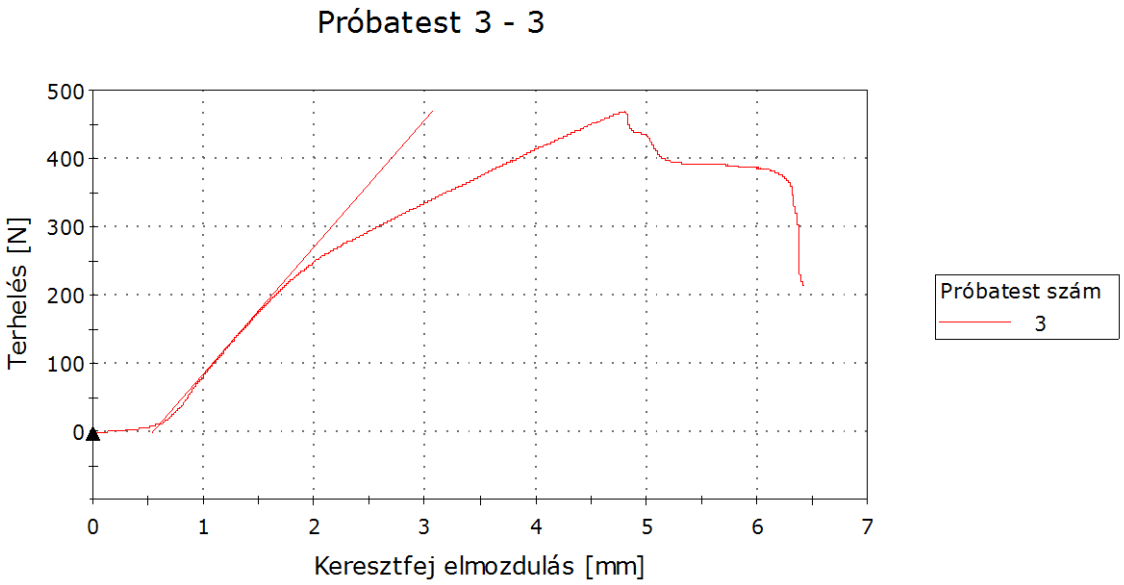
Próbatest 3 - 3
Terhelés [N]
500
400
300
200
100
0
0
1
2
3
4
5
6
7
Keresztfej elmozdulás [mm]
Próbatest szám
3

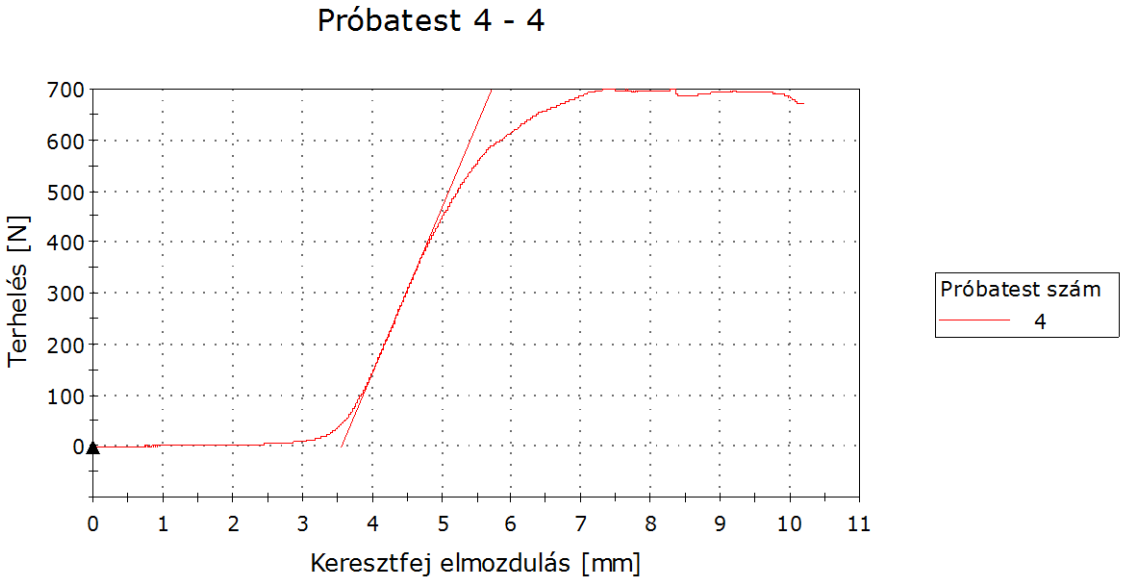
Próbatest 4 - 4
Terhelés [N]
700
600
500
400
300
200
100
0
0 1 2 3 4 5 6 7 8 9 10 11
Keresztfej elmozdulás [mm]
Próbatest szám
4

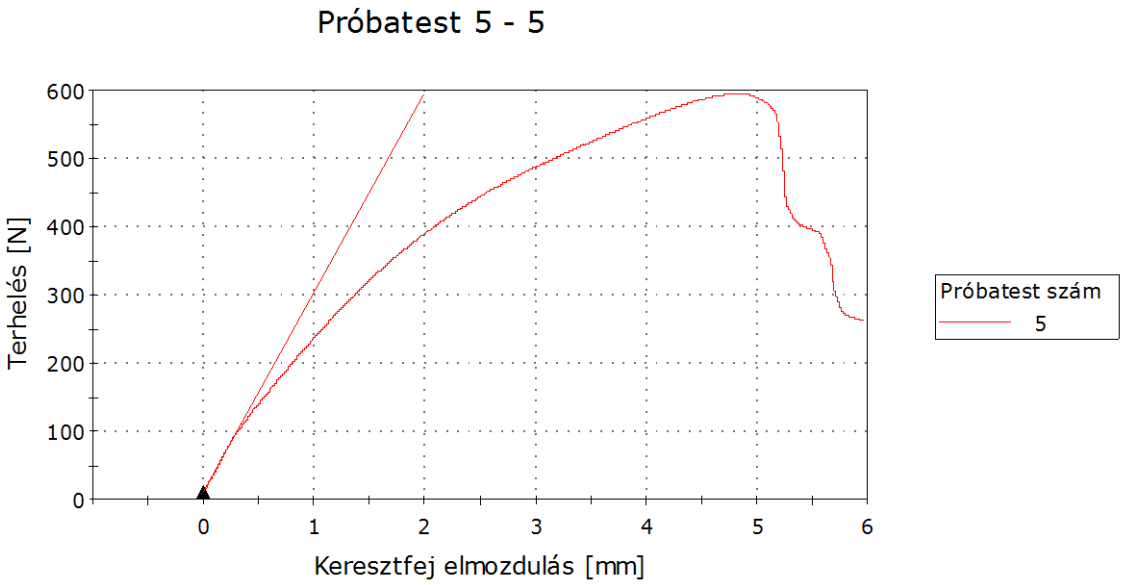
Próbatest 5 - 5
Terhelés [N]
600
500
400
300
200
100
0
0 1 2 3 4 5 6
Keresztfej elmozdulás [mm]
Próbatest szám
5

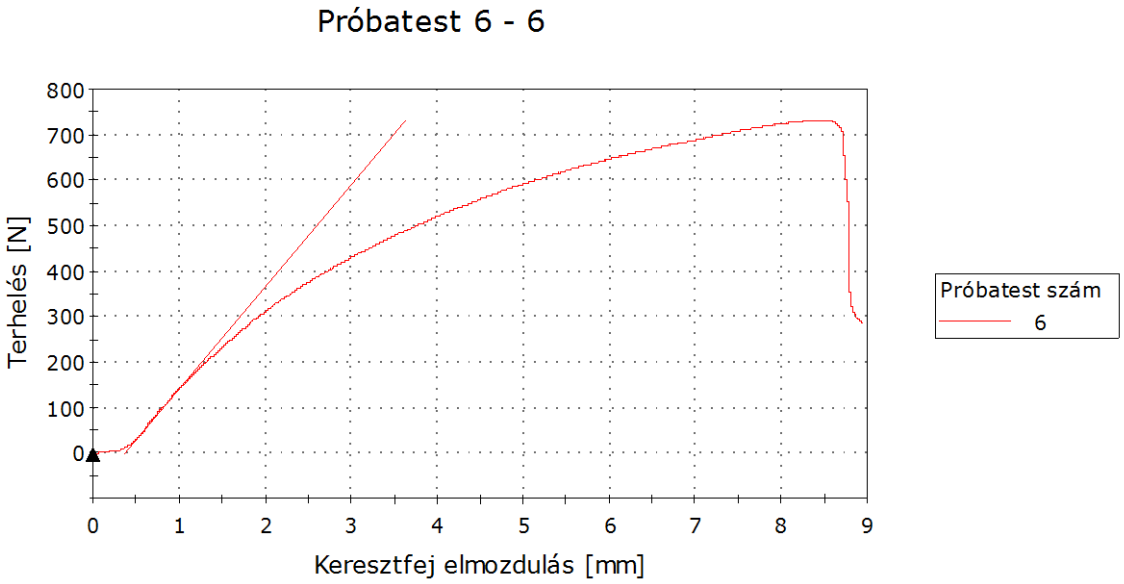
Próbatest 6 - 6
Terhelés [N]
800
700
600
500
400
300
200
100
0
0
1
2
3
4
5
6
7
8
9
Keresztfej elmozdulás [mm]
Próbatest szám
6

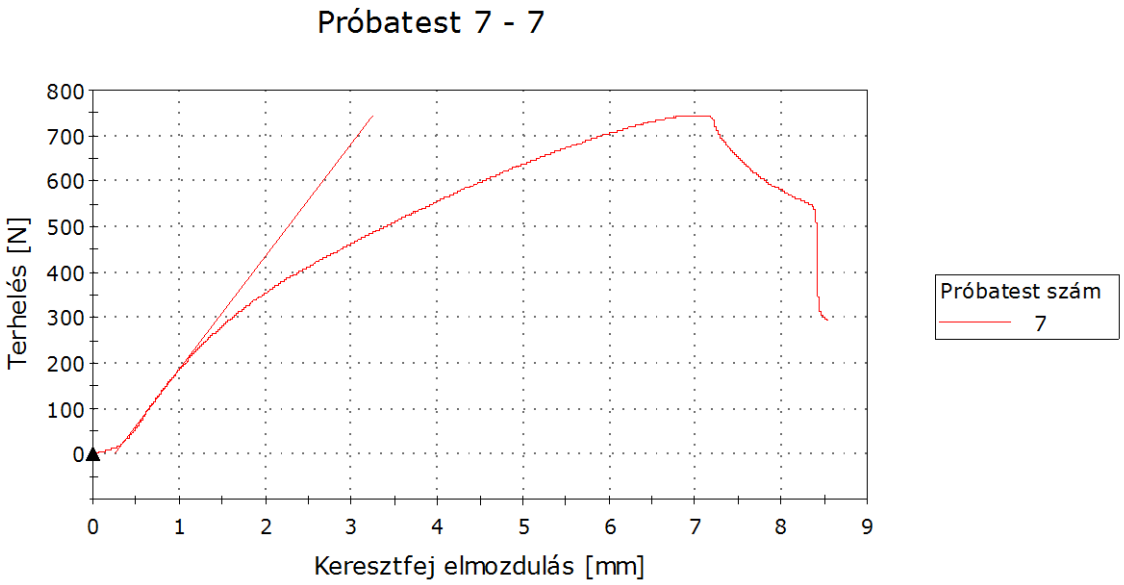
Próbatest 7 - 7
Terhelés [N]
800
700
600
500
400
300
200
100
0
0
1
2
3
4
5
6
7
8
9
Keresztfej elmozdulás [mm]
Próbatest szám
7

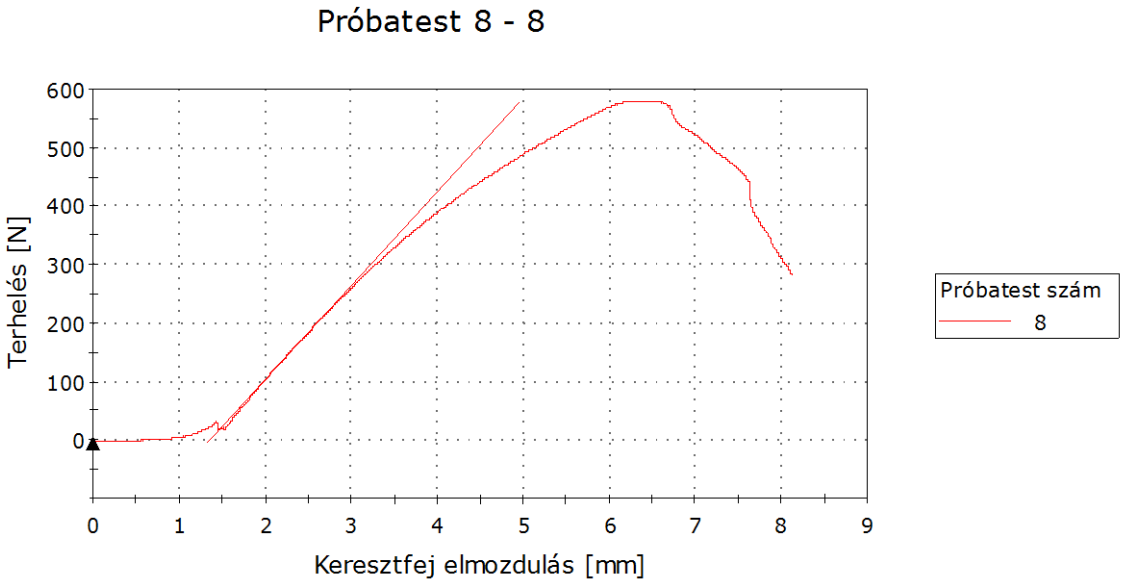
Próbatest 8 - 8
Terhelés [N]
600
500
400
300
200
100
0
0
1
2
3
4
5
6
7
8
9
Keresztfej elmozdulás [mm]
Próbatest szám
8

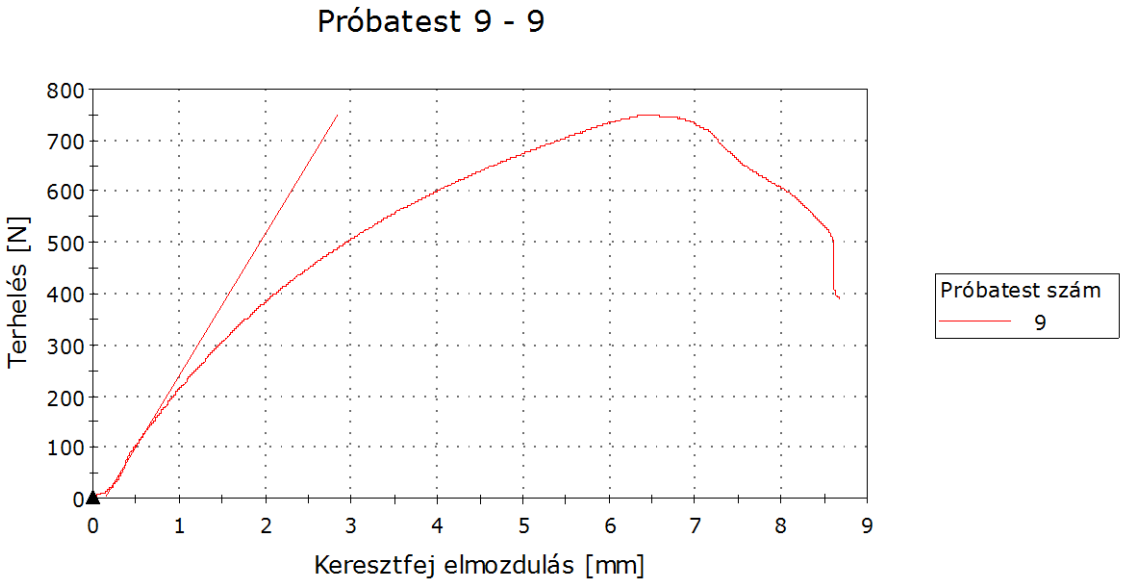
Próbatest 9 - 9
Terhelés [N]
800
700
600
500
400
300
200
100
0
0
1
2
3
4
5
6
7
8
9
Keresztfej elmozdulás [mm]
Próbatest szám
9

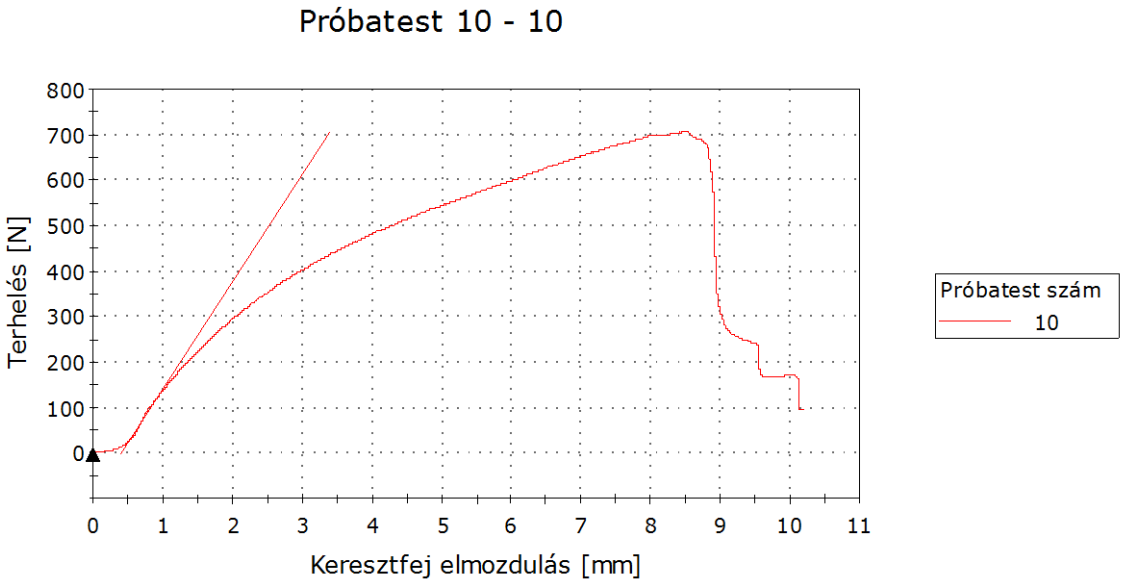

Figures A-19 to -28 Load-displacement curves. LBC-type specimens, bending by tensile force

3. Withdrawal tets of T-joints

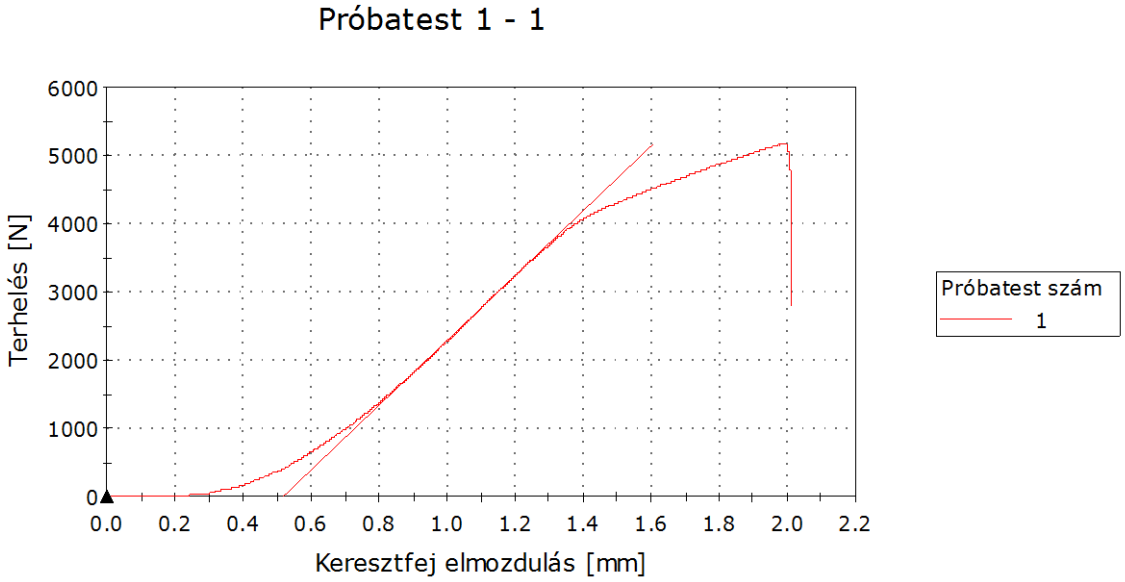

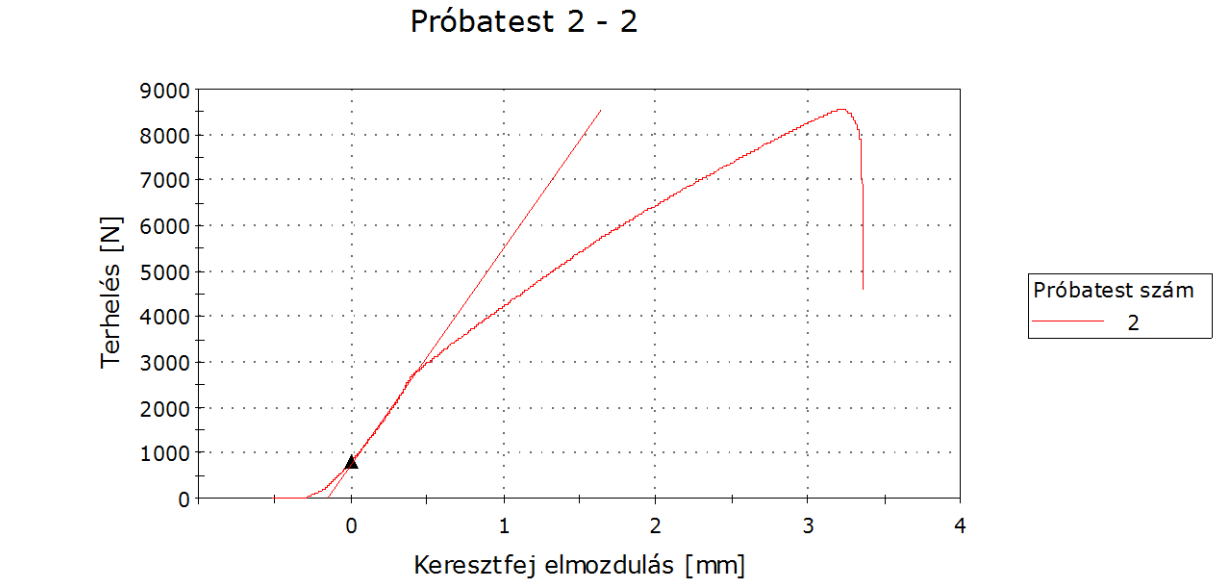
Próbatest 2 - 2
Terhelés [N]
9000
8000
7000
6000
5000
4000
3000
2000
1000
0
0
1
2
3
4
Keresztfej elmozdulás [mm]
Próbatest szám
2

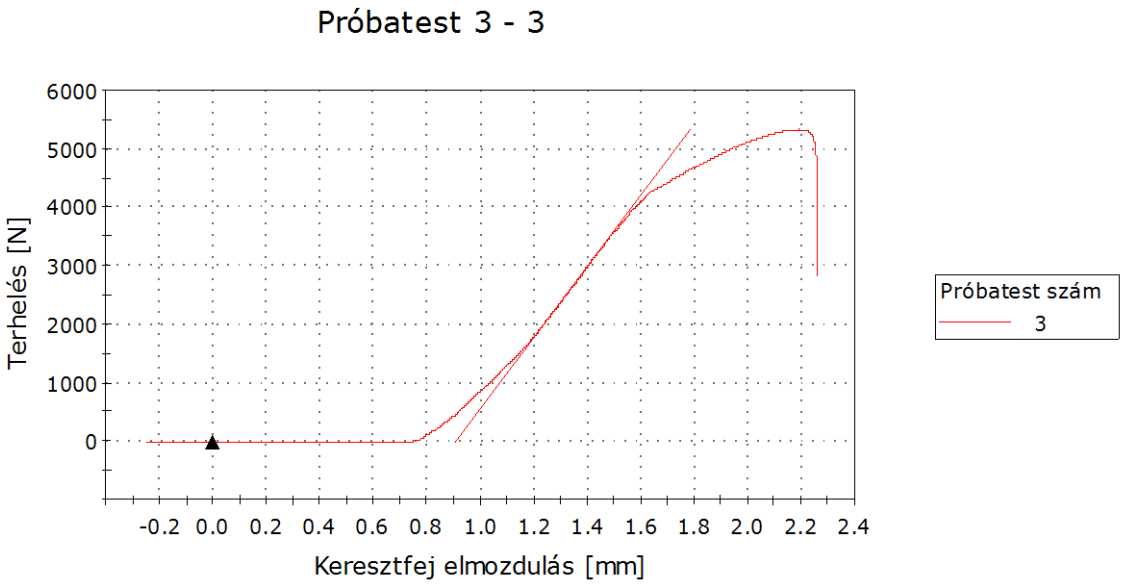
Próbatest 3 - 3
Terhelés [N]
6000
5000
4000
3000
2000
1000
0
-0.2
0.0
0.2
0.4
0.6
0.8
1.0
1.2
1.4
1.6
1.8
2.0
2.2
2.4
Keresztfej elmozdulás [mm]
Próbatest szám
3

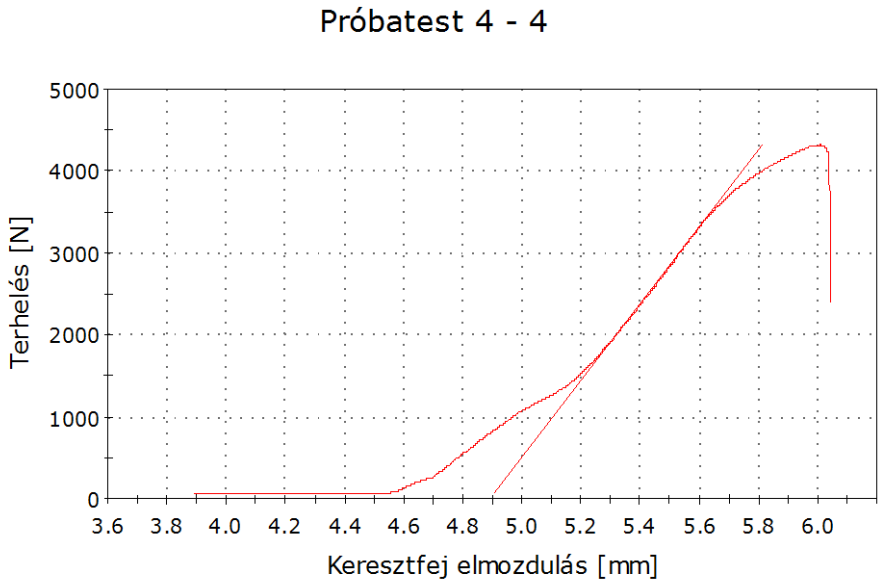
Próbatest 4 - 4
Terhelés [N]
5000
4000
3000
2000
1000
0
3.6
3.8
4.0
4.2
4.4
4.6
4.8
5.0
5.2
5.4
5.6
5.8
6.0
Keresztfej elmozdulás [mm]

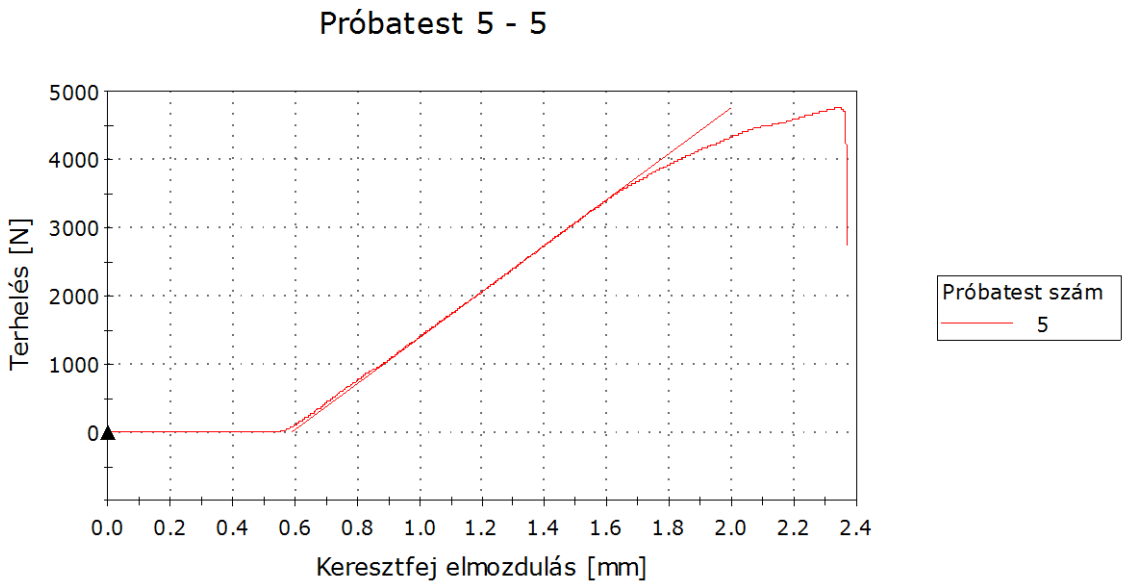
Próbatest 5 - 5
Terhelés [N]
5000
4000
3000
2000
1000
0
0.0
0.2
0.4
0.6
0.8
1.0
1.2
1.4
1.6
1.8
2.0
2.2
2.4
Keresztfej elmozdulás [mm]
Próbatest szám
5

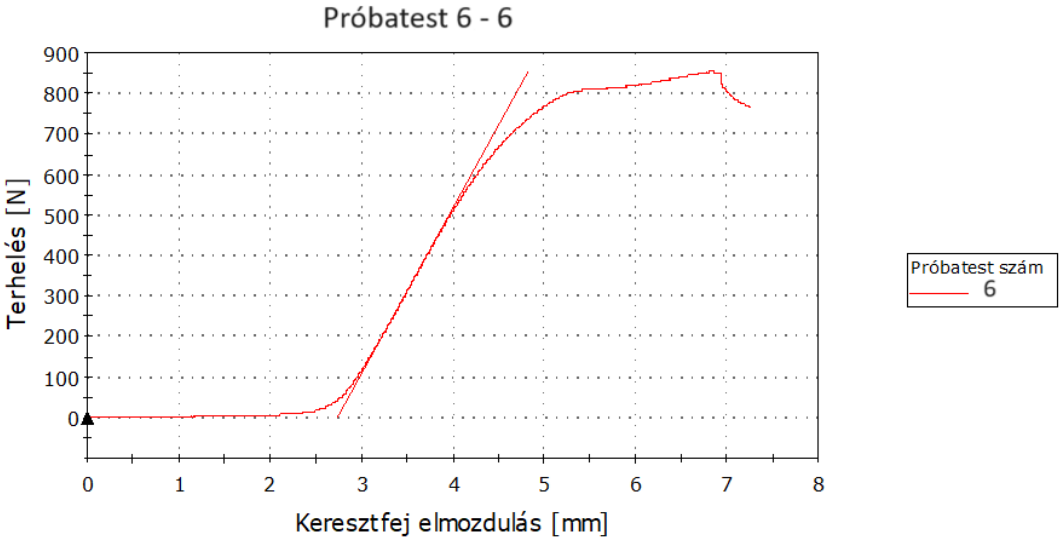
Próbatest 6 - 6
Terhelés [N]
900
800
700
600
500
400
300
200
100
0
0
1
2
3
4
5
6
7
8
Keresztfej elmozdulás [mm]
Próbatest szám
6

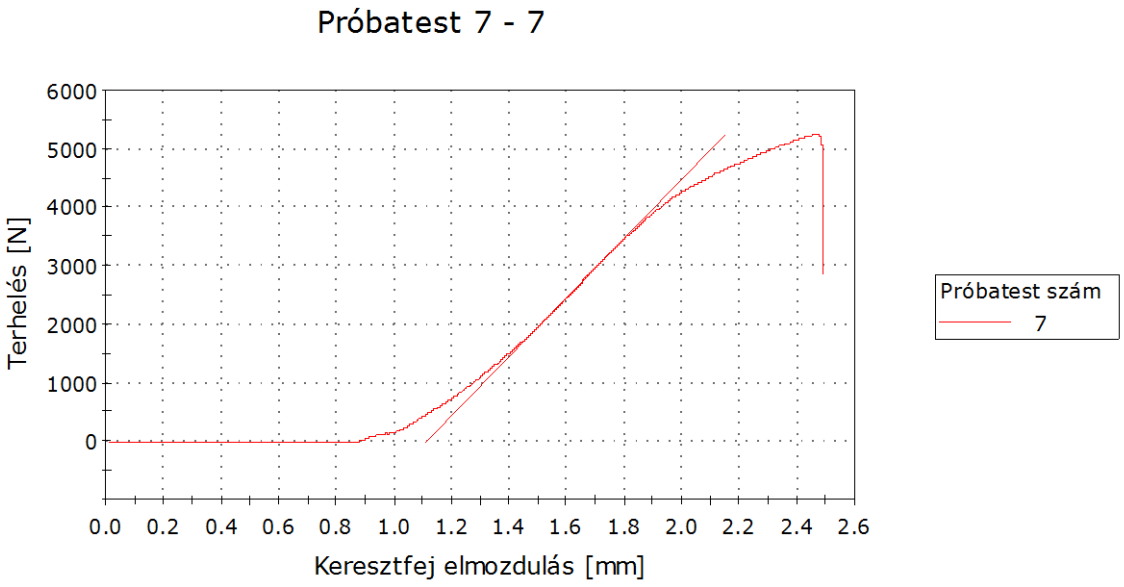
Próbatest 7 - 7
Terhelés [N]
6000
5000
4000
3000
2000
1000
0
0.0
0.2
0.4
0.6
0.8
1.0
1.2
1.4
1.6
1.8
2.0
2.2
2.4
2.6
Keresztfej elmozdulás [mm]
Próbatest szám
7

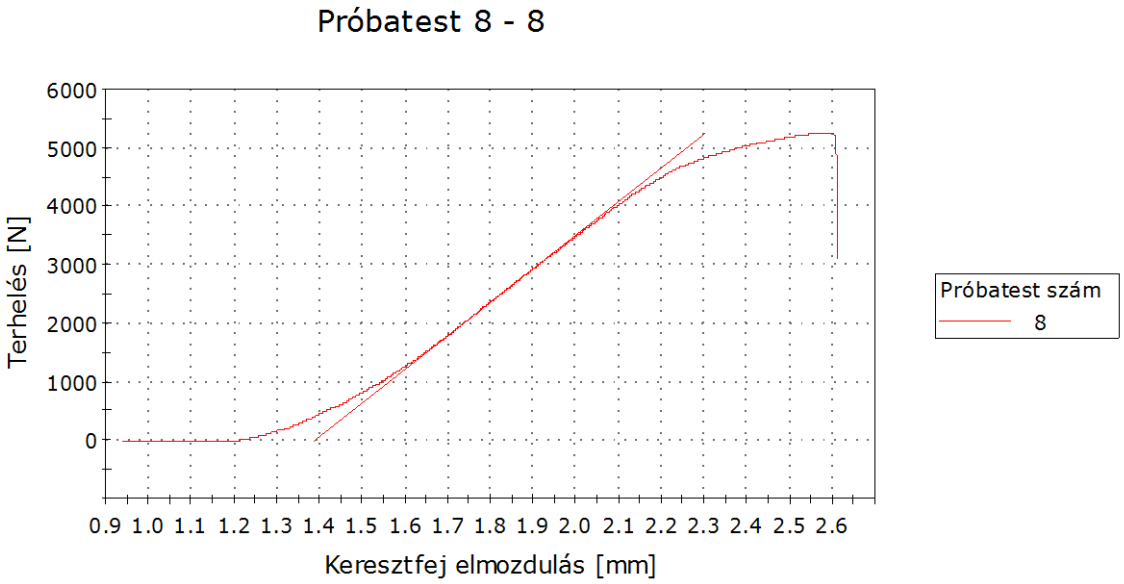
Próbatest 8 - 8
Terhelés [N]
6000
5000
4000
3000
2000
1000
0
0.9 1.0 1.1 1.2 1.3 1.4 1.5 1.6 1.7 1.8 1.9 2.0 2.1 2.2 2.3 2.4 2.5 2.6
Keresztfej elmozdulás [mm]
Próbatest szám
8

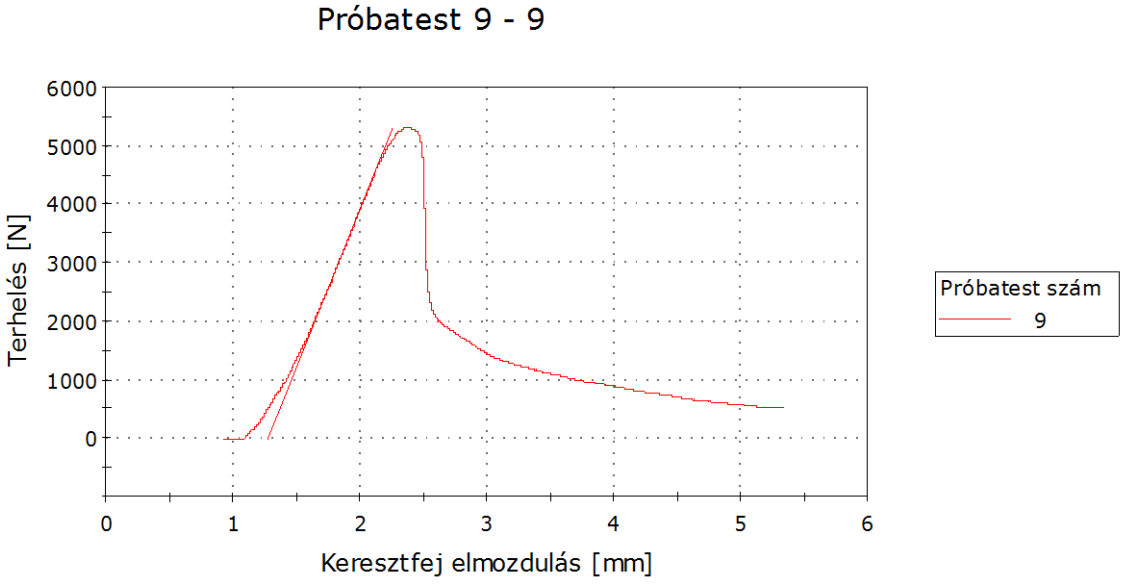
Próbatest 9 - 9
Terhelés [N]
6000
5000
4000
3000
2000
1000
0
0 1 2 3 4 5 6
Keresztfej elmozdulás [mm]
Próbatest szám
9

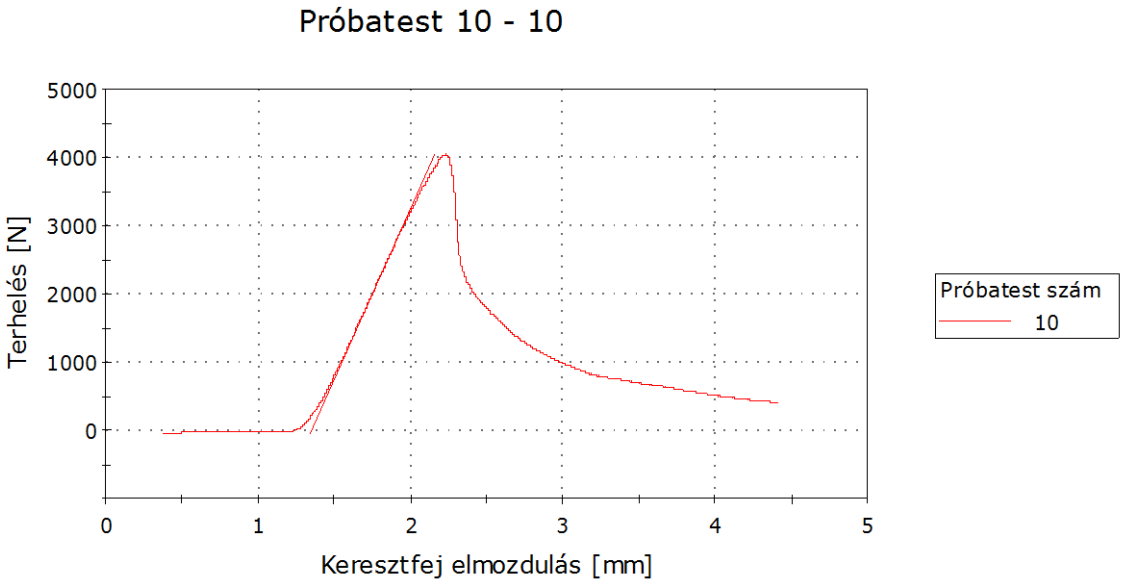

Figures A-29 to -38 Load-displacement curves. TBWD-type specimens, withdrawal test

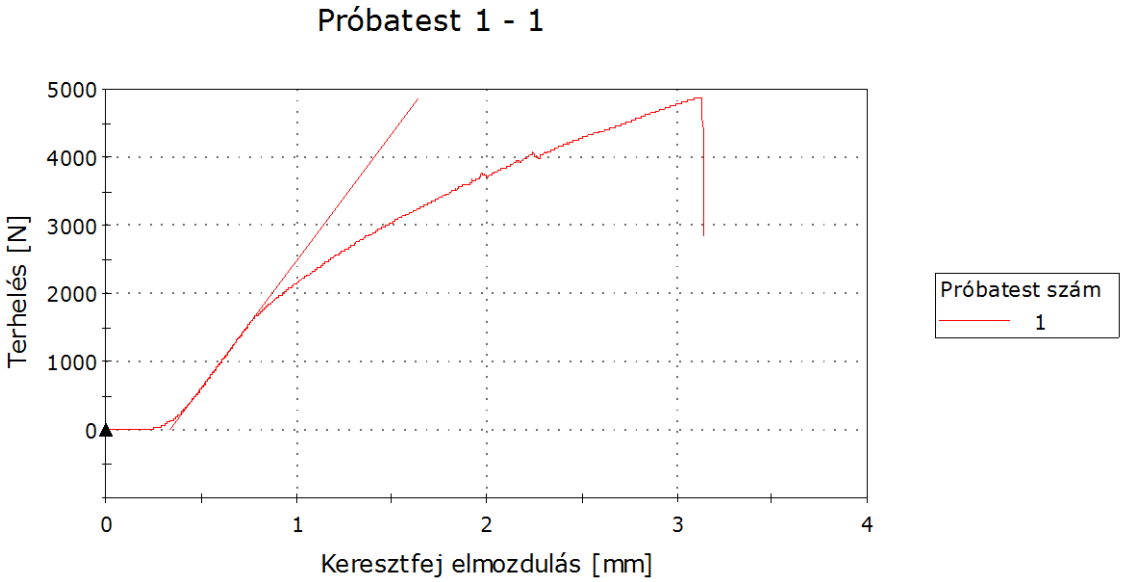

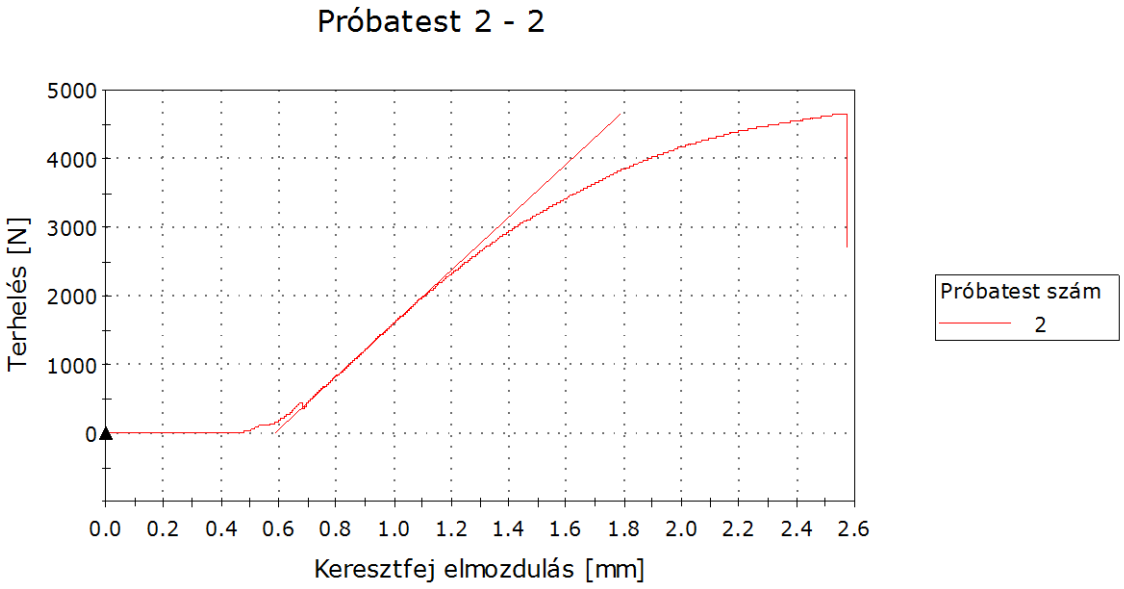
Próbatest 2 - 2
Terhelés [N]
5000
4000
3000
2000
1000
0
0.0
0.2
0.4
0.6
0.8
1.0
1.2
1.4
1.6
1.8
2.0
2.2
2.4
2.6
Keresztfej elmozdulás [mm]
Próbatest szám
2

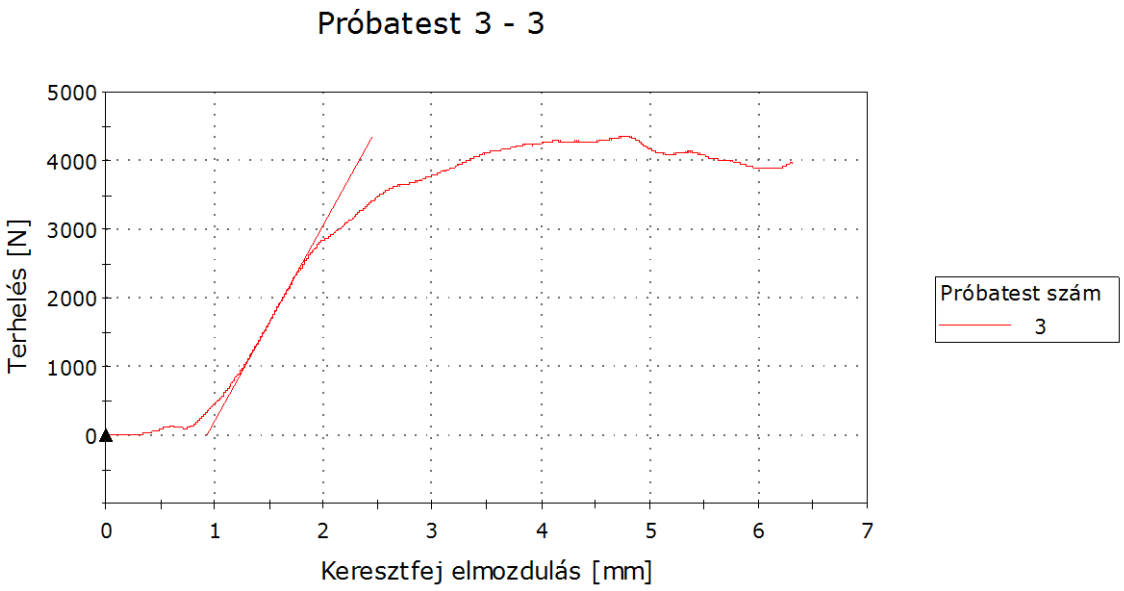
Próbatest 3 - 3
Terhelés [N]
5000
4000
3000
2000
1000
0
0
1
2
3
4
5
6
7
Keresztfej elmozdulás [mm]
Próbatest szám
3

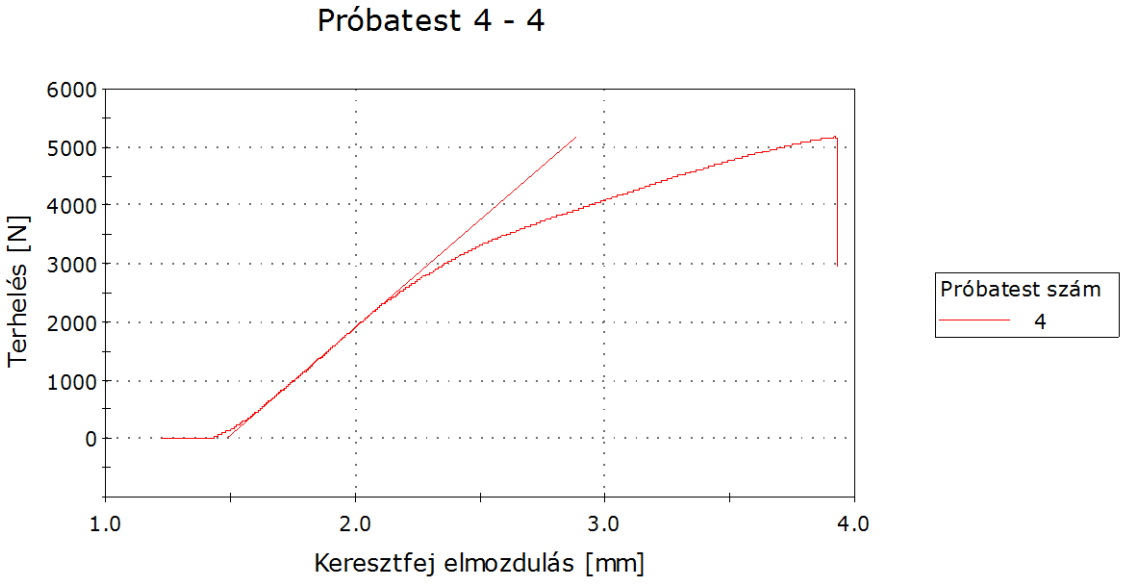
Próbatest 4 - 4
Terhelés [N]
6000
5000
4000
3000
2000
1000
0
1.0
2.0
3.0
4.0
Keresztfej elmozdulás [mm]
Próbatest szám
4

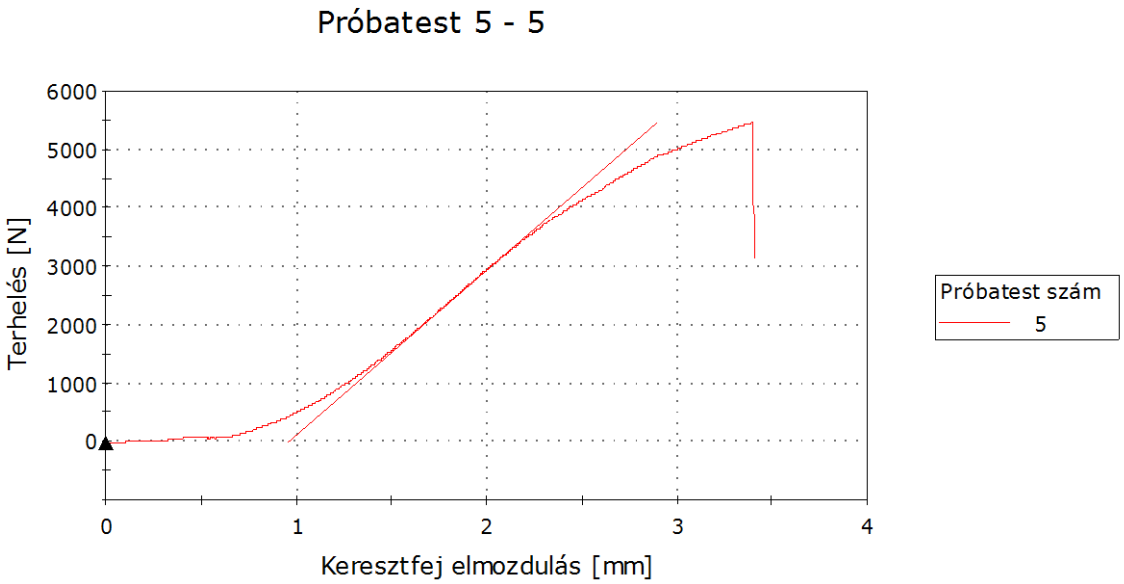
Próbatest 5 - 5
Terhelés [N]
6000
5000
4000
3000
2000
1000
0
0
1
2
3
4
Keresztfej elmozdulás [mm]
Próbatest szám
5

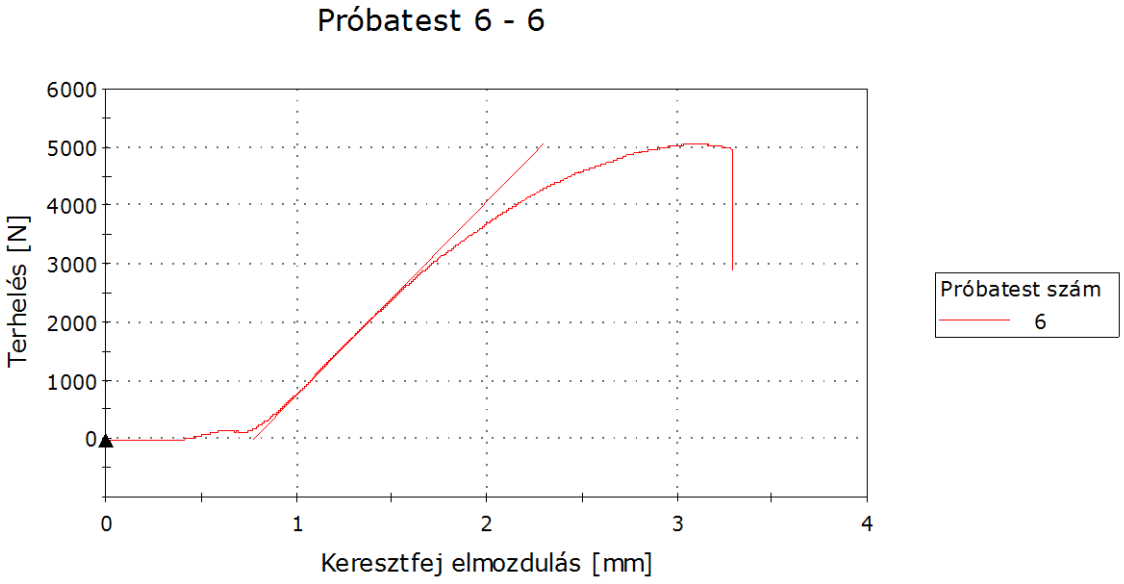
Próbatest 6 - 6
Terhelés [N]
6000
5000
4000
3000
2000
1000
0
0
1
2
3
4
Keresztfej elmozdulás [mm]
Próbatest szám
6

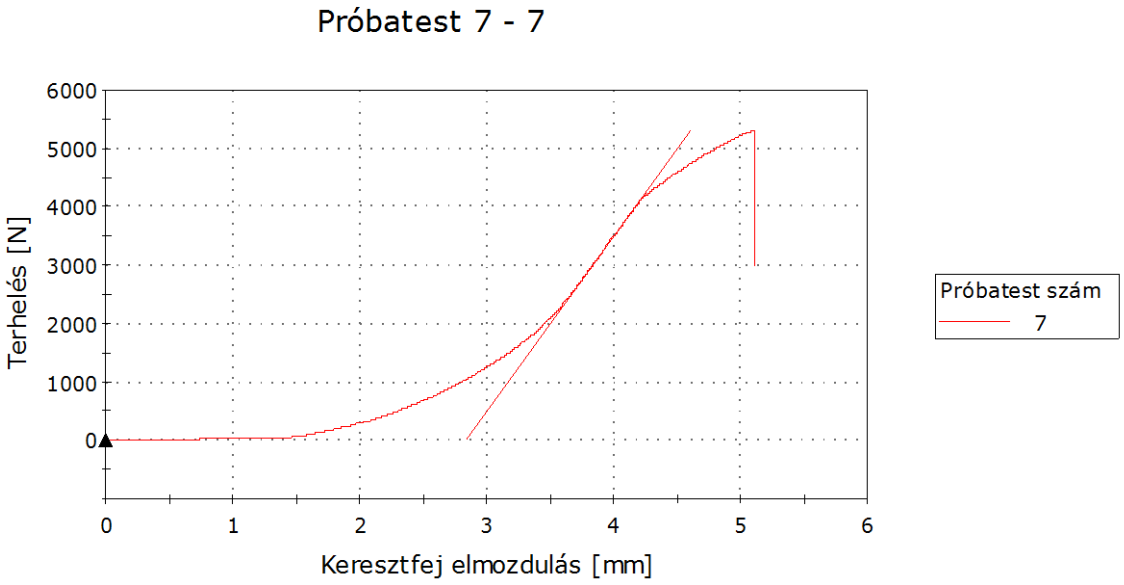
Próbatest 7 - 7
Terhelés [N]
6000
5000
4000
3000
2000
1000
0
0
1
2
3
4
5
6
Keresztfej elmozdulás [mm]
Próbatest szám
7

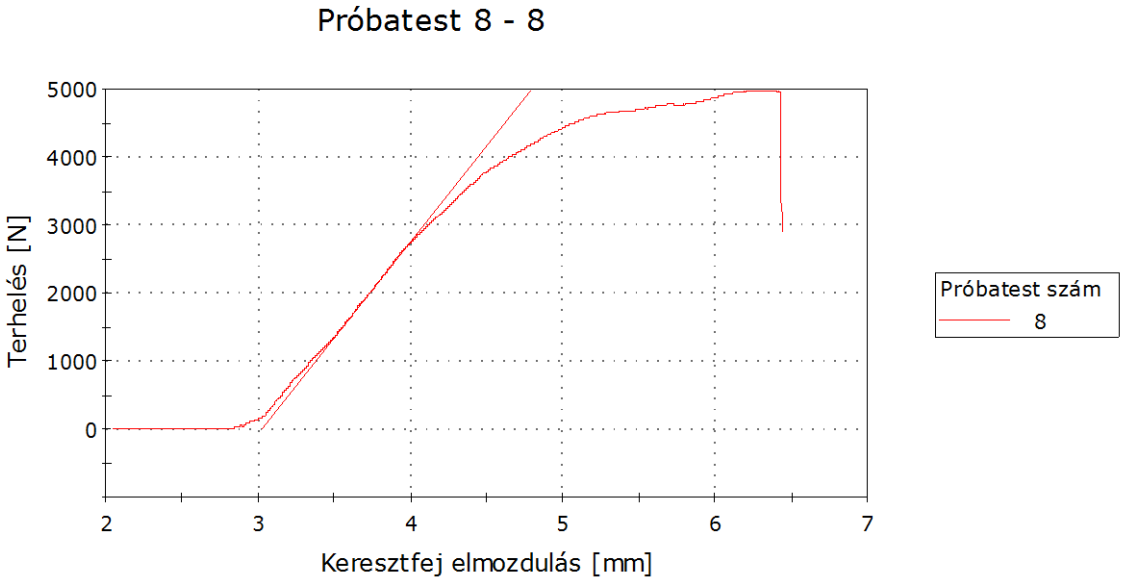
Próbatest 8 - 8
Terhelés [N]
5000
4000
3000
2000
1000
0
2
3
4
5
6
7
Keresztfej elmozdulás [mm]
Próbatest szám
8

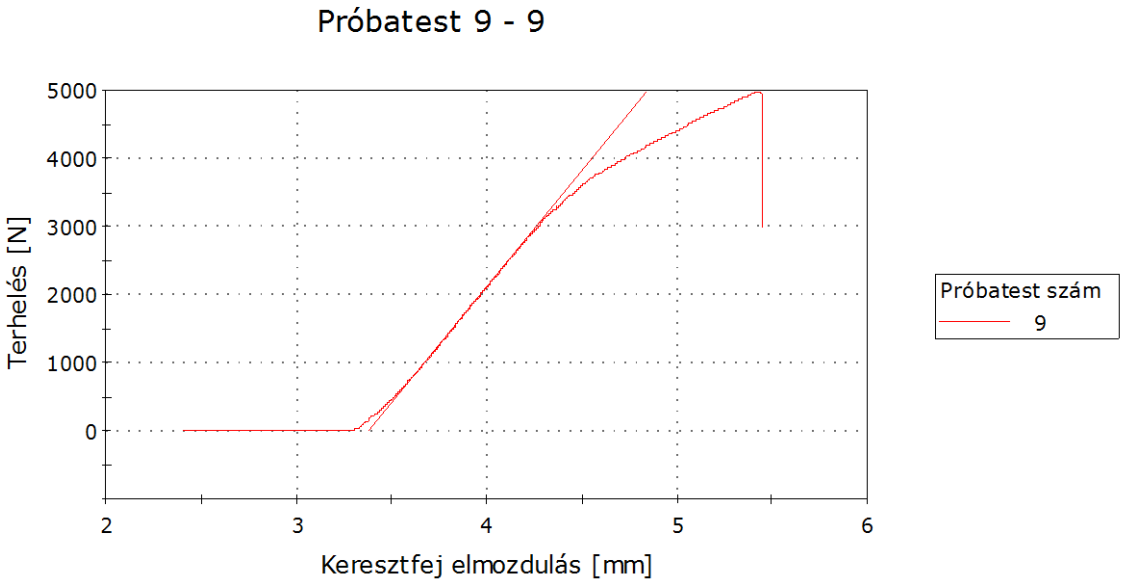
Próbatest 9 - 9
Terhelés [N]
5000
4000
3000
2000
1000
0
2
3
4
5
6
Keresztfej elmozdulás [mm]
Próbatest szám
9

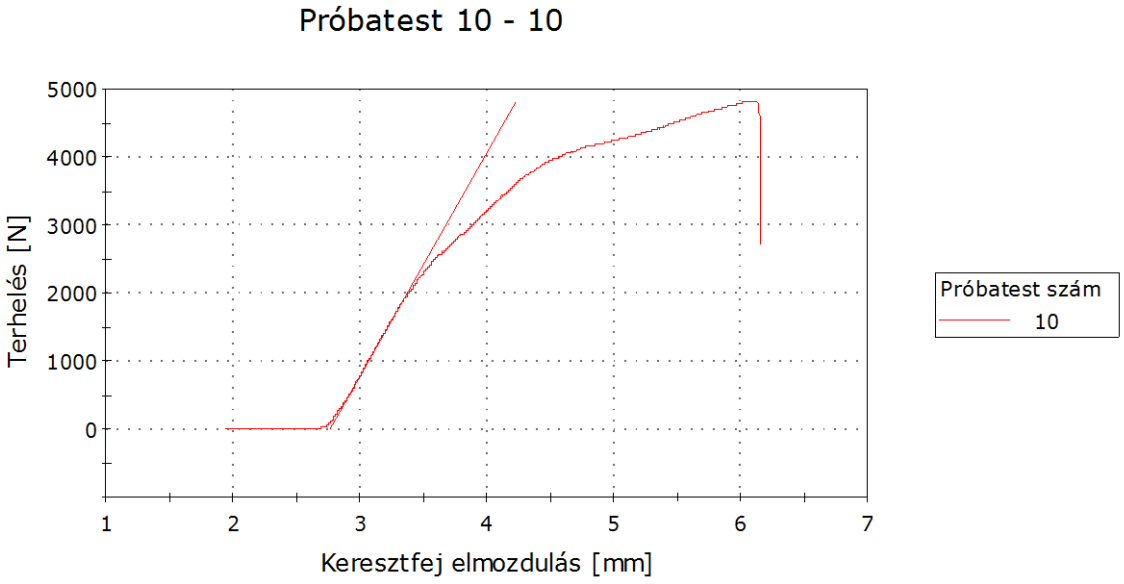

Figures A-39 to -48 Load-displacement curves. TBWD-type specimens, withdrawal test

B - Time-dependent deflection curves of the test specimens of creep study

The first 0.0 data-point corresponds to the state before load application

Big-size corner joints with Domino wood dowel

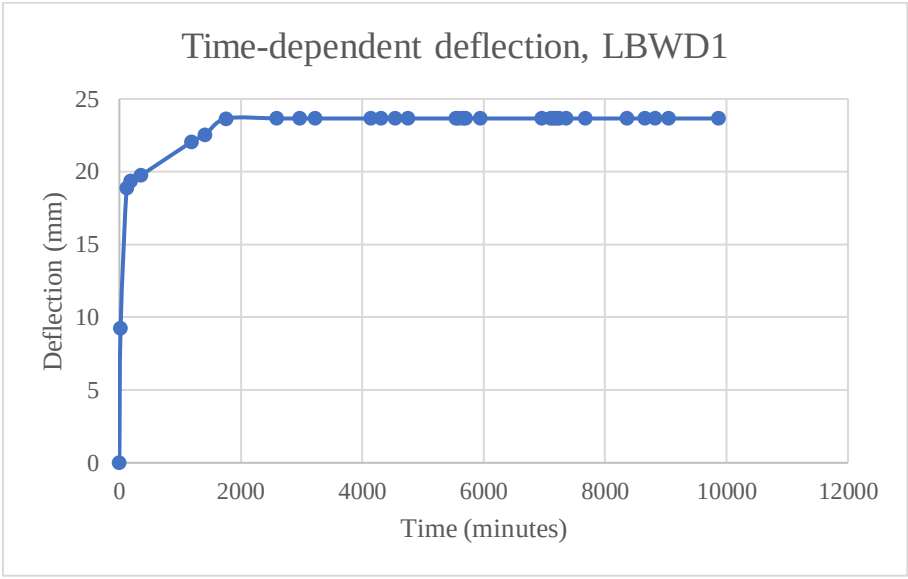

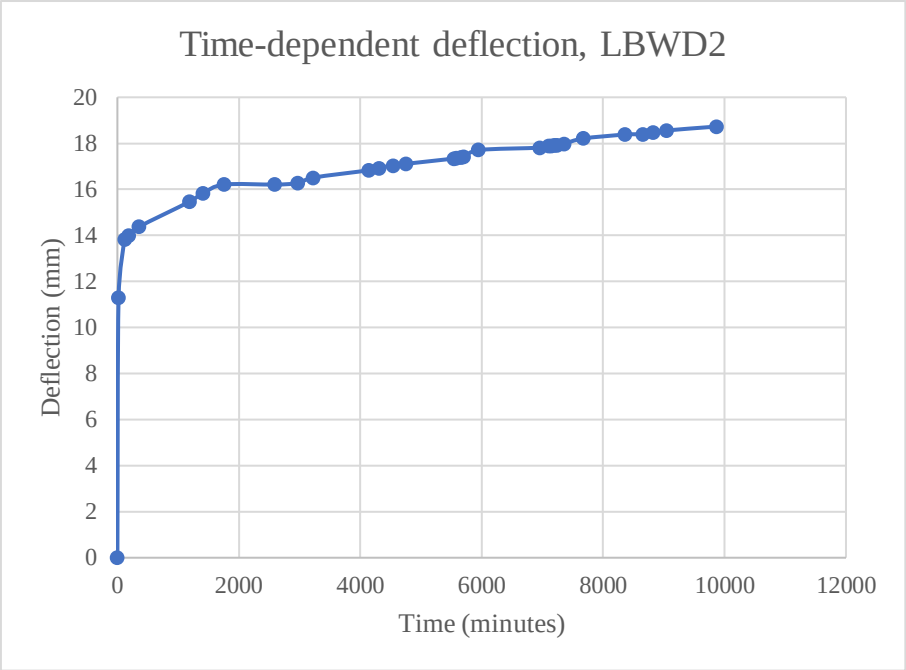
Time-dependent deflection, LBWD2
Deflection (mm)
0
2
4
6
8
10
12
14
16
18
20
0
2000
4000
6000
8000
10000
12000
Time (minutes)

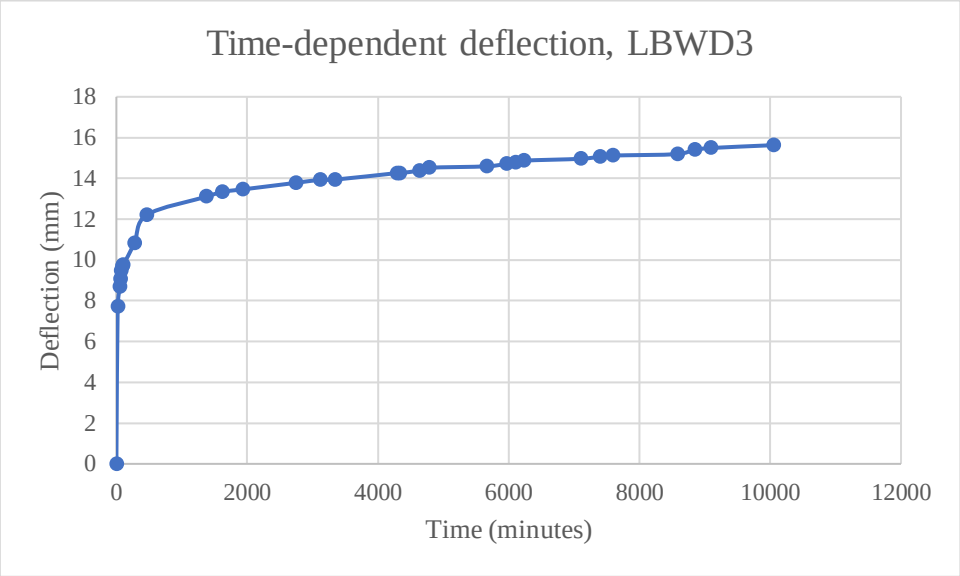
Time-dependent deflection, LBWD3
Deflection (mm)
0
2
4
6
8
10
12
14
16
18
0
2000
4000
6000
8000
10000
12000
Time (minutes)

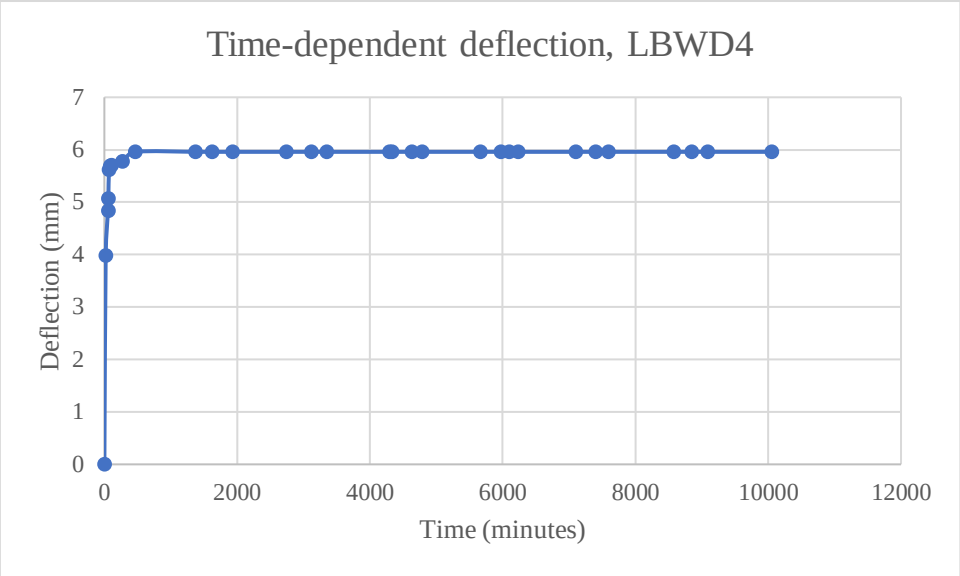

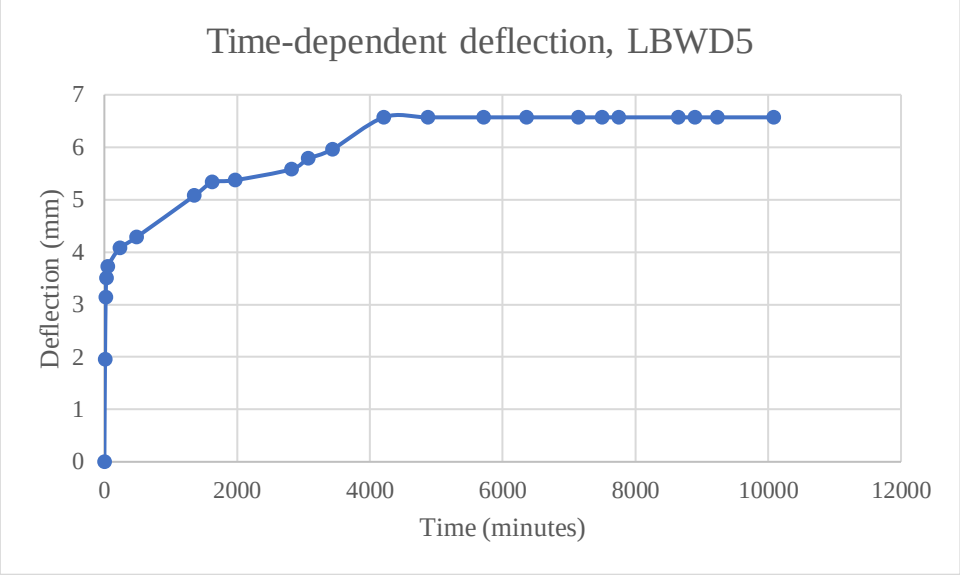

Big-size T joints with Domino wood dowel

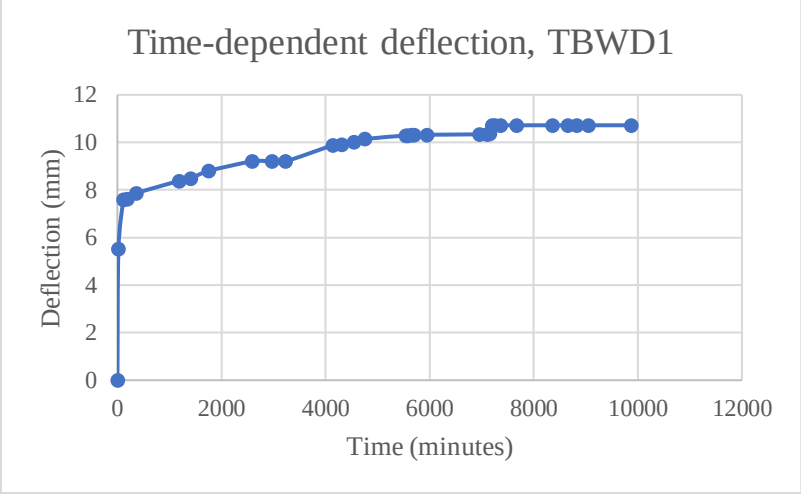

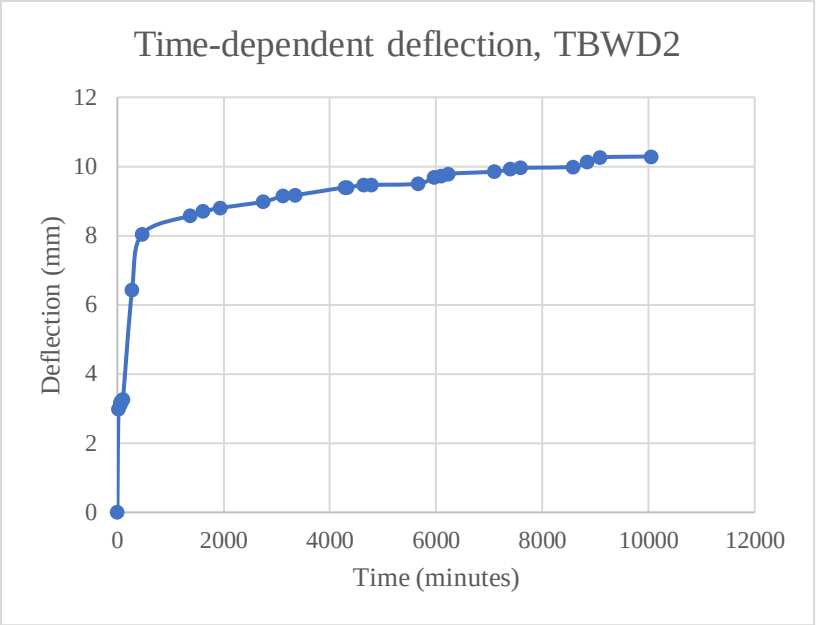

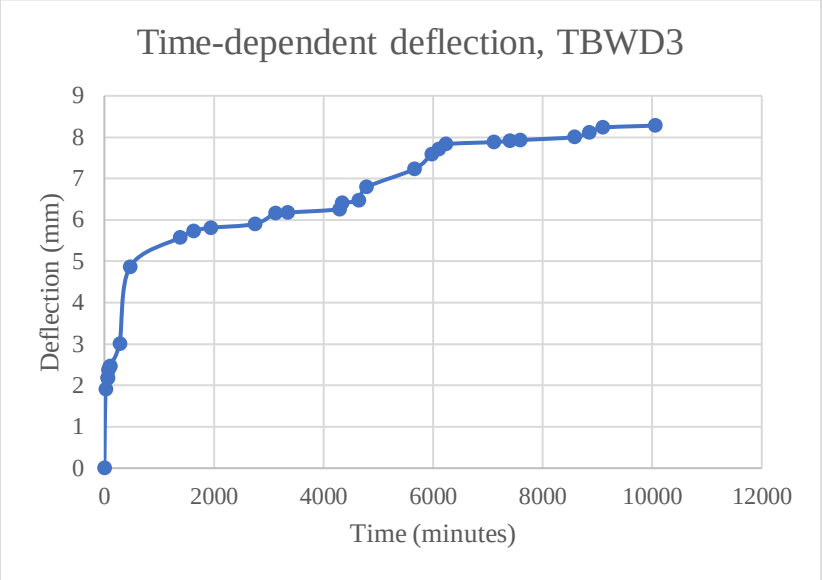

Small-size corner joints with Domino wood dowel

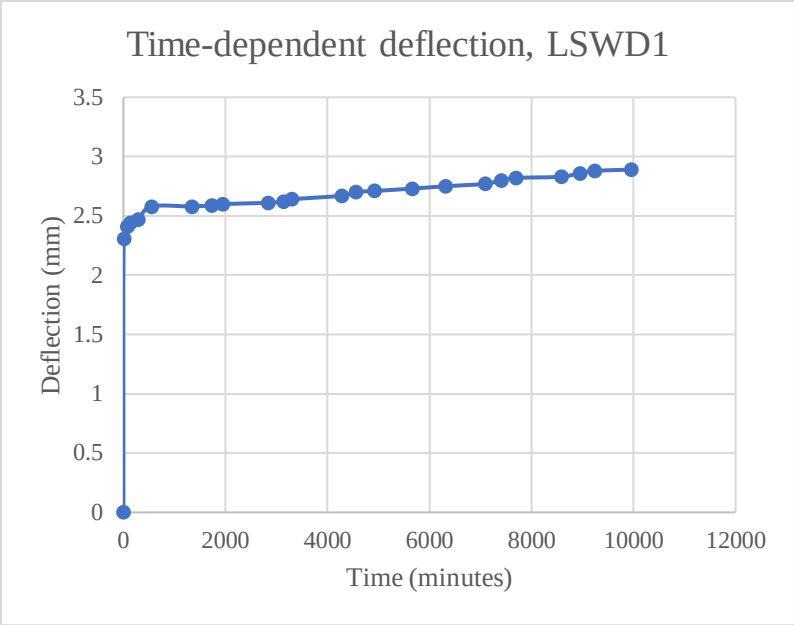
Time-dependent deflection, LSWD1
Deflection (mm)
3.5
3
2.5
2
1.5
1
0.5
0
0
2000
4000
6000
8000
10000
12000
Time (minutes)

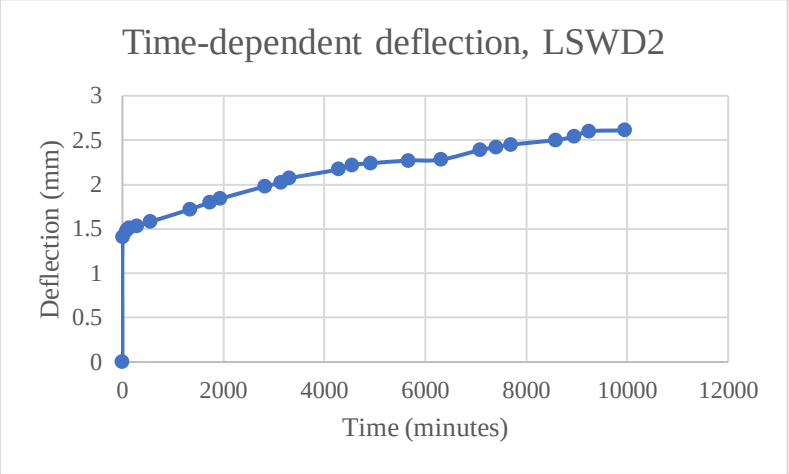
Time-dependent deflection, LSWD2
Deflection (mm)
3
2.5
2
1.5
1
0.5
0
0
2000
4000
6000
8000
10000
12000
Time (minutes)

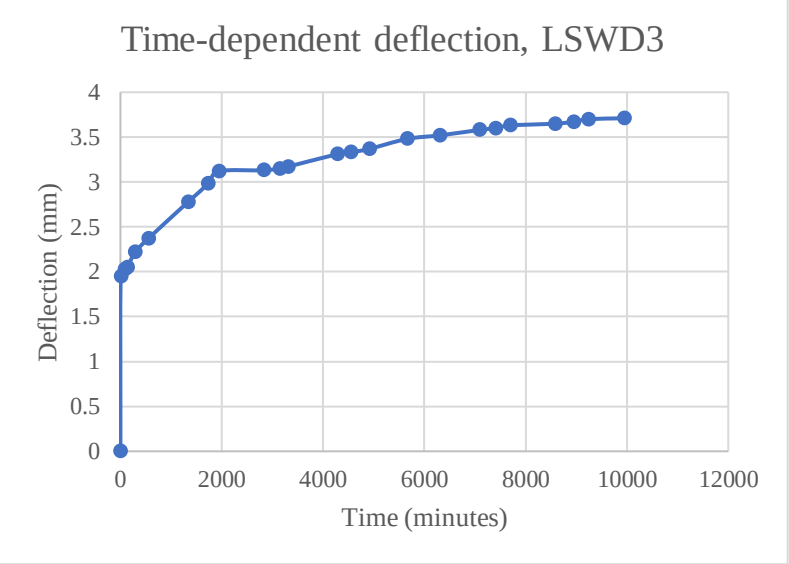
Time-dependent deflection, LSWD3
Deflection (mm)
4
3.5
3
2.5
2
1.5
1
0.5
0
0
2000
4000
6000
8000
10000
12000
Time (minutes)

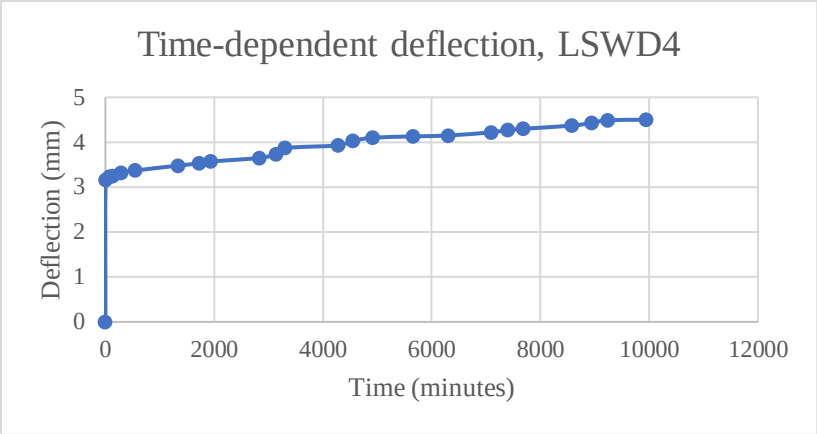

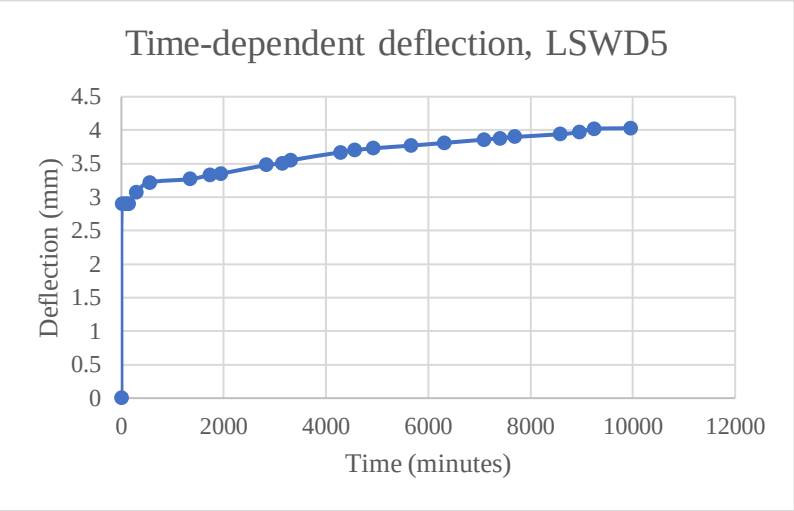

Small-size T joints with Domino wood dowel

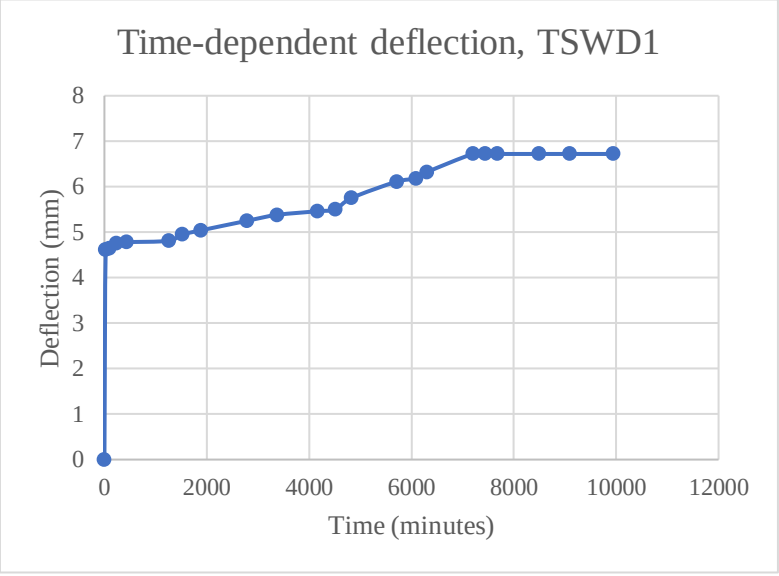

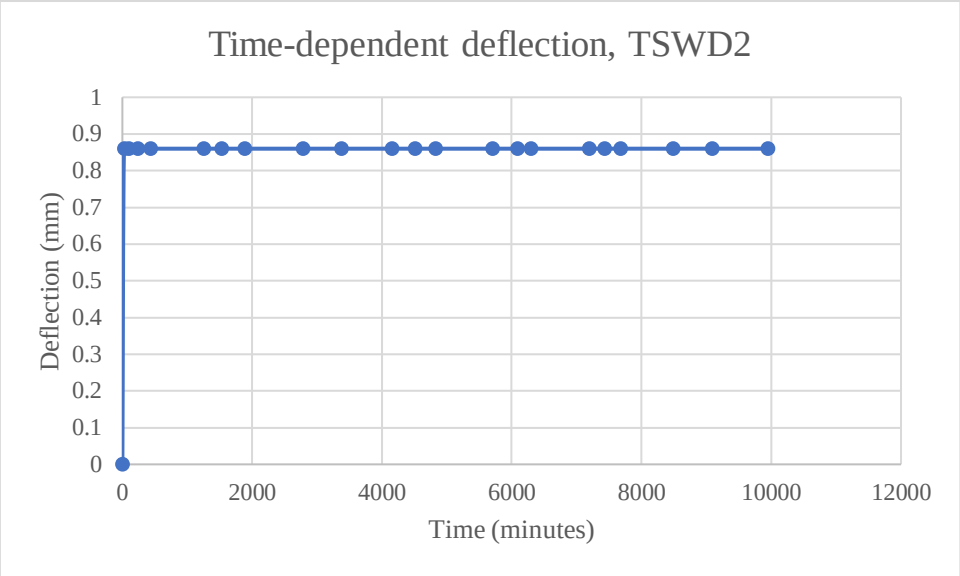
Time-dependent deflection, TSWD2
Deflection (mm)
1
0.9
0.8
0.7
0.6
0.5
0.4
0.3
0.2
0.1
0
0
2000
4000
6000
8000
10000
12000
Time (minutes)

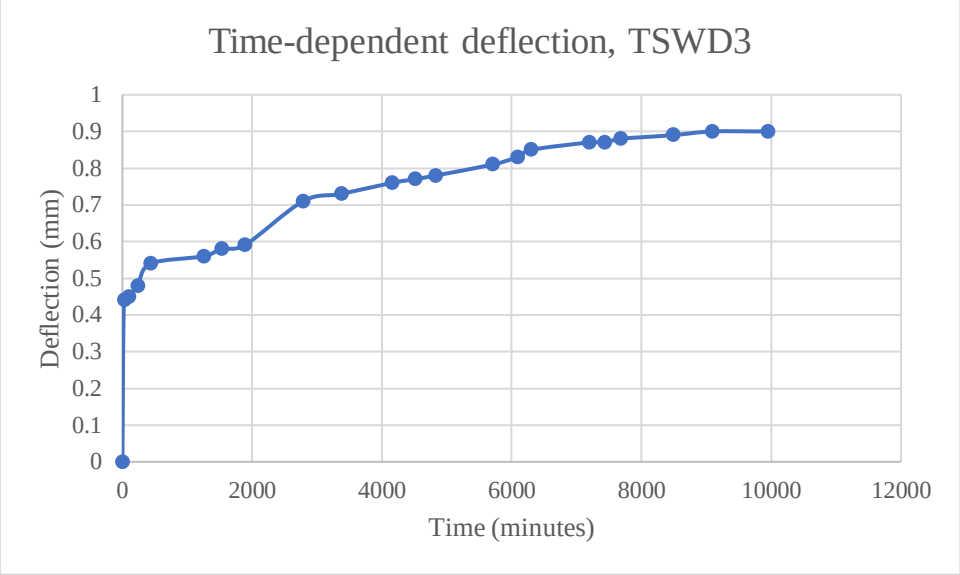
Time-dependent deflection, TSWD3
Deflection (mm)
1
0.9
0.8
0.7
0.6
0.5
0.4
0.3
0.2
0.1
0
0
2000
4000
6000
8000
10000
12000
Time (minutes)

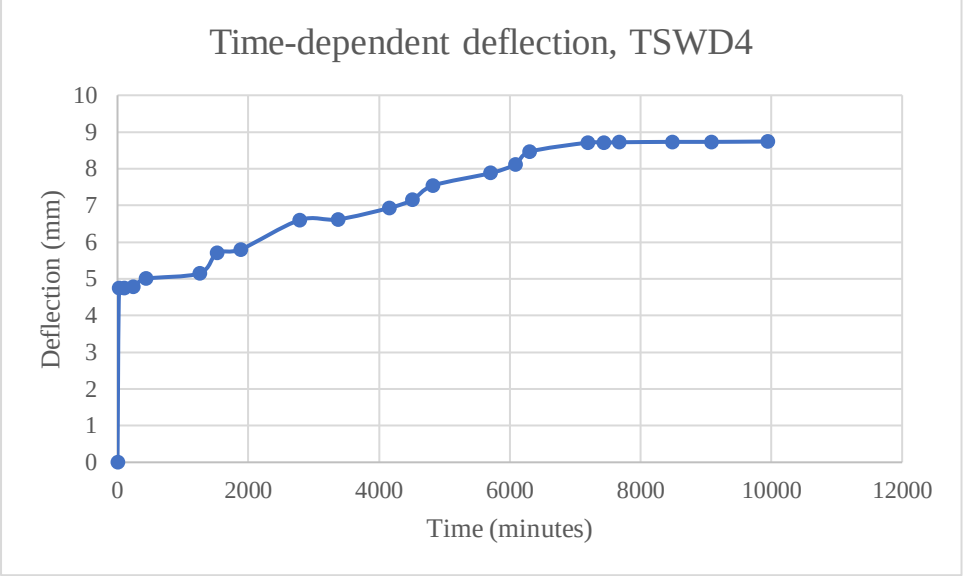
Time-dependent deflection, TSWD4
Deflection (mm)
10
9
8
7
6
5
4
3
2
1
0
0
2000
4000
6000
8000
10000
12000
Time (minutes)

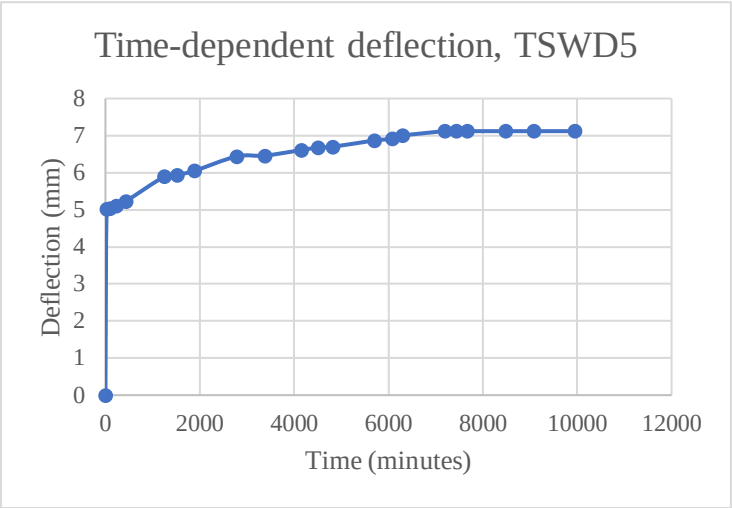

Big-size corner joints with metallic Domino connector

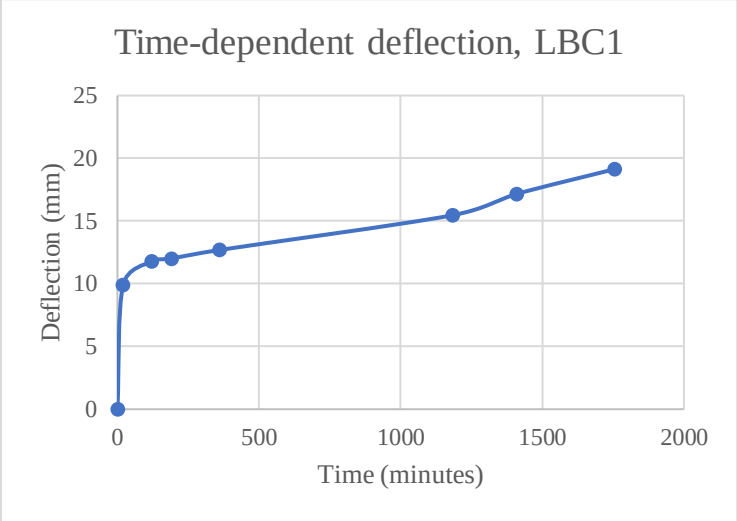

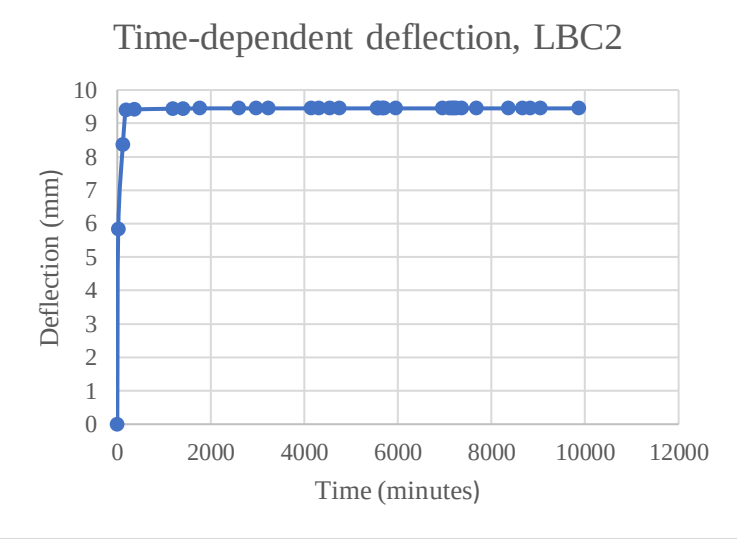

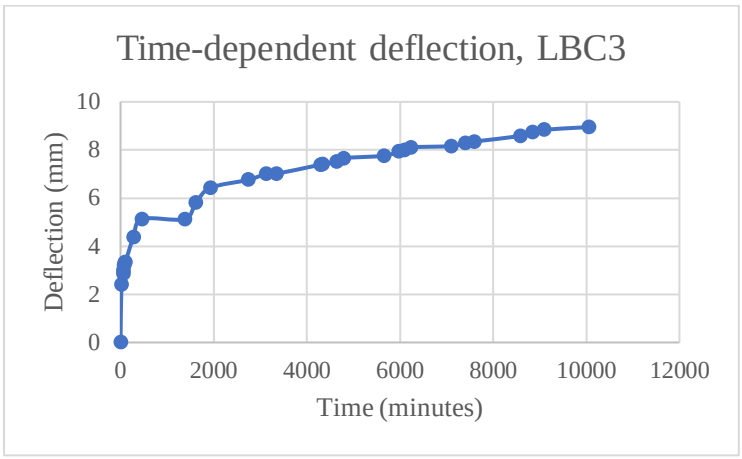
Time-dependent deflection, LBC3
Deflection (mm)
0
2
4
6
8
10
0
2000
4000
6000
8000
10000
12000
Time (minutes)

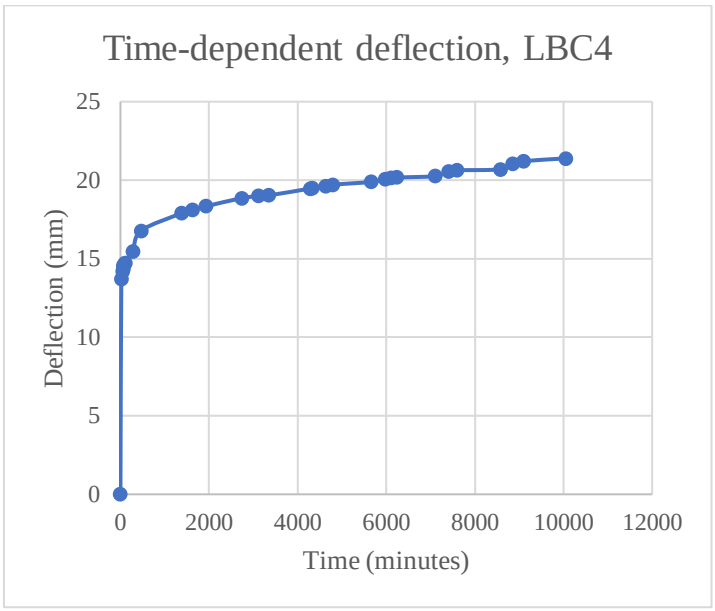
Time-dependent deflection, LBC4
Deflection (mm)
0
5
10
15
20
25
0
2000
4000
6000
8000
10000
12000
Time (minutes)

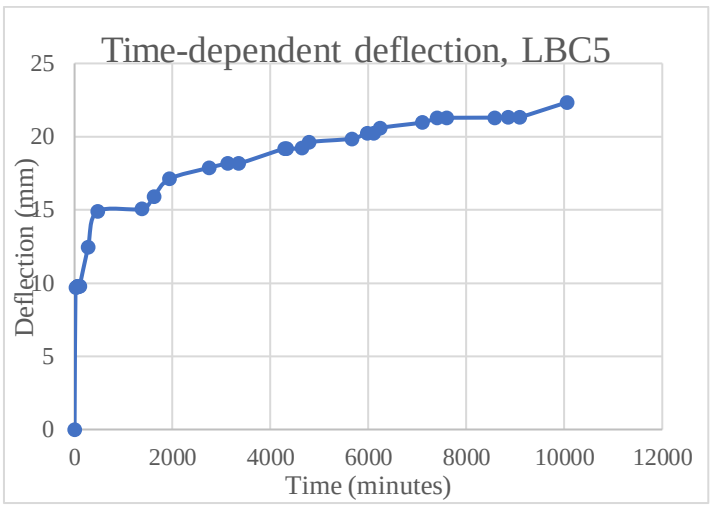
Time-dependent deflection, LBC5
Deflection (mm)
0
5
10
15
20
25
0
2000
4000
6000
8000
10000
12000
Time (minutes)

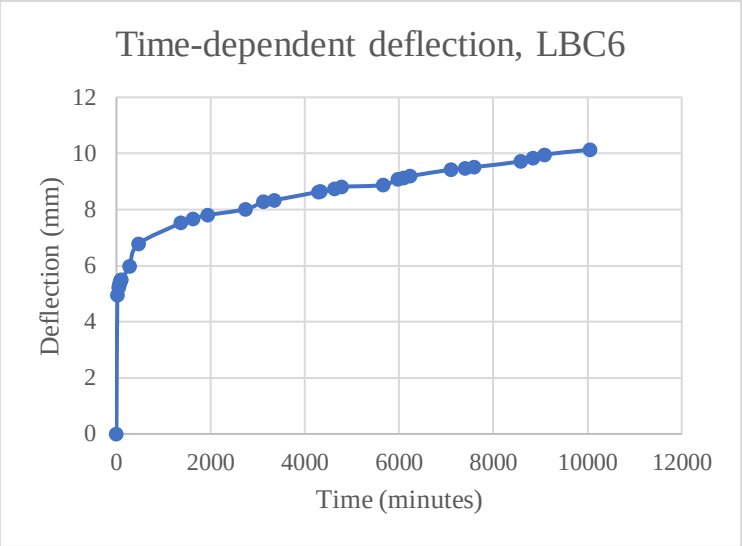

Big-size T joints with metallic Domino connector

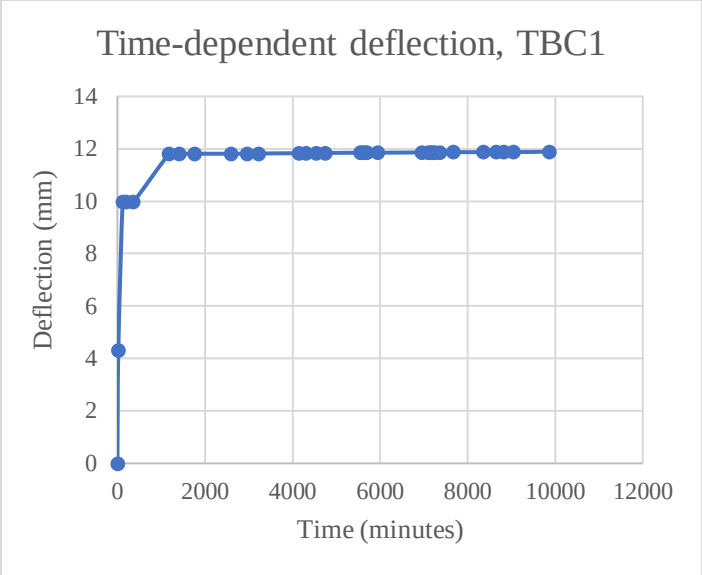

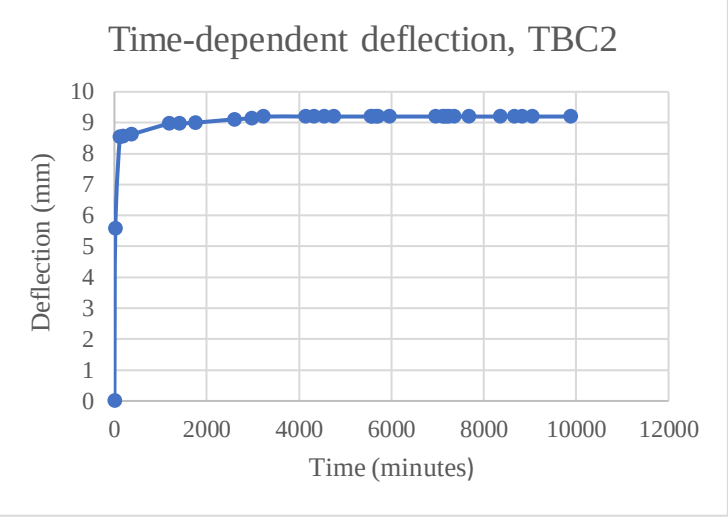

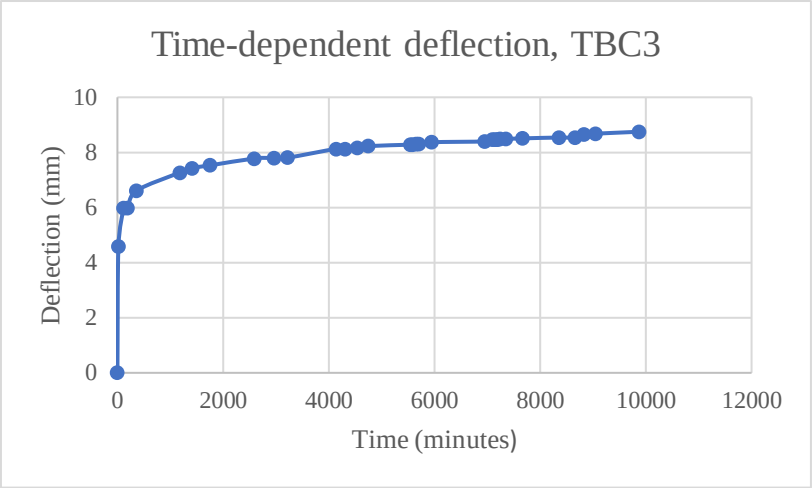

Small-size corner joints with metallic Domino connector

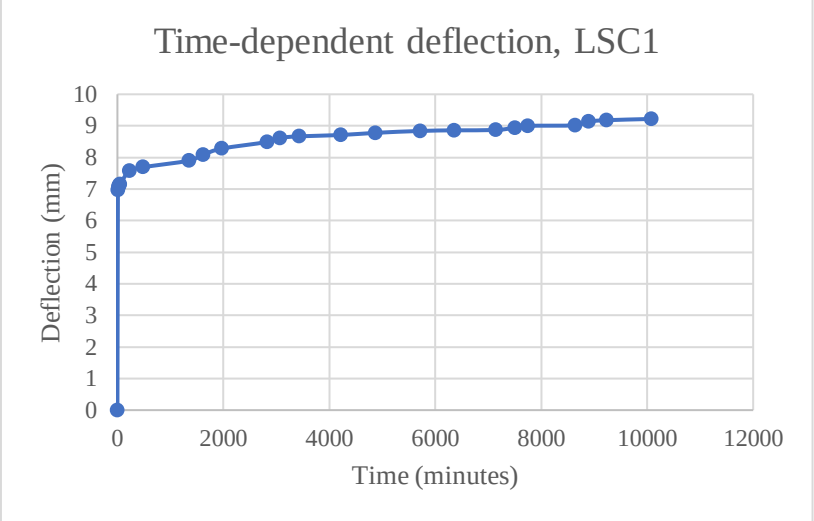

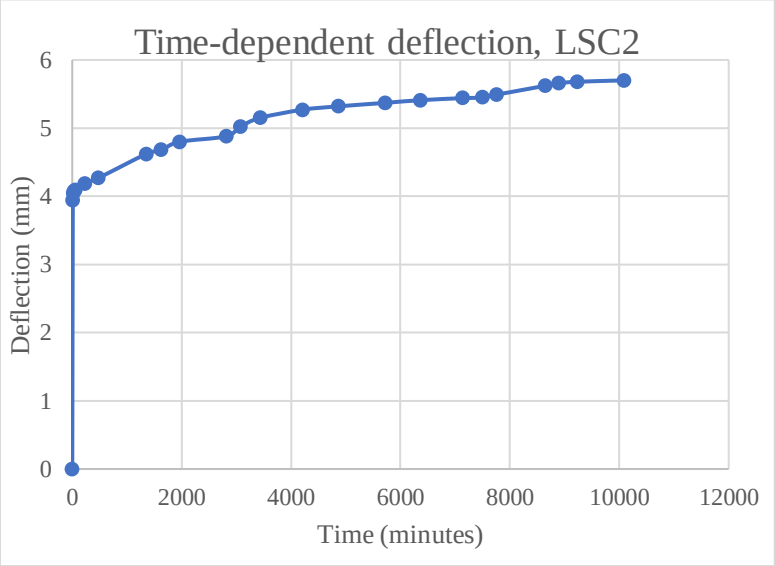

Time-dependent deflection
Deformation (mm)
0
1
2
3
4
5
6
7
0
10
20
30
Time (minute)

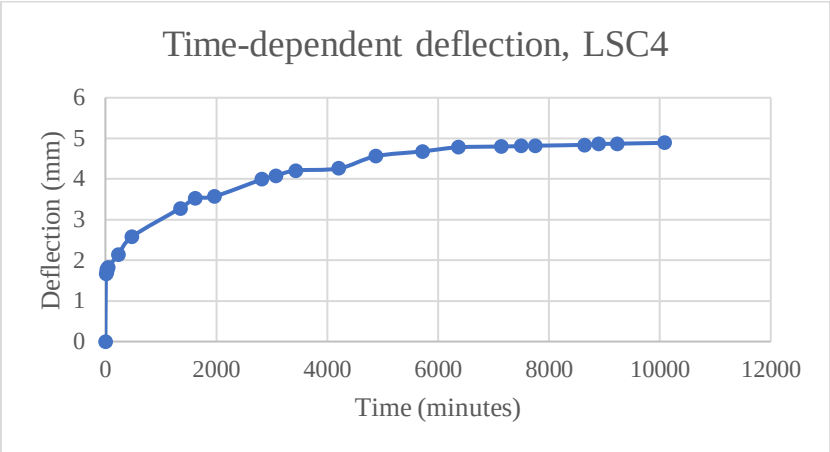
Time-dependent deflection, LSC4
Deflection (mm)
0
1
2
3
4
5
6
0
2000
4000
6000
8000
10000
12000
Time (minutes)

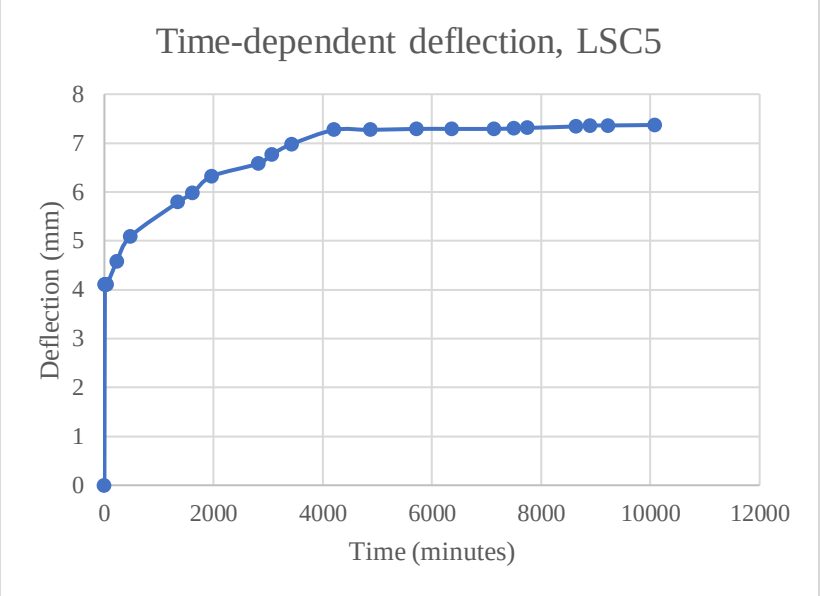
Time-dependent deflection, LSC5
Deflection (mm)
0
1
2
3
4
5
6
7
8
0
2000
4000
6000
8000
10000
12000
Time (minutes)

Small-size T joints with metallic Domino connector

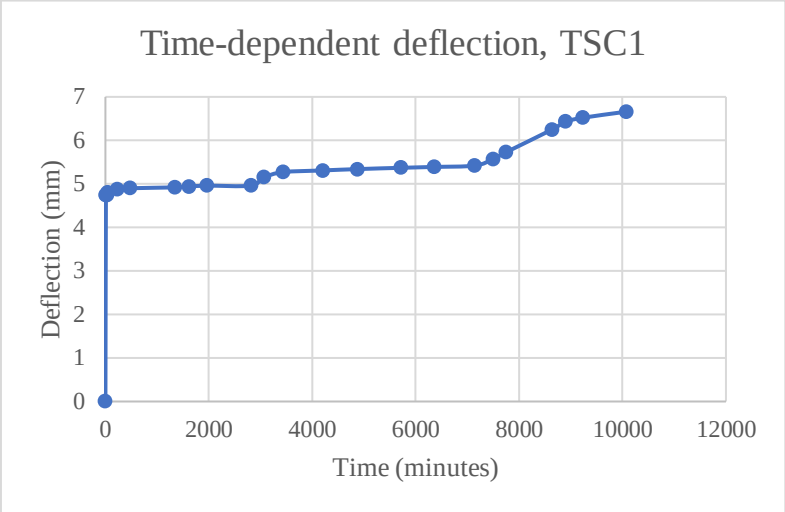

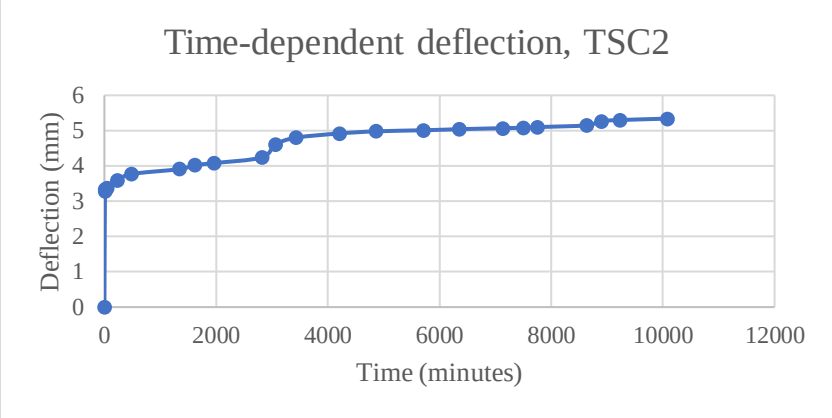

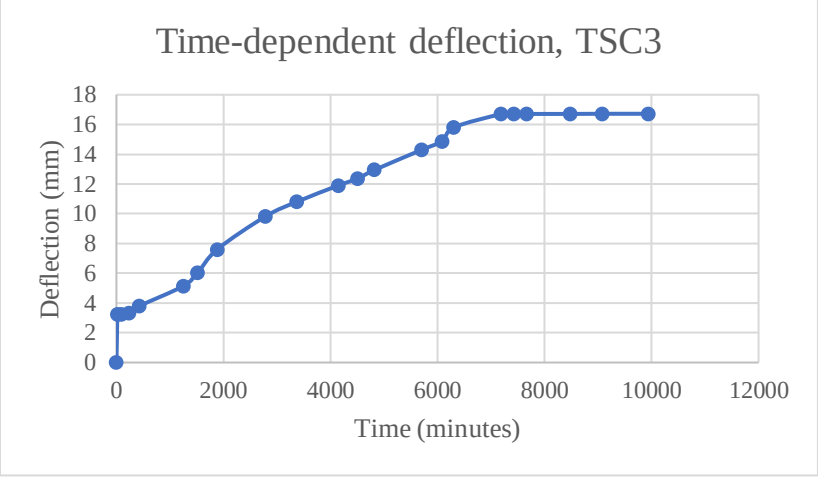

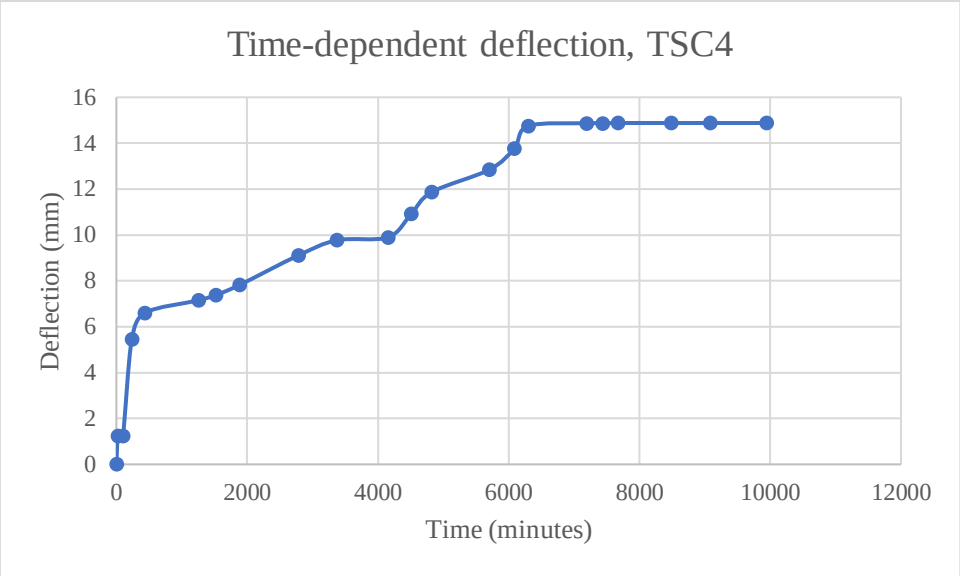
Time-dependent deflection, TSC4
Deflection (mm)
16
14
12
10
8
6
4
2
0
0
2000
4000
6000
8000
10000
12000
Time (minutes)

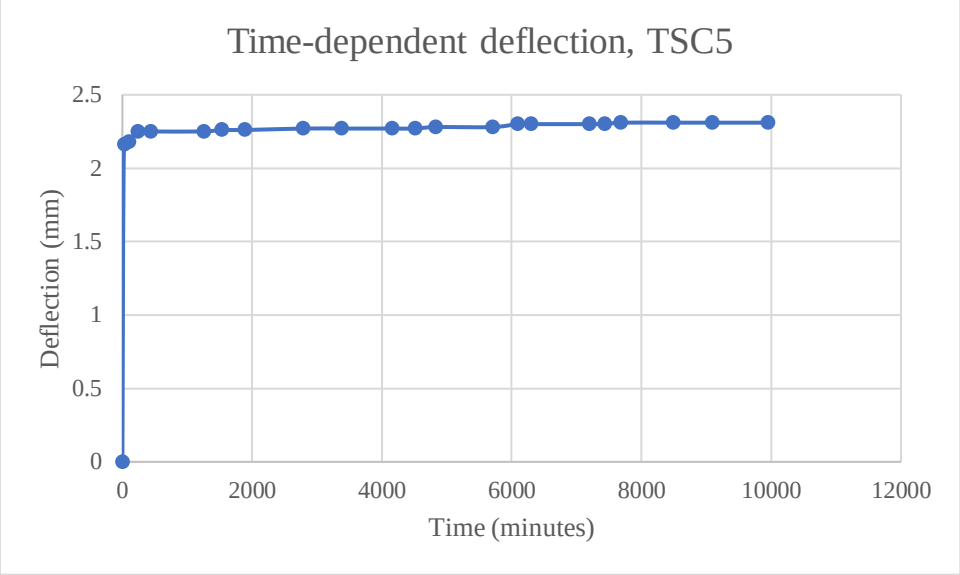
Time-dependent deflection, TSC5
Deflection (mm)
2.5
2
1.5
1
0.5
0
0
2000
4000
6000
8000
10000
12000
Time (minutes)

C – Logarithmic curve fitting to creep factor data

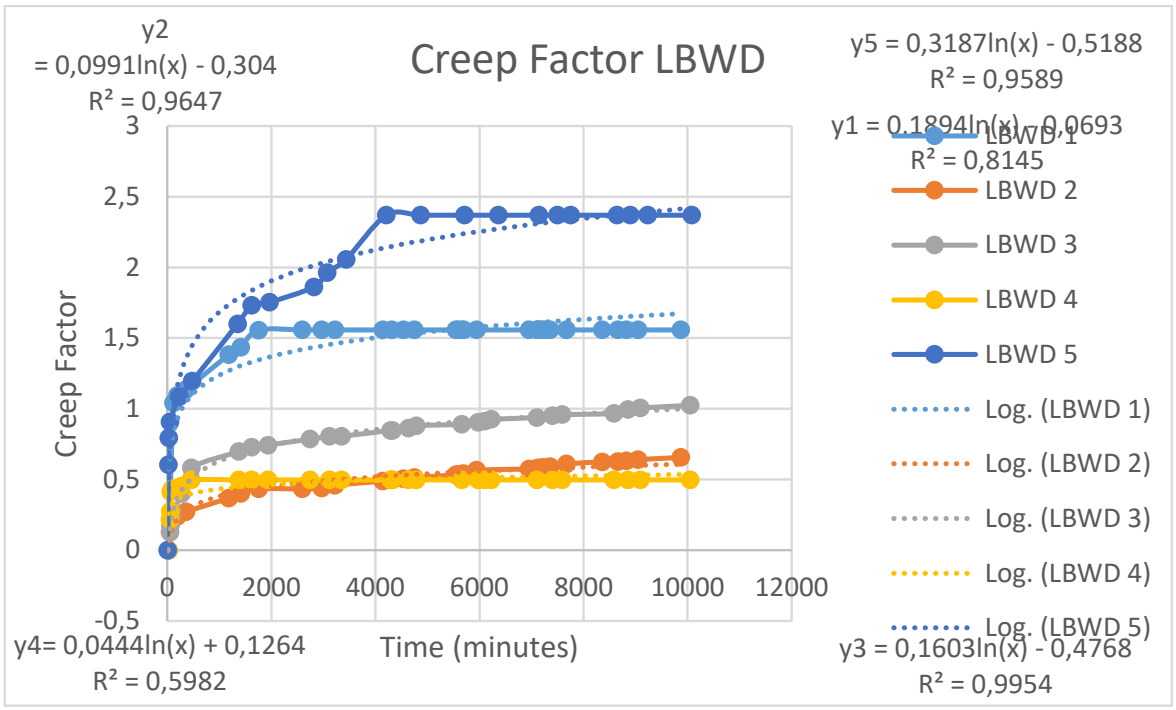

Figure B-1 Logarithmic curve fitting to creep data factor of LBWD-type specimens

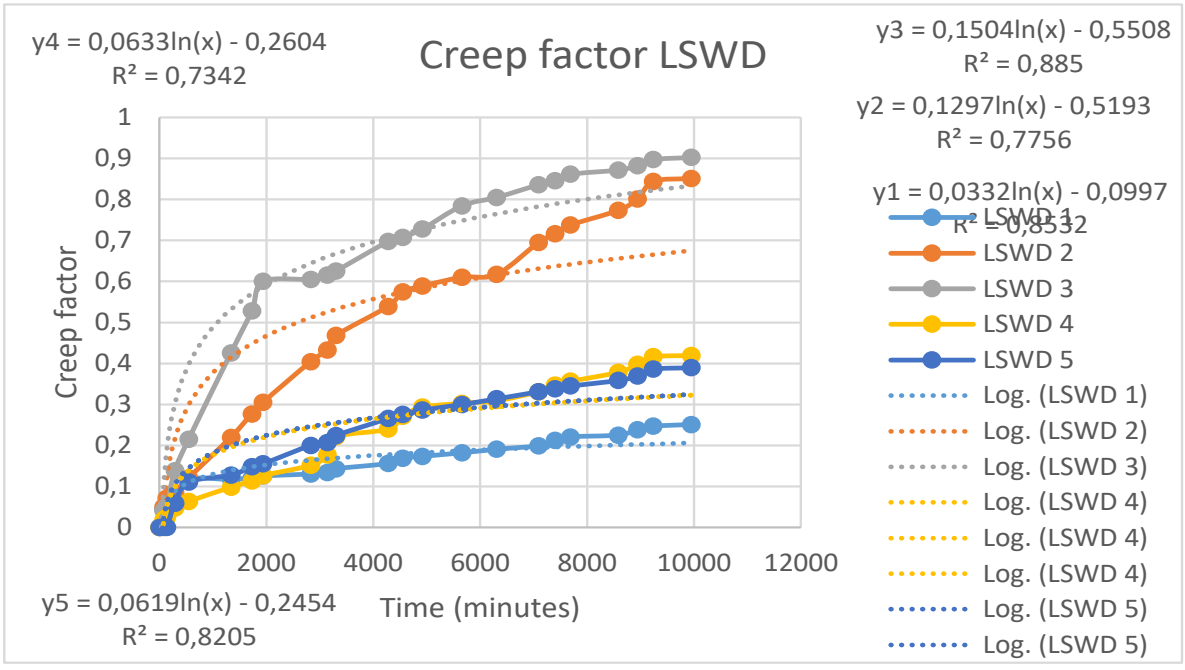

Figure B-2 Logarithmic curve fitting to creep data factor of LsWD-type specimens

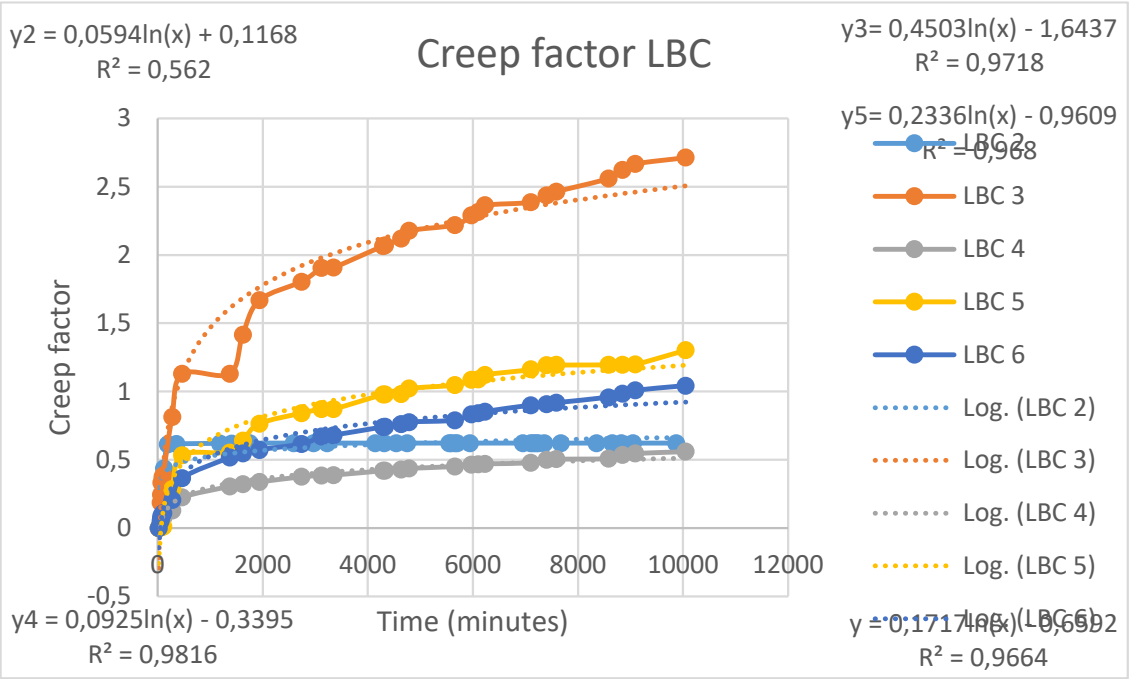

Figure B-3 Logarithmic curve fitting to creep data factor of LBC-type specimens

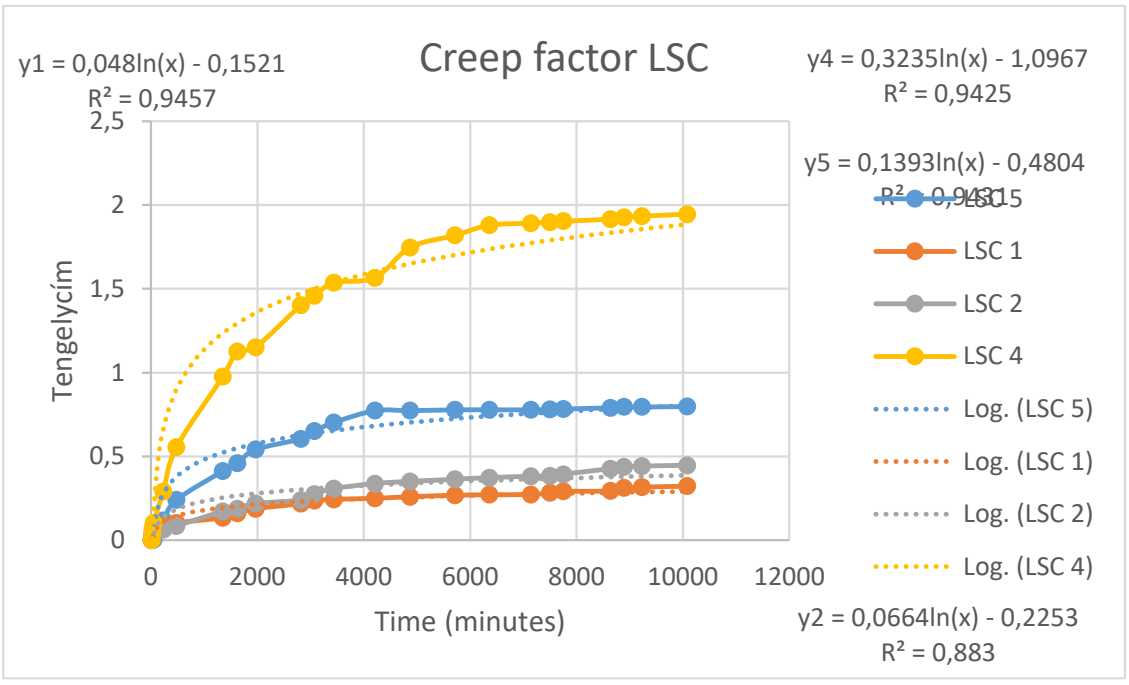

Figure B-4 Logarithmic curve fitting to creep data factor of LSC-type specimens

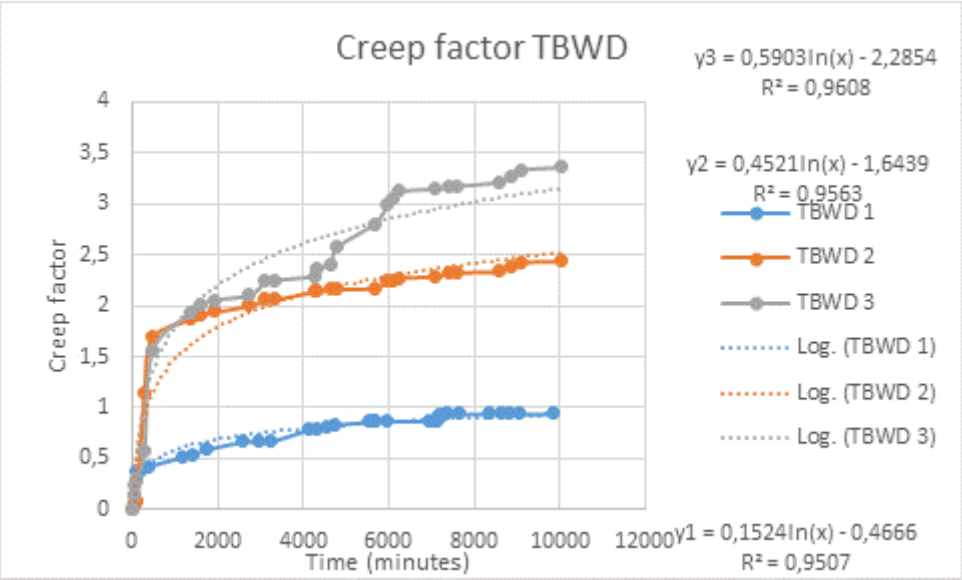

Figure B-5 Logarithmic curve fitting to creep data factor of TBWD-type specimens

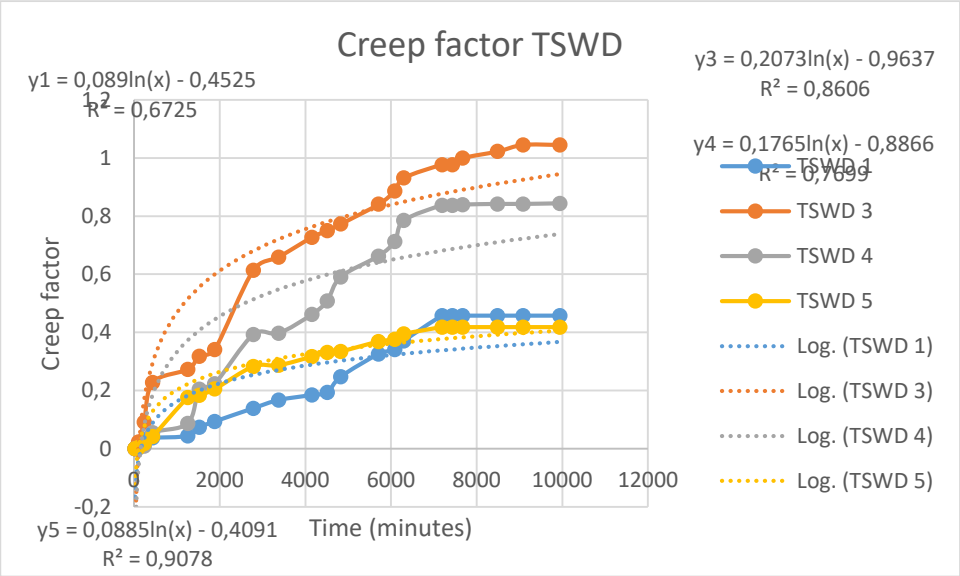

Figure B-6 Logarithmic curve fitting to creep data factor of TSWD-type specimens

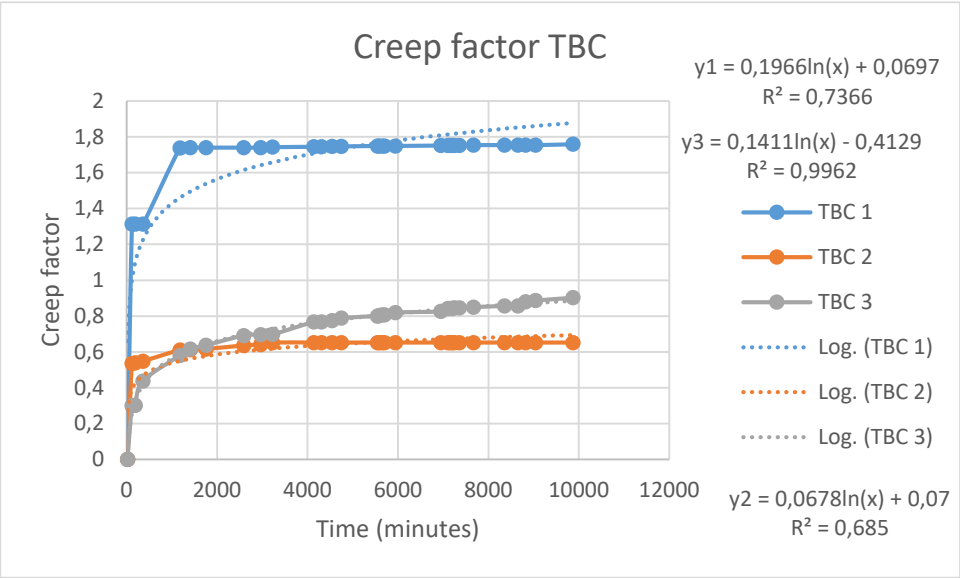

Figure B-7 Logarithmic curve fitting to creep data factor of TBC-type specimens

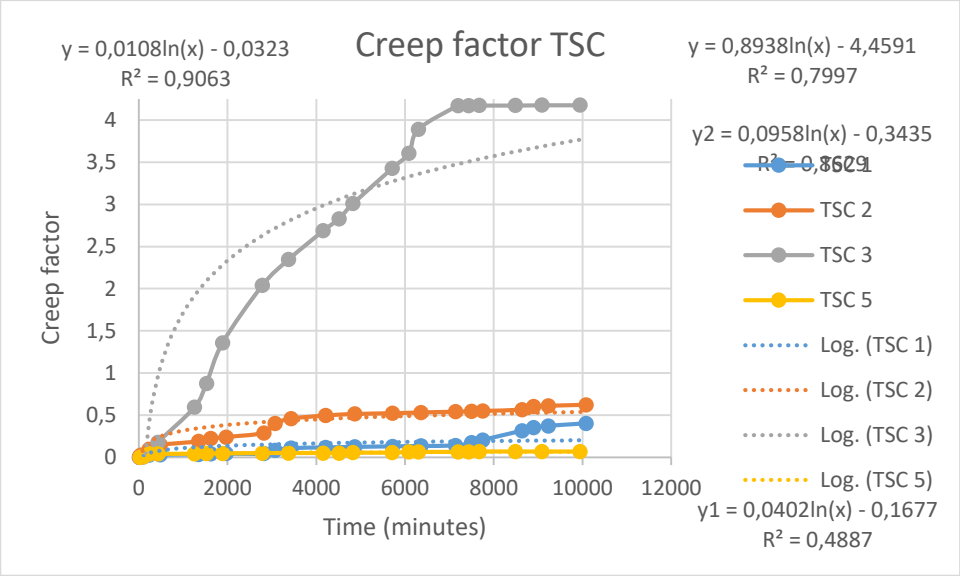

Figure B-7 Logarithmic curve fitting to creep data factor of TSC-type specimens

5. REFERENCES

1. Postell, J., *Furniture design*. 2012: John Wiley & Sons.
2. Demirel, S. and S. Bas, Evaluation of creep characteristics of singlestaple furniture joints made of different wood species. Drvna industrija, **72**(2021), 179-186.
3. Hope, T. and T.U. Walter, Household furniture and interior decoration, in Nineteenth-Century Interiors. 1807, Routledge. p. 213-225.
4. Gloag, J., *A short dictionary of furniture*. 2013: Read Books Ltd.
5. KURTOĞLU, A., Mobilya yapımında kullanılan ağaç malzemeler. Journal of the Faculty of Forestry Istanbul University, **34**(1984), 86-97.
6. Yıldız, S. and A. Can, Isıl işlem uygulanmış ladin, karaçam, kayın ve kavak odunlarının korozyon özellikleri. (2012).
7. Bal, B.C. and İ. Bektaş, Okaliptüs, kayın ve kavak soyma kaplamaları ile üretilen tabakalı kaplama kerestelerin (TKK) bazı fiziksel özellikleri. (2013).
8. Branowski, B., M. Zabłocki, and M. Sydor, Experimental analysis of new furniture joints. BioResources, **13**(2018), 370-382.
9. Eckelman, C.A. and E. Haviarova, Withdrawal capacity of joints constructed with 9.5-mm and 15.9-mm through-bolts and diameter nominal 15-mm and 25-mm pipe-nut connectors. Forest products journal, **61**(2011), 257-264.
10. Zwerger, K., *Wood and wood joints: building traditions of Europe, Japan and China*. 2023: Birkhäuser.
11. Jelínek, L., *Tesařské Konstrukce [Carpentry Construction]*. 2008, ČKAIT, Prague, Czech Republic.
12. Horman, I., et al., Numerical Analysis of Stress and Strain in a Wooden Chair. Wood Industry/Drvna Industrija, **61**(2010).
13. Nutsch, W., *Příručka pro truhláře*. 2006: Európa-Sobotáles.
14. Záborský, V., et al., The effect of selected factors on domino joint stiffness. BioResources, **13**(2018), 2424-2439.
15. Osten, M., *Práce s Lepidly a Tmely [Work with Adhesives and Fillers]*. 1996, Grada, Prague, Czech Republic.
16. BAŞ, S., L. Dénes, and C. Csiha, Performance comparison of domino pin and domino connector fastened corner joints. (2022).
17. Richardson, D.B., et al., Manufacturing methods, in Mechanical Engineer's Reference Book. 1994, Elsevier. p. 16-1-16-112.
18. Suwannatee, N. and M. Yamamoto, Single-Pass Process of Square Butt Joints without Edge Preparation Using Hot-Wire Gas Metal Arc Welding. Metals, **13**(2023), 1014.
19. Miller, H. and H. Miller, Wood Joints. Hand and Machine Woodwork,(1962), 140-153.
20. Norvydas, V., A. BALTRUŠAITIS, and I. JUODEIKIENĖ, Investigation of miter corner joint strength of case furniture from particleboard. Materials Science, **18**(2012), 352-357.
21. Fatheree, T.C., A Comparative Analysis of Furniture Dowel Joint Strength Among Various Dowel Styles. (2017).
22. Hao, J., et al., Analysis and modeling of the dowel connection in wood T type joint for optimal performance. Composite Structures, **253**(2020), 112754.
23. Mollahassani, A., et al., Dynamic and static comparison of beech wood dovetail, tongue and groove, halving, and dowel joints. BioResources, **15**(2020), 3787-3798.
24. Dalvand, M., et al. Combined stress analysis of mitered spline furniture joints under diagonal loading. in The XXVIth Conference Research for Furniture Industry. 2013.
25. Petrova, B., V. Jivkov, and N. Yavorov, Possibilities for Efficient Furniture Construction Made of Thin and Ultra-Thin Materials by Using Mitre Joints. Materials, **16**(2023), 6855.
26. Krzyżaniak, Ł. and J. Smardzewski, Impact damage response of L-type corner joints connected with new innovative furniture fasteners in wood-based composites panels. Composite Structures, **255**(2021), 113008.

27. Yu, S., et al., Experimental Study on Tenon and Mortise Joints of Wood-Structure Houses Reinforced by Innovative Metal Dampers. Forests, **13**(2022), 1177.
28. Erdil, Y., A. Kasal, and C. Eckelman, Bending moment capacity of rectangular mortise and tenon furniture joints. Forest products journal, **55**(2005), 209.
29. Shang, B., et al., A comprehensive mortise and tenon structure selection method based on Pugh's controlled convergence and rough Z-number MABAC method. Plos one, **18**(2023), e0283704.
30. Patel, V., S. Masood, and T. Waterman, Investigation of butt joint failure mode in sofa frame. Assembly Automation, **29**(2009), 371-377.
31. Segovia, C. and A. Pizzi, Performance of dowel-welded wood furniture linear joints. Journal of adhesion science and technology, **23**(2009), 1293-1301.
32. Diler, H., et al., Withdrawal force capacity of T-type furniture joints constructed from various heat-treated wood species. (2017).
33. Lang, E.M. and T. Fodor, Finite element analysis of cross-halved joints for structural composites. Wood and fiber science,(2002), 251-265.
34. Eckelman, C., et al., Withdrawal capacity of pinned and unpinned round mortise and tenon furniture joints. Forest products journal, **54**(2004).
35. Kasal, A., et al., Numerical analyses of various sizes of mortise and tenon furniture joints. (2016).
36. OMRANI, P., G. Ebrahimi, and M. Kahvand, The investigation of the affecting factors on withdrawal resistance of the wooden biscuit joints. Iranian Journal of Wood and Paper Industries, **11**(2020), 121-131.
37. TANKUT, A.N. and N. TANKUT, Effect of some factors on the strength of furniture corner joints constructed with wood biscuits. Turkish Journal of Agriculture and Forestry, **28**(2004), 301-309.
38. Malyshev, B. and R.L. Salganik, The strength of adhesive joints using the theory of cracks. International Journal of Fracture Mechanics, **1**(1965), 114-128.
39. Candea, V.N., et al., OPTIMIZING BUTT WELDING JOINTS OF SHEETS TO PROCESS 111-135 NORM EN 287-1/92. Metalurgia, **65**(2013).
40. Yin, T., et al., Shear performance of tongue-and-groove joints for CLT. Construction and Building Materials, **322**(2022), 126449.
41. Dvorak, G.J., J. Zhang, and O. Canyurt, Adhesive tongue-and-groove joints for thick composite laminates. Composites science and technology, **61**(2001), 1123-1142.
42. Seda, B., C. CSIHA, and L. DÉNES, Performance comparison of wood furniture joints fastened with Domino tenons and connectors. (2023).
43. Bas, S., L. Denes, and C. Csiha, Performance of Wood Dowels and Same Size Metallic Connectors Used for Furniture Joints. Bulletin of the Transilvania University of Brasov. Series II: Forestry• Wood Industry• Agricultural Food Engineering,(2023), 23-38.
44. Green, D.W., J.E. Winandy, and D.E. Kretschmann, Mechanical properties of wood. Wood handbook: wood as an engineering material. Forest Products Laboratory,(1999).
45. Prekrat, S., A. Jazbec, and S. Pervan, Analysis of the bending moment of innovative corner joints during static testing. Wood research, **49**(2004), 21-32.
46. Uluata, A.R., Ağaç malzemenin mekanik özelliklerine etki eden faktörler. Atatürk Üniversitesi Ziraat Fakültesi Dergisi, **18**(2011).
47. Clouser, W.S., Creep of small wood beams under constant bending load. (1959).
48. Yiğiter, H., *Betonarme donatısında klorid korozyonu gelişiminin elektrokimyasal yöntemlerle belirlenmesi*. 2008, DEÜ Fen Bilimleri Enstitüsü.
49. Marsoem, S., P. Bordonné, and T. Okuyama, Mechanical responses of wood to repeated loading, 2: Effect of wave form on tensile fatigue. Journal of the Japan Wood Research Society (Japan),(1987).
50. Gong, M. and I. Smith, Effect of waveform and loading sequence on low-cycle compressive fatigue life of spruce. Journal of materials in civil engineering, **15**(2003), 93-99.

51. Holzer, S.M., J.R. Loferski, and D.A. Dillard, A review of creep in wood: concepts relevant to develop long-term behavior predictions for wood structures. Wood and Fiber Science,(1989), 376-392.
52. Navi, P. and S. Stanzl-Tschegg, Micromechanics of creep and relaxation of wood. A review COST Action E35 2004–2008: Wood machining–micromechanics and fracture. (2009).
53. Du, Y., N. Yan, and M.T. Kortschot, An experimental study of creep behavior of lightweight natural fiber-reinforced polymer composite/honeycomb core sandwich panels. Composite Structures, **106**(2013), 160-166.
54. Hanhijärvi, A., Advances in the knowledge of the influence of moisture changes on the long-term mechanical performance of timber structures. Materials and Structures, **33**(2000), 43-49.
55. Ogawa, K., Y. Sasaki, and M. Yamasaki, Theoretical estimation of the mechanical performance of traditional mortise–tenon joint involving a gap. Journal of Wood Science, **62**(2016), 242-250.
56. Chevalier, L., et al., Cyclic virtual test on wood furniture by Monte Carlo simulation: from compression behavior to connection modeling. Mechanics & Industry, **20**(2019), 606.
57. Navi, P. and D. Sandberg, *Thermo-hydro-mechanical wood processing*. 2012: Crc Press.
58. Dubois, F., H. Randriambololona, and C. Petit, Creep in wood under variable climate conditions: numerical modeling and experimental validation. Mechanics of Time-Dependent Materials, **9**(2005), 173-202.
59. Zhou, Y., et al., Bending creep behavior of wood under cyclic moisture changes. Journal of Wood Science, **45**(1999), 113-119.
60. Demirel, S. and S. Bas, Procjena obilježja puzanja spojeva namještaja s klamericom izrađenih od različitih vrsta drva. Drvna industrija, **72**(2021), 179-186.
61. Gibson, E., Creep of wood: Role of water and effect of a changing moisture content. Nature, **206**(1965), 213-215.
62. Hunt, D.G., Creep trajectories for beech during moisture changes under load. Journal of materials science, **19**(1984), 1456-1467.
63. Reichel, S. and M. Kaliske, Hygro-mechanically coupled modelling of creep in wooden structures, Part I: Mechanics. International Journal of Solids and Structures, **77**(2015), 28-44.
64. Haygreen, J., et al., Studies of flexural creep behavior in particleboard under changing humidity conditions. Wood and Fiber Science,(1975), 74-90.
65. Bodig, J. and B.A. Jayne, Mechanics of wood and wood composites. (1982).
66. Nilsson, J. and J. Johansson, Bending and creep deformation of a wood-based lightweight panel: an experimental study. Wood and Fiber Science, **51**(2019), 16-25.
67. Demirel, S., et al., Face lateral shear resistance of one-row multistaple joints in oriented strandboard. Forest Products Journal, **63**(2013), 207-212.
68. Meyer, R.W. and R.M. Kellogg, *Structural uses of wood in adverse environments*. 1982.
69. Barrett, J., Effects of loading time on design. Structural uses of wood in adverse environments. Society of Wood Science and Technology, Van Nostrand Reinhold Company, New York,(1982), 301-316.
70. Mack, J., Creep in nailed joints. Nature, **193**(1962), 1313-1313.
71. Boyd, J., The significance of basic and applied research on mechanical fasteners for residential construction in Australia. Building Science, **1**(1965), 33-44.
72. Brock, G. The behavior of nailed joints under wood and short duration loading. in Proc., CAB TRADE Int. Symp. on Joints in Timber Struct. 1968.
73. Norén, B., *Nailed joints-Their strength and rigidity under short-term and long-term loading*. 1968, National swedish institute for building research.
74. Kuipers, J., Long duration tests on timber joints. CIB-WI8, Stockholm. February,(1977).
75. Polensek, A., Creep prediction for nailed joints under constant and increasing loading. (1982).
76. Feldborg, T., Slip in joints under long-term loading. Structral Division CIB-W18.,(1987).
77. Smith, I., et al., Design properties of laterally loaded nailed or bolted wood joints. Canadian Journal of Civil Engineering, **15**(1988), 633-643.

78. Huang, Y., Creep behavior of wood under cyclic moisture changes: interaction between load effect and moisture effect. Journal of wood science, **62**(2016), 392-399.
79. Owen, D.M. and T.G. Langdon, Low stress creep behavior: An examination of Nabarro—Herring and Harper—Dorn creep. Materials Science and Engineering: A, **216**(1996), 20-29.
80. Hazzledine, P. and J. Schneibel, Theory of coble creep for irregular grain structures. Acta metallurgica et materialia, **41**(1993), 1253-1262.
81. Blum, W., P. Eisenlohr, and F. Breutinger, Understanding creep—a review. Metallurgical and Materials Transactions A, **33**(2002), 291-303.
82. Gittus, J., Theory of dislocation creep for a material subjected to bombardment by energetic particles role of thermal diffusion. Philosophical Magazine, **30**(1974), 751-764.
83. Hirth, G. and D.L. Kohlstedt, Experimental constraints on the dynamics of the partially molten upper mantle: 2. Deformation in the dislocation creep regime. Journal of Geophysical Research: Solid Earth, **100**(1995), 15441-15449.
84. Liu, P., et al., Relationship between constant-load creep, decreasing-load creep and stress relaxation of titanium alloy. Materials Science and Engineering: A, **638**(2015), 106-113.
85. Hunt, D.G., A unified approach to creep of wood. Proceedings of the Royal Society of London. Series A: Mathematical, Physical and Engineering Sciences, **455**(1999), 4077-4095.
86. Costa, I. and J. Barros, Tensile creep of a structural epoxy adhesive: Experimental and analytical characterization. International Journal of Adhesion and Adhesives, **59**(2015), 115-124.
87. Smardzewski, J., R. Klos, and B. Fabisiak, Determination of the impact of creeping of furniture joints on their rigidity. Turkish Journal of Agriculture and Forestry, **37**(2013), 802-811.
88. Xu, W., Z. Wu, and J. Zhang, Compressive creep and recovery behaviors of seat cushions in upholstered furniture. Wood and Fiber Science, **47**(2015), 431-444.
89. Nakai, T., K. Toba, and H. Yamamoto, Creep and stress relaxation behavior for natural cellulose crystal of wood cell wall under uniaxial tensile stress in the fiber direction. Journal of Wood Science, **64**(2018), 745-750.
90. GÜNTEKİN, E., Ahşap ve Ahşap Kompozitlerinde Sünmeyi Etkileyen Faktörler. Turkish Journal of Forestry, **4**(2003), 87-102.
91. Navi, P., V. Pittet, and C. Plummer, Transient moisture effects on wood creep. Wood Science and Technology, **36**(2002), 447-462.
92. Hoseinzadeh, F., S.M. Zabihzadeh, and F. Dastoorian, Creep behavior of heat treated beech wood and the relation to its chemical structure. Construction and Building Materials, **226**(2019), 220-226.
93. Georgiopoulos, P., E. Kontou, and A. Christopoulos, Short-term creep behavior of a biodegradable polymer reinforced with wood-fibers. Composites Part B: Engineering, **80**(2015), 134-144.